Universidade do Minho
Escola de Ciências

Arunava Pradhan

Impacts of nanoparticles to microbes and invertebrates: from community responses to cellular targets

June 2013

Arunava Pradhan **Impacts of nanoparticles to microbes and invertebrates: from community responses to cellular targets**

UMinho | 2013

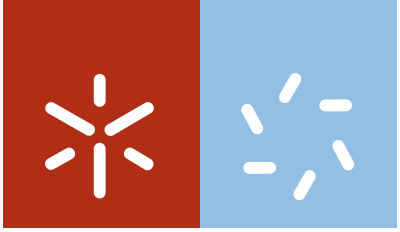

Universidade do Minho
Escola de Ciências

Arunava Pradhan

Impacts of nanoparticles to microbes and invertebrates: from community responses to cellular targets

Ph. D. Thesis in Sciences
Specialization in Biology

Supervised by
Prof. Dr. Fernanda Cássio
Co-supervised by
Prof. Dr. Cláudia Pascoal
Co-supervised by
Dr. Seena Sahadevan

June 2013

É AUTORIZADA A REPRODUÇÃO INTEGRAL DESTA TESE APENAS PARA EFEITOS DE INVESTIGAÇÃO, MEDIANTE DECLARAÇÃO ESCRITA DO INTERESSADO, QUE A TAL SE COMPROMETE

Universidade do Minho, June 2013

(Arunava Pradhan)

Acknowledgements

First of all I am grateful to the Portuguese Foundation for Science and Technology (FCT) for supporting me with the Ph. D. grant (SFRH/BD/45614/2008) and the work developed through the projects NANOECOTOX (PTDC/AAC-AMB/121650/2010), FCT-DAAD 2010-2011, FEDER-POFC-COMPETE and PEst-C/BIA/UI4050/2011.

I am very much thankful to my supervisor Prof. Dr. Fernanda Cássio and my co-supervisors Prof. Dr. Cláudia Pascoal and Dr. Seena Sahadevan for providing me the excellent opportunity of doing my doctoral research, all the precious scientific advices and supports with huge freedom and the nice friendly environment to enjoy my research and stay in Portugal.

My very special gratitude to CBMA and Department of Biology of University of Minho for providing such a nice platform for doing research and all kind of help and also I would like to thank Prof. Dr. Cândida Lucas, the director of CBMA, for her fruitful advices and helps, all the professors, researchers, technicians and supporting staffs of the department for their kind and friendly nature and helpful supports.

Starting the exciting journey in beginning of the year 2009 from India to Portugal with microbiology and molecular biology as my scientific background, it was a big challenge to establish and fulfill the research aim and objectives within four years in a new emerging field “nanoecotoxicology” at the new lab of a different cultural country. The journey was very special to me because that was the threasold period of the entire research group to stepping into the “nanoresearch” and I was the most fortunate person to receive the responsibility from my supervisors with complete freedom and faith inspite of our limited funding. Indeed, the target could not be achieved without the help and contribution of our whole lab group members. My very special thanks to Paulo for his helping hand in part of my work and friendship, to Sofia and Isabel for all kind of friendly helps and for sharing their knowledge and experiences, and to Daniela, Eva, Ana, Diana, Francisco, Bruno, Zé, Maria João, Carla, Bárbara for their helps and friendships. Also I would like to thank the other professors and group members of the lab especially Prof. Dr. Maria Teresa Almeida, Célia, Fábio and Joanna for their friendly advices, helps and supports; the professors and researchers from other labs: Prof. Dr. Margarida Casal, Prof. Dr. Pedro Gomes, Prof. Dr. Filipe Costa for their helping advices and Tony, Monica, Björn, Sandra, Ronaldo, Susana, Raul, Andreia, Franklin, Marslin, João, Andrei and many others for their friendly helps and cheering natures. Also I would like to thank Dr. Catarina Gonçalves and Dina from Department of Biological Engineering for their friendly helps and Elsa Ribeiro for her help in SEM.

I would also like to thank our all collaborators especially from Germany, Prof. Dr. Gerd-Joachim Krauss, Prof. Dr. Dietmar Schlosser, Dr. Dirk Dobritzsch, Melanie Dobritzsch, Stefan Helm, Katharina Gerth and Anja Reupsch. My special thanks to Prof. Dr. Manuel

Graça for his helpful workshop and advices on scientific paper writing and to Prof. Dr. Stephen J Klein and Prof. Dr. James F Ranville for their fruitful friendly scientific advices on nanoecotoxicology and to Prof. Dr. Klement Tockner and Prof. Dr. Guy Woodward for their influencing advices on career development strategies in research.

My research life started in West Bengal University of Technology (WBUT), India. Therefore my immense gratitude to all my teachers and professors in WBUT especially, my ex-supervisor of M.Sc. thesis Dr. Shaon Ray Chaudhuri, ex-Vice Chancellor of WBUT Prof. Dr. Ashoke Ranjan Thakur, Prof. Dr. Subrata Kumar Dey, Dr. Jaya Bandyopadhyay, Dr. Srimonti Sarkar, Dr. Anindita Seal, Dr. Soumalee Basu, Dr. Indrani Roy, Prof. Dr. Timir Baran Samanta, Prof. Dr. Arunabha Adhikari, Prof. Dr. Bishnupada Chatterjee, Dr. Raja Banerjee, Dr. Joydeep Mitra for their encouraging teaching, research training, valuable advices and friendly support. Also I would like to thank Dr. Sukla Ghosh and all other professors and researchers especially Subhra da, Aditi di, Indrashis and Piyasi di from Department of Biophysics, Molecular Biology and Bioinformatics, University of Calcutta, India for their help and support.

Additionally, I would like to express my very special gratitude to those who always support me in any situation of life, my beloved friends, Udatto, Soumen, Soma, Tanmoyda, Poulomi, Poonam di, Pranami, Sumita, Sumana, Sanhita di, Jayeeta and Madhu di. Thanks also to all my junior and senior friends from WBUT for their love, support and all help.

Also thanks to my friends in Portugal, Swagata, Soma di, Kalyan da, Angshu boudi, Aneesh, Manab, Kallol da, Rima boudi, Debarati, Smriti, Raghu, Francielle and all my friends from Erasmus student network for always cheering and supporting me.

My special thanks to the teachers and professors of Department of Microbiology, Botany, Zoology and Chemistry of Modern College of Arts, Science and Commerse under University of Pune, India. My special gratitude to Snehal Shinde Sir, Harsh Gaikwad Sir, Jayant Randive sir, Sneha Ogale Madam and Gogi Madam for growing my interest and motivations in science.

I would also like to express my very special thanks to all of my relatives who always supported me mentally throughout this special journey of my life, especially Babu da, Bapi da, my all uncles, aunts and cousins.

The list of the people who always help and support me is very long and I am very much grateful to all of them.

At the end I would like to dedicate this dissertation to my sister and parents; without their unconditional support, love, guidance and understanding I could not reach to this stage of life. Thank you so much for your eternal love and blessings on me.

Impacts of nanoparticles to microbes and invertebrates: from community responses to cellular targets

Abstract

The incredible development in nanotechnology since the last decade has brought the “nanoworld” to our regular life. However, the extensive global growth in commercial production and usage of nanomaterial-based products raised the question whether nanomaterials when released to the environment can constitute a potential risk to biota and ecosystem processes. Being large reservoirs, natural waters are likely to be the ultimate sink of nanomaterials. In forested streams, microbes, predominantly fungi, decompose plant litter from riparian vegetation and transfer carbon and energy via invertebrate shredders to higher trophic levels. Freshwater decomposers are sensitive to changes in water quality with implications to ecosystem functioning. Considering the recent development of nanotechnology, assessing the potential toxicity of nanomaterials against freshwater decomposers and examining their ecological and physiological responses to nanoparticle exposure will contribute to a safer use of nanomaterials.

In this study, by using a microcosm approach, we found that nanocopper oxide (nanoCuO), nanosilver, and their ionic precursors severely affected leaf litter decomposition by stream-dwelling microbes, as indicated by a decrease in microbial biomass, fungal sporulation and species richness. Moreover, the analysis of fungal and bacterial communities, based on DNA fingerprints from denaturing gradient gel electrophoresis and fungal sporulating species, revealed shifts in species composition and changes towards a better adapted community under the stress induced by nano and ionic metals. Moreover, the negative effects of metal nanoparticles were less pronounced than those of their ionic forms.

Nanoparticle size (12, 50 and 80 nm) and the presence of humic acid (HA) influenced the toxicity of nanoCuO against stream-dwelling microbial decomposers. The toxicity of nanoCuO increased in a dose-dependent manner and with the decrease in nanoparticle size. Bacteria were more sensitive than fungi to nanoCuO, because EC_{50} values for biomass of bacteria were much lower than those of fungi. Fungal reproduction was more sensitive to nanoCuO than leaf decomposition or microbial biomass. HA alone also had negative effects on microbial diversity and activity, but the presence of HA alleviated the negative effects of smaller size nanoCuO (12 or 50 nm). Alterations in leaf surface morphology further supported the impacts of nanoparticles and HA on microbial activity on decomposing leaves, as shown by scanning electron microscopy.

We also showed that nanoCuO had lethal and sublethal effects on *Allogamus ligonifer*, a common invertebrate shredder in Southwest European streams that prefers high quality stream water. The feeding behaviour and growth of the invertebrate were affected in a dose-dependent manner. Effects were due to both nanoCuO and ionic copper leached from nanoCuO that adsorbed or accumulated in the shredder body. The feeding behaviour of the invertebrate shredder was more inhibited as nanoparticle size decreased. The toxicity of

smaller size nanoCuO to the shredder was alleviated by the presence of HA. A post-exposure feeding experiment showed a very low recovery of the invertebrate feeding behaviour after stress removal.

The exposure of aquatic fungal populations to nanoCuO led to a decrease in biomass production, alterations in cell-wall morphology, increased biosorption of nanoCuO and induction of extracellular laccase activity in a time and dose-dependent manner. Fungal populations from metal-polluted streams were more resistant/tolerant to the stress induced by nanoCuO than those from non-polluted streams. Differences in laccase activity among fungi appeared to be related to the presence of laccase-like genes in the copper-binding domain.

Exposure to nanoCuO or ionic copper led to lower intracellular accumulation of reactive oxygen species (ROS), plasma membrane disruption, and DNA-strand breaks in fungal populations isolated from metal-polluted streams than in those from non-polluted streams. The activities of glutathione reductase and superoxide dismutase were higher in fungi from metal-polluted than from non-polluted streams, but the opposite was found for glutathione peroxidase activity. Results suggested that fungi from metal-polluted streams have higher capacity to deal with the oxidative stress induced by nanoCuO, probably due to their ability to maintain a high ratio of reduced glutathione (GSH) to oxidized glutathione (GSSG).

In contrast to metal nanoparticles, polyhydroxy fullerene (PHF) nanoparticles stimulated the growth of the yeast *Saccharomyces cerevisiae*, which was used as model of eukaryotic organism. Moreover, the oxidative stress induced by cadmium ions to yeast cells was mitigated by the presence of PHF. A maximum growth recovery was obtained after 26h of exposure to 500 ppm PHF at pH 6.8. Results suggested that PHF nanoparticles have antioxidant and free-radical scavenging properties.

Efeitos das nanopartículas em microrganismos e invertebrados: das comunidades aos alvos celulares

Resumo

Na última década ocorreu um desenvolvimento exponencial da nanotecnologia o que trouxe o "nanomundo" à nossa vida do dia a dia. No entanto, o crescimento a nível global da produção e do uso de produtos com base em nanomateriais levanta a questão de saber se os nanomateriais, quando libertados para o meio ambiente, podem constituir um risco potencial para as comunidades biológicas e para os processos dos ecossistemas a elas associados. Os ecossistemas de água doce são susceptíveis de constituir o reservatório final dos nanomateriais. Nos rios e ribeiros florestados, os microrganismos, principalmente os fungos, decompõem o material vegetal proveniente da vegetação ribeirinha e promovem a transferência do carbono e da energia para os níveis tróficos superiores através da actividade dos invertebrados trituradores. Os decompositores de água doce são sensíveis a alterações na qualidade da água, com implicações para o funcionamento do ecossistema. Assim, a avaliação da potencial toxicidade dos nanomateriais para os decompositores de água doce e a análise das suas respostas ecológicas e fisiológicas à exposição a nanopartículas contribuirá para uma utilização mais segura dos nanomateriais.

Neste estudo, usando uma abordagem em microcosmos, mostrámos que as nanopartículas de óxido de cobre, as nanopartículas de prata, e os seus precursores iónicos afectavam negativamente a decomposição da folhada por comunidades de microrganismos aquáticos, como indicado por uma diminuição da biomassa microbiana (fungos e bactérias), da esporulação dos fungos e da riqueza em espécies de fungos. A análise da comunidades de fungos, por electroforese em gradiente desnaturante do DNA microbiano e com base na morfologia das conídias libertadas da folhada em decomposição, revelou alterações na estrutura das comunidades no sentido de uma comunidade melhor adaptada ao stress induzido pelos metais quer nas formas nano quer iónicas. Além disso, os efeitos negativos das nanopartículas metálicas foram menos pronunciados do que os das suas formas iónicas.

O tamanho das nanopartículas de óxido de cobre (12, 50 e 80 nm) e a presença do ácido húmico (HA) influenciou a toxicidade das nanopartículas para os microrganismos decompositores. A toxicidade das nanopartículas de óxido de cobre aumentou com a dose e com a diminuição do tamanho das partículas. As bactérias foram mais sensíveis do que os fungos às nanopartículas de óxido de cobre, porque os valores de EC_{50} para a biomassa de bactérias foram muito mais baixos do que os dos fungos. A reprodução dos fungos foi mais sensível à exposição às nanopartículas de óxido de cobre do que a decomposição da folhada ou a biomassa microbiana. O HA sozinho também teve efeitos negativos sobre a diversidade e a actividade dos microrganismos. Contudo, a presença de HA mitigou os efeitos negativos das nanopartículas de óxido de cobre de menor tamanho (12 ou 50 nm). As alterações na morfologia da superfície da folhada, reveladas por microscopia electrónica

de varrimento, corroboraram os efeitos das nanopartículas e do HA na actividade microbiana nas folhas em decomposição.

Os nossos resultados também mostraram que as nanopartículas de óxido de cobre tiveram efeitos letais e subletais em *Allogamus ligonifer*, um invertebrado detritívoro comum em rios do Sudoeste Europeu com elevada qualidade ecológica. A presença de nanopartículas de óxido de cobre afectou o comportamento alimentar e o crescimento do invertebrado de uma forma dependente da dose. Os efeitos negativos no animal pareceram ser devidos à adsorção ou acumulação no corpo do invertebrado de nanopartículas e de cobre iónico libertado das nanopartículas. O comportamento alimentar dos invertebrados foi mais inibido na presença de nanopartículas de menor tamanho comparativamente às de maior tamanho. A toxicidade das nanopartículas de óxido de cobre de menor tamanho para o invertebrado foi atenuada pela presença de HA. Uma experiência de alimentação de pós-exposição mostrou uma baixa recuperação do comportamento alimentar dos invertebrados após a remoção do stress imposto pelas nanopartículas.

A exposição de populações de fungos aquáticos às nanopartículas de óxido de cobre levou a uma diminuição da biomassa produzida, a alterações na morfologia da parede celular, ao aumento da bioadsorção das nanopartículas de óxido de cobre e à indução da actividade de lacases extracelulares de uma forma dependente da dose e do tempo. As populações de fungos isoladas de rios poluídos com metais foram mais resistentes/tolerantes ao stress induzido pelas nanopartículas metálicas do que as isoladas de rios não poluídos. As diferenças observadas na actividade das lacases entre os fungos pareceram estar associadas à presença ou ausência de genes do tipo das lacases.

A exposição a nanopartículas de óxido de cobre ou a cobre iónico induziu menor acumulação intracelular de espécies reactivas de oxigénio e menos danos na membrana plasmática e no DNA de fungos isolados de rios poluídos com metais do que em fungos isolados de rios não poluídos. As actividades da glutationa reductase e da superóxido dismutase foram mais elevadas em fungos isolados de rios poluídos com metais do que em fungos isolados de rios não poluídos. Contudo, o oposto foi observado para a actividade da glutationa peroxidase. Os resultados sugerem que os fungos de rios poluídos com metais têm maior capacidade para lidar com o stress oxidativo induzido pelas nanopartículas de óxido de cobre provavelmente devido à sua capacidade de manter uma razão elevada de glutationa reduzida (GSH) em relação à glutationa oxidada (GSSG) nas células.

Em contraste com o observado para as nanopartículas metálicas, as nanopartículas de poli-hidroxi-fulereno (PHF) estimularam o crescimento da levedura *Saccharomyces cerevisiae*, a qual foi utilizada neste trabalho como modelo de organismo eucariota. Por outro lado, o stress oxidativo induzido por iões de cádmio na levedura foi atenuado pela presença de PHF. A recuperação máxima do crescimento da levedura foi obtida após 26 horas de exposição a 500 mg L^{-1} de PHF e a pH 6,8. Os resultados sugerem que as nanopartículas de PHF têm propriedades antioxidantes.

Table of Contents

Chapter 3

Toxicity of nanoCuO to microbial decomposers depends on nanoparticle size and concentration of humic acid in freshwaters

Chapter 4

Copper oxide nanoparticles can induce toxicity to the freshwater shredder *Allogamus ligonifer*

Chapter 5

Size-dependent effects of nanoCuO on the feeding behaviour of freshwater shredders may change in the presence of natural organic matter

Chapter 6

Physiological responses to nanoCuO in fungi from non-polluted and metal-polluted streams

List of Figures

List of Tables

List of Manuscripts for Scientific Publication

The chapters in this dissertation are developed based on the following manuscripts already published or under preparation for submission into scientific journals:

1. Pradhan A, Seena S, Pascoal C, Cássio F. 2011. Can Metal Nanoparticles Be a Threat to Microbial Decomposers of Plant Litter in Streams? Microbial Ecology, 62, 58–68.

2. Pradhan A, Geraldes P, Seena S, Pascoal C, Cássio F. 2013. Toxicity of nanoCuO to microbial decomposers depends on nanoparticle size and concentration of humic acid in freshwaters (under preparation).

3. Pradhan A, Seena S, Pascoal C, Cássio F. 2012. Copper oxide nanoparticles can induce toxicity to the freshwater shredder *Allogamus ligonifer*. Chemosphere, 89, 1142–1150.

4. Pradhan A, Geraldes P, Seena S, Pascoal C, Cássio F. 2013. Size-dependent effects of nanoCuO on the feeding behaviour of freshwater shredders may change in the presence of natural organic matter (under preparation).

5. Pradhan A, Seena S, Dobritzsch D, Helm S, Gerth K, Dobritzsch M, Krauss G-J, Schlosser D, Pascoal C, Cássio F. 2013. Physiological responses to nanoCuO in fungi from non-polluted and metal-polluted streams (submitted).

6. Pradhan A, Seena S, Schlosser D, Gerth K, Helm S, Dobritzsch M, Krauss G-J, Dobritzsch D, Pascoal C, Cássio F. 2013. Fungi from metal-polluted streams have high ability to cope with the stress induced by nanoCuO (under preparation).

7. Pradhan A, Seena S, Pascoal C, Cássio F. 2013. Polyhydroxy fullerene can stimulate yeast growth and mitigate oxidative stress induced by cadmium (under preparation).

Chapter 1

General introduction

1.1. Historical overview and advances in nanotechnology

The word “nano” probably evolved from the Greek word “*νᾶνος*” (*nanos*), meaning "dwarf", and was officially recognized by the International System (SI) of units as a standard metric prefix in 1960. The “nanometre” is one billionth of a metre (1 nm=10^{-9} m, SI units). Although there is no accepted international definition for a nanoparticle, according to the new PAS71 document developed in UK, a material with one or more dimensions lower than 100 nm should be considered a nanomaterial, (http://www.malvern.com/labeng/industry/nanotechnology/nanoparticles_definition.htm). Unlike the bulk-sized particles, nanoparticles are under the limelight of the current research owning to its special properties. The increased surface area per unit mass and discontinuous behaviour of delocalized surface electrons by quantum confinement effects induce changes in chemical, mechanical, optical, electric, and magnetic properties of nanomaterials (Burda et al., 2005; Buzea et al., 2007).

Nanotechnology was recognised by the scientific community in the 20th century. However, nanomaterial-based products were already in use at least for the last two millenniums, as indicated by metallographic analyses of ancient products, such as the purple surface of shakudō or the techniques of lusterware (Northover, 2008). Some tiny spiral-shaped metallic objects were found in the Narada River (eastern side of the Ural Mountains in Russia) dating from past 20,000 to 318,000 years. These objects were composed of an alloy of copper, tungsten and molybdenum; the smallest size being 1/10,000th of an inch justifying the designation of micro to nano size metals (Igan, 2005). Metal nanoparticles, such as silver, gold and copper, were used in pottery during the Renaissance to generate a glittering effect on the surface of pots. Gold nanoparticles were used in the Roman Lycurgus cup dated to the 4th century AD. Iron oxide nanoparticles were used in Maya blue paint during ~700 AD (José-Yacamán et al., 1996).

The first scientific description about the optical properties of metal particles with very minute dimensions was given by Michael Faraday (Faraday, 1857). Richard Zsigmondy, an Austrian-Hungarian chemist, was the first to report about size measurements of nanoparticles in the first decade of the 20th century (Zsigmondy, 1909). A number of subsequent studies further determined the size distribution of tiny particles in colloid chemistry and the observed nanometre size particles were expressed as “mμ” or “μμ” (Svedberg and Nichols, 1923; Svedberg

and Rinde, 1924). In 1959, the physicist Richard P. Feynman described for the first time the concept of “nanoscience” in a lecture to the American Physical Society (Gribbin and Gribbin, 1997; Park, 2007) and the term “nanotechnology” was coined by the Japanese scientist Norio Taniguchi in 1974 (Taniguchi, 1974). Later, Kim Eric Drexler disseminated the concept of nanotechnology into the public domain with the publication of “Engines of Creation: The Coming Era of Nanotechnology” and founded the field of molecular nanotechnology (Drexler, 1986).

At present, nanomaterial-based products have become part of our daily life. A large number of companies are currently involved in the production and application of nanomaterial-based products in several areas, such as cosmetics, electronics, biopharmaceutical and biomedicines and laboratory equipments (Salata, 2004; Aitken et al., 2006). Examples of different types of tailored nanomaterials and their applications are summarized in Table 1.1.

1.2. Sources of nanomaterials in the environment

The source of nanoparticles in the environment can be natural or anthropogenic. The most common natural sources of nanoparticles are combustions including forest and grass fires, soot, naturally occurring aerosols, volcanic elements, rock erosion, photochemical and biogenic reactions. Combustions, like forest and grass fires or from burnt charcoal, can occur naturally (by lightning and wind or heat) or be caused directly or indirectly by humans, leading to the production of smoke, soot and ash which contain large amounts of nanomaterials (Buzea et al., 2007). Most aerosols in the environment occur naturally and contain large number of nanoparticulate matter; only one tenth of the aerosols are produced by human activities, mainly from industrial exhausts and burnt residues from vehicles in urban areas (Taylor, 2002). Aerosols can be produced in large quantity from the dust storms mainly in the desert areas. Huge amount of mineral nanoparticles with size ranging between 120 and 160 nm have been detected in aerosols of the desert Sahara (d’Almeida and Schütz, 1983). Volcanic soils or products contain nanoparticles of metals including heavy metals (Yano et al., 1990; Buzea et al., 2007). Metals and metal oxide nanoparticles (e.g. Au, Ag, TiO_2, Fe-oxides and magnetite) often have atmospheric or geogenic sources; they are found in the dust aerosols, soils, rocks, sea salts and rivers (Nowack and Bucheli, 2007; Wigginton et al., 2007). Carbon nanoparticles, like C_{60} or C_{70} fullerenes and their derivatives and CNTs, can be found in the soot, fly ashes and aerosols, hard and soft rocks,

fossilised dinosaur eggs and charcoals (Heymann et al., 2003; Nowack and Bucheli, 2007). Also other organic nanoscale substances, like humic substances, can be present in natural colloids (Gibson et al., 2007). Biogenic source of nanoparticles are often reported. Naturally occurring organic nanoparticles have been isolated from the English ivy (*Hedera helix*) and have UV-protective effects (Xia et al., 2010). Many microorganisms, including bacteria, are able to produce metal nanoparticles, e.g. silver (50-100 nm) and gold (10-20 nm) nanoparticles (He et al., 2007; Minaeian et al., 2008). Biosynthesis of silver nanoparticles using fungi has been reported by Sadowski et al. (2008). Nanoparticles of Au, Ag and Au-Ag of size ranging from 15 to 150 nm have shown to be biosynthesised by *Volvariella volvacea*, an edible mushroom (Philip, 2009).

Anthropogenic sources of nanoparticles in the environment include aerosols, cosmetics, other daily life products, biomedicines and wastewater treatment plants. Aerosols containing nanoparticles can be generated from industrial combustion, automobile exhausts, smokes, multistorage building re-constructions, road constructions, roadside traffic, etc. (Shi et al., 2001; Buzea et al., 2007). Anthropogenic sources are mostly responsible for spreading and contaminating manufactured nanoparticles to the environment. Some of the regularly used materials like flame of candles, refrigerator, vacuum cleaner, cigarette, stoves, electrospray or other room-freshener spray and room heater may also emit nanoparticles indoors (Buzea et al., 2007). Metal by-products such as Pt and Rh with size in nanometer range are often found in aerosols (Zereini et al., 2001). Intense industrial and urban development led to the presence of huge amount of fullerenes and their derivatives in the aerosols of Mediterranean Sea atmosphere (Sanchís et al., 2012). Temporal association between very small size nanoparticles (3-7 nm) and solar radiation was observed in urban atmosphere in the absence of other local sources, suggesting the importance of homogeneous nucleation as a source of nanoparticles in urban areas (Shi et al., 2001). Increased quantity of other regular use products like sunscreen, cosmetics, electronics, antimicrobial paints, clothes, washing machines and biomedicines, which contain nanoparticles such as Ag, Au, CuO, ZnO, TiO_2, and SiO_2, may also release manufactured nanoparticles that will probably contaminate (intentionally or unintentionally) the environment through leaching into soil and natural surface waters. Other anthropogenic sources (unintentional) of nanoparticles that can contaminate the soil or surface waters are

wastewater treatment plants, filtration units in drinking water purification plants and metallic pipes (Wigginton et al., 2007; Kim et al., 2010; Lau, 2011).

Table 1.1 Engineered nanomaterials and their potential applications for human benefit

Type of nanomaterial	Example	Major application	Reference
Spherical nanometals	Ag, Au, Zn, Cu, Si, Pt, Pd	In ornaments, antimicrobial paints, textiles, fabrics, electronics consumer goods, biomedical and therapeutic research, drug delivery and gene therapy, antimicrobial therapy, anti-HIV drug development strategy, anticancer drug development	Elechiguerra et al., 2005 Jin and Ye, 2007 Kim et al., 2007 Kumar et al., 2008 Luechinger et al., 2008 Agasti et al., 2009 Zhang et al., 2009 Matthews et al., 2010
Spherical nanometal oxides	ZnO, CuO, TiO_2, SiO_2, CeO_2, Al_2O_3, Fe_2O_3	In ornaments, cosmetics, sunscreens, antimicrobial paints, textiles, electrospray disinfectants, biomedical and therapeutic research, drug delivery and gene therapy, antimicrobial therapy,	Nel et al., 2006 Jin and Ye, 2007 Becheri et al., 2008 Kathirvelu et al., 2009 Hochmannova and Vytrasova, 2010 Matthews et al., 2010 Wang et al., 2010
Nanocrystals/ nanocrystallites/ quantum dots	CdS, CdSe, CdTe, PbSe, GaAs, CdSe/ZnS, CdSeS/ZnS	As semiconductor for biological imaging, cell tracking, pathogen and toxin detection, Fluorescent labelling of cellular proteins, Gene technology	Jamieson et al., 2005 Jin et al., 2011
Nanotubes/nanowires of metals/metal oxides	Cu, SiO_2, ZnO, TiO_2	In electronic devices as semiconductor	Mo and Kaxiras, 2007
Carbon nanotubes	CNT, single-walled or multi-walled	In electronic devices as semiconductors, electrical circuits, batteries, computation, electronics, catalytic reactions, strength absorber, flexible displays, fuel cell and solar cell In biomedical fields, biosensing, drug delivery, diagnostics, tissue engineering and anticancer therapeutics	Endo et al., 2004 Bandaru, 2007 Fisher et al., 2012
Noble metal nanoparticles/carbon nanotubes nanohybrids	CNT/DEN/Au, PtRu/CNT, Pt/CNT, Pt/Au/CNT, Pd/HPW-PDDA-MWCNTs	In heterogeneous catalysis, electrocatalysis, fuel cells and chemo/biosensors	Wu et al., 2011
Buckyball or buckminsterfullerenes and functionalized derivatives	C_{60}, C_{70}, $C_{60}(OH)_x$, C_3 (e,e,e-$C_{60}(C(COOH_2))_3$)	Fullerenes in HIV-1 protease inhibition, DNA-photocleavage, antimicrobial therapy Water soluble functionalized derivatives of fullerene as potent antioxidant agent and free radical scavenger in prevention of excitotoxic and apoptotic death of neurons, protection against ischemia-reperfused lungs, protecting brain against alcoholic injury, preventing hepatotoxicity in rats and human cell lines, anti-tumour therapy HIV-1 protease inhibition	Friedman et al., 1993 Dugan et al., 1996 Ros et al., 2001 Chen et al., 2004 Injac et al., 2008b Tykhomyrov et al., 2008 Krishna et al., 2010

1.3. Aquatic environment: the ultimate sink of nanomaterials

Increased industrial production and commercial application of engineered nanoparticles enhance the possibility of their release to the environment (Colvin, 2003). Natural waters constitute a large environmental compartment and are likely to serve as a terminal repository of natural and engineered nanoparticles via industrial waste-release, soil runoff and atmospheric deposition. The average concentration of nanoparticles in natural waters is 10^7-10^8 L^{-1} (Lau, 2011). Because the surface properties of natural nanoparticles are often similar to those of engineered nanoparticles, natural nanoparticles may provide some information to predict the fate and behaviour of engineered nanoparticles in natural waters. Metal oxide natural nanoparticles, like crystalline TiO_2, were found in rivers of western Montana, USA (Wigginton et al., 2007). Nanoparticles can be released from mechanical milling of rocks in slipping zones of faults (Han et al., 2011). Iron oxides and Pb nanoparticles with 20 nm were detected in drinking water but it was not clear if those nanoparticles had a natural origin in the river or an anthropogenic origin from the water treatment plant or from the corrosion of pipes (Wigginton et al., 2007). Iron oxide nanoparticles with similar size were also observed in riverine and glacial melt water environments (Poulton and Raiswell, 2005). Ferrihydrite nanocrystallites and nanocrystalline iron oxides were observed in main rivers of the Amazon Basin in Brazil, and were involved in transporting iron and organic matter (Allard et al., 2004). High amounts of organic nanoparticulate fraction with particle size smaller than 5 nm have been reported in lakes and rivers near Birmingham, UK (Baalousha and Lead, 2007). Metal sulphide nanoparticles are often found in rivers (Rozan et al., 2000), but the actual sources of these nanoparticles are not clear.

Natural biosynthesis of metal nanoparticles may also occur in surface waters. Silver nanoparticles can be produced by microbes. For example, Ag nanoparticles can be synthetized by several *Fusarium oxysporum* strains (Durán et al., 2005) and *Fusarium* sp. has been associated with plant-litter in freshwaters (Fernandes et al., 2009). Carbon nanoparticles, such as fullerenes, naturally occurring in rivers appear to be produced by algae (Heymann et al., 2003). Organic nanoparticles (1-5 nm) sitting on coherent nanoscale surface films (3 nm thick) can be formed in natural waters at low pH (Gibson et al., 2007). The presence of nanoparticles in salt waters has also been reported. Nanoparticles of trace metals were found in water samples from the San Francisco Bay estuary, USA. At the lower salinity sites of the estuary, about 84% of the total dissolved fraction consisted of Al,

Ag and Fe nanoparticles, while 16-20% of that fraction consisted of Cu and Mn nanoparticles with sizes <200 nm; at sites with higher salinity, Fe nanoparticles were the most abundant (ca. 40%), followed by nanoparticles of Al, Mn and Cu (<10%) and nanoparticles of Zn (<3%), and about <2% of the fraction contained Ni nanoparticles at the river endmember (Sañudo-Wilhelmy et al., 1996). Nanoparticles of bioactive metals with 200-800 nm were detected in the Narragansett Bay, RI, USA with a decreasing order of nanoparticle load as follows: Fe>Mn>Zn>Cu>Ni (Wells et al., 2000).

There is also evidence of the release of tailored nanoparticles into streams from anthropogenic sources (Nowack, 2008). TiO_2 nanoparticles (20 and 300 nm size) from the exterior facade paints were discharged into surface waters (Kaegi et al., 2008). Inorganic metal nanoparticles and carbon nanoparticles are often used for detection and removal of chemical and biological substances, including heavy metals, from wastewaters (Tiwari et al., 2008). Ag_2S nanocrystals with 5-20 nm size have been found in sewage sludge products indicating the transformation of Ag nanoparticles during the wastewater treatment process (Kim et al., 2010). Copper concentration in the chemical mechanical planarization wastewaters of Taiwan often exceeds 100 ppm (mainly due to incineration of fly ashes), up to 49% of which may consist of CuO nanoparticles (Hsiao et al., 2001; Huang et al., 2006). Silver nanoparticles are widely used in textiles and plastic industries and they can be a source of Ag in natural waters. Indeed, from the estimated 500 t $year^{-1}$ of global production of nano Ag (Muller and Nowack, 2008), about 20–130 t $year^{-1}$ have been predicted to reach EU freshwaters mainly from ionic leaching of polymer embedded nanoAg from biocidal plastics and textiles, which accounts for about 15% of the total silver released into EU freshwaters (Blaser et al., 2008). Predicted environmental concentrations (PECs) of nano size Ag in Europe, with lower and upper quartiles ($Q_{0.15}$ and $Q_{0.85}$) based on regular life use of nanomaterials, are 0.5−2 ng L^{-1} in surface waters, 32–111 ng L^{-1} in sewage treatment plant effluents, and 1.3–4.4 mg kg^{-1} in sewage sludge (Gottschalk et al., 2009; Fabrega et al., 2011), and these values are predicted to increase in the near future (Balser et al., 2008; Gottschalk et al., 2009; Mueller and Nowack, 2008). Although a number of techniques have proved suitable for characterization of engineered metal nanoparticles (e.g. Ag, Al, Au, Cu, Fe, Si and Zn) or metal oxide nanoparticles (e.g. NiO, ZnO, SiO_2, TiO_2, Al_2O_3, CeO_2, CuO and Fe_2O_3) released to the environment from textile industry wastewaters and waters from hospitals or hotel laundries (Rezić, 2011), studies on

the detection and characterization of engineered nanoparticles in natural waters are still scarce.

1.4. Ecotoxicity of metal-based nanoparticles and carbon-based nanoparticles

Metal/metal oxide nanoparticles and carbon-based nanoparticles are among the most widely used types of engineered nanomaterials (Griffitt et al., 2008). These nanoparticles represent a fundamental cornerstone of nanotechnology due to their contribution to various fields of applications (Table 1.1). Indeed, they are used worldwide in a vast range of regular life products and find applications in various research fields including electronics, biomedical and pharmaceutical areas.

Metal-based nanoparticles have special catalytic and photoactive properties, which are different from those of carbon-based nanoparticles. For example, metal nanoparticles are less hydrophobic compared to most of carbon-based nanoparticles in aqueous environments and, thus, the aggregation or deposition rates of inorganic nano metals/metal oxides are relatively lower than that of carbon nanoparticles. The adverse impacts of nano metals/metal oxides against aquatic biota have been associated with their ability to generate reactive oxygen species (Limbach et al., 2007; Petersen and Nelson, 2010). On the other hand, there are controversial reports on the potential toxicity and/or antioxidative activity of fullerenes and their derivatives. Some studies have reported toxicity and ecotoxicity of fullerene via oxidative stress (Oberdörster et al., 2006). Due to differences in properties, surface chemistry and abiotic or biotic degradation rates it is difficult to have real comparative toxicity studies between metal-based and carbon-based nanoparticles. Very few attempts were made to compare the toxicity of these two types of nanomaterials in individual organisms and human cell lines.

The OECD enlisted most of metal oxide nanoparticles (TiO_2, Al_2O_3, CeO_2, ZnO and SiO_2), two metal nanoparticles (Ag and Fe) and four carbon-based nanoparticles (fullerene C_{60}, SWCNTs, MWCNTs and carbon black) as representative manufactured nanomaterials seeking ecotoxicity tests and risk assessment (OECD, 2010). Most of the studies with carbon-based nanoparticles have shown very low lethal effects and much more pronounced sublethal effects on invertebrates; whereas most of metal and metal oxide nanoparticles have exhibited lethal and sublethal effects on invertebrates although depending on nanoparticle type and size (Cattaneo et al., 2009). Within the carbon nanoparticles, fullerenes

seemed to be more toxic than CNTs; however, the toxicity of fullerenes prepared with the solvent tetrahydrofuran (THF) is generally higher than when prepared by stirring and sonication in water because THF itself can be toxic (Cattaneo et al., 2009). In a comparative study, ZnO nanoparticles induced phytotoxicity by inhibiting seed germination and root growth, whereas MWCNTs did not (Lin and Xing, 2007). Consistently, CuO and ZnO nanoparticles showed higher cytotoxicity than MWCNT against human lung epithelial cell lines, and the genotoxicity of CuO and TiO_2 nanoparticles was also higher than that of MWCNT (Karlsson et al., 2009). The TiO_2 nanoparticles were more phototoxic and promoted higher production of superoxide ions in bacteria compared to fullerenes or their hydroxyl derivatives (Brunet et al., 2009). Blaise et al. (2008) demonstrated the toxicity of 11 nano-powders against various aquatic organisms; fullerene C_{60} was classified as “harmful” or “nontoxic”, while most of metal oxide nanoparticles were classified as “very toxic”, “toxic” or “harmful” according to the categories in the EU Commission Guideline 93/67/EEC. However, the pristine form of fullerene (C_{60}) was more toxic against human cell lines than its derivatives (Sayes et al., 2004).

The functionalised fullerene polyhydroxy fullerene (PHF) is commercially more attractive because it is reported to be non-toxic, water soluble, stable in aqueous environment due to the presence of hydroxyl groups and antioxidant properties (Lai et al., 2000; Injac et al., 2008a; Vávrová et al., 2012). PHF has been reported to decrease excitotoxic and apoptotic death of neurons, tumour in rat, prevent ischemia-reperfused lungs, alcoholic injury in brain and hepatotoxicity in rats and human cell lines (Table 1.1). On the contrary, few studies reported the cytotoxicity of PHF (Sayes et al., 2004; Xu et al., 2009; Johnson-Lyles et al., 2010; Wielgus et al., 2010) and have shown that under photoexcitation, PHF can generate free radical species (Pickering and Wiesner, 2005) leading to early apoptosis and lipid peroxidation (Wielgus et al., 2010). However, Kong et al. (2009) provided evidence of extensive mineralization of PHF (up to 47% of PHF) by direct photolysis. Moreover, white rot fungi are capable of mineralising PHF and also incorporate minor amounts of carbon from PHF into lipid biomass (Schreiner et al., 2009). In addition to its antioxidant function, possible utilisation of PHF as a nutrition source was also reported because it stimulated growth and lifespan of algae, fungi and plants (Gao et al., 2011). Increase in lifespan of mice by carboxyfullerene, another antioxidant functionalized fullerene, has also been reported (Quick et al., 2008).

In spite of the reported toxicity of carbon-based nanoparticles, metal and metal oxide nanoparticles are of greater concern for the environment due to their abundant applications, special surface properties by delocalized resonating electrons, lesser degradation rate and longer biological life. Moreover, considerable amounts of bioavailable ionic forms leached from metal/metal oxide nanoparticles have been reported increasing the probability of their contribution to nanoparticle toxicity (Franklin et al., 2007; Aruoja et al., 2009). Also, physical and chemical properties of water (e.g., pH, conductivity and organic matter) are expected to affect leaching and bioavailability of metal ions, as well as agglomeration/aggregation of nanoparticles, and, thus, a priority of the toxicological researchers is to examine such aspects to better predict the fate and behaviour of engineered metal nanoparticles in aqueous environments.

1.5. Physico-chemical properties of metal nanoparticles

The physico-chemical properties of metal/metal oxide nanoparticles are very important to understand their fate and behaviour in the environmental compartments. Nanoparticle toxicity to biota may also depend on the properties of nanomaterials. Nanoparticle chemistry, such as elemental composition and structure, can influence the biological activity (Navarro et al., 2008). Moreover, the size of metal/metal oxide nanoparticles is among the factors that influence toxicity. Often size is inversely related to the toxicity of metal nanoparticles by modification of surface properties. The uptake of nanometals can depend on the particle size; very small size nanometals can penetrate the blood-brain barrier, which in turn may cause neurotoxicity to mammals, including humans (Panyala et al., 2008). Lethal effects of bulk metal oxides were less severe than those promoted by nanometal oxides to the aquatic bacterium *Vibrio fischeri* and to the aquatic crustaceans *Daphnia magna* and *Thamnocephalus platyurus* (Heinlaan et al. 2008). In the microalgae *Pseudokirchneriella subcapitata* the lower toxicity of bulk CuO particles compared to nanoCuO particles was probably due to 141-folds higher bioavailability of nanoparticles (Aruoja et al., 2009). Also, the toxicity of TiO_2 nanoparticles to the freshwater green alga *P. subcapitata* was size dependent (Hartmann et al., 2010). The decreased toxicity of larger particles suggests self-aggregation of metal nanoparticles with the increase in size.

Nano metals/metal oxides may have different shapes, such as spheres, tubes, rods and wires (Pinna and Niederberger, 2008). Differences in the shape may

affect the dispersion, mobility and stability due to self-aggregation and biological sorption in aqueous conditions changing the biological activity/toxicity. For instance, the toxicity of CNTs can differ from that of spherical fullerene due to the variation in shapes. Similarly, inorganic metallic nanotubes have some special properties like semiconductivity (Mo and Kaxiras, 2007), which may not be found in spherical forms. Due to lower width, the penetration impacts of nanotubes on biological cells may be higher comparing to the nanospheres. The optical properties of metal-based nanoparticles are also influenced by shape and dielectric environment (Kelly et al., 2003).

The nanoparticle form can also influence their toxicity to living organisms. For example, TiO_2 nanoparticles occur in four different forms, but anatase and rutile are the naturally occurring crystals more used in the industry. Both size and crystal structure of TiO_2 nanoparticles determine toxicity but the mechanism of cell death depends on the crystal structure regardless of size (Braydich-Stolle et al. 2009). Moreover, anatase induced cell necrosis, while rutile induced apoptosis by generating reactive oxygen species (ROS).

The surface/volume ratio depends on the nanoparticle size; the ratio increases with the decrease in size and, thus, an increased number of atoms are free to be displayed in the surface instead of lining to each other in the inner core region of the metal lattice (Lowry and Wiesner, 2007). This increases the number of delocalized surface electrons, which are very active as they came from the displayed atoms of potentially active groups. Hence, the number of these surface active groups per unit mass increases with the decrease in nanoparticle size, and, therefore, the nanoparticles become very reactive. Also, the number of nanoparticles per unit mass increases with the decrease in size. Therefore, biological interactions with metal nanoparticles tend to increase with the increase in surface area. Indeed, the pulmonary inflammatory response against TiO_2 was higher when nanoparticles had higher surface area (Duffin et al., 2002).

The surface of metal nanoparticles may have electric charge when dispersed in aqueous environment depending on the particle nature, shape, size and the surrounding environment (Kelly et al., 2003). The surface charge and chemistry of metal nanoparticles may affect the mobility and dispersion of nanoparticles in aqueous environments. Engineered nanoparticles are often made with surface coatings for longer stabilization and dispersion to avoid aggregation. Generally, organic molecules containing hydrophilic and biocompatible terminal functional

groups, such as –OH, –COOH, –CN, and $–NH_2$, are used for the surface coating. For example, silver or gold nanoparticles may be stabilised with citrate. The surface charge and chemical composition may influence the surrounding ionic strength, and the cellular uptake or biosorption of chemicals with implications to toxicity.

Metal nanoparticles can release metal ions, which may be a key factor in their toxicity against living organisms (Kahru et al., 2008; Brunner et al., 2006). Metal ions have been found in the medium after exposure of *Saccharomyces cerevisiae* to nanoparticles of ZnO, CuO and TiO_2 (Kasemets et al., 2009). Part of the toxicity of metal/metal oxide nanoparticles against various aquatic organisms has also been explained by the presence of bioavailable metal ions leached from the nanoparticles (Heinlaan et al., 2008; Aruoja et al., 2009; Blinova et al., 2010). Also, the cytotoxicity of quantum dots, like CdSe, was partially explained by the liberation of free Cd^{2+} ions due to deterioration of CdSe lattice (Derfus et al., 2004).

Aggregation of metal-based nanoparticles is often observed and it depends on the size, surface charge, surface chemistry and several environmental factors; aggregation can occur during nanoparticle synthesis, storage and application (Hartmann et al., 2010). For example, high aggregation of nanoparticles was observed in seawater due to high salinity (Buffet et al., 2011). Aggregation of nanoparticles affects their stability and may result in sedimentation that, in turn, may compromise the toxicity of nanoparticles against living organisms (Gajjar et al., 2009).

1.6. Aquatic ecotoxicity: impacts of metal nanoparticles and mode of action

1.6.1. Lethal and sublethal effects

Aquatic ecotoxicity of nanoparticles to organisms can result in mortality (acute lethal effects) or in adverse structural or functional changes (sublethal effects). Lethality tests are of primary importance in ecotoxicological assays to determine the sensitivity, viability and acute stress responses of biota (Valenti et al., 2005). Acute toxicity induced by metal and metal oxide nanoparticles is reported in a wide range of aquatic organisms. Silver nanoparticles can induce toxicity to zebrafish embryos (LC_{50} at 72 h post-fertilization = 25-50 mg L^{-1}) (Asharani et al., 2008). In acute toxicity tests, the microalgae *P. subcapitata* was sensitive to several metal oxide nanoparticles and the order of toxicity based on EC_{50} (72 h) was

ZnO>CuO>TiO_2 (Aruoja et al., 2009). The increased bioavailability of metal ions with the decrease in particle size contributed to explain the toxicity level of each metal nanoparticle (Franklin et al., 2007; Aruoja et al., 2009; Heinlaan et al., 2008). Also, acute lethal effects of CuO and ZnO nanoparticles were reported against aquatic crustaceans and protozoa, and the toxicity was mainly attributed to solubilised ions (Blinova et al., 2010). However, leached ionic metals only explained part of nanotoxicity (Kasemets et al. 2009). Acute lethal toxicity of Ag and Cu nanoparticles against zebrafish, daphnids and algae was higher comparing to Ni, Al, Co and TiO_2 nanoparticles although the leached Ag and Cu ions had a minor role in toxicity (Griffitt et al., 2008). However, toxicity can also be caused by intracellular dissolution of nanoparticles; the oral toxicity of Cu nanoparticles to mice was a consequence of the high reactivity of Cu nanoparticles that led to metabolic alkalosis and intracellular accumulation of copper ions (Meng et al., 2007).

In bioassays, as those proposed by the EU Commission Guideline 93/67/EEC, it was shown that the majority of metal oxide nanoparticles causes acute toxicity against many aquatic organisms, such as bacteria, invertebrates and fishes (Blaise et al. 2008). However, the mode of toxicity of the tested nanoparticles may not be similar. Nanoparticles of TiO_2 under natural UV radiation were toxic to aquatic microbes by generation of ROS and cell membrane damage (Battin et al., 2009). The acute lethal toxicity of metal nanoparticles is generally higher for organisms from lower trophic levels (filter-feeding invertebrates) compared to higher trophic levels (fish) (Griffitt et al., 2008).

Although many acute toxicity tests for metal nanoparticles to aquatic organisms have been carried out, few studies are available on their sublethal effects. Sublethal effects of TiO_2 nanoparticles to *Arenicola marina* (lugworm) were observed with a significant decrease in the casting rate, increase in cellular and DNA damages in coelomocytes. Under these conditions, nanoparticle aggregates were observed in the lumen of the gut and outer epithelium of the worms (Galloway et al., 2010). Also, TiO_2 nanoparticles posed sublethal toxicity to the rainbow trout involving oxidative stress, organ pathologies, and the induction of antioxidant defences (Federici et al., 2007). Sublethal doses of CuO nanoparticles in seawater also caused impairment of burrowing and feeding behaviour in the marine invertebrate *Scrobicularia plana* (Buffet et al., 2011). Dietary exposure of rainbow trout (aged < 1 year) to TiO_2 nanoparticles (10 and 100 mg kg^{-1} for 8 weeks) caused changes in Cu and Zn ion levels in the brain, with biochemical alterations in the gills

and gut (Ramsden et al., 2009). Also, the chronic exposure to TiO_2 nanoparticles can result in bioaccumulation of nanoparticles that may interfere with the feeding and inhibit the growth and reproduction of daphnids (Zhu et al., 2010).

1.6.2. Responses at the community level

Knowledge on the structural and functional responses of aquatic organisms to various metal-based nanoparticles is required to predict the risks of these chemicals to aquatic ecosystems. There are only few studies that determined the impacts of nano size metals/metal oxides at the community level in aquatic environments. Toxicity of TiO_2 nanoparticles against planktonic and biofilm communities was reported under natural levels of UV radiation and low TiO_2 concentrations in surface waters (up to 5.3 mg L^{-1}) (Battin et al., 2009). The observed generation of intracellular ROS explained the TiO_2 nanoparticle-induced toxicity to cells of aquatic microbial communities (Battin et al., 2009). However, the exposure to low concentrations of Ag nanoparticles (up to 1000 µg L^{-1}) induced minor changes in genetic diversity of bacterial communities from estuarine sediments, as shown by the negligible differences in DGGE profiles (Bradford et al., 2009).

1.6.3. Responses at the individual level

Although some studies have been conducted to understand the individual response of organisms to nanoparticles, there are many gaps that should be addressed to have a complete picture. Individual response of zebrafish to Ag nanoparticles resulted in high acute mortality of embryos or larvae, and the embryos/larvae that survived showed various phenotypic deformities, including bent and twisted notochord, blood accumulation in the blood vessels near the tail, low heart rate, pericardial edema, distorted yolk sac and degeneration of body parts (Lee et al., 2007; Asharani et al., 2008). Nanoparticles of Ag and CuO have bactericidal effects against the beneficial soil microbe *Pseudomonas putida* KT2440, while ZnO nanoparticles showed bacteriostatic effect (Gajjar et al., 2009). Griffitt et al. (2008) reported high lethality for individuals of different trophic levels, such as algae, daphnids and fishes, under exposure to Ag and Cu nanoparticles, while nanoparticles of Ni, Cu, Al, Co and TiO_2 exhibited lower toxicity to organisms of higher trophic levels (zebrafish). ZnO and CuO nanoparticles caused mortality in the

aquatic ciliated protozoa *Tetrahymena thermophila*; however, the toxic effects of both nanoparticles to protozoa were caused by their solubilised fraction (Mortimer et al., 2010). The core–shell CuO nanoparticles induced cellular aggregation in *Chlamydomonas reinhardtii*, and inhibited the photosystem II and the electron transport in this green alga (Saison et al., 2010). Exposure to CeO_2 nanoparticles and two different sizes of SiO_2 nanoparticles induced lethal toxicity against *D. magna* and the larva of the aquatic midge *Chironomus riparius* (Lee et al., 2009). In a short-term toxicity study, tin dioxide nanoparticles were shown to penetrate into the blood of the fish *Poecilia reticulata* through the gills and intestine that might mobilize to various organs, but no acute toxic effects were found (Krysanov et al., 2009).

1.6.4. Responses at cellular and biochemical level

Toxicity of various metal and metal oxide nanoparticles (Ag, Fe_3O_4, Al, MoO_3 and TiO_2) in mammalian cells (rat liver derived cell line BRL 3A) has been associated with decreased functions of mitochondria and increased membrane permeability. A decrease in the mitochondrial membrane potential and a significant depletion of reduced glutathione (GSH) were observed in those cells after exposure to Ag nanoparticles (Hussain et al., 2005). Ag nanoparticles induced apoptosis or programmed cell death in zebrafish embryos (Asharani et al., 2008). The exposure of the fish *Japanese Medaka* to Ag nanoparticles led to high DNA damage and oxidative stress, induction and upregulation of genes related to metal detoxification, metabolic regulation and free radical scavenging activity (Chae et al., 2009). TiO_2 nanoparticles were reported to decrease the Na^+/K^+-ATPase activity in cells of gills and intestine, alteration of total glutathione levels in some organs (e.g. gills and liver) and minor changes in fatty acids of hepatocytes in the rainbow trout; but some of them had apoptotic bodies (Federici et al., 2007). Dietary exposure of rainbow trout to TiO_2 nanoparticles reduced by 50% the activity of brain Na^+/K^+-ATPase and the thiobarbituric acid reactive substances (TBARS) in the gill and intestine (Ramsden et al., 2009). Ti accumulation was detected in several fish organs (gills, gut, liver, brain and spleen) (Ramsden et al., 2009). Metal oxide nanoparticles induced oxidative stress biomarkers by increasing the activity of catalase, glutathione-S-transferase and superoxide dismutase and the levels of metallothionein-like proteins in marine invertebrates (Buffet et al., 2011).

Histological and biochemical analysis revealed that the gills of zebrafish could be the primary target for Cu nanoparticles (Griffitt et al., 2007). Cu nanoparticles decreased gill Na^+/K^+-ATPase activity up to 58% and the transcription of stress responsive genes in the gills: the exposure to 1.5 mg L^{-1} Cu nanoparticles increased the activity of hypoxia-inducible factor 1 (HIF-1, ~24 folds), heat-shock protein 70 (HSP-70, 14 folds) and copper transport regulatory protein (CTR, ~12 folds) (Griffitt et al., 2007). The exposure for 48 h to CuO nanoparticles led to ultrastructural changes in the midgut epithelium of daphnids, including protrusion of epithelial cells into the lumen, and to the presence of nanoparticles in circular structures, analogous to membrane vesicles from holocrine secretion (Heinlaan et al., 2011). Increased DNA damage has been observed in freshwater invertebrates after exposure to CeO_2 nanoparticles (Lee et al., 2009). Aqueous exposure of the freshwater mussel *Elliption complanata* to cadmium–telluride (CdTe) quantum dots (1.6 to 8 mg L^{-1}) led to high oxidative stress with lipid peroxidation, genotoxicity and DNA strand breaks in the digestive glands and gills, and to a decreased viability and activity of hemocytes, and 15% of CdTe was found in the dissolved phase (Gagné et al., 2008). Many studies have revealed an increase in the production of ROS in various biological tissues exposed to different metal-based nanoparticles (Hussain et al., 2005; Lin et al., 2006), which can be one of the key mechanisms of nanoparticle toxicity against organisms (Petersen and Nelson, 2010).

1.7. Fate of metal nanoparticles in aquatic environments

1.7.1. Stability, mobility and transformation

The properties and behaviour of metal nanoparticles in the environment are very similar to the natural colloids and, therefore, various physical and chemical factors can interfere with their fate and stability in natural waters, such as pH, composition, ionic strength, salinity, natural organic matter and dissolved organic carbon (Omelia, 1980; Lowry and Wiesner, 2007; Hartmann et al., 2010). Blinova et al. (2010) found that toxicity of CuO nanoparticles to crustaceans in natural waters was lower (up to 140-folds) than that found in artificial freshwaters probably due to differences in concentration of dissolved organic carbon. Natural organic matter, such as humic acid, is present in natural waters (Wall and Choppin, 2003; Steinberg et al., 2006) and can interfere with the stability or mobility of metal nanoparticles. Exposure to different sizes (10, 30 and 300 nm) of TiO_2 nanoparticles may alter the

toxicity of ionic metals; the 300 nm size nanoTiO_2 reduced the toxicity of Cd^{2+} to freshwater algae by decreasing Cd bioavailability due to its sorption/complexation to TiO_2 surface. However, the co-exposure to 30 nm TiO_2 nanoparticles and Cd^{2+} promoted a growth inhibition greater than that expected from effects of Cd^{2+} alone (Hartmann et al., 2010). This indicates that in addition to nanoparticle toxicity, potential interactions with existing environmental contaminants are also important to consider when assessing toxicity of nanoparticles (Hartmann et al., 2010). Salinity and substances excreted by organisms may also induce aggregation of nanoparticles and may interfere with their toxicity against aquatic organisms (Nielsen et al., 2008). The electrophoretic mobility, state of aggregation, and rate of sedimentation of different metal oxide nanoparticles (TiO_2, ZnO and CeO_2) in seawater, freshwaters, and groundwater were affected by the presence of natural organic matter (NOM) and ionic strength, but not by pH; NOM adsorbed to nanoparticles reduced aggregation and stabilized nanoparticles (Keller et al., 2010). Dissolved organic matter may adsorb to metal/metal oxide nanoparticles through surface charge interactions interfering with the aggregation state and changing their mobility in aqueous environments (Chen et al., 2006). The size and shape of nanoparticles influence their stability and mobility. Size and shape of metal nanoparticles may change with pH and fulvic acids, a component of NOM (dos Santos et al., 2005). Except for nanosilica, nanoparticles of TiO_2, Fe_2O_3, ZnO and NiO rapidly aggregated in tap water due to electric double layer compression; nanosilica remained stable in tap water due to electric double layer compression and its low Hamaker constant (Zhang et al., 2008). Highly dispersed and stable nanoparticles in surface waters have high mobility but the mobility of nanoparticles may decrease in porous media, such as ground water aquifers, where nanoparticles may attach to mineral surfaces or to highly surface active particles. Some water treatment plants use filters with active surfaces to retain nanoparticles. Depending on the intrinsic properties and environmental factors, the primary particles can agglomerate/aggregate to form bulk size in aqueous environment (Buffet et al., 2011) affecting stability and thus their mobility and transformation.The stability of nanoparticles can increase with steric hindrance/steric repulsion or electrostatic repulsive forces, and agglomeration may occur due to hydrophobicity of the particles as generally found for carbon-based nanoparticles in aqueous suspension. Surface coating can also promote the stability of those nanoparticles which have surface charge weaker than required for steric or electrostatic repulsive forces as generally

observed for nanotubes; surface coating overcomes the weaker attractive electrostatic forces or van der Waal forces. However, addition of salts may lead to agglomeration by interfering with the surface charge and chemical composition of nanoparticles; this can be one of the important factors for nanoparticle mobility and abiotic transformation in natural waters because they are rich in salts or cations. Agglomeration increases nanoparticle size up to few folds of the single nanoparticle, but they may not settle or deposit down in aqueous suspensions due to high buoyancy ability against gravity (Lowry and Wiesner, 2007). The abiotic transformation of nanoparticles may depend on the hydrodynamics of the surrounding environment based on the laws of thermodynamics. For instance, transformation of 3 nm ZnS nanoparticles having methanol surface occurred by structural modification and significantly reducing distortions of surface and interior core due to natural binding of water to the nanoparticles at room temperature (Zhang et al., 2003). Oxidation may also cause transformations of nanoparticles and may change the stability and mobility of nanoparticles in aqueous environment. For example, long exposure to oxygenated water may lead the oxidation of hydrophobic fullerenes or zero-valence metal nanoparticles to be more stable in water (Brant et al., 2005; Liu et al., 2005; Oberdörster et al., 2006). Due to the existence of a huge number of living organisms in aquatic ecosystems, it is expected that the manufactured nanoparticles that are likely to be released to the surface waters would interact with organisms. Therefore, biotransformation of nanoparticles can also occur although no sufficient knowledge on this is available.

1.7.2. Detection and characterization

The available data on the fate and behaviour of manufactured nanoparticles is limited mainly because efficient procedures to detect and characterize nanomaterials in aquatic environments are lacking. Therefore, detection and characterization of nanomaterials in environmental samples is a big challenge in nanoecotoxicology. Difficulties are found for complete characterization of physico-chemical properties and morphology of nanoparticles in natural waters and for distinguishing natural from engineered nanoparticles.

To determine and characterise the properties of nanoparticles, multiple approaches are used involving different methods and instruments: scanning or transmission electron microscopy (SEM or TEM) and atomic force microscopy (AFM) for determining particle diameter, surface area and aggregation state;

dynamic light scattering (DLS) for size distribution, dispersion and agglomeration in aqueous suspension without any sample distortion; zeta potential and electrophoretic mobility for determining surface charge; X-ray diffraction (XRD) to analyse crystal structure; the Brunauer, Emmett, Teller (BET) method (Brunauer et al., 1938) for measuring specific surface area of nanoparticles, inductively coupled plasma mass spectroscopy or optical emission spectrometry (ICP-MS or ICP-OES) and flame-atomic absorption spectroscopy (flame-AAS) for elemental composition analysis; SEM or TEM coupled with energy dispersive X-ray spectrometer (EDX/EDS) for determining chemical composition of nanoparticles, optical UV–visible or X-ray spectroscopy for determining optical property or surface chemistry; mass spectroscopy (MS) or infrared spectroscopy (IR) for determining carbon-based nanoparticles. Examples of methods to characterize nanoparticles can be found elsewhere (Lead et al., 2005; Hassellöv et al., 2008; Weinberg et al., 2011).

Nanoparticle characteristics also depend on sample handling because sampling inhomogeneity or agglomeration may occur. Complete and reliable detection and characterization of nanoparticles may require the development and combination of multiple advanced techniques and reduction of sampling errors. Currently, environmental scanning electron microscopy (ESEM) has been used for analysing nanoparticles in complex environmental samples including natural water samples (Hassellöv et al., 2008). Confocal laser scanning microscopy (CLSM) is also used for determining the colloidal distributions in the samples. Another powerful tool used in natural aquatic samples is the field-flow fractionation (FFF). The most commonly used is the flow-FFF, which can separate nanoparticles according to their size based on their diffusion coefficients in a very thin open channel (Stolpe et al., 2005; Hassellöv et al., 2008). The flow-FFF in combination with other advanced techniques might be a very good tool for detection and characterisation of metal nanoparticles in natural waters and their interactions with environmental factors, such as pH and the content in natural organic matter (Stolpe et al., 2005; Baalousha and Lead, 2007; Gibson et al., 2007; Weinberg et al., 2011; Zänker and Schierz, 2012).

1.8. Aquatic risk assessment framework for metal nanoparticles

1.8.1. Importance of risk assessment for nanotechnology: learning from past mistakes

The enhanced benefit of humans from the use of nanomaterials in daily life is leading to an increasing demand of manufactured nanoparticles, ultimately promoting higher production and wider applications of nanomaterials. A major concern about the increased used of manufactured or engineered nanoparticles is their behaviour in the environment and potential interactions with biota; this demands stringent environmental risk assessment. Most nanoparticles are not easily biodegradable, have long biological life (e.g., metal nanoparticles and some fullerenes) and exhibit cytotoxicity and ecotoxicity to a wide range of biota, thereby hampering the functioning of key ecosystem processes. We have already witnessed the environmental devastating results of the application of DDT and PCBs due to the lack of risk assessment studies despite the early warnings. Similarly to DDT or PCBs, some engineered nanoparticles, such as fullerenes, are lipophilic (Oberdörster, 2004; Oberdörster et al., 2006) and have low biodegradation rates resulting in their bioaccumulation. So, they may spread via biotransportation and biotransformation through the foodwebs in various ecosystems. In addition, the reported wide range of adverse biological impacts should be considered as potential warnings and we should focus on risk assessment studies. For that, a complete framework of environmental and human health risk assessment of manufactured nanoparticles are required, considering their interactions with the various interlinked ecosystems, the role of biota from different ecological niches, and the complex dynamics of the environmental compartments for complete understanding of their fate and behaviour in different environments.

1.8.2. Scientific organisations, guidelines and protocols

Due to the increasing data on potential negative effects of engineered nanoparticles to biota, several environmental health regulatory advisory committees all over the world are developing guidelines on the handling and environmental risk assessment of engineered nanoparticles. Most guidelines advise to consider the engineered nanoparticles as emergent materials with potential hazardous properties. The Environmental Protection Agency (EPA), created by the United

States for protecting human health and the environment, under the EPA Nanotechnology branch, developed during 2007-2012 a framework for quantifying nanoparticles in the environment and understanding whether engineered nanoparticles with great potential to be released into the environment and/or trigger a hazard concern, pose significant risks to human health or ecosystems, considering their life cycles (Neumann, 2010). They recommended that further research should focus on environmental detection, fate and behaviour (mobility, transformation, exposure pathways) of engineered nanoparticles, and necessary developments for assessing their biological toxicity. EPA is working with other international agencies, including the Organization of Economic Cooperation and Development's (OECD), to fulfil the goal of developing a safer nanotechnology-based world. The OECD Chemicals Committee has a significant role in the regulatory health and safety by testing various commercially emerging chemicals and by developing standard protocols/guidelines (OECD, 2010). To deal with the emerging manufactured nanoparticles, the OECD Working Party on Manufactured Nanomaterials (WPMN) has been establishing science-based and internationally harmonised standard approaches to ensure the efficient risk assessment of nanomaterials, to avoid adverse effects from the use of these materials at short and longer term (OECD, 2010). The OECD Sponsorship Programme of Testing a Representative Set of Manufactured Nanomaterials was established to develop dossiers of the engineered nanoparticles, including detection, identification and intrinsic physicochemical properties of nanoparticles for determining the proper risk assessment strategies (OECD, 2010). Based on the outcome of a number of risk assessment studies, projects and publications, a test guideline was developed by OECD, the 'Guidance Manual for the Testing of Manufactured Nanomaterials' (OECD, 2010), to provide guidance to ensure scientifically comparable risk assessment among the contributing partners. The guideline also provided important information and suggestions regarding the advanced methods for characterization, development and standardization of biological and environmental toxicity tests with endpoints considering the organisms from different ecological niches to determine and understand the environmental fate and behaviour of engineered nanoparticles. Due to significant increases in the commercial production and use of nanomaterials, OECD has already listed nanomaterials based on their potential frequencies of commercialization seeking for risk assessment (OECD, 2010). According to the EC (European Commission, 2011) a nanomaterial should consist of 50% or more

particles having one or more dimensions in the size range of 1–100 nm or when the volume specific surface area of the material is > 60 m^2 cm^{-3} (Rauscher et al., 2012). The Registration, Evaluation, Authorisation and Restriction of Chemicals (REACH) is a European Union regulation addressing the production and use of chemical substances and their potential impacts on human health and environment. Recently, the European Chemicals Agency (ECHA) launched a number of guidelines on how to address nanomaterials in REACH registration dossiers (Rauscher et al., 2012). These guidelines are expected to be benefited from the recent definition of nanomaterials suggested by EC for further developing and designing the framework on human and environmental risk assessment of manufactured nanoparticles.

1.8.3. Practical problems, needs of improvement and future challenges

Although the produced guidelines and the development of scientific contributions for handling and assessing the human and environmental risks of engineered nanoparticles, knowledge on their environmental fate and behaviour is still limited. There is a huge discrepancy between the experimental approach proposed in the guidelines and the approaches followed by researchers. For example, there is a tendency among ecotoxicologists to use relatively short-term experiments with easily controlled biological model organisms. Most of the available guidelines do not provide suggestions on how to test impacts at the community level to better assess effects on ecologically complex inter-trophic relationships at long term. Indeed, just measuring toxicity of nanoparticles to individuals may not reveal the actual potential risk against humans or other organisms from different trophic levels; individual responses may differ from community responses because individuals from different species can respond in different ways.

Although most guidelines have mentioned that nanoparticles not included in the OECD list can be important in the future, most assessments have focused only on the nanoparticles enlisted in OECD. Indeed, impacts of accidental or flash exposure to unlisted nanoparticles should not be ignored, as shown by the recent accidental oil spill in the Gulf of Mexico (2010) that greatly affected marine life and the associated ecosystems. Due to a wide range of reported toxicity of engineered nanomaterials, care should be taken until nanomaterials are proved to be safe for humans and environment. Actions should also be taken at the consumer level because potentially hazardous nanoparticles are already in use. For that, awareness

of consumers is needed, which can only be possible by the combined support of governmental and non-governmental organisations.

Detailed studies on the detection, characterization, mobility, transformation, and toxicity, with clarification of the underlying mechanisms, at different trophic levels are needed, together with the knowledge on clearance of engineered nanoparticles in the environment. This will help to develop regulatory frameworks for a safer and cleaner environment, by controlling exposure levels (e.g., limiting the production and reducing the bioactivity) and or using biocompatible and environmentally friendly nanoparticles.

1.9. Objectives and outline of the thesis

Owing to the rapid growth of nanotechnology-based industries enormous amounts of nanomaterials are being manufactured and utilized since the past decade (Aitken et al., 2006). This will certainly lead to an increased released of nanomaterials to the environment, and natural surface waters are likely to serve as the ultimate sink of nanomaterials. In forested streams, microbes, predominantly aquatic fungi, decompose plant material from riparian vegetation and mediate carbon and energy transfer to invertebrate shredders (Graça 2001; Pascoal and Cássio, 2004). Freshwater decomposers are sensitive to changes in water quality with implications to ecosystem functioning (Pascoal et al., 2001, 2005; Fernandes et al., 2009). In this study, the potential impacts of nanoparticles on plant litter decomposition and associated biota, namely fungi, bacteria and invertebrates were assessed. In addition, effects of nanoparticles were also tested on the ubiquitous yeast *Saccharomyces cerevisiae*, which is a well-known eukaryotic model. Responses to nanoparticle exposure were assessed at different levels of biological organization: from community, to individual and cellular levels. Nanoparticle size, potential for aggregation and interactions with plant litter and biota were analysed to better understand effects of nanoparticles under experimental conditions.

Chapter 1 provides the current knowledge on a wide range of human-beneficial applications of nanoparticles as well as their potential toxicological risks. Specific characteristics, detection techniques and sources of nanoparticle contamination in aquatic environments are also considered.

In Chapter 2, we used a microcosm approach to test the effects of copper oxide nanoparticles (nanoCuO) and nanosilver, and their ionic precursors, on leaf litter decomposition by stream-dwelling microbial communities. The measured endpoints were leaf mass loss, fungal and bacterial biomass, and fungal reproduction and diversity. In Chapter 3, we examined the interactive effects of nanoparticle size (12, 50 and 80 nm) and of increasing concentrations of humic acid on the toxicity of nanoCuO against microbial decomposers of plant litter.

In Chapter 4, we showed lethal and sublethal impacts of CuO nanoparticles on *Allogamus ligonifer*, a common invertebrate shredder in Southwest European streams that prefers high quality stream water. We expected that nanoparticles would affect the feeding behaviour and the growth of the invertebrate due to both nanoCuO and ionic copper leached from nanoCuO. In Chapter 5, we assessed how nanoparticle size and the presence of humic acids affect the toxicity of nanoCuO to the invertebrate shredder *A. ligonifer*. A post-exposure feeding experiment was also conducted to examine the ability of the animal to recover after stress removal.

In Chapter 6, we investigated the physiological impacts of nanoCuO in four aquatic fungal populations with different background under the hypothesis that fungal populations collected from metal-polluted streams would be more tolerant/resistant to the stress induced by nanoCuO than those from non-polluted streams. Effects were assessed on fungal growth, morphology of fungal mycelium and on the activity of extracellular laccases. In Chapter 7, we examined the effects of CuO nanoparticles on cellular targets and antioxidant defences in five aquatic fungi collected from metal-polluted or non-polluted streams, under the hypotheses that nanoCuO might induce oxidative stress in aquatic fungi, and that fungal isolates from metal-polluted streams would be able to cope better with the stress induced by nanoCuO. The measured endpoints were: intracellular accumulation of ROS, plasma membrane integrity, DNA strand breaks, induction of intracellular protein and activities of glutathione reductase, glutathione peroxidase and superoxide dismutase.

In Chapter 8, we examined the effects of cadmium ions and carbon-based nanoparticles, namely polyhydroxy fullerene (PHF), alone or in mixtures on cells of *S. cerevisiae* under the hypothesis that oxidative stress induced by cadmium might be mitigated by PHF nanoparticles due to its antioxidant and free-radical scavenging properties.

Finally, in Chapter 9, the major outcomes are integrated to provide an overall perspective of results and to point possible lines of future research.

References

Agasti SS, Chompoosor A, You CC, Ghosh P, Kim CK, Rotello, VM, 2009. Photoregulated release of caged anticancer drugs from gold nanoparticles. J Am Chem Soc 131, 5728–5729.

Aitken RJ, Chaudhry MQ, Boxall ABA, Hull M, 2006. Manufacture and use of nanomaterials: current status in the UK and global trends. Occup Med 56, 300–306.

Allard T, Menguy N, Salomon J, Calligaro T, Weber T, Calas G, Benedetti MF, 2004. Revealing forms of iron in river-borne material from major tropical rivers of the Amazon Basin (Brazil). Geochim. Cosmochim Acta 68, 3079–3094.

Aruoja V, Dubourguier HC, Kasemets K, Kahru A, 2009. Toxicity of nanoparticles of CuO, ZnO and TiO_2 to microalgae *Pseudokirchneriella subcapitata*. Sci Total Environ 407, 1461–1468.

Asharani PV, Wu LY, Gong Z, Valiyaveettil S, 2008. Toxicity of silver nanoparticles in zebrafish models. Nanotechnology 19, 255102 (8 pp.).

Baalousha M, Lead JR, 2007. Characterization of natural aquatic colloids (<5 nm) by flow-field flow fractionation and atomic force microscopy. Environ Sci Technol, 41, 1111–1117.

Bandaru PR, 2007. Electrical properties and applications of carbon nanotube structures. J Nanosci Nanotechnol, 7, 1–29.

Battin TJ, Kammer FVD, Weilhartner A, Ottofuelling S, Hofmann T, 2009. Nanostructured TiO_2: transport behavior and effects on aquatic microbial communities under environmental conditions. Environ Sci Technol 43, 8098–8104.

Becheri A, Dürr M, Nostro PL, Baglioni P, 2008. Synthesis and characterization of zinc oxide nanoparticles: application to textiles as UV-absorbers. J Nanopart Res 10, 679–689.

Blaise C, Gagné F, Férard J, Eullaffroy P, 2008. Ecotoxicity of selected nano-materials to aquatic organisms. Environ Toxicol 23, 591–598.

Blaser SA, Scheringer M, MacLeod M, Hungerbühler K, 2008. Estimation of cumulative aquatic exposure and risk due to silver: Contribution of nano-functionalized plastics and textiles. Sci Total Environ 390, 396–409.

Blinova I, Ivask A, Heinlaan M, Mortimer M, Kahru A, 2010. Ecotoxicity of nanoparticles of CuO and ZnO in natural water. Environ Pollut 158, 41–47.

Bosi S, Ros TD, Spalluto G, Prato M, 2003. Fullerene derivatives: an attractive tool for biological applications. Eur J Med Chem 38, 913–923.

Bradford A, Handy RD, Redman JW, Atfield A, Mühling M, 2009. Impact of silver nanoparticle contamination on the genetic diversity of natural bacterial assemblages in estuarine sediments. Environ Sci Technol 43, 4530–4536.

Brant J, Lecoanet H, Wiesner MR, 2005. Aggregation and deposition characteristics of fullerene nanoparticles in aqueous systems. J Nanoparticle Res 7, 545–553.

Brunauer S, Emmet PH, Teller E, 1938. Adsoprtion of gases in multimolecular layers. J Am Chem Soc 60, 309–319.

Braydich-Stolle LK, Schaeublin NM, Murdock RC, Jiang J, Biswas P, Schlager JJ, Hussain AM, 2009. Crystal structure mediates mode of cell death in TiO_2. J Nanopart Res 11, 1361–1374.

Brunet L, Lyon DY, Hotze EM, Alvarez PJ, Wiesner MR, 2009. Comparative photoactivity and antibacterial properties of C_{60} fullerenes and titanium dioxide nanoparticles. Environ Sci Technol 4355–4360.

Brunner TJ, Wick P, Manser P, Spohn P, Grass RN, Limbach LK, Bruinink A, Stark WJ, 2006. In vitro cytotoxicity of oxide nanoparticles: comparison to asbestos, silica, and the effect of particle solubility. Environ Sci Technol 40, 4374–4381.

Buffet PE, Tankoua OF, Pan J-F, Berhanu D, Herrenknecht C, Poirier L, Amiard-Triquet C, Amiard JC, Bérard JB, Risso C, Guibbolini M, Roméo M, Reip P, Valsami-Jones E, Mouneyrac C, 2011. Behavioural and biochemical responses of two marine invertebrates *Scrobicularia plana* and *Hediste diversicolor* to copper oxide nanoparticles. Chemosphere 84, 166 – 174.

Burda C, Chen X, Narayanan R, El-Sayed MA, 2005. Chemistry and properties of nanocrystals of different shapes. Chem Rev 105, 1025–1102.

Buzea C, Blandino IIP, Robbie K, 2007. Nanomaterials and nanoparticles: sources and toxicity. Biointerphases 2, MR17–MR172.

Cattaneo AG, Gornati R, Chiriva-Internati M, Bernardini G, 2009. Ecotoxicology of nanomaterials: the role of invertebrate testing. Invertebrate Surviv J 6, 78–97.

Chae YJ, Pham CH, Lee J, Bae E, Yi J, Gu MB, 2009. Evaluation of the toxic impact of silver nanoparticles on Japanese medaka (*Oryzias latipes*). Aquat Toxicol 94, 320–327.

Chen YW, Hwang KC, Yen CC, Lai YL, 2004. Fullerene derivatives protect against oxidative stress in RAW 264.7 cells and ischemia-reperfused lungs. Am J Physiol Regul Integr Comp Physiol 287, R21–R26.

Chen KL, Mylon SE, Elimelech M, 2006. Aggregation kinetics of alginate-coated hematite nanoparticles in monovalent and divalent electrolytes. Environ Sci Technol 40, 1516–1523.

Colvin VL, 2003. The potential environmental impact of engineered nanomaterials. Nat Biotechnol 21, 1166–1170.

d'Almeida GA, Schütz L, 1983. Number, mass and volume distributions of mineral aerosol and soil of the Sahara. J Appl Meteorol 22, 233–243.

Derfus AM, Chan WC, Bhatia SN, 2004. Probing the cytotoxicity of semiconductor quantum dots. Nano Lett 4, 11–18.

dos Santos DSJr, Alvarez-Puebla RA, Oliveira ONJr, Aroca RF, 2005. Controlling the size and shape of gold nanoparticles in fulvic acid colloidal solutions and their optical characterization using SERS. J Mater Chem 15, 3045–3049.

Duffin R, Tran CL, Clouter A, Brown DM, MacNee W, Stone V, Donaldson K, 2002. The importance of surface area and specific reactivity in the acute pulmonary inflammatory response to particles. Ann Occup Hyg 46, 242–245.

Dugan LL, Gabrielsen JK, Yu SP, Lin TS, Choi DW, 1996. Buckminsterfullerenol free radical scavengers reduce excitotoxic and apoptotic death of cultured cortical neurons. Neurobiol Dis 3, 129–135.

Durán N, Marcato PD, Alves OL, Souza GIHD, Esposito E, 2005. Mechanistic aspects of biosynthesis of silver nanoparticles by several *Fusarium oxysporum* strains. J Nanobiotechnology 3 (7 pp.).

Drexler KE (foreword by Minsky, M.), 1986. Engines of Creation: The Coming Era of Nanotechnology. http://www.physics.utu.fi/projects/kurssit/UFYS3084/Engines%20of%20Creation.pdf

ECB, 2003. Technical guidance document on risk assessment, part 2. in support of Commission Directive 93/67/EEC on Risk Assessment for new notified substances, Commission Regulation (EC) No 1488/94 on Risk Assessment for existing substances and Directive 98/8/EC of the European Parliament and of the Council concerning the placing of biocidal products on the market. European Commission Joint Research Centre, European Communities.

Elechiguerra JL, Burt JL, Morones JR, Camacho-Bragado A, Gao X, Lara HH, Yacaman MJ, 2005. Interaction of silver nanoparticles with HIV-1. J Nanobiotechnology 3, (10 pp.).

Endo M, Hayashi T, Kim YA, Terrones M, Dresselhaus MS, 2004. Applications of carbon nanotubes in the twenty-first century. Phil Trans R Soc Lond A 362, 2223–2238.

European Commission, 2011. Commission Recommendation of 18 October 2011 on the definition of nanomaterial. Official Journal of the European Union. L 275, 38–40.

Fabrega J, Luoma SN, Tyler CR, Galloway TS, Lead JR, 2011. Silver nanoparticles: behaviour and effects in the aquatic environment. Environ Int 37, 517–531.

Faraday M, 1857. The Bakerian lecture: experimental relations of gold (and other metals) to light. Phil Trans R Soc Lond 147, 145–181.

Federici G, Shaw BJ, Handy RD, 2007. Toxicity of titanium dioxide nanoparticles to rainbow trout (*Oncorhynchus mykiss*): Gill injury, oxidative stress, and other physiological effects. Aquat Toxicol 84, 415–430.

Fernandes I, Uzun B, Pascoal C, Cássio F, 2009. Responses of aquatic fungal communities on leaf litter to temperature-change events. Internat Rev Hydrobiol 94, 410–418.

Fisher C, Rider AE, Han ZJ, Kumar S, Levchenko I, Ostrikov KK, 2012. Applications and nanotoxicity of carbon nanotubes and graphene in biomedicine. J Nanomater 2012 (19 pp.).

Franklin NM, Rogers NJ, Apte SC, Batley GE, Gadd GE, Casey PS, 2007. Comparative toxicity of nanoparticulate ZnO, bulk ZnO, and $ZnCl_2$ to a freshwater microalga (*Pseudokirchneriella subcapitata*): the importance of particle solubility. Environ Sci Technol 41, 8484–8490.

Friedman SH, DeCamp DL, Sijbesma RP, Srdanov G, Wudl F, Kenyon GL, 1993. Inhibition of the HIV-1 protease by fullerene derivatives: model building studies and experimental verification. J Am Chem SOC 115, 6506–6509.

Gagné F, Auclair J, Turcotte P, Fournier M, Gagnon C, Sauvé S, Blaise C, 2008. Ecotoxicity of CdTe quantum dots to freshwater mussels: impacts on immune system, oxidative stress and genotoxicity, Aquat Toxicol 86, 333–340.

Gajjar P, Pettee B, Britt DW, Huang W, Johnson WP, Anderson AJ, 2009. Antimicrobial activities of commercial nanoparticles against an environmental soil microbe, *Pseudomonas putida* KT2440. J Biol Eng 3, pp 13, doi:10.1186/1754-1611-3-9.

Galloway T, Lewis C, Dolciotti I, Johnston BD, Moger J, Regoli F, 2010. Sublethal toxicity of nano-titanium dioxide and carbon nanotubes in a sediment dwelling marine polychaete. Environ Pollut 158, 1748–1755.

Gao J, Wang Y, Folta KM, Krishna V, Bai W, Indeglia P, Georgieva A, Nakamura H, Koopman B, Moudgil B, 2011. Polyhydroxy fullerenes (fullerols or fullerenols): beneficial effects on growth and lifespan in diverse biological models. PLoS One 6, e19976, pp 8.

Gibson CT, Turner IJ, Roberts CJ, Lead JR, 2007. Quantifying the dimensions of nanoscale organic surface layers in natural waters. Environ Sci Technol 41, 1339–1344.

Gottschalk F, Sonderer T, Scholz RW, Nowack B, 2009. Modeled environmental concentrations of engineered nanomaterials (TiO2, ZnO, Ag, CNT, fullerenes) for different regions. Environ Sci Technol 43, 9216–9222.

Graça MAS, 2001. The role of invertebrates on leaf litter decomposition in streams – a Review. Int Rev Hydrobiol 86, 383–393.

Gribbin J, Gribbin M, 1997. Richard Feynman: A Life in Science. Dutton pp. 170.

Griffitt RJ, Luo J, Bonzongo JC, Barber DS, 2008. Effects of particle composition and species on toxicity of metallic nanomaterials in aquatic organisms. Environ Toxicol Chem 27, 1972–1978.

Griffitt RJ, Weil R, Hyndman KA, Denslow ND, Powers K, Taylor D, Barber DS, 2007. Exposure to copper nanoparticles causes gill injury and acute lethality in zebrafish (*Danio rerio*). Environ Sci Technol 41, 8178–8186.

Han R, Hirose T, Shimamoto T, Lee Y, Ando J, 2011. Granular nanoparticles lubricate faults during seismic slip. Geology 39, 599–602.

Hartmann NB, Kammer FVD, Hofmann T, Baalousha M, Ottofuelling S, Baun A, 2010. Algal testing of titanium dioxide nanoparticles--testing considerations, inhibitory effects and modification of cadmium bioavailability. Toxicology 269, 190–197.

Hassellöv M, Readman JW, Ranville JF, Tiede K, 2008. Nanoparticle analysis and characterization methodologies in environmental risk assessment of engineered nanoparticles. Ecotoxicology 17, 344–361.

He S, Guo Z, Zhang Y, Zhang S, Wang J, Gu N, 2007. Biosynthesis of gold nanoparticles using the bacteria *Rhodopseudomonas capsulata*. Mater Lett 61, 3984–3987.

Heinlaan M, Ivask A, Blinova I, Dubourguier HC, Kahru A, 2008. Toxicity of nanosized and bulk ZnO, CuO and TiO_2 to bacteria *Vibrio fischeri* and crustaceans *Daphnia magna* and *Thamnocephalus platyurus*. Chemosphere 71, 1308–1316.

Heinlaan M, Kahru A, Kasemets K, Arbeille B, Prensier G, 2011. Changes in the *Daphnia magna* midgut upon ingestion of copper oxide nanoparticles: A transmission electron microscopy study. Water Res 45, 179–190.

Heymann D, Jenneskens LW, Jehlička J, Koper C, Vlietstra E, 2003. Terrestrial and Extraterrestrial Fullerenes. Fuller Nanotub Car N 11, 333–370.

Hochmannova L, Vytrasova J, 2010. Photocatalytic and antimicrobial effects of interior paints. Prog Org Coat 67, 1–5.

Hsiao MC, Wang HP, Yang YW, 2001. EXAFS and XANES studies of copper in a solidified fly ash. Environ Sci Technol 35, 2532–2535.

Huang HL, Wang HP, Wei GT, Sun IW, Huang JF, Yang YW, 2006. Extraction of nanosize copper pollutants with an ionic liquid. Environ Sci Technol 40, 4761–4764.

Hussain SM, Hess KL, Gearhart JM, Geiss KT, Schlager JJ, 2005. In vitro toxicity of nanoparticles in BRL 3A rat liver cells. Toxicol in Vitro 19, 975–983.

Igan M, 2005. Earths forbidden history: part one, searching for the past, pp. 36, The Crowhouse (http://www.thecrowhouse.com/projects.html).

Injac R, Perse M, Obermajer N, Djordjevic-Milic V, Prijatelj M, Djordjevic A, Cerar A, Strukelj B, 2008b. Potential hepatoprotective effects of fullerenol $C_{60}(OH)_{24}$ in doxorubicin-induced hepatotoxicity in rats with mammary carcinomas. Biomaterials 29, 3451–3460.

Injac R, Radic N, Govedarica B, Djordjevic A, Strukelj B, 2008a. Bioapplication and activity of fullerenol $C_{60}(OH)_{24}$. Afr J Biotechnol 7, 4940–4050.

Jamieson T, Bakhshi R, Petrova D, Pocock R, Imanib M, Seifalian AM, 2007. Biological applications of quantum dots. Biomaterials 28, 4717–4732.

Jin S, Ye K, 2007. Nanoparticle-mediated drug delivery and gene therapy. Biotechnol Prog 23, 32–41.

Jin S, Hu Y, Gu Z, Liu L, Wu HC, 2011. Application of quantum dots in biological imaging. J Nanomater 2011 (13 pp.).

José-Yacamán M, Rendon L, Arenas J, Serra Puche MC, 1996. Maya blue paint: An ancient nanostructured material. Science 273, 223–225.

Kaegi R, Ulrich A, Sinnet B, Vonbank R, Wichser A, Zuleeg S, Simmler H, Brunner S, Vonmont H, Burkhardt M, Boller M, 2008. Synthetic TiO_2 nanoparticle emission from exterior facades into the aquatic environment. Environ Pollut 156, 233–239.

Kahru A, Dubourguier HC, Blinova I, Ivask A, Kasemets K, 2008. biotests and biosensors for ecotoxicology of metal oxide nanoparticles: A minireview. Sensors 8, 5153–5170.

Karlsson HL, Gustafsson J, Cronholm P, Möller L, 2009. Size-dependent toxicity of metal oxide particles–A comparison between nano- and micrometer size. Toxicol Lett 188, 112–118.

Kasemets K, Ivask A, Dubourguier HC, Kahru A, 2009. Toxicity of nanoparticles of ZnO, CuO and TiO_2 to yeast *Saccharomyces cerevisiae*. Toxicol in Vitro 23, 1116–1122.

Kathirvelu S, D'Souza L, Dhurai B, 2009. UV protection finishing of textiles using ZnO nanoparticles. Indian J Fibre Text 34, 267–273.

Keller AA, Wang H, Zhou D, Lenihan HS, Cherr G, Cardinale BJ, Miller R, Ji Z, 2010. Stability and aggregation of metal oxide nanoparticles in natural aqueous matrices. Environ Sci Technol 44, 1962–1967.

Kelly KL, Coronado E, Zhao LL, Schatz GC, 2003. The optical properties of metal nanoparticles: the influence of size, shape, and dielectric environment. J Phys Chem B 107, 668–677.

Kim JS, Kuk E, Yu KN, Kim JH, Park SJ, Lee HJ, Kim SH, Park YK, Park YH, Hwang CY, Kim YK, Lee YS, Jeong DH, Cho MH, 2007. Antimicrobial effects of silver nanoparticles. Nanomedicine 3, 95–101.

Kim B, Park CS, Murayama M, Hochella MF, 2010. Discovery and characterization of silver sulfide nanoparticles in final sewage sludge products. Environ Sci Technol 44, 7509–7514.

Kong L, Tedrow O, Chan YF, Zepp RG, 2009. Light-initiated transformations of fullerenol in aqueous media. Environ Sci Technol 43, 9155–9160.

Krishna V, Singh A, Sharma P, Iwakuma N, Wang Q, Zhang Q, Knapik J, Jiang H, Grobmyer SR, Koopman B, Moudgil B, 2010. Polyhydroxy fullerenes for non-invasive cancer imaging and therapy. Small 6, 2236–2241.

Krysanov EYu, Demidova TB, Pel'gunova LA, Badalyan SM, Rumyantsevab MN, Gas'kov AM, 2009. Effect of Hydrated Tin Dioxide ($SnO_2.xH_2O$) Nanoparticles on Guppy (*Poecilia reticulate* Peters, 1860), Dokl Biol Sci 426, 288–289.

Kumar A, Vemula PK, Ajayan PM, John G, 2008. Silver-nanoparticle-embedded antimicrobial paints based on vegetable oil. Nat Mater 7, 236–241.

Lai HS, Chen WJ, Chiang LY, 2000. Free radical scavenging activity of fullerenol on the ischemia-reperfusion intestine in dogs. World J Surg 24, 450–454.

Lau BLT, 2011. Understanding how nanoparticles behave in natural and engineered waters. J Am Water Works Assoc 103, 20–22.

Lead JR, Muirhead D, Gibson CT, 2005. Characterization of freshwater natural aquatic colloids by atomic force microscopy (AFM). Environ Sci Technol 39, 6930–6936.

Lee KJ, Nallathamby PD, Browning LM, Osgood CJ, Xu XHN, 2007. In Vivo Imaging of Transport and Biocompatibility of Single Silver Nanoparticles in Early Development of Zebrafish Embryos. ACS Nano 1, 133–143.

Lee SW, Kim SM, Choi J, 2009. Genotoxicity and ecotoxicity assays using the freshwater crustacean *Daphnia magna* and the larva of the aquatic midge *Chironomus riparius* to screen the ecological risks of nanoparticle exposure. Environ Toxicol Pharmacol 28, 86–91.

Lin W, Huang YW, Zhou XD, Ma Y, 2006. Toxicity of cerium oxide nanoparticles in human lung cancer cells. Int J Toxicol 25, 451–457.

Lin D, Xing B, 2007. Phytotoxicity of nanoparticles: Inhibition of seed germination and root growth. Environ Pollut 150, 243–250.

Liu YQ, Majetich SA, Tilton RD, Sholl DS, Lowry GV, 2005. TCE dechlorination rates, pathways, and efficiency of nanoscale iron particles with different properties. Environ Sci Technol 39, 1338–1345.

Lowry GV, Wiesner MR, 2007. Environmental considerations: occurrences, fate, and characterization of nanoparticles in the environment. In Nanotoxicology: characterization, dosing and health effects (ed: Monteiro-Riviere, N.A., Tran, C.L.), Informa Healthcare USA, Inc., NY, 369–389.

Luechinger NA, Athanassiou EK, Stark WJ, 2008. Graphene-stabilized copper nanoparticles as an air-stable substitute for silver and gold in low-cost ink-jet printable electronics. Nanotechnology 19:445201 (6 pp.)

Matthews L, Kanwar RK, Zhou S, Punj V, Kanwar JR., 2010. Applications of nanomedicine in antibacterial medical therapeutics and diagnostics. Open Trop Med J 3, 1–9.

Meng H, Chen Z, Xing G, Yuan H, Chen C, Zhao F, Zhang C, Zhao Y, 2007. Ultrahigh reactivity provokes nanotoxicity: Explanation of oral toxicity of nanocopper particles. Toxicol Lett 175, 102–110.

Minaeian S, Shahverdi AR, Nohi AS, Shahverdi HR, 2008. Extracellular biosynthesis of silver nanoparticles by some bacteria. J Sci I A U (JSIAU) 17 (4 pp.).

Mo Y, Kaxiras E, 2007. Semiconducting cyanide–transition-metal nanotubes. Small 3, 1253–1258.

Mortimer M, Kasemets K, Kahru A, 2010. Toxicity of ZnO and CuO nanoparticles to ciliated protozoa *Tetrahymena thermophila*. Toxicology 269, 182–189.

Mueller NC, Nowack B, 2008. Exposure modeling of engineered nanoparticles in the environment. Environ Sci Technol 42, 4447–4453.

Navarro E, Baun A, Behra R, Hartmann NB, Filser J, Miao AJ, Quigg A, Santschi PH, Sigg L, 2008. Environmental behavior and ecotoxicity of engineered nanoparticles to algae, plants, and fungi. Ecotoxicology 17, 372–386.

Nel A, Xia T, Mädler L, Li N, 2006. Toxic potential of materials at the nanolevel. Science 311, 622–627.

Neumann RV, 2010. EPA's nanotechnology research framework (U.S. Environmental Protection Agency). In nanotechnology and the environment (ed. Neumann , R.V.). Nova Science Publishers, Inc. NY, pp. 113–114.

Nielsen HD, Berry LS, Stone V, Burridge TR, Fernandes TF, 2008. Interactions between carbon black nanoparticles and the brown algae *Fucus serratus*: Inhibition of fertilization and zygotic development. Nanotoxicology 2, 88–97.

Northover P, 2008. Metallographic analysis. In encyclopedia of archaeology, vol. 2, Pearsall, D.M. (editor in chief), Elsevier, Oxford, pp. 1608–1613.

Nowack B, 2008. Pollution prevention and treatment using nanotechnology. In: Nanotechnology (ed. Krug, H.). Wiley-VCS Verlag GmbH & Co, Weinheim, pp. 1–15.

Nowack B, Bucheli TD, 2007. Occurrence, behavior and effects of nanoparticles in the environment. Environ Pollut, 150, 5–22.

Oberdörster, E., 2004. Manufactured nanomaterials (fullerenes, C_{60}) induce oxidative stress in the brain of juvenile largemouth bass. Environ. Health. Perspect., 112, 1058–1062.

Oberdörster E, Zhu S, Blickley TM, McClellan-Green P, Haasch ML, 2006. Ecotoxicology of carbon-based engineered nanoparticles: effects of fullerene (C_{60}) on aquatic organisms. Carbon 44, 1112–1120.

OECD, 2010. Guidance manual for the testing of manufactured nanomaterials: OECD's sponsorship programme, ENV/JM/MONO(2009)20REV; OECD environment, health and safety publications, series on the safety of manufactured nanomaterials No. 25; Organisation for economic co-operation and development: Paris.

Omelia CR, 1980. Aquasols – the behavior of small particles in aquatic systems. Environ Sci Technol 14, 1052–1060.

Panyala NR, Peña-Méndez EM, Havel J, 2008. Silver or silver nanoparticles: a hazardous threat to the environment and human health? J Appl Biomed 6, 117–119.

Park B, 2007. Current and future applications of nanotechnology. In nanotechnology: consequences for human health and the environment (Hester, R.E., Harrison, R.M.), R Soc Chem, pp. 1.

Pascoal C, Cássio F, Gomes P, 2001. Leaf breakdown rates: a measure of water quality? Int Rev Hydrobiol 86, 407–416.

Pascoal C, Cássio F, 2004. Contribution of fungi and bacteria to leaf litter decomposition in a polluted river. Appl Environ Microbiol 70, 5266–5273.

Pascoal C, Cássio F, Marvanová L, 2005. Anthropogenic stress may affect aquatic hyphomycete diversity more than leaf decomposition in a low-order stream. Arch Hydrobiol 162, 481-496.

Petersen EJ, Nelson BC, 2010. Mechanisms and measurements of nanomaterial-induced oxidative damage to DNA. Anal Bioanal Chem 398, 613–650.

Philip D, 2009. Biosynthesis of Au, Ag and Au–Ag nanoparticles using edible mushroom extract. Spectrochim Acta A 73, 374–381.

Pinna N, Niederberger M, 2008. Surfactant-free nonaqueous synthesis of metal oxide nanostructures. Angew Chem Int Ed, 47, 5292–5304.

Poulton SW, Raiswell R, 2005. Chemical and physical characteristics of iron oxides in riverine and glacial meltwater sediments. Chem Geol 218, 203–221.

Quick KL, Ali SS, Arch R, Xiong C, Wozniak D, Dugan LL, 2008, A carboxyfullerene SOD mimetic improves cognition and extends the lifespan of mice. Neurobiol Aging 29, 117–128.

Ramsden CS, Smith TJ, Shaw BJ, Handy RD, 2009. Dietary exposure to titanium dioxide nanoparticles in rainbow trout (*Oncorhynchus mykiss*): no effect on growth, but subtle biochemical disturbances in the brain. Ecotoxicology 18, 939–951.

Rauscher H, Sokull-Klüttgen B, Stamm H, 2012. The European Commission's recommendation on the definition of nanomaterial makes an impact. Nanotoxicology doi:10.3109/17435390.2012.724724.

Rezić I, 2011. Determination of engineered nanoparticles on textiles and in textile wastewaters. Trends Analyt Chem 30, 1159–1167.

Ros TD, Spalluto G, Prato M, 2001. Biological applications of fullerene derivatives: a brief overview. Croat Chem Acta 74, 743–755.

Rozan TF, Lassman ME, Ridge DP, Lutter GW, 2000. Evidence for iron, copper and zinc complexation as multinuclear sulphide clusters in oxic rivers. Nature 406, 879–882.

Sadowski Z, Maliszewska IH, Grochowalska B, Polowczyk I, Koźlecki T, 2008. Synthesis of silver nanoparticles using microorganisms. Mater Sci-Poland, 26, 419–424.

Saison C, Perreault F, Daigle JC, Fortin C, Claverie J, Morin M, Popovic R, 2010. Effect of core-shell copper oxide nanoparticles on cell culture morphology and photosynthesis (photosystem II energy distribution) in the green alga, *Chlamydomonas reinhardtii*. Aquat Toxicol 96, 109–114.

Salata OV, 2004. Applications of nanoparticles in biology and medicine. J Nanobiotechnol 2 (6 pp).

Sanchís J, Berrojalbiz N, Caballero G, Dachs J, Farré M, Barceló D, 2012. Occurrence of aerosol-bound fullerenes in the mediterranean sea atmosphere. Environ Sci Technol 46, 1335–1343.

Sañudo-Wilhelmy SA, Rivera-Duarte I, Flegal AR, 1996. Distribution of colloidal trace metals in the San Francisco Bay estuary. Geochim Cosmochim Acta 60, 4933–4944.

Sayes CM, Fortner JD, Guo W, Lyon D, Boyd AM, Ausman KD, Tao YJ, Sitharaman B, Wilson LJ, Hughes JB, West JL, Colvin VL, 2004. The differential cytotoxicity of water-soluble fullerenes. Nano Lett 4, 1881–1887.

Schreiner KM, Filley TR, Blanchette RA, Bowen BB, Bolskar RD, Hockaday WC, Masiello CA, Raebiger JW, 2009. White-rot basidiomycete-mediated decomposition of C_{60} fullerol. Environ Sci Technol 43, 3162–3168.

Shi JP, Evans DE, Khan AA, Harrison RM, 2001. Sources and concentration of nanoparticles (<10nm diameter) in the urban atmosphere. Atmos Environ 35, 1193–1202.

Stolpe B, Hassellöv M, Andersson K, Turner D, 2005. High resolution ICPMS as an on-line detector for flow field-flow fractionation: multi-element determination of colloidal size distributions in a natural water sample. Anal Chim Acta 535, 109–121.

Svedberg T, Nichols JB, 1923. Determination of size and distribution of size of particle by centrifugal methods. J Am Chem Soc 45, 2910–2917.

Svedberg T, Rinde H, 1924. The ultra-centrifuge, a new instrument for the determination of size and distribution of size of particle in amicroscopic colloids. J Am Chem Soc 46, 2677–2693.

Taniguchi N, 1974. Proc Intl Conf Prod Eng Tokyo, Part II, Japan Society of Precision Engineering.

Taylor DA, 2002. Dust in the wind. Environ Health Perspect 110, A80–A87.

Tiwari DK, Behari J, Sen P, 2008. Application of nanoparticles in waste water treatment. World Appl Sci J 3, 417–433.

Tykhomyrov AA, Nedzvetsky VS, Klochkov VK, Andrievsky GV, 2008. Nanostructures of hydrated C_{60} fullerene (C_{60}HyFn) protect rat brain against alcohol impact and attenuate behavioral impairments of alcoholized animals. Toxicology 246, 158–165.

Valenti W, Chaffin JL, Cherry DS, Schreiber ME, Valett HM, Charles M, 2005. Bioassessment of an appalachian headwater stream influenced by an abandoned arsenic mine. Arch Environ Contam Toxicol 49, 488–496.

Vávrová J, Řezáčová M, Pejchal J, 2012. Fullerene nanoparticles and their anti-oxidative effects: a comparison to other radioprotective agents. J Appl Biomed 10, 1–8.

Wang Z, Lee YH, Wu B, Horst A, Kang Y, Tang YJ, Chen DR, 2010. Anti-microbial activities of aerosolized transition metal oxide nanoparticles. Chemosphere 80, 525–529.

Weinberg H, Galyean A, Leopold M, 2011. Evaluating engineered nanoparticles in natural waters. Trends Analyt Chem 30, 72–83.

Wells ML, Smith GJ, Bruland KW, 2000. The distribution of colloidal and particulate bioactive metals in Narragansett Bay, RI. Mar Chem 71, 143–163.

Wigginton NS, Haus KL, Hochella MF, 2007. Aquatic environmental nanoparticles. J Environ Monit 9, 1306–1316.

Wu B, Kuang Y, Zhang X, Chen J, 2011. Noble metal nanoparticles/carbon nanotubes nanohybrids: Synthesis and applications. Nano Today 6, 75–90.

Xia L, Lenaghan SC, Zhang M, Zhang Z, Li Q, 2010. Naturally occurring nanoparticles from English ivy: an alternative to metal-based nanoparticles for UV protection. J Nanobiotechnology 8 (9 pp).

Yano E, Yokoyama Y, Higashi H, Nishii S, Maeda K, Koizumi A, 1990. Health effects of volcanic ash: a repeat study. Arch Environ Health 45, 367–373.

Zänker H, Schierz A, 2012. Engineered nanoparticles and their identification among natural nanoparticles. Annu Rev Anal Chem 5, 107–132.

Zereini F, Wiseman C, Alt F, Messerschmidt J, Müller J, Urban H, 2001. Platinum and rhodium concentrations in airborne particulate matter in Germany from 1988 to 1998. Environ Sci Technol 35, 1996–2000.

Zhang HZ, Gilbert B, Huang F, Banfield JF, 2003. Water-driven structure transformation in nanoparticles at room temperature. Nature 424, 1025–1029.

Zhang Y, Chen Y, Westerhoff P, Hristovski K, Crittenden JC, 2008. Stability of commercial metal oxide nanoparticles in water. Water Res 42, 2204–2212.

Zhang F, Wu X, Chen Y, Lin H, 2009. Application of silver nanoparticles to cotton fabric as an antibacterial textile finish. Fibers Polym 10, 496–501.

Zhu X, Chang Y, Chen Y, 2010. Toxicity and bioaccumulation of TiO_2 nanoparticle aggregates in *Daphnia magna.* Chemosphere 78, 209–215.

Zsigmondy R, 1909. Colloids and the Ultramicroscope. J Am Chem Soc 31, 951–952.

Chapter 2

Can metal nanoparticles be a threat to microbial decomposers of plant litter in streams?

Published as:

Can metal nanoparticles be a threat to microbial decomposers of plant litter in streams?

Pradhan A, Seena S, Pascoal C, Cássio F

***Microbial Ecology*, 62, 58–68 in 2011**

Abstract

The extensive use of nanometal-based products increases the chance of their release into aquatic environments, raising the question whether they can pose a risk to aquatic biota and the associated ecological processes. Aquatic microbes, namely fungi and bacteria, play a key role in forested streams by decomposing plant litter from terrestrial vegetation. Here, we investigated the effects of nanocopper oxide and nanosilver on leaf litter decomposition by aquatic microbes and the results were compared with the impacts of their ionic precursors. Alder leaves were immersed in a stream of Northwest Portugal to allow microbial colonization before being exposed in microcosms to increased nominal concentrations of nanometals (CuO, 100, 200 and 500 mg L^{-1}; Ag, 100 and 300 mg L^{-1}) and ionic metals (Cu^{2+} in $CuCl_2$, 10, 20 and 30 mg L^{-1}; Ag^{+} in $AgNO_3$, 5 and 20 mg L^{-1}) for 21 days. Results showed that rates of leaf decomposition decreased with exposure to nano and ionic metals. Nano and ionic metals inhibited bacterial biomass (from 68.6 to 96.5% of control) more than fungal biomass (from 28.5 to 82.9% of control). The exposure to increased concentrations of nano and ionic metals decreased fungal sporulation rates from 91.0 to 99.4%. These effects were accompanied by shifts in the structure of fungal and bacterial communities based on DNA fingerprints and fungal spore morphology. The impacts of metal nanoparticles on leaf decomposition by aquatic microbes were less pronounced compared to their ionic forms, despite metal ions were applied at one order of magnitude lower concentrations. Overall, results indicate that the increased release of nanometals to the environment may affect aquatic microbial communities with impacts on organic matter decomposition in streams.

Keywords: silver nanoparticles; copper oxide nanoparticles; ionic metals; streams; litter decomposition; microbial communities

2.1. Introduction

Owing to the rapid growth of nanotechnology-based industries enormous amounts of nanomaterials are being manufactured and utilized since the past decade (Aitken et al., 2006). Nanometal-based products have become part of our regular life in the form of cosmetics (Perugini et al., 2002), antimicrobial paints (Kaegi et al., 2008), textile fabrics (Zhang et al., 2009) and electronic devices (Luechinger et al., 2008). Nanometals are also employed in biomedical and pharmaceutical applications, like cancer therapy, protein detection, tissue engineering, drug delivery and gene therapy (Salata, 2004). With the accelerated usage of nanoparticles, aquatic ecosystems most likely will serve as terminal repository for the discharged nanomaterials (Kaegi et al., 2008). For instance, the engineered nanoparticle TiO_2 was detected in aquatic environments as a consequence of being leached from the paint of house facades into the neighbouring stream (Kaegi et al., 2008). Hence, the research pertaining to impacts of nanoparticles and its ionic forms on aquatic biota has become a topic of major importance.

Ionic metals are used as precursors for production of many nanomaterials; for instance, silver nitrate and copper chloride are known to be the ionic precursors of nanosilver and nanocopper oxide, respectively (Wang et al., 2002; Saquing et al., 2009). A number of studies have reported toxicity of metal ions against aquatic organisms ranging from microbes to vertebrates (Birceanu et al., 2008; Gopalakrishnan et al., 2008; Azevedo et al., 2009) but very little is known about the effects of their nanoparticle forms (but see e.g., Navarro et al., 2004; Aruoja et al., 2009).

Nanosilver and nanocopper oxide are used widely (e.g., medical research/applications (Nair and Laurencin, 2007; Ren et al., 2009) and textiles (Zhang et al., 2009)) and are becoming the focus of toxicological investigations. These nanoparticles can have toxic effects on various organisms, including yeasts (Kasemets et al., 2009), bacteria (Kim et al., 2007), fungi (Kim et al., 2008), the marine diatom *Thalassiosira weissflogii* (Miao et al., 2009), *Chlamydomonas* (Saison et al., 2010) and fish, like zebrafish (Griffitt et al., 2009), and may also pose risks to human health (Panyala et al., 2008; Karlsson et al., 2009). However, the existing data on the effects of nano-sized silver and copper oxide are mainly based on individual responses of organisms and are clearly insufficient to predict its

impacts on biotic communities (but see reports from Bradford et al. (2009) and Shah and Belozerova (2009) for estuarine and soil bacterial assemblages, respectively) and ecosystem processes.

Predicting the risks of nanoAg or nanoCuO to aquatic ecosystems is currently limited by difficulties in estimating the levels of nanometals in surface waters. However, from the 500 t y^{-1} of worldwide production of nanoAg (Mueller and Nowack, 2008), 20–130 t y^{-1} are expected to reach EU freshwaters mainly from ionic leaching of polymer embedded nanosilver from biocidal plastics and textiles (Blaser et al., 2008). The concentration of copper in the chemical mechanical planarization waste water in Taiwan often exceeds 100 mg L^{-1} (mainly due to incineration of fly ashes (Hsiao et al., 2001)) of which 49% was nanoCuO (Huang et al., 2006). Hence, further research is needed on the fate of the nano and ionic forms of Ag and CuO and their effects on aquatic biota and processes.

In freshwaters, plant-litter decomposition is a key ecosystem process associating riparian vegetation with microbial and invertebrate activities Pascoal et al., 2003, 2005a). Fungi, mainly aquatic hyphomycetes, have been distinguished as dominant microbial decomposers (Pascoal and Cássio, 2004) and are responsible for transferring carbon and energy from plant litter to higher trophic levels in streams (Graça, 2001). Bacteria have been recognized to play a role after partial breakdown of plant material (Pascoal and Cássio, 2004). Previous studies demonstrated that litter decomposition is sensitive to changes in water chemistry (Pascoal et al., 2003; Pascoal and Cássio, 2004; Fernandes et al., 2009) and this integrative process was proposed as a functional measure to assess the health of freshwater ecosystems (Pascoal et al., 2001, 2003).

Even though the ionic forms of metals, such as zinc, copper and cadmium, have been reported to affect litter decomposition and the associated communities in freshwaters (Niyogi et al., 2002; Sridhar et al., 2005; Duarte et al., 2008a; Fernandes et al., 2009; Medeiros et al., 2010; Moreirinha et al., 2011), studies exploring the impacts of nanometals on this ecosystem process are unknown. Earlier studies on individual aquatic organisms demonstrated that the toxicity of ionic metals might be higher (20 – 50 times) than that of their nano forms (Heinlaan et al., 2008; Aruoja et al., 2009), and the lower toxicity of nanometals was attributed to a reduced bioavailability of the leached metal ions from nanoparticles.

The aim of this study was to investigate the effects of nanocopper oxide and nanosilver, and their ionic precursors, on leaf litter decomposition by freshwater

microbial communities. Due to the small size and reactive surface characteristics of nanoparticles, they are prone to aggregation and sorption onto organic materials (Holsapple et al., 2005), such as submerged plant detritus in streams. Therefore, a close interaction between nanometals and benthic microbes involved in plant litter decomposition is expected to occur. We hypothesized that nanometals might have impacts on freshwater microbial decomposer communities and their associated ecological functions, but the effects would be less pronounced than those of their ionic precursors. We also expected that bacteria might be more sensitive than fungi to nanometals, as previously found for ionic metals (Duarte et al., 2008b, 2009). We used stream-dwelling microbial communities in microcosms to mimic the natural environment under controlled conditions, and the measured parameters were leaf mass loss, fungal and bacterial biomass and diversity, and fungal reproduction.

2.2. Material and Methods

2.2.1. Microbial colonization in the stream

The sampling site was located at the Maceira stream (N 41°45'58.79", W 8°08'49.39", altitude 867 m) in the Peneda-Gerês National Park (Northwest Portugal). At the sampling site, the stream is 0.3-0.5 m deep and 0.5-1.0 m wide and the geological substratum was constituted by granitic rocks, pebbles, gravels and sand. The dominant riparian vegetation was *Quercus pyrenaica* Wild, *Quercus robur* L., *Chamaecyparis* sp. and *Ilex aquifolium* L.

Leaves of *Alnus glutinosa* (L.) Gaertn. (alder) were collected from a single tree in autumn and air dried at room temperature. This leaf species was chosen because it is among the most common and dominant riparian trees in the Iberian Peninsula. The leaves were soaked in deionised water and cut into 12 mm-diameter disks. Sets of 40 disks were placed into each of 105 fine mesh bags (15 × 15 cm, 0.5-mm mesh size, to prevent macroinvertebrate colonization) that were immersed in the stream for 7 days to allow microbial colonization. After 30 min of leaf immersion, 3 randomly selected leaf bags were retrieved and transported to the laboratory to determine initial leaf mass.

Conductivity and pH of the stream water were measured *in situ* with field probes (Multiline F/set 3 no. 400327, WTW, Weilheim, Germany). Stream water

samples were collected into sterile dark glass bottles, transported in a cold box (4°C) to the laboratory to determine the concentrations of nitrate (HACH kit, programme 351), nitrite (HACH kit, programme 371) and phosphate (HACH kit, programme 490) using a HACH DR/2000 photometer (HACH, Loveland, CO).

2.2.2. Microcosm experiment

After retrieval from the stream, leaf disks from each of 102 bags were rinsed with deionised water and placed into 150 mL sterile Erlenmeyer flasks with 80 mL of filtered (MN GF-3 filter paper, Macherey-Nagel, Germany) and sterilized stream water (121°C, 20 min). Stream water had a pH of 5.9, a conductivity of 16 µS cm^{-1}, and contained 40 µg L^{-1} $N\text{-}NO_3^-$, 2 µg L^{-1} $N\text{-}NO_2^-$ and 20 µg L^{-1} $P\text{-}PO_4^{3-}$. Stream water was supplemented with increasing nominal concentrations of nanometals or ionic metals as follows: 0, 100, 200 and 500 mg L^{-1} of nanocopper oxide (CuO nanopowder <50 nm, 99.5%); 0, 100 and 300 mg L^{-1} of nanosilver (Ag nanopowder, <100 nm, 99.5%); 0, 10, 20 and 30 mg L^{-1} of Cu^{2+} ($CuCl_2.2H_2O$, > 99%); and 0, 5 and 20 mg L^{-1} of Ag^+ ($AgNO_3$, > 99%). Nano and ionic metals were purchased from Sigma-Aldrich (St. Louis, MO). Stock suspensions of the two nanometals were sonicated (42 kHz, 100 W, Branson 2510, Danbury, CT, USA) for 30 min in dark before used (Heinlaan et al., 2008). The pH of stock suspensions of nanometals and stock solutions of ionic metals were adjusted to 6.0 ± 0.2.

All microcosms were kept under shaking (150 rpm) at 13°C (stream water temperature), and solutions were renewed every 7 days. After 7, 14 and 21 days of exposure, a set of 33 microcosms (3 replicates of each treatment per time) was sacrificed and leaf disks were freeze dried to determine leaf mass loss, microbial biomass and diversity as described below. In addition, the content of 3 leaf bags was used to determine leaf mass loss and microbial parameters at the beginning of microcosm experiment.

2.2.3. Fungal sporulation rates

After 21 days of exposure to the nano and ionic metals, suspensions of released fungal conidia from each replicate microcosm were mixed with Triton X-100 (40 µl of 15%), to avoid conidial adherence to the flask, and the conidia were fixed with 2% formaldehyde. Then, appropriate aliquots of conidial suspensions were filtered (5 µm pore size, Millipore, Billerica, MA) and stained with 0.05% cotton

blue in lactic acid. Conidia of aquatic hyphomycetes were identified and counted under a light microscope (Leica Biomed, Heerbrug, Switzerland) at 400× magnification.

2.2.4. Microbial biomass

Concentration of ergosterol was measured to estimate fungal biomass associated with decomposing leaves (Pascoal and Cássio, 2004; Gessner, 2005). Lipids were extracted from sets of 6 leaf disks per replicate by heating (30 min, 80°C) in 0.8% KOH-methanol and the extract was purified by solid-phase extraction and eluted in isopropanol. Ergosterol was quantified by high-performance liquid chromatography (HPLC) using a LiChrospher RP18 column (250 × 4 mm, Merck) connected to a Beckmann Gold liquid chromatographic system. The system was run isocratically with HPLC-grade methanol at 1.4 mL min^{-1} and 33°C. The peaks of ergosterol were detected at 282 nm and standard series of ergosterol (Sigma) in isopropanol were used to estimate the ergosterol concentration in the samples. Ergosterol concentration was converted to fungal biomass assuming 5.5 µg ergosterol mg^{-1} mycelial dry mass (Gessner, 2005).

To estimate bacterial biomass, sets of 4 leaf disks per replicate were placed into 15 mL falcon tubes with 10 mL of phosphate buffered formalin (2% final concentration) and kept at 4°C until processed. Bacterial cells were dislodged from leaf disks in a sonication bath (42 kHz, 100 W; Branson 2510, Danbury, CT, USA) for 5 min (samples were cooled in ice after each 1 min of sonication) (Pascoal and Cássio, 2004; Duarte et al., 2009). Aliquots of 2 mL of appropriate dilutions of bacterial suspensions were incubated with 4′,6-diamidino-2-phenylindole (DAPI, 50 µL of 0.1 mg mL^{-1}; Molecular Probes) for 10 min in the dark, before filtered through black polycarbonate membranes (0.2 µm pore size, GTTP, Millipore, Billerica, MA). Filters were mounted between two drops of immersion oil on grease free slides, covered with cover slips and bacterial cells were counted using a fluorescence microscope (Leitz Laborlux Heerbrug, Switzerland) at magnification of 1000×. Bacterial numbers were converted to bacterial biomass considering a mean bacterial biomass of 20 fg $cell^{-1}$ (Norland, 1993).

2.2.5. Denaturing gradient gel electrophoresis

DNA was extracted from 3 leaf disks (pooling 2 half disks of each replicate) using the UltraClean Soil DNA kit (MoBio Laboratories, Solana Beach, CA, USA). The ITS2 region of fungal genomic rDNA was amplified with the primer pair ITS3GC and ITS4 (White et al., 1990; Duarte et al., 2008a) and the V3 region of bacterial 16S rDNA was amplified with the primer pair 338F_GC and 518R (Duarte et al., 2008a). The 40-bp GC tail on the 5′ end of the forward primers ensured the amplicon separation by denaturing gradient gel electrophoresis (DGGE). All primers were purchased from MWG Biotech AG. For polymerase chain reaction (PCR), 1x Go Taq Green Master Mix (Promega), 0.8 µM of each primer and 2 µL of extracted fungal or bacterial DNA were mixed gently with nuclease free water in a final volume of 50 µL. PCR was carried out in the iCycler Thermal Cycler (BioRad Laboratories, Hercules, CA, USA). DNA amplification programme was started with a denaturation for 5 min at 94°C, followed by 36 cycles of denaturation for 30 s at 94°C, primer annealing for 30 s at 55°C and extension for 1 min at 72°C, concluding with an extension for 3 min at 72°C (Duarte et al., 2008a). The PCR products were separated by DGGE using the DCode™ Universal Mutation Detection System (BioRad Laboratories, Hercules, CA, USA). For fungal DNA, 20–40 µL from the amplified products of 380–400 bp were loaded on 8% (w/v) polyacrylamide gel in 1x Tris–Acetate–EDTA (TAE) with a denaturing gradient from 30% to 70% (100% denaturant corresponds to 40% formamide and 7 M urea). For bacterial DNA, 20 µL from the amplified products of 200 bp were loaded on 8% (w/v) polyacrylamide gels in 1x TAE with a denaturing gradient from 35% to 80%. DNA mixtures of 5 species of fungi or bacteria were used as reference bands to calibrate the gels. The gels were run at 55 V for 16 h at 56°C and stained with 1x GelStar (Lonza Rockland, Inc., USA). The gel images were captured under UV light in a transiluminator Eagle eye II (Stratagene, La Jolla, CA, USA).

2.2.6. Leaf mass loss

To determine leaf mass loss, freeze-dried (Christ alpha 2–4, B. Braun, Germany) leaf disks from each replicate before and after stream colonization, and after microcosm exposure were weighed to the nearest 0.001 mg.

2.2.7. Nanometals in stock suspensions

The nanometals in suspensions were analysed by UV-visible spectrophotometry (UV – 1700 PharmaSpec, Shimadzu, Kyoto, Japan) and by scanning electron microscopy (SEM, Leica Cambridge S 360, Cambridge, UK) coupled to an energy dispersive X-ray microanalysis setup (EDX, 15 KeV). For SEM analysis, 20 µl of stock suspension of each nanometal was mounted on a clean grease free slide in dark, air dried and coated with gold in vacuum by using a Fisons Instruments SC502 sputter coater. Nanosilver and nanocopper oxide showed plasmon peaks at 416 nm and 359 nm, respectively. Scanning electron microscopy confirmed the size of copper oxide nanoparticles (30 to 50 nm) and silver nanoparticles (near 100 nm). The presence of Cu and O in copper oxide nanoparticles and Ag in silver nanoparticles was confirmed by EDX (Fig. 2.1A and B). Additional peaks were found: Au from the coated gold, Si probably from the glass slide, and Na, Ca and Mg probably from the stream water.

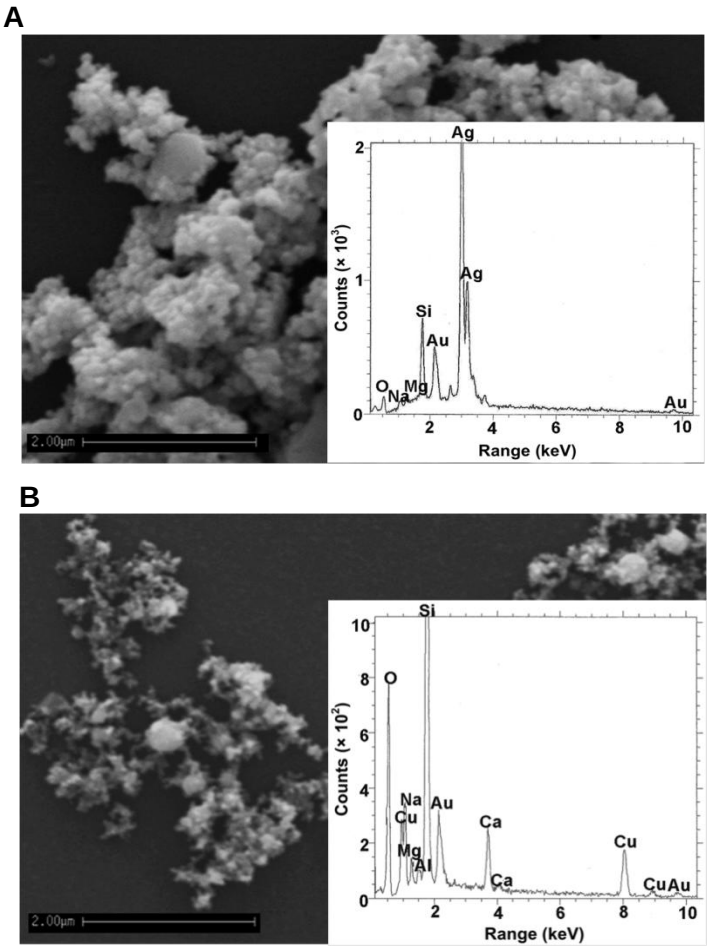

Figure 2.1 Scanning electron microscopy (SEM) with energy dispersive X-ray (EDX) microanalysis (insight) of nanosilver (A) and nanocopper oxide (B) in stock suspensions.

2.2.8. Data analyses

Rates of leaf decomposition (k) were estimated according to the exponential model as follows: $W_t = W_0 \times e^{-kt}$, where W_t is the leaf dry mass remaining at time t, W_0 is the initial leaf dry mass and t is the time in days. Regression lines of ln-transformed values of leaf dry mass against time were compared by analysis of covariance (ANCOVA) (Zar, 2009). Two-way analysis of variance (two-way ANOVA) (Zar, 2009) was used to determine the effects of exposure time and concentration of nano or ionic metal form on fungal and bacterial biomass. Each metal type and metal form were analysed separately. One-way ANOVA was used to test the effect of concentration of nano or ionic form of each metal on fungal sporulation rate and on the percentage contribution of each aquatic hyphomycete species to the total conidial production after 21 days of exposure. Significant differences between control and treatments were analysed by Bonferroni post-tests (Zar, 2009). To achieve normal distribution and homoscedasticity, data of percentage contribution of each fungal species to the total conidial production were arcsine square root transformed and the remaining data were ln-transformed (Zar, 2009). Univariate analyses were performed with Statistica 6.0 (Statsoft, Inc., Tulsa, OK, USA).

Cluster analyses of fungal and bacterial communities based on relative intensity of each DGGE band was done by Unweighted Pair-Group Method Average (UPGMA) using the Pearson correlation coefficient (Fernandes et al., 2009). Each band in the gel was considered one operational taxonomic unit (OTU). Gel and cluster analyses were done with the GelCompar II program (Applied Maths, Sint-Martens-Latem, Belgium).

2.3. Results

2.3.1. Effects of nano and ionic metals on microbially-mediated leaf litter decomposition

The decomposition rate of alder leaves was high corresponding to 0.0368 day^{-1} (Table 2.1). The exposure to nano or ionic metals led to a significant decrease in leaf decomposition rate (ANCOVA, $P<0.05$). The lowest decomposition rates were found at the highest concentrations of nano and ionic silver (k = 0.0214 and

0.0209 day^{-1} for 300 mg L^{-1} nanosilver and 20 mg L^{-1} ionic silver, respectively) or nanocopper oxide and ionic copper (k = 0.0165 day^{-1} and 0.0153 day^{-1} for 500 mg L^{-1} of nanocopper oxide and 30 mg L^{-1} of ionic copper, respectively).

Table 2.1 Effects of nano and ionic metals on decomposition rates (k) of alder leaves

Treatments	k (day^{-1}) ± SE	W_0 (%)	r^2
Control	0.0368 ± 0.0042	105.6	0.86
AgNP1	0.0237 ± 0.0027*	98.6	0.86
AgNP2	0.0214 ± 0.0029*	99.4	0.81
Ag1	0.0218 ± 0.0032*	97.3	0.79
Ag2	0.0209 ± 0.0026*	97.1	0.84
CuONP1	0.0208 ± 0.0022*	98.0	0.87
CuONP2	0.0186 ± 0.0021*	98.5	0.86
CuONP3	0.0165 ± 0.0018*	98.7	0.87
Cu1	0.0219 ± 0.0028*	97.8	0.83
Cu2	0.0176 ± 0.0018*	96.9	0.88
Cu3	0.0153 ± 0.0024*	95.8	0.75

AgNP1: 100 mg L^{-1} nanoAg; AgNP2: 300 mg L^{-1} nanoAg; Ag1: 5 mg L^{-1} Ag^{+}; Ag2: 20 mg L^{-1} Ag^{+}; CuONP1: 100 mg L^{-1} nanoCuO; CuONP2: 200 mg L^{-1} nanoCuO; CuONP3: 500 mg L^{-1} nanoCuO; Cu1: 10 mg L^{-1} Cu^{2+}; Cu2: 20 mg L^{-1} Cu^{2+}; Cu3: 30 mg L^{-1} Cu^{2+}; Control: without addition of any form of metals. *, treatments that differ significantly from control (ANCOVA, Bonferroni test, $P < 0.05$). SE: standard error; r^2: coefficient of determination; W_0: initial leaf dry mass.

After 7 days of colonization in the stream, fungal biomass on decomposing leaves was 10 mg g^{-1} leaf dry mass and increased to 53 mg g^{-1} leaf dry mass after 21 days in control microcosms (Fig. 2.2A and B). Concentrations of nano and ionic forms of silver or ionic copper and exposure time had negative effects on fungal biomass (two-way ANOVAs, *P<0.05*; Table 2.2). Significant interactions were found between exposure time and concentration of ionic forms of each metal (*P<0.05*; Table 2.2). Exposure time, but not concentrations of nanocopper oxide, affected fungal biomass (two-way ANOVA, *P<0.05* and *P>0.05,* respectively; Table 2.2). After 21 days of exposure to the highest concentration of nanosilver (Fig. 2.2A) or nanocopper oxide (Fig. 2.2B) a 40% inhibition of fungal biomass was found (Bonferroni tests, *P<0.05*). Fungal biomass was inhibited earlier by exposure to the highest concentrations of ionic silver (15 and 9 mg g^{-1} leaf dry mass at 20 mg L^{-1} for 14 and 21 days, respectively; Bonferroni tests, *P<0.05*; Fig. 2.2A) or ionic copper (24 and 18 mg g^{-1} leaf dry mass at 30 mg L^{-1} for 14 and 21 days, respectively; Bonferroni tests, *P<0.05*; Fig. 2.2B). A significant decrease in fungal biomass was also observed at the longest exposure time to the lowest concentration of ionic silver (17 mg g^{-1} leaf dry mass at 5 mg L^{-1}; Bonferroni test, *P<0.05*; Fig. 2.2A) or ionic

copper (30 and 18 mg g^{-1} leaf dry mass at 10 and 20 mg L^{-1} for 21 days, respectively; Bonferroni test, *P<0.05*; Fig. 2.2B).

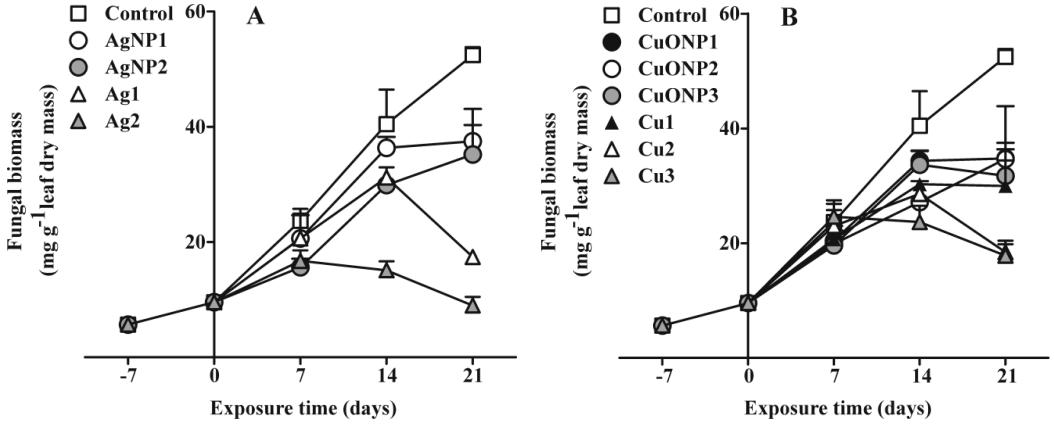

Figure 2.2 Fungal biomass on decomposing alder leaves exposed to nano or ionic silver (A), nanocopper oxide or ionic copper (B) in microcosms. AgNP1 and AgNP2: 100 and 300 mg L^{-1} nanoAg; Ag1 and Ag2: 5 and 20 mg L^{-1} Ag^{+}; CuONP1, CuONP2 and CuONP3: 100, 200 and 500 mg L^{-1} nanoCuO; Cu1, Cu2 and Cu3: 10, 20 and 30 mg L^{-1} Cu^{2+}, respectively; Control: without addition of any form of metals. Mean ± SEM, n=3.

Before microcosm exposure, bacterial biomass on decomposing leaves was 0.02 mg g^{-1} leaf dry mass and increased to 0.26 mg g^{-1} leaf dry mass after 21 days in microcosms (Fig. 2.3A and B). The exposure to all concentrations of nano or ionic silver led to a significant decrease in bacterial biomass at all times (two-way ANOVAs; Bonferroni test, *P<0.05*, Table 2.2, Fig. 2.3A) with strongest effects for silver ions (0.01 mg g^{-1} leaf dry mass). Interactions between exposure time and concentration of nano or ionic forms of silver or copper were significant (*P<0.05*, Table 2.2). Bacterial biomass was negatively affected by concentration of nanocopper oxide or ionic copper and exposure time (two-way ANOVAs, *P<0.05*; Table 2.2). The exposure to the highest concentrations of nanocopper oxide (200 and 500 mg L^{-1}) or ionic copper (20 and 30 mg L^{-1}) led to a significant decrease in bacterial biomass at all times, whereas the lowest tested concentrations of these materials (100 mg L^{-1} of nanocopper oxide and 10 mg L^{-1} of ionic copper) decreased the biomass only after 14 and 21 days of exposure (Bonferroni test, *P<0.05,* Fig. 2.3B).

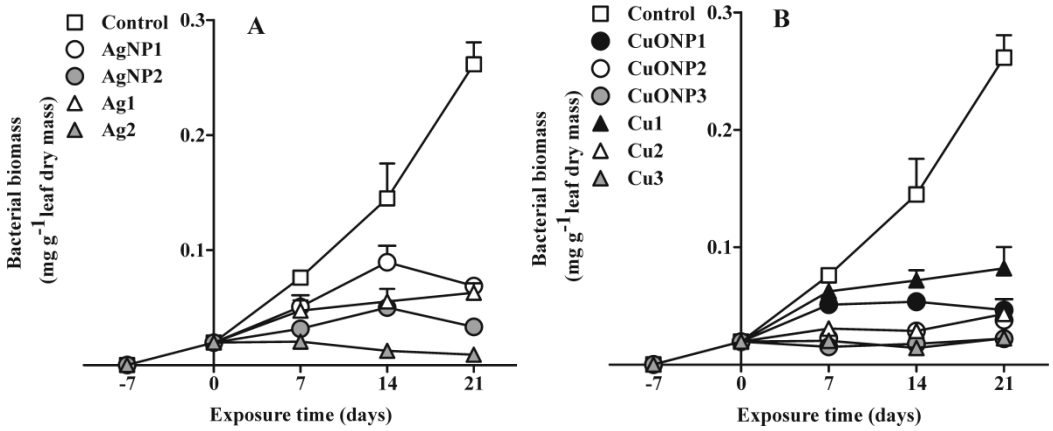

Figure 2.3 Bacterial biomass on decomposing alder leaves exposed to nano or ionic silver (A), nanocopper oxide or ionic copper (B) in microcosms. AgNP1 and AgNP2: 100 and 300 mg L^{-1} nanoAg; Ag1 and Ag2: 5 and 20 mg L^{-1} Ag^{+}; CuONP1, CuONP2 and CuONP3: 100, 200 and 500 mg L^{-1} nanoCuO; Cu1, Cu2 and Cu3: 10, 20 and 30 mg L^{-1} Cu^{2+}, respectively; Control: without addition of any form of metals. Mean ± SEM, n=3.

In control microcosms, sporulation rate of aquatic hyphomycetes attained 245 × 10^3 spores g^{-1} leaf dry mass day^{-1} and was significantly inhibited (up to 99.4%) by exposure for 21 days to all concentrations of nano or ionic forms of silver or copper (one-way ANOVAs, *P<0.05*; Fig. 2.4A and B; Table 2.2).

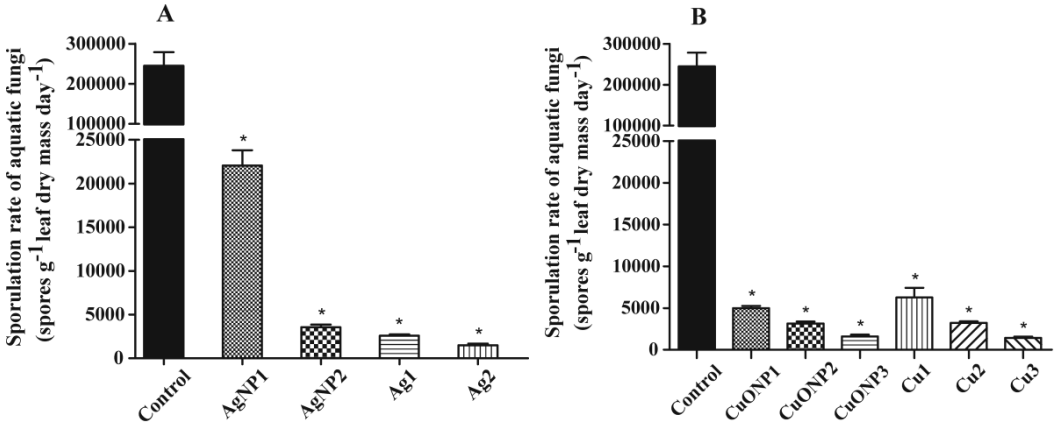

Figure 2.4 Fungal sporulation from decomposing alder leaves after 21 days exposure to nano or ionic silver (A), nanocopper oxide or ionic copper (B) in microcosms. AgNP1 and AgNP2: 100 and 300 mg L^{-1} nanoAg; Ag1 and Ag2: 5 and 20 mg L^{-1} Ag^{+}; CuONP1, CuONP2 and CuONP3: 100, 200 and 500 mg L^{-1} nanoCuO; Cu1, Cu2 and Cu3: 10, 20 and 30 mg L^{-1} Cu^{2+}, respectively; Control: without addition of any form of metals. Mean ± SEM, n=3. *, treatments that differ significantly from control (Bonferroni tests, P<0.05).

Table 2.2 ANOVAs of effects of exposure time, nano or ionic metal concentrations on fungal biomass, bacterial biomass and fungal sporulation (only significant effects are shown). Metal type and metal form were analysed separately

Parameter		Effect	d.f.	*F*	*P*-value
Fungal biomass					
	NanoAg				
		Time	4	173.3	<0.0001
		Concentration	2	6.223	<0.05
	Ag^+				
		Time	4	158.6	<0.0001
		Concentration	2	35.92	0.0005
		Time*Concentration	8	19.88	<0.0001
	NanoCuO				
		Time	4	199.3	<0.0001
	Cu^{2+}				
		Time	4	185.8	<0.0001
		Concentration	3	10.65	<0.005
		Time*Concentration	12	4.652	<0.0005
Bacterial biomass					
	NanoAg				
		Time	4	1950	<0.0001
		Concentration	2	96.56	<0.0001
		Time*Concentration	8	19.21	<0.0001
	Ag^+				
		Time	4	1779	<0.0001
		Concentration	2	99.56	<0.0001
		Time*Concentration	8	59.49	<0.0001
	NanoCuO				
		Time	4	1356	<0.0001
		Concentration	3	121.8	<0.0001
		Time*Concentration	12	17.42	<0.0001
	Cu^{2+}				
		Time	4	1612	<0.0001
		Concentration	3	115.8	<0.0001
		Time*Concentration	12	19.68	<0.0001
Fungal sporulation rate (21 days)					
	NanoAg				
		Concentration	2	358.4	<0.0001
	Ag^+				
		Concentration	2	518.4	<0.0001
	NanoCuO				
		Concentration	3	428.8	<0.0001
	Cu^{2+}				
		Concentration	3	280.0	<0.0001

d.f., degree of freedom

2.3.2. Effects of nano and ionic metals on the structure of microbial decomposer community

Based on conidial morphology, a total of 11 aquatic hyphomycete species were identified on decomposing leaves after 21 days in control microcosms (Table 2.3). The exposure to nano or ionic metals decreased fungal species richness,

particularly in the case of copper (5 species in treatments with concentrations ≥ 200 mg L^{-1} of nanocopper and 4 species with 30 mg L^{-1} of ionic copper; Table 2.3). In addition, nano or ionic metals led to shifts in fungal species composition (Table 2.3). In control, *Articulospora tetracladia* (51.2%) was the dominant species followed by *Flagellospora* sp. (32.8%) (Table 2.3). The exposure to nanosilver, nanocopper or ionic copper significantly increased the contribution of *A. tetracladia* to overall conidial production (one-way ANOVAs, Bonferroni tests, $P<0.05$), whereas ionic silver did not lead to any significant change (Table 2.3). The exposure to nano and ionic metals significantly decreased the contribution of *Flagellospora* sp. (Bonferroni test, $P<0.05$; Table 2.3) but increased that of *Heliscus lugdunensis* (Bonferroni test, $P<0.05$; Table 2.3).

DNA fingerprinting based on DGGE showed that fungal and bacterial communities were affected by nano and ionic metals (Fig. 2.5A and B, Table 2.3). Thirty one fungal OTUs and 36 bacterial OTUs were found in control communities (Fig. 2.5A and B, Table 2.3). The number of fungal or bacterial OTUs decreased with increasing concentrations of nano or ionic metals, particularly in the case of the latter form of the metals, with maximum reduction at the highest concentration of ionic silver (Fig. 2.5A and B, Table 2.3).

Cluster analysis of fungal communities exposed to the highest ionic silver concentration formed an outgroup (Fig. 2.5A). Further, fungal communities exposed to nanosilver clustered together and were separated from control communities or communities exposed to other treatments. Cluster analysis of bacteria discriminated 3 groups: control communities, communities exposed to silver and communities exposed to copper (Fig. 2.5B). Bacterial communities exposed to nano and ionic forms of each metal were further separated.

Table 2.3 Microbial community composition on decomposing leaves as number and composition of fungal sporulating species and number of fungal and bacterial OTUs from DGGE fingerprints after 21 days of exposure to increasing concentrations of nano or ionic metals in microcosms

Species	% of conidia in treatments										
	Control	AgNP1	AgNP2	Ag1	Ag2	CuONP1	CuONP2	CuONP3	Cu1	Cu2	Cu3
Alatospora acuminata Ingold	0.2	0.4	nd	nd	nd	nd	nd	nd	nd	nd	nd
Anguillospora filiformis Greath	4.3	1.4	2.2	6.3	nd	nd	nd	nd	nd	nd	nd
Articulospora tetracladia Ingold	51.2	76.0	76.1	53.2	55.5	51.6	56.1	60.7	66.7	68.0	73.3
Culicidospora aquatica R.H. Petersen	0.1	0.4	nd	nd	nd	nd	nd	nd	0.4	nd	nd
Flagellospora sp.	32.8	9.3	6.7	15.6	15.9	9.1	11.4	7.5	10.9	11.8	6.5
Fontanospora eccentrica (R.H. Petersen) Dyko	0.2	0.4	nd	nd	nd	nd	nd	nd	nd	nd	nd
Fontanospora fusiramosa Marvanová, P.J. Fisher, Descals & Bärlocher	3.9	2.4	2.2	6.3	5.4	5.3	4.0	4.6	3.6	2.4	nd
Heliscus lugdunensis Sacc. & Therry	1.8	6.1	8.1	12.5	17.8	27.5	24.4	22.6	12.3	11.7	15.2
Lunulospora curvula Ingold	0.9	2.0	2.2	nd	nd	1.6	nd	nd	1.7	2.4	nd
Tricladium splendens Ingold	0.1	nd	nd	nd	nd	nd	nd	nd	nd	nd	nd
Varicosporium elodeae W. Kegel	4.5	1.7	2.2	6.3	5.4	4.8	4.0	4.6	4.4	3.9	5.1
Nº of fungal morphotypes	11	10	7	6	5	6	5	5	7	6	4
Nº of fungal DGGE OTUs	31	26	24	20	11	26	25	23	19	17	16
Nº of bacterial DGGE OTUs	36	28	24	24	19	27	25	24	26	25	24

AgNP1: 100 mg L^{-1} nanoAg; AgNP2: 300 mg L^{-1} nanoAg; Ag1: 5 mg L^{-1} Ag^{+}; Ag2: 20 mg L^{-1} Ag^{+}; CuONP1: 100 mg L^{-1} nanoCuO; CuONP2: 200 mg L^{-1} nanoCuO; CuONP3: 500 mg L^{-1} nanoCuO; Cu1: 10 mg L^{-1} Cu^{2+}; Cu2: 20 mg L^{-1} Cu^{2+}; Cu3: 30 mg L^{-1} Cu^{2+}; Control: without addition of any form of metals. nd, not detected.

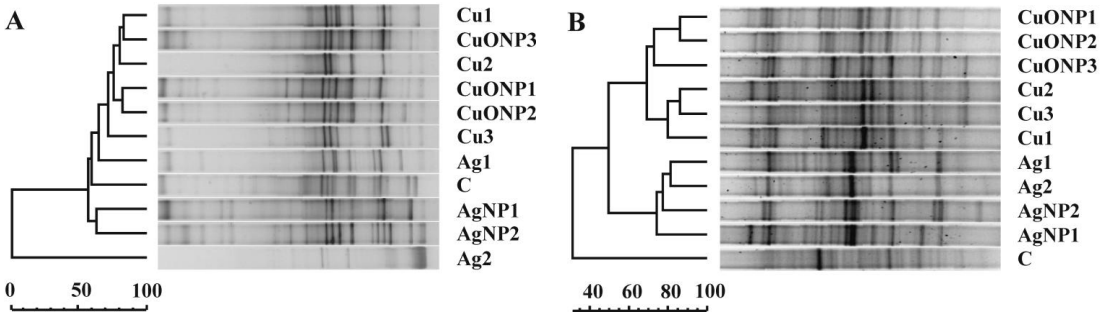

Figure 2.5 DNA fingerprints from DGGE and cluster analysis of fungal (A) and bacterial (B) communities exposed to nano and ionic silver or nanocopper oxide and ionic copper for 21 days in microcosms. Dendograms were constructed from UPGMA analysis based on the Pearson coefficient of similarity. AgNP1 and AgNP2: 100 and 300 mg L^{-1} nanoAg; CuONP1, CuONP2 and CuONP3: 100, 200 and 500 mg L^{-1} nanoCuO; Ag1 and Ag2: 5 and 20 mg L^{-1} Ag^{+}; Cu1, Cu2 and Cu3: 10, 20 and 30 mg L^{-1} Cu^{2+}, respectively; C: Control without addition of any form of metals.

2.4. Discussion

Our study shows that nano and ionic metals can have impacts on microbial communities and reduce leaf litter decomposition in freshwater ecosystems. The exposure to elevate concentrations of nano and ionic metals reduced microbial biomass on decomposing leaves. The biomass of bacteria was strongly inhibited even at short exposure times (7 days). Indeed, many nanometals including nanosilver and nanocopper are known to have anti-bacterial properties (< 100 mg L^{-1} in axenic cultures) (Yoon et al., 2007). However, negligible effects of nanosilver or nanocopper on bacterial abundance, diversity (as fatty acid methyl-ester or DGGE profiles) or activity (as metabolic profile) are reported in communities of soil (Shah and Belozerova, 2009) and estuarine sediments (Bradford et al., 2009). The discrepancy between our results and those in the two latter studies might be explained by the two order of magnitude lower concentrations of the nanometals used in those studies and differences in environmental conditions. Indeed, pH, temperature and oxygen availability (Rispoli et al., 2010), as well as nanoparticle properties (e.g., size (Choi and Hu, 2008)) may affect nanoparticle bioavailability and account for different effects on biota.

In this study, nano and ionic silver or copper inhibited bacterial biomass (68.6 – 96.5% of control) more than fungal biomass (28.5 – 82.9% of control) suggesting that the biomass of bacteria was more sensitive to these metals. This agrees with earlier reports showing that, contrary to bacterial biomass (Duarte et al., 2008b, 2009), fungal biomass is not very sensitive to moderate metal stress and decline only under high stress levels (Niyogi et al., 2002; Duarte et al., 2008b, 2009). The greater sensitivity of bacterial cells to nano and ionic metals may be partially due to the higher surface to volume ratio in bacteria, allowing a higher contact between nano and ionic metals and living cells. The structure of bacterial communities, based on DNA fingerprint, also appeared to discriminate well the stress imposed by ionic and nano forms of silver and copper. It is conceivable that the response of fungal communities become clearer at longer exposure times, as shown by Duarte et al. (2008a) in microbial communities exposed to copper and zinc ions. Moreover, a differential response of aquatic microbial communities to each nanometal and respective ionic form was found, suggesting different modes of action of these different forms of metals. This is supported by distinct gene

expression profiles in zebrafish gills after exposure to nano or ionic metals (Griffitt et al., 2009).

The analysis of aquatic hyphomycete communities based on identification of released spores from decomposing leaves also showed shifts in community composition after exposure to nano and ionic metals. For instance, the dominant fungal species *A. tetracladia* was stimulated by exposure to all compounds, except ionic silver. Moreover, the co-dominant species *Flagellospora* sp. was inhibited by exposure to nano or ionic metals, being replaced by *H. lugdunensis* at the highest exposure concentrations. *Articulospora tetracladia* and *H. lugdunensis* are reported to occur in metal contaminated streams (Jaeckel et al., 2005; Pascoal et al., 2005b) and some strains of these species were found to be resistant to high concentrations of metals (Braha et al., 2007). The shift in species composition in this study probably indicates a change towards a better-adapted community, which may play an ecological role under the stress imposed by nanometals and/or their ionic precursors.

The significant reduction in leaf decomposition rate by stream-dwelling microbes in the presence of nano or ionic metals was probably due to the observed decrease in fungal and bacterial diversity (based on spore morphology and/or DGGE OTUs) and activity (based on sporulation rates and/or biomass production) on leaf litter. Although biomass of fungi was apparently less affected by these stressors than that of bacteria, fungal biomass on decomposing leaves was two orders of magnitude higher. This agrees with previous studies pointing to a dominant role of fungi during litter decomposition in freshwaters (Pascoal and Cássio, 2004; Pascoal et al., 2005a) and is consistent with a more effective production of extracellular degradative enzymes by fungi than bacteria (Schneider et al., 2010). Therefore, it is conceivable that the observed reduction in litter decomposition was mainly due to the negative effects of nano and ionic metals on fungal activity. Unfortunately, we do not have data on the activity of plant litter degrading enzymes in aquatic fungi under nano or ionic metal stress. However, in the white rot fungus *Trametes versicolor*, the production of lignocellulose degrading enzymes, such as ß-glucosidase, cellobiohydrolase and ß-xylosidase, decreased by the presence of ionic copper and aggregated nanoparticles (Shah et al., 2010).

In our study, the impacts of nano and ionic metals were more pronounced on fungal sporulation than on fungal biomass or diversity. This has ecological implications because if fungal reproductive output is affected, it may further

compromise fungal dispersal and survival in freshwaters with impacts to leaf eating invertebrates that are dependent on fungal activity. Moreover, sporulation rate was one of the most sensitive microbial parameters to nano or ionic metals. Also, other studies point to reproduction of aquatic hyphomycetes as a sensitive measure of water quality (Duarte et al., 2008a, 2009; Medeiros et al., 2010) with possible applications in stream monitoring programmes.

Besides the impacts of nano and ionic metals on fungal communities and their ecological functions, the observed negative effects on bacterial communities cannot be neglected. Bacteria also play a role in detritus foodwebs by providing food and energy to higher trophic levels, particularly after partial decomposition of leaf litter by fungi (Pascoal and Cássio, 2004).

Even though we used concentrations of ionic metals one order of magnitude lower than those of nanometals, the negative effects of ionic forms were more pronounced compared to their nano forms. Also, the toxicity of nanocopper oxide to the protozoa *Tetrahymena thermophila* ($EC_{50,14h}$ = 128 mg L^{-1}) was 120 times lower than that of the ionic copper (Mortimer et al., 2010). This may be attributed to the low bioavailability of nano forms in water. The toxicity of nanometals to bacteria (Heinlaan et al., 2008), aquatic algae (Aruoja et al., 2009), and to the eukaryotic model yeast *Saccharomyces cerevisiae* (Kasemets et al., 2009) was attributed to soluble metal ions originating from the metal oxide particles. Conversely, others found that the toxicity of nanocopper and nanosilver in zebrafish and *Daphnia pulex* is unlikely to be merely explained by particle dissolution (Griffitt et al., 2008). Therefore, more investigation on the mechanisms of action of nanoparticles is needed to clarify this aspect.

The effects of nanocopper oxide appeared to be stronger than those of nanosilver on leaf decomposition rate, bacterial biomass, fungal diversity and reproduction. However, it should be taken into account that the size of metal nanoparticles used in our study was lower for nanocopper oxide (30-50 nm) than for nanosilver (near 100 nm). Data from literature have shown that nanometal toxicity to several cell lines (Pan et al., 2007; Karlsson et al., 2009) and organisms, including aquatic species of different trophic levels, tend to increase with the decrease of particle size (Heinlaan et al., 2008; Van Hoecke et al., 2009). However, the toxicity of nanometals does not appear to be a generic response to exposure to nano-sized particles; rather, it seems that particular nanometals have an intrinsic property that confers toxicity (Karlsson et al., 2009).

Overall, our study provides the novel information that nanometals may be a threat to microbial communities that drive plant litter decomposition in streams by reducing diversity and activity of fungi and bacteria. Although the negative effects of ionic forms were more pronounced compared to their nano forms, accumulation or adsorption of nanometals to microbial cells is conceivable to occur (Battin et al., 2009). If so, nanometals may enter aquatic detritus foodwebs with impacts to higher trophic levels. This study clearly indicates the emerging risks of nano and ionic forms of metals to aquatic microbiota and associated ecosystem processes. Moreover, our study suggests that biomass of aquatic bacteria and sporulation of aquatic fungi might be useful tools in ecotoxicological studies to assess nano or ionic metal impacts.

References

Aitken RJ, Chaudhry MQ, Boxall ABA, Hull M, 2006. Manufacture and use of nanomaterials: current status in the UK and global trends. Occup Med 56, 300–306.

Aruoja V, Dubourguier HC, Kasemets K, Kahru A , 2009. Toxicity of nanoparticles of CuO, ZnO and TiO2 to microalgae *Pseudokirchneriella subcapitata*. Sci Total Environ 407, 1461–1468.

Azevedo MM, Almeida B, Ludovico P, Cássio F, 2009. Metal stress induces programmed cell death in aquatic fungi. Aquat Toxicol 92, 264–270.

Blaser SA, Scheringer M, MacLeod M, Hungerbühler K, 2008. Estimation of cumulative aquatic exposure and risk due to silver: Contribution of nano-functionalized plastics and textiles. Sci Total Environ 390, 396–409.

Battin TJ, Kammer FVD, Weilhartner A, Ottofuelling S, Hofmann T, 2009. Nanostructured TiO_2: transport behavior and effects on aquatic microbial communities under environmental conditions. Environ Sci Technol 43, 8098–8104.

Birceanu O, Chowdhury MJ, Gillis PL, McGeer JC, Wood CM, Wilkie MP, 2008. Modes of metal toxicity and impaired branchial ionoregulation in rainbow trout exposed to mixtures of Pb and Cd in soft water. Aquat Toxicol 89, 222–231.

Bradford A, Handy RD, Redman JW, Atfield A, Mühling M, 2009. Impact of silver nanoparticle contamination on the genetic diversity of natural bacterial assemblages in estuarine sediments. Environ Sci Technol 43, 4530–4536.

Braha B, Tintemann H, Krauss G, Ehrman J, Bärlocher F, Krauss GJ , 2007. Stress response in two strains of the aquatic hyphomycete *Heliscus lugdunensis* after exposure to cadmium and copper ions. BioMetals 20, 93–105.

Choi O, Hu Z, 2008. Size dependent and reactive oxygen species related nanosilver toxicity to nitrifying bacteria. Environ Sci Technol 42, 4583–4588.

Duarte S, Pascoal C, Alves A, Correia A, Cássio F, 2008a. Copper and zinc mixtures induce shifts in microbial communities and reduce leaf litter decomposition in streams. Freshwat Biol 53, 91–101.

Duarte S, Pascoal C, Cássio F, 2008b. High diversity of fungi may mitigate the impact of pollution on plant litter decomposition in streams. Microb Ecol 56, 688–695.

Duarte S, Pascoal C, Cássio F, 2009. Functional stability of stream-dwelling microbial decomposers exposed to copper and zinc stress. Freshwat Biol 54, 1683–1691.

Fernandes I, Duarte S, Pascoal C, Cássio F, 2009. Mixtures of zinc and phosphate affect leaf litter decomposition by aquatic fungi in streams. Sci Total Environ 407, 4283–4288.

Gessner MO, 2005. Ergosterol as a measure of fungal biomass. In: Graça MAS, Bärlocher F, Gessner MO (Eds) Methods to study litter decomposition: a practical guide, Springer, Dordrecht, Netherlands, pp 189–196.

Gopalakrishnan S, Thilagam H, Raja PV, 2008. Comparison of heavy metal toxicity in life stages (spermiotoxicity, egg toxicity, embryotoxicity and larval toxicity) of Hydroides elegans. Chemosphere 71, 515–528.

Graça MAS, 2001. The role of invertebrates on leaf litter decomposition in streams – a Review. Int Rev Hydrobiol 86, 383–393.

Griffitt RJ, Luo J, Gao J, Bonzango JC, Barber DS, 2008. Effects of particle composition and species on toxicity of metallic nanoparticles in aquatic organisms. Environ Toxicol Chem 27, 1972–1978.

Griffitt RJ, Hyndman K, Denslow ND, Barber DS, 2009. Comparison of molecular and histological changes in zebrafish gills exposed to metallic nanoparticles. Toxicol Sci 107, 404–415.

Heinlaan M, Ivask A, Blinova I, Dubourguier HC, Kahru A, 2008. Toxicity of nanosized and bulk ZnO, CuO and TiO_2 to bacteria *Vibrio fischeri* and crustaceans *Daphnia magna* and *Thamnocephalus platyurus*. Chemosphere 71, 1308–1316.

Holsapple MP, Farland WH, Landry TD, Monteiro-Riviere NA, Carter JM, Walker NJ, Thomas KV, 2005. Research strategies for safety evaluation of nanomaterials, part II: toxicological and safety evaluation of nanomaterials, current challenges and data needs. Toxicol Sci 88, 12–17.

Hsiao MC, Wang HP, Yang YW, 2001. EXAFS and XANES studies of copper in a solidified fly ash. Environ Sci Technol 35, 2532–2535.

Huang HL, Wang HP, Wei GT, Sun IW, Huang JF, Yang YW, 2006. Extraction of nanosize copper pollutants with an ionic liquid. Environ Sci Technol 40, 4761–4764.

Jaeckel P, Krauss GJ, Krauss G, 2005. Cadmium and zinc response of the fungi *Heliscus lugdunensis* and *Verticillium* cf. *alboatrum* isolated from highly polluted water. Sci Total Environ 346, 274–279.

Kaegi R, Ulrich A, Sinnet B, Vonbank R, Wichser A, Zuleeg S, Simmler H, Brunner S, Vonmont H, Burkhardt M, Boller M, 2008. Synthetic TiO_2 nanoparticle emission from exterior facades into the aquatic environment. Environ Pollut 156, 233–239.

Karlsson HL, Gustafsson J, Cronholm P, Möller L, 2009. Size-dependent toxicity of metal oxide particles–A comparison between nano- and micrometer size. Toxicol Lett 188, 112–118.

Kasemets K, Ivask A, Dubourguier HC, Kahru A, 2009. Toxicity of nanoparticles of ZnO, CuO and TiO_2 to yeast *Saccharomyces cerevisiae*. Toxicol in Vitro 23, 1116–1122.

Kim JS, Kuk E, Yu KN, Kim JH, Park SJ, Lee HJ, Kim SH, Park YK, Park YH, Hwang CY, Kim YK, Lee YS, Jeong DH, Cho MH, 2007. Antimicrobial effects of silver nanoparticles. Nanomedicine 3, 95–101.

Kim KJ, Sung WS, Moon SK, Choi JS, Kim JG, Lee DG, 2008. Antifungal effect of silver nanoparticles on dermatophytes. J Microbiol Biotechnol 18, 1482–1484.

Luechinger NA, Athanassiou EK, Stark WJ, 2008. Graphene-stabilized copper nanoparticles as an air-stable substitute for silver and gold in low-cost ink-jet printable electronics. Nanotechnology 19, 445201 (6 pp).

Medeiros A, Duarte S, Pascoal C, Cássio F, Graça MAS, 2010. Effects of Zn, Fe and Mn on leaf litter breakdown by aquatic fungi: a microcosm study. Internat Rev Hydrobiol 95, 12–26.

Miao AJ, Schwehr KA, Xu C, Zhang SJ, Luo Z, Quigg A, Santschi PH, 2009. The algal toxicity of silver engineered nanoparticles and detoxification by exopolymeric substances. Environ Pollut 157, 3034–3041.

Moreirinha C, Duarte S, Pascoal C, Cássio F, 2011. Effects of cadmium and phenanthrene mixtures on aquatic fungi and microbially mediated leaf litter decomposition. Arch Environ Contam Toxicol 61, 211–219.

Mortimer M, Kasemets K, Kahru A, 2010. Toxicity of ZnO and CuO nanoparticles to ciliated protozoa *Tetrahymena thermophila*. Toxicology 269, 182–189.

Mueller NC, Nowack B, 2008. Exposure modeling of engineered nanoparticles in the environment. Environ Sci Technol 42, 4447–4453.

Nair LS, Laurencin CT, 2007. Silver nanoparticles: synthesis and therapeutic applications. J Biomed Nanotech 3, 301–316.

Navarro E, Baun A, Behra R, Hartmann NB, Filser J, Miao, AJ, Quigg A, Santschi PH, Sigg L, 2008. Environmental behavior and ecotoxicity of engineered nanoparticles to algae, plants, and fungi. Ecotoxicology 17, 372–386.

Niyogi DK, Lewis Jr WM, McKnight DM, 2002. Effects of stress from mine drainage on diversity, biomass, and function of primary producers in mountain streams. Ecosystems 5, 554–567.

Norland S, 1993. The relationship between biomass and volume of bacteria. In: Kemp PF, Sherr BF, Sherr EB, Cole JJ (Eds) Handbook of Methods in Aquatic Microbial Ecology, Lewis publishers, Boca Raton, Florida, pp 303–307.

Pan Y, Neuss S, Leifert A, Fischler M, Wen F, Simon U, Schmid G, Brandau W, Jahnen-Dechent W, 2007. Size-dependent cytotoxicity of gold nanoparticles. Small 3, 1941–1949.

Panyala NR, Peña-Méndez EM, Havel J, 2008. Silver or silver nanoparticles: a hazardous threat to the environment and human health? J Appl Biomed 6, 117–119.

Pascoal C, Cássio F, 2004. Contribution of fungi and bacteria to leaf litter decomposition in a polluted river. Appl Environ Microbiol 70, 5266–5273.

Pascoal C, Cássio F, Gomes P, 2001. Leaf breakdown rates: a measure of water quality? Int Rev Hydrobiol 86, 407–416.

Pascoal C, Cássio F, Marcotegui A, Sanz B, Gomes P, 2005a. Role of fungi, bacteria, and invertebrates in leaf litter breakdown in a polluted river. J N Am Benthol Soc 24, 784–797.

Pascoal C, Marvanová L, Cássio F, 2005b. Aquatic hyphomycete diversity in streams of Northwest Portugal. Fungal Divers 19, 109–128.

Pascoal C, Pinho M, Cássio F, Gomes P, 2003. Assessing structural and functional ecosystem condition using leaf breakdown: studies on a polluted river. Freshwat Biol 48, 2033–2044.

Perugini P, Simeoni S, Scalia S, Genta I, Modena T, Conti B, Pavanetto F, 2002. Effect of nanoparticle encapsulation on the photostability of the sunscreen agent, 2-ethylhexyl-p-methoxycinnamate. Int J Pharm 246, 37–45.

Ren G, Hu D, Cheng EWC, Vargas-Reus MA, Reip P, Allaker RP, 2009. Characterisation of copper oxide nanoparticles for antimicrobial applications. Int J Antimicrob Ag 33, 587–590.

Rispoli F, Angelov A, Badia D, Kumar A, Seal S, Shah V, 2010. Understanding the toxicity of aggregated zero valent copper nanoparticles against *Escherichia coli*. J Hazard Mater 180, 212–216.

Saison C, Perreault F, Daigle JC, Fortin C, Claverie J, Morin M, Popovic R, 2010. Effect of core–shell copper oxide nanoparticles on cell culture morphology and photosynthesis (photosystem II energy distribution) in the green alga, *Chlamydomonas reinhardtii*. Aquat Toxicol 96, 109–114.

Salata OV, 2004. Applications of nanoparticles in biology and medicine. J Nanobiotechnol 2 (6 pp).

Saquing CD, Manasco JL, Khan SA, 2009. Electrospun nanoparticle–nanofiber composites via a one-step Synthesis. Small 5, 944–951.

Schneider T, Gerrits B, Gassmann R, Schmid E, Gessner MO, Richter A, Battin T, Eberl L, Riedel K, 2010. Proteome analysis of fungal and bacterial involvement in leaf litter decomposition. Proteomics 10, 1819–1830.

Shah V, Belozerova I, 2009. Influence of metal nanoparticles on the soil microbial community and germination of lettuce seeds. Water Air Soil Pollut 197, 143–148.

Shah V, Dobiášová P, Baldrian P, Nerud F, Kumar A, Seal S, 2010. Influence of iron and copper nanoparticle powder on the production of lignocellulose degrading enzymes in the fungus *Trametes versicolor*. J Hazard Mater 178, 1141–1145.

Sridhar KR, Bärlocher F, Krauss GJ, Krauss G, 2005. Response of aquatic hyphomycete communities to changes in heavy metal exposure. Int Rev Hydrobiol 90, 21–32.

Van Hoecke K, Quik JT, Mankiewicz-Boczek J, De Schamphelaere KA, Elsaesser A, Van der Meeren P, Barnes C, McKerr G, Howard CV, Van de Meent D, Rydzyński K, Dawson KA, Salvati A, Lesniak A, Lynch I, Silversmit G, De Samber B, Vincze L, Janssen CR, 2009. Fate and effects of CeO_2 nanoparticles in aquatic ecotoxicity tests. Environ Sci Technol 43, 4537–4546.

Wang W, Zhan Y, Wang X, Liu Y, Zheng C, Wang G, 2002. Synthesis and characterization of CuO nanowhiskers by a novel one-step, solid-state reaction in the presence of a nonionic surfactant. Mater Res Bull 37, 1093–1100.

White TJ, Bruns T, Lee S, Taylor JW, 1990. Amplification and direct sequencing of fungal ribosomal RNA genes for phylogenetics. In: Innis MA, Gelfand DH, Sninsky JJ, White TJ (Eds) PCR Protocols: A Guide to Methods and Applications, Academic Press, Inc, New York, pp 315–322.

Yoon KY, Byeon JH, Park JH, Hwang J, 2007. Susceptibility constants of *Escherichia coli* and *Bacillus subtilis* to silver and copper nanoparticles. Sci Total Environ 373, 572–575.

Zar JH, 2009. Biostatistical Analysis, fifth ed, Prentice-Hall, Upper Saddle River, New Jersey.

Zhang F, Wu X, Chen Y, Lin H, 2009. Application of silver nanoparticles to cotton fabric as an antibacterial textile finish. Fibers Polym 10, 496–501.

Chapter 3

Toxicity of nanoCuO to microbial decomposers depends on nanoparticle size and concentration of humic acid in freshwaters

Abstract

In aquatic environments, the reactive surface area of nanoparticles prone to interact with natural organic matter (NOM) may determine the impacts of nanometal oxides on biota. In streams, heterotrophic microbes, predominantly fungi, play a key role in detritus food webs by transferring energy from plant-litter to higher trophic levels. We investigated the impacts of three sizes of nanoCuO (12, 50 and 80 nm powder; ≤400 mg L^{-1}) and of humic acid (HA; ≤100 mg L^{-1}), a major component of NOM, on stream-dwelling microbes associated with decomposing leaf litter. Results showed that the exposure to increasing concentrations of decreasing size of nanoCuO reduced leaf decomposition, microbial biomass, and fungal reproduction and diversity. Alterations in leaf surface morphology further supported the impacts of nanoparticles on microbial activity on decomposing leaves. Bacteria were more sensitive than fungi to nanoCuO, because EC_{50} values for biomass of bacteria were much lower than those of fungi (50-times lower for 12 and 50 nm nanoCuO, and 12-times lower for 80 nm nanoCuO). Fungal reproduction was more sensitive to nanoCuO than leaf decomposition or microbial biomass. Microbial activity on decomposing leaves was also inhibited by exposure to increasing concentrations of HA in the absence of nanoCuO. The adverse effects of smaller size nanoCuO were alleviated by the presence of HA.

Keywords: NanoCuO size, humic acid, fungi, bacteria, leaf decomposition, streams.

3.1. Introduction

The engineered nanocopper oxide (nanoCuO) has a wide range of applications for human welfare, mostly in the fields of electronics and biomedicines (Carnes and Klabunde, 2003; Dutta et al., 2003; Zhang et al., 2008; Ren et al., 2009), and has been reported to be toxic to a wide range of living biota including aquatic organisms, such as bacteria, protozoa, algae and invertebrates (Heinlaan et al., 2008; Mortimer et al., 2010; Saison et al., 2010). However, most studies are based on individual responses of organisms that are inadequate to predict the impacts of nanoCuO on aquatic communities and associated ecosystem processes (but see Pradhan et al., 2011). Studies have demonstrated that effects of metal oxide nanoparticles on aquatic biota can differ from those of their bulk counterparts (Kahru et al., 2008; Aruoja et al., 2009), but only few studies have explored how toxicity of nanometal oxides to biota may vary with the nanoparticle size (Van Hoecke et al., 2009; Bang et al., 2011; Azam et al., 2012).

In freshwaters, humic acid (HA) is a significant part of natural or dissolved organic matter (NOM or DOM) (Ma et al., 2001), which is often expressed as dissolved organic carbon (DOC) (Al-Reasi et al., 2011). Concentration of HA in natural waters may rise up to several hundreds mg L^{-1} of DOC (Wall and Choppin, 2003); however, in oligotrophic streams, the concentration of HA ranges between 1–100 mg L^{-1} (Steinberg et al., 2006). Humic acid has been reported to exhibit toxicity against living organisms including freshwater invertebrates (Meems et al., 2004; Yang et al., 2004; Timofeyev et al., 2006). However, several ionic metals can bind to carboxylic groups of HA decreasing metal bioavailability and toxicity (Tsiridis et al 2005). Some reports explained changes in metal oxide toxicity to biota based on the quantity of DOC in the stream water (e.g. Blinova et al., 2010). The protective role of HA against Cu^{2+} toxicity to some aquatic organisms (e.g. sea urchin larvae, Lorenzo et al 2002; photobacterium *Vibrio fischeri*, Tsiridis et al., 2005) has been reported. However, studies on the impact of HA on nanoCuO toxicity in aquatic biotic communities are not available.

In low order forested streams, plant-litter decomposition of riparian vegetation by microbes and invertebrates is a key ecosystem process ensuring organic matter turnover and energy transfer from plant litter to higher trophic levels (Pascoal et al., 2005a). Both fungi and bacteria play a significant role in this ecological process. Fungi are recognized to have a dominant role at earlier stages

of litter decomposition, while bacteria appear to gain importance after partial decomposition of plant-litter (Pascoal and Cássio, 2004). Plant-litter decomposition is sensitive to water quality and this integrative process was proposed as a functional measure to assess the health of stream ecosystems (Pascoal et al., 2001; Gessner and Chauvet, 2002; Pascoal et al., 2005a). In microcosm experiments, the structure and function of microbial communities were affected by exposure to ionic copper (Fernandes et al., 2009) or nanoCuO (Pradhan et al., 2011). However, no information is available on how microbial communities and the ecological processes they drive respond to different nanoparticle sizes and to the concomitant presence of dissolved organic matter in the stream water.

We investigated the interactive effects between CuO nanoparticle sizes and humic acid on microbial communities involved in leaf-litter decomposition in streams under the hypotheses that: i) smaller nanoparticles would exhibit higher toxicity than larger nanoparticles because of their higher reactive surface area, ii) in the absence of nanoCuO, HA would have negative impacts on microbial communities, iii) effects of nanoCuO and HA would be dose-dependent, and iv) HA would alleviate nanoCuO toxicity to biota if interactions with nanoparticles decreased nanoCuO bioavailability. We used a microcosm approach with stream-dwelling microbial communities that were exposed to increasing concentrations of nanoCuO with three sizes in the absence or presence of HA. The measured endpoints were leaf decomposition, fungal and bacterial biomass, and fungal reproduction and diversity. In addition, surface of leaves unexposed or exposed to the chemicals were analysed by scanning electron microscopy to monitor the surface integrity and biosorption of the chemicals.

3.2. Material and Methods

3.2.1. Microbial colonization of leaves

Leaves of *Alnus glutinosa* (L.) Gaertn. (alder), a common riparian tree in the Iberian Peninsula, were collected from a single tree in autumn just before abscission, and air dried at room temperature. The leaves were soaked in deionised water, cut into 12 mm-diameter disks, and sets of 80 disks were placed into fine-mesh bags (15 × 15 cm, 0.5-mm size mesh for preventing invertebrate colonization).

Leaf bags were immersed in the Maceira Stream (N 41°45'58.79'', W 8°08'49.39'', altitude 867 m, National Park of Peneda-Gerês, Portugal) for 7 days to allow microbial colonization. Further details of the sampling site can be found in Pradhan et al. (2011).

At the time of leaf immersion, stream water had a temperature of 13.8°C, a pH of 5.8 and a conductivity of 16 µS cm^{-1} measured *in situ* with field probes (Multiline F/set 3 no. 400327, WTW, Weilheim, Germany). Stream water samples were collected in sterile dark bottles, and transported in a cold box at 4ºC to the laboratory to determine the concentrations of inorganic nutrients with a HACH DR/2000 photometer (HACH, Loveland, CO, USA). Nutrient concentrations were: 30 µg L^{-1} $N\text{-}NO_3^-$ (HACH kit, programme 351), 2 µg L^{-1} $N\text{-}NO_2^-$, (HACH kit, programme 371) and 20 µg L^{-1} $P\text{-}PO_4^{3-}$ (HACH kit, programme 490).

3.2.2. Preparation of nanocopper oxide and humic acid (HA) stocks and characterization of nanoparticles

Stock suspensions of three size nanocopper oxides, namely i) 12 nm CuO nanopowder (99.5%, Ionic Liquid Technology (IO-LI-TEC), Heilbronn, Germany), ii) 50 nm CuO nanopowder (99.5%, Sigma-Aldrich, St. Louis, MO), and iii) 80 nm (99.9%, IO-LI-TEC), were prepared in autoclaved stream water (121°C, 20 min) by sonication at 42 kHz in a sonication bath (Branson 2510, Danbury, CT, USA) for 30 min in dark before use (Heinlaan et al., 2008). Stock solution of humic acid (Sigma-Aldrich, St. Louis, MO, USA) was prepared in sterile stream water by stirring for 10 h at room temperature prior to use. The pH of all nanoCuO suspensions and HA solution was adjusted to the stream water pH (5.8 ± 0.2).

NanoCuO size in the stock suspensions was analysed by scanning electron microscopy (SEM, Leica Cambridge S 360, Cambridge, UK) coupled to an energy dispersive X-ray microanalysis setup (EDX, 15 KeV) and by dynamic light scattering (DLS) using a zetasizer (Malvern, Zetasizer Nano ZS), as described by Pradhan et al. (2011, 2012). SEM analyses of nanoCuO suspensions of 12, 50 and 80 nm powder revealed that the size of CuO nanoparticles ranged between 10–30 nm, 30–50 nm and 80–120 nm, respectively (not shown). DLS showed that nanoparticles had an average size larger than the primary particles measured by SEM, and corresponded to 101.8 nm (PdI 0.137), 202.4 nm (PdI 0.181) and 267.6 nm (PdI 0.296) for 12, 50 and 80 nm, respectively. These results suggested agglomeration of

nanoparticles in the stream water as described before (Buffet et al., 2011; Pradhan et al., 2012).

3.2.3. Microcosm experiment

Bags containing microbially-colonized leaf disks were retrieved from the stream and brought to the laboratory. Leaf disks from each bag were rinsed with deionised water and placed into 150 mL sterile Erlenmeyer flasks with 80 mL of filtered (MN GF-3 filter paper, Macherey-Nagel, Germany) and autoclaved stream water. To determine the impacts of nanoCuO and/or HA, stream water was supplemented with: i) increasing concentrations of each size nanoCuO (0, 50, 100, 200 or 400 mg L^{-1}), ii) increasing concentrations of HA (0, 20 or 100 mg L^{-1}), and iii) all combinations of each concentration and size of nanoCuO with HA. Three replicate flasks were prepared per treatment. Microcosms were incubated at 14ºC under shaking at 140 rpm (Certomat BS 3, Melsungen, Germany), and solutions were renewed after 10 days. At the end of the experiment (20 days), leaf disks were collected for quantification of leaf mass loss and microbial biomass, and microcosm solutions were used for assessing fungal sporulation as described below.

3.2.4. Leaf decomposition

Leaf mass loss in each microcosm was determined as the difference between leaf dry mass at the beginning and at the end of microcosm experiment. Leaf disks from each replicate were freeze-dried (Christ alpha 2–4 LD Plus, B. Braun, Germany) to constant mass (72 h) and weighed to the nearest 0.001 mg.

3.2.5. Microbial biomass

Fungal biomass associated with decomposing leaves was estimated based on ergosterol concentration on leaves (Gessner, 2005). Lipids were extracted from sets of 6 leaf disks per replicate by heating (30 min, 80°C) in 0.8% KOH-methanol and the extract was purified by solid-phase extraction and eluted in isopropanol. Ergosterol was quantified by high-performance liquid chromatography (HPLC) using a LiChrospher RP18 column (250 × 4 mm, Merck) connected to a Beckmann Gold liquid chromatographic system running isocratically with HPLC-grade methanol at 1.4 mL min^{-1} and 33°C. The peak of ergosterol was detected at 282 nm. A standard

series of ergosterol (Sigma) in isopropanol were used to estimate the ergosterol concentration which was further converted to fungal biomass assuming 5.5 µg ergosterol mg^{-1} mycelial dry mass (Gessner, 2005).

To estimate bacterial biomass, sets of 4 leaf disks from each replicate were placed into falcon tubes with 10 mL of phosphate buffered formalin (2% final concentration) and kept at 4°C until processed. Bacterial cells were dislodged from leaves by sonication in a bath (42 kHz, 100 W; Branson 2510, Danbury, CT, USA) for 5 min, with cooling in ice after each 1 min of sonication to avoid cell damage. Serial dilutions of bacterial suspensions were prepared, and 2 mL aliquot of each bacterial suspension was mixed with 4′,6-diamidino-2-phenylindole (DAPI, 40 µL of 0.1 mg mL^{-1}; Molecular Probes, Eugene, OR, USA) and incubated for 10 min in the dark to stain bacterial cells. Bacterial suspensions were filtered through black polycarbonate membranes (0.2 µm pore size, GTTP, Millipore, Billerica, MA, USA), and filters were mounted on slides between two drops of immersion oil. Bacterial cells were counted under an epifluorescence microscope (1000× magnification; Leitz Laborlux Heerbrug, Switzerland), and bacterial numbers were converted to bacterial biomass considering a mean biomass of 20 fg $cell^{-1}$ (Norland, 1993).

3.2.6. Fungal sporulation rates

Suspensions with released fungal conidia from each replicate microcosm were mixed with Triton X-100 (40 µl of 15%), to minimize conidial adherence to the flask, and the conidia were fixed with 2% formaldehyde. Adequate volumes of conidial suspensions were filtered (5 µm pore size, Millipore, Billerica, MA, USA), and the conidia were stained with 0.05% cotton blue in lactic acid, and identified and counted under a light microscope (400× magnification; Leica Biomed, Heerbrug, Switzerland).

3.2.7. Morphology of leaves under SEM

Freeze-dried leaves were fixed in 2.5% (v/v) glutaraldehyde for 24 h, and glued onto 12.7-mm diameter metallic SEM pin stub specimen mounts, coated with gold under vacuum and scanned by SEM-EDX as above.

3.2.8. Data analyses

Analyses of variance were used to test significant effects of chemicals on leaf mass loss, fungal biomass, bacterial biomass and fungal sporulation as follows: three-way ANOVAs were used to test the effects of concentrations of nanoCuO and HA at different nanoparticle sizes. Because HA did not have a significant effect on fungal biomass when overall data was considered, a separate one-way ANOVA was used to test the effects of HA concentrations in the absence of nanoCuO. Bonferroni post-tests were used to check in which treatments significant differences occurred (Zar, 2009). To achieve normal distribution and homoscedasticity, data in percentage were arcsine square root transformed (Zar, 2009). Analyses were performed with Statistica 6.0 (Statsoft, Inc., Tulsa, OK, USA). The effective concentration of each size nanoCuO inducing 50% of decrease (EC_{50}, 95% C.I.) in leaf decomposition, fungal or bacterial biomass, and fungal sporulation rate was calculated using PriProbit 1.63 (Sakuma, 1998).

3.3. Results

3.3.1. Effects of nanoCuO and HA on fungal diversity

After 20 days of experiment, a total of 12 fungal species were identified in control microcosms based on conidial morphology (Table 3.1). The exposure to nanoCuO decreased fungal species richness in a concentration-dependent manner, and effects became more pronounced as nanoparticle size decreased (4, 5 and 8 species after exposure to 400 mg L^{-1} nanoCuO with 12, 50 and 80 nm, respectively) (Table 3.1). The exposure to 100 mg L^{-1} of HA alone decreased fungal richness to 8 species (Table 3.1). However, fungal species richness was less inhibited when fungi were co-exposed to HA and smaller size nanoparticles (Table 3.1).

In control, *Articulospora tetracladia* was the dominant species (83.3%) followed by *Flagellospora* sp. (8.3%) (Table 3.1). Exposure to the highest concentrations of nanoCuO and/or HA decreased the contribution of *Flagellospora* sp. but increased that of *Heliscus lugdunensis* (Table 3.1). The percentage contribution of *H. lugdunensis* increased with the decrease in nanoCuO size (Table 3.1).

Table 3.1 Contribution of aquatic fungal sporulating species on decomposing leaves to the total spore production and species richness after 20 days of exposure to CuO nanoparticles (NP; 400 mg L^{-1}) with different sizes (12, 50 and 80 nm) and/or humic acid (HA; 100 mg L^{-1})

Fungal species	% of conidia							
	Control	HA	NP 12	NP 50	NP 80	NP 12 + HA	NP 50 + HA	NP 80 + HA
Alatospora acuminata Ingold	0.2	nd	nd	nd	nd	nd	nd	nd
Anguillospora filiformis Greath	1.1	0.5	nd	nd	0.2	0.4	0.7	1.0
Articulospora tetracladia Ingold	83.3	76.0	66.5	69.2	72.4	73.2	75.1	74.4
Culicidospora aquatica R.H. Petersen	0.1	nd	nd	nd	nd	nd	nd	nd
Flagellospora sp.	8.3	5.9	4.1	4.4	5.7	7.1	6.9	6.3
Fontanospora eccentrica (R.H. Petersen) Dyko	1.5	2.2	nd	nd	1.4	1.0	1.3	1.5
Fontanospora fusiramosa Marvanová, P.J. Fisher, Descals & Bärlocher	2.2	5.3	4.0	4.3	5.1	3.3	4.0	4.5
Heliscus lugdunensis Sacc. & Therry	0.3	6.9	25.4	21.5	12.6	13.8	10.2	9.5
Lunulospora curvula Ingold	0.1	nd	nd	nd	nd	nd	nd	nd
Tricladium attenuatum Iqbal	0.7	1.5	nd	nd	1.2	0.4	0.7	1.0
Tricladium splendens Ingold	0.2	nd	nd	nd	nd	nd	nd	nd
Varicosporium elodeae W. Kegel	2.0	1.7	nd	0.6	1.4	0.8	1.1	1.8
Fungal species richness	12	8	4	5	8	8	8	8

nd: not detected.

3.3.2. Effects of nanoCuO and HA on fungal sporulation

After 20 days, sporulation rate of aquatic hyphomycetes attained 302 × 10^3 spores g^{-1} leaf dry mass day^{-1} in control microcosms. Fungal sporulation was significantly affected by nanoCuO size and concentration and by HA concentration (three-way ANOVAs, *P<0.05*). In the absence of HA, the effects were stronger at smaller size and higher concentrations of CuO nanoparticles with inhibitions of fungal sporulation up to 99.5% (Fig. 3.1A-C). The EC_{50} value increased with the increase in nanoparticle size (EC_{50}: 3.0, 8.3 and 46.9 mg L^{-1} for nanoCuO with 12, 50 and 80 nm, respectively; Table 2). The exposure to HA alone also inhibited fungal sporulation up to 82.4% at the highest HA concentration (Fig. 3.1A-C). However, the presence of HA alleviated the toxicity of smaller size nanoCuO (12 and 50 nm) in a dose-dependent manner (*P<0.05*; Fig. 3.1A and B). Maximum

alleviating effects of HA on nanoCuO toxicity occurred when fungi were exposed to 100 mg L^{-1} HA and 400 mg L^{-1} of 12 nm nanoCuO (41.4% recovery; Fig. 3.1A).

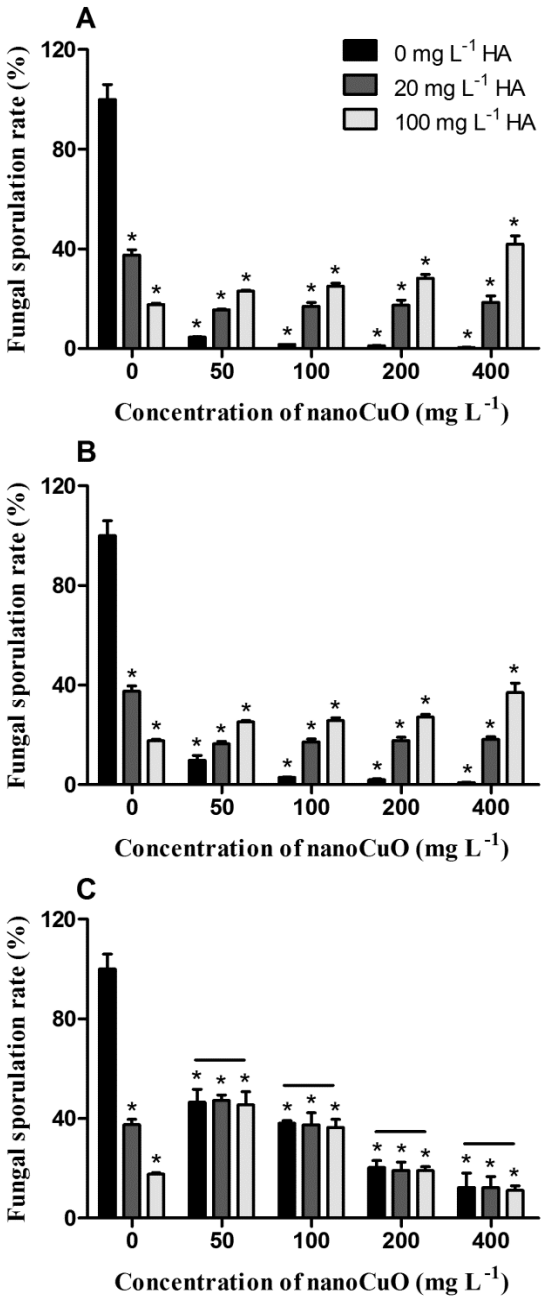

Figure 3.1 Fungal sporulation rate (% of control) on decomposing alder leaves exposed for 20 days to increasing concentrations of three sizes of nanoCuO or humic acid (HA) alone or in mixtures. NanoCuO sizes were: 12 nm (A), 50 nm (B) and 80 nm (C). Mean ± SEM, n=3. *, treatments that differ significantly from control. Horizontal lines indicate no significant differences between HA treatments.

3.3.3. Effects of nanoCuO and HA on microbial biomass

After 20 days, fungal biomass on leaves attained 68.8 mg g^{-1} leaf dry mass in the control (not shown). When overall data was considered, fungal biomass was

affected by the size and concentration of nanoCuO, but not by HA (three-way ANOVA, *P<0.05* for significant effects; Fig. 3.2A-C). Fungal biomass decreased with increasing nanoCuO concentration and decreasing nanoparticle size. At the highest concentration of nanoparticles, fungal biomass inhibitions were: 47.7, 60.8 and 67.1% for 12, 50 and 80 nm nanoCuO, respectively (Fig. 3.2A-C). The lowest observed effective concentrations (LOEC) for ascending nanoCuO size were 50, 100 and 400 mg L^{-1}, respectively (*P<0.05*; Table 2). The lowest EC_{50} value for nanoCuO with smaller size also indicated higher toxicity of smaller nanoparticles to fungal biomass production (EC_{50}: 272.5, 735.4, 1850.4 mg L^{-1} for 12, 50 and 80 nm nanoCuO, respectively; Table 2).

In the absence of nanoparticles, the exposure to the highest HA concentration (100 mg L^{-1}) decreased fungal biomass by 35.9% (one-way ANOVA, *P<0.05*; Fig. 3.2A-C). HA alleviated the inhibitory effects of increasing concentrations of 12 or 50 nm nanoCuO on fungal biomass (*P<0.05*; Fig. 3.2A and B). The highest recovery of fungal biomass (41.0%) was observed after co-exposure to 100 mg L^{-1} of HA and 400 mg L^{-1} of 12 nm nanoCuO (Fig. 3.2A and B). However, HA did not alleviate the effects of 80 nm of nanoCuO on fungal biomass (*P>0.05*; Fig. 3.2C).

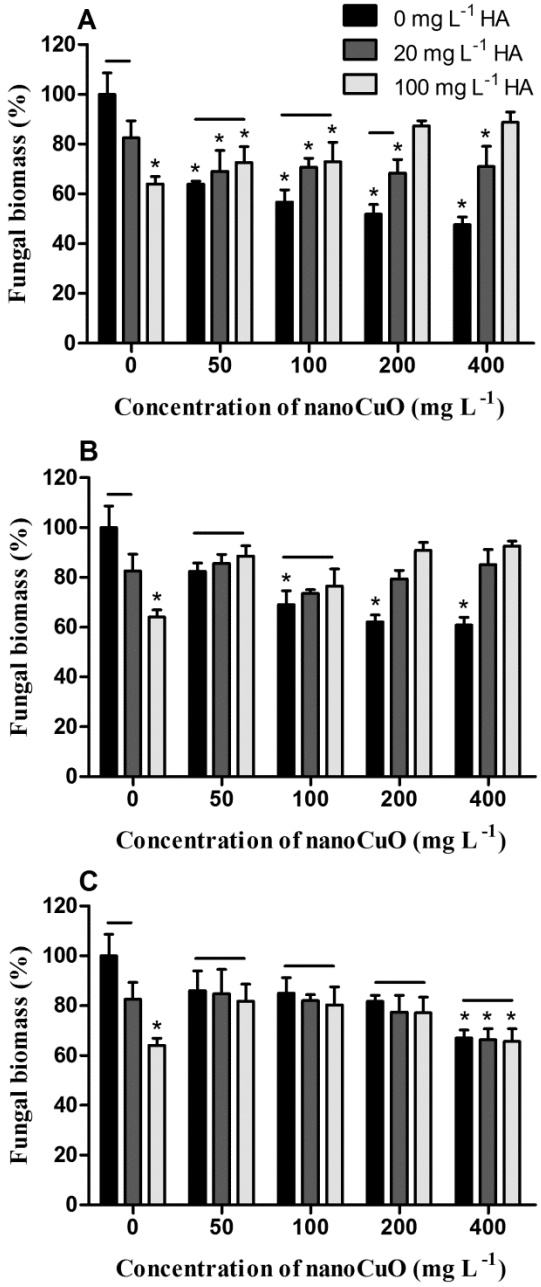

Figure 3.2 Fungal biomass (% of control) on the decomposing alder leaves exposed for 20 days to increasing concentrations of three sizes of nanoCuO or humic acid (HA) alone or in mixtures. NanoCuO sizes were: 12 nm (A), 50 nm (B) and 80 nm (C). Mean ± SEM, n=3. *, treatments that differ significantly from control. Horizontal lines indicate no significant differences between HA treatments.

Bacterial biomass on leaves in control microcosms was 0.31 mg g^{-1} leaf dry mass (not shown). Bacterial biomass was affected by exposure to HA and to nanoCuO of different sizes and concentrations (three-way ANOVA, *P<0.05*; Fig. 3.3A-C). Bacterial biomass decreased significantly after exposure to all nanoparticle sizes at all tested concentrations (LOEC was 50 mg L^{-1} for all nanoCuO sizes;

P<0.05; Table 2; Fig. 3.3A-C). The effects were stronger at higher concentrations and smaller nanoparticle size, with minimum bacterial biomass at 400 mg L^{-1} of nanoCuO (6.6, 9.6 and 31.2% for 12, 50 and 80 nm nanoCuO, respectively comparing to control; Fig. 3.3A-C). The EC_{50} values showed that effect of smaller size nanoCuO was stronger than that of larger size nanoCuO on bacterial biomass (EC_{50}: 5.0, 14.1 and 156.6 mg L^{-1} for 12, 50 and 80 nm nanoCuO, respectively; Table 2).

Bacterial biomass decreased significantly by exposure to increasing concentration of HA alone, with a maximum inhibition of 56.0% at 100 mg L^{-1} of HA (*P<0.05*; Fig. 3A-C). Exposure to increasing concentrations of smaller size (12 nm and 50 nm) nanoparticles with increasing concentration of HA led to a significant recovery of bacterial biomass comparing to the effects promoted by nanoCuO in the absence of HA (*P<0.05*; Fig. 3.3A and B). Maximum recovery of biomass was observed at the highest concentrations of nanoCuO and HA (recovery: 11.4% and 10.4% for 12 nm and 50 nm, respectively; Fig. 3.3A and B). However, HA did not alleviate the effects promoted by the larger size nanoCuO (80 nm) on bacterial biomass (*P>0.05*; Fig. 3.3C).

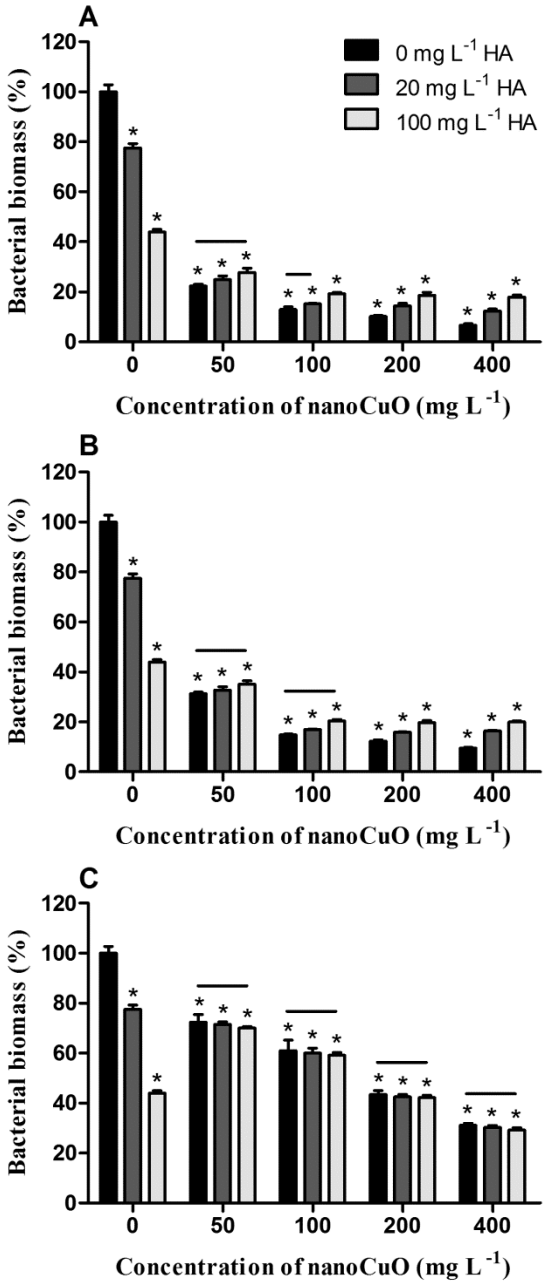

Figure 3.3 Bacterial biomass (% of control) on decomposing alder leaves exposed for 20 days to increasing concentrations of three sizes of nanoCuO or humic acid (HA) alone or in mixtures. NanoCuO sizes were: 12 nm (A), 50 nm (B) and 80 nm (C). Mean ± SEM, n=3. *, treatments that differ significantly from control. Horizontal lines indicate no significant differences between HA treatments.

3.3.4. Effects of nanoCuO and HA on leaf decomposition

After 20 days, leaf mass loss in control microcosms was 48.7%. Humic acid, size and concentration of nanoCuO had significant effects on leaf decomposition (three-way ANOVA, *P<0.05*; Fig. 3.4A-C). Leaf decomposition was lowest after exposure to the highest concentration (400 mg L^{-1}) of smallest size nanoCuO

(27.3% for 12 nm, 45.0% for 50 nm and 59.1% for 80 nm, comparing to control; Fig. 3.4A-C). The LOEC for 12, 50 and 80 nm CuO nanoparticles on leaf decomposition were 50, 100 and 400 mg L^{-1}, respectively (*P<0.05*; Table 2). The EC_{50} values for nanoCuO increased as nanoparticle size increased (EC_{50}: 83.1, 286.7 and 680.1 mg L^{-1} for ascending size of nanoCuO; Table 2).

The presence of HA alone decreased significantly leaf decomposition, and a maximum inhibition of 67.5% was found at the highest concentration of HA (100 mg L^{-1}) (*P<0.05*, Fig. 3.4A-C). However, the exposure to HA alleviated the effects caused by 12 and 50 nm nanoCuO on leaf decomposition (*P<0.05*; Fig. 3.4A and B). The co-exposure to HA (100 mg L^{-1}) with 200 or 400 mg L^{-1} of 12 nm nanoCuO led to a recovery in leaf decomposition of about 35.4 and 49.7%, respectively (Fig. 3.4A). However, no significant recovery in leaf decomposition was observed when leaves were co-exposed to larger size nanoCuO (80 nm) and HA (*P>0.05*; Fig. 3.4C).

Table 3.2 Lowest observed effective concentration (LOEC) and effective concentration inducing 50% inhibition (EC_{50}) of leaf decomposition (LD), fungal biomass (FB) and bacterial biomass (BB), and fungal sporulation (FS) after 20 days exposure to three sizes of nanoCuO

NanoCuO size (nm)	LOEC (mg L^{-1})				EC_{50} (mg L^{-1})			
	LD	FB	BB	FS	LD	FB	BB	FS
12	50	50	50	50	83.1 (45.7–117.9)	272.5 (145.5–6150.6)	5.0 (0.07–18.7)	3.0 (0.01–7.4)
50	100	100	50	50	286.7 (192.5–650.6)	735.4 (378.5–6402.2)	14.1 (1.8–29.5)	8.3 (0.08–21.5)
80	400	400	50	50	680.1 (427.7–1759.7)	1850.4 (714.9–61337.8)	156.6 (122.6–203.8)	46.9 (26.5–65.1)

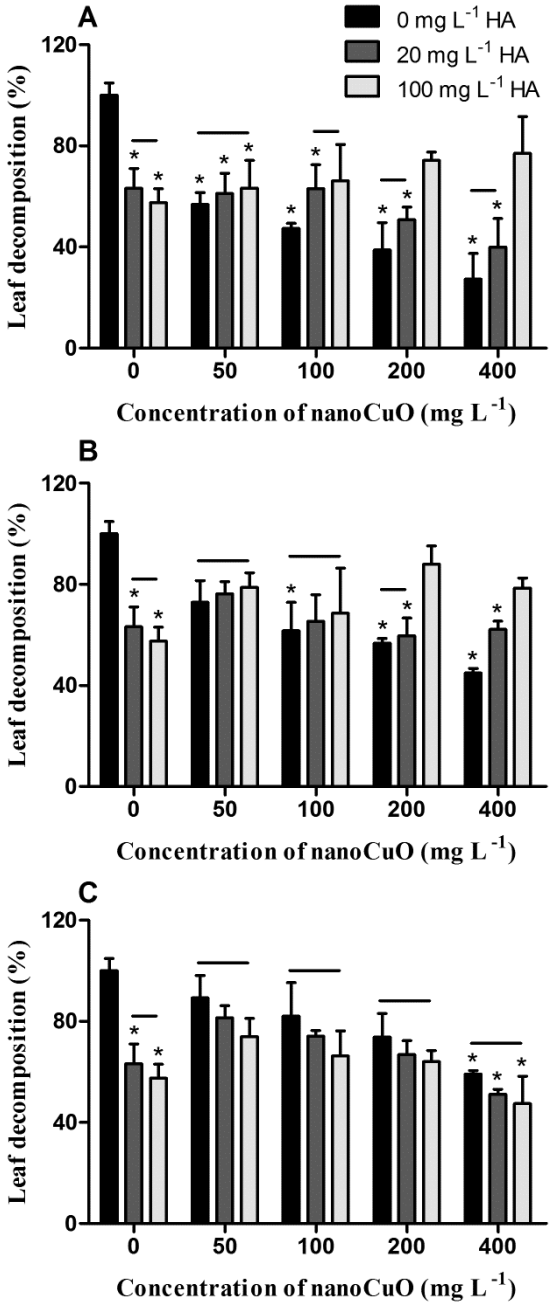

Figure 3.4 Decomposition of alder leaves (% of control) exposed for 20 days to increasing concentrations of three sizes of nanoCuO or humic acid (HA) alone or in mixtures. NanoCuO sizes were: 12 nm (A), 50 nm (B) and 80 nm (C). Mean ± SEM, n=3. *, treatments that differ significantly from control. Horizontal lines indicate no significant differences between HA treatments.

3.3.5. Leaf litter surface after exposure to nanoCuO and HA

After 20 days, SEM analysis revealed that the surface of control leaves had evidence of high decomposition because the outer and inner tissues of the leaves were poorly preserved (Fig. 3.5, panel I) and colonization by microbes was visible

(Fig. 3.5, panel II). After exposure to all nanoCuO sizes, the leaves were less decomposed and nanoparticles were adsorbed to leaf surface (Fig. 3.5). The presence of copper was confirmed by EDX (not shown). Self-aggregation and adsorption of nanoCuO varied with nanoparticle size: self-aggregation was lower and adsorption was higher in treatments with smaller size (12 and 50 nm) nanoparticles (Fig. 3.5, panel II). In the absence of nanoCuO, the leaves exposed to HA showed more preserved surfaces but evidence of microbial colonization was found (Fig. 3.5, panel II). Leaf surfaces seemed to be more decomposed after co-exposure to HA and smaller size nanoCuO than when exposed to each chemical alone (Fig. 3.5, panel I). However, no remarkable differences in leaves were observed after exposure to 80 nm nanoCuO with or without HA (Fig. 3.5). Under these conditions, aggregation of nanoCuO and/or HA was observed on leaves.

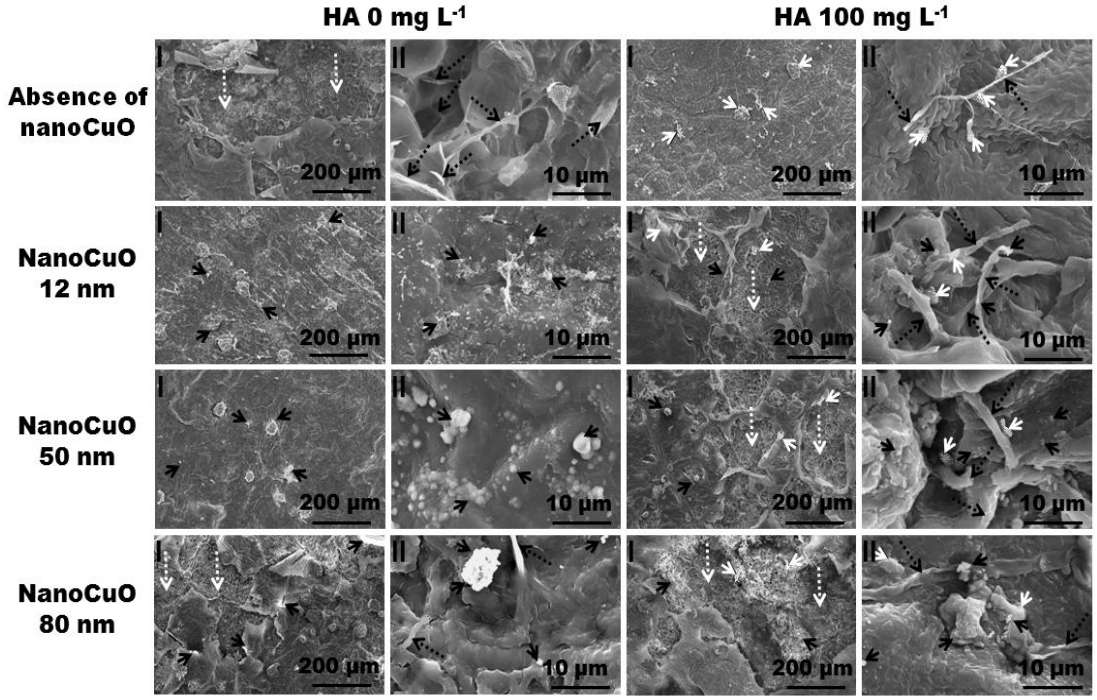

Figure 3.5 SEM visualization of surface of decomposing alder leaves unexposed or exposed for 20 days to the highest concentration (400 mg L^{-1}) of 12, 50 or 80 nm size of nanoCuO or to the highest concentration of humic acid (HA; 100 mg L^{-1}) alone or in mixtures. Panels I and II denote different magnification. Black arrows indicate nanoCuO; white arrows indicate HA; black dotted arrows indicate microbes; white dotted arrows indicate loss of epidermal tissues/cuticle layer.

3.4. Discussion

Our study showed that leaf-litter decomposition mediated by microbes was affected by exposure to nanoCuO, and effects varied with nanoparticle size and concentration. Earlier studies reported negative effects of nanoCuO to freshwater

and marine organisms, including bacteria, microalgae and invertebrates (Heinlaan et al., 2008; Aruoja et al., 2009; Buffet et al., 2011), but our study provides evidence that impacts at the community-level and on ecosystem processes cannot be neglected. Similar to that found in a previous study (Pradhan et al., 2011), increasing concentrations of nanoCuO had negative effects on microbial decomposers of plant litter, but in the present study we showed that effects became stronger with decreasing nanoparticle size. Indeed, the maximum inhibition to leaf decomposition (72.7%) was found after exposure to the highest concentration (400 mg L^{-1}) of the smallest size (12 nm) nanoCuO. Exposure to increasing size of nanoparticles promoted less but still severe impacts on this ecological process (55.0 and 40.9% for nanoCuO with 50 and 80 nm, respectively). The lower LOEC and EC_{50} values of smaller size nanoCuO for the effects on leaf decomposition also supported the higher toxicity of smaller nanoparticles. The surface of leaves exposed to nanoCuO was more preserved than that of control leaves, and leaf-associated microbes were hardly found under exposure conditions. Leaf surface integrity decreased and microbial colonization increased as nanoparticle size increased. Evidence of nanoparticle aggregation on leaf surface was observed after exposure to nanoCuO. Also, in metal-polluted streams, submerged leaves can be coated by a layer of metals, resulting in a low density of fungal hyphae and a well-preserved leaf surface (Ehrman et al., 2008).

Increasing concentrations of different size nanoCuO also affected the biomass of microbial communities. The lower LOEC and EC_{50} values for fungal and bacterial biomass supported the more pronounced effects of smaller than larger size nanoCuO. However, LOEC and EC_{50} values for bacterial biomass were lower than those for fungal biomass. These findings support that bacteria were more sensitive than fungi to nanoCuO, with biomass inhibitions ranging from 68.8 to 93.4% for bacteria and from 32.9 to 52.3% for fungi after exposure to 400 mg L^{-1} of nanoCuO with descending nanoparticle size (from 80 to 12 nm). This corroborates our earlier study in which bacterial biomass was inhibited up to 91.6%, while fungal biomass was inhibited up to 39.5% after exposure to 500 mg L^{-1} of 50 nm size nanoCuO (Pradhan et al., 2011). Interestingly, other reports also revealed that bacteria are more sensitive than fungi to metal stress (Niyogi et al., 2002; Duarte et al., 2008, 2009). The higher surface to volume ratio of bacteria than fungi could be partially responsible for the higher bacterial sensitivity, allowing higher contact and interactions between nanoparticles and cells. Moreover, fungal hyphae can

penetrate and grow inside leaf tissues, which may protect fungi from direct exposure to nanoparticles.

In our study, the effects of nanoCuO on fungal sporulation were similar to those found for leaf decomposition and microbial biomass, but sporulation was much more sensitive to nanoCuO than the other endpoints. The high sensitivity of fungal sporulation to nanoCuO (this study) and to other stressors (copper and zinc, Duarte et al., 2009; cadmium and phenantrene, Moreirinha et al., 2011; cadmium and temperature, Batista et al 2012) points to fungal reproduction as a potential measure to be used in ecotoxicity tests.

Stronger inhibitory effects of smaller TiO_2 nanoparticles (<10 nm) than larger TiO_2 nanoparticles (30 and 300 nm) have been shown at lower exposure concentration to freshwater algae (Hartmann et al., 2010). Increased toxicity with decreased nanoparticle size of nanoCuO was illustrated on Gram-positive and Gram-negative bacteria (Azam et al., 2012), many of which are found in natural waters. The increased toxicity of smaller size nanometal oxides could be attributed to differences in the reactive surface area available to interact with biota (Van Hoecke et al., 2009). Indeed, SEM and DLS analyses indicated increased self-agglomeration/aggregation of nanoCuO in the stream water with the increase in nanoparticle size, suggesting a decrease in the reactive surface area of larger particles comparing to smaller particles. However, the influence of size on other physico-chemical properties of nanoCuO cannot be ignored because it may affect its toxicity to biota.

In the absence of nanoCuO, humic acid also had negative effects on microbial decomposers of leaf litter (inhibition of decomposition up to 42.5%, fungal biomass up to 35.9%, bacterial biomass up to 56.0%, and fungal reproduction up to 82.4%). Adverse effects of HA were reported to freshwater organisms, such as cyanobacteria and invertebrates (Meems et al., 2004; Sun et al., 2006), probably due to HA ability to induce accumulation of reactive oxygen species or free radicals (Pflugmacher et al., 2001; Timofeyev et al., 2004, 2006). In contrast, the individual toxicity of HA or smaller size (12 or 50 nm) nanoCuO was reduced by co-exposure to both chemicals. The presence of NOM or HA can alleviate the toxicity of ionic or nano metals to living organisms (De Schamphelaere et al., 2002; Blinova et al., 2010; Li et al., 2011), but our study clearly shows that particle size is a critical factor when assessing nanoparticle impacts because no alleviating effects were found when microbial decomposers were co-exposed to HA and larger size nanoCuO (80

nm). The alleviating effects of NOM on nanoparticle toxicity can also vary with other factors, including its source (Al-Reasi et al., 2011), composition (Glover et al., 2005), concentration and time of exposure (Fabrega et al., 2009). The effects of HA were consistent with alterations in leaf surface as shown by SEM-EDX. After exposure to the highest concentration of HA, leaves were well preserved, and adsorption of HA to leaf surface was visible. Leaves co-exposed to smaller size nanoCuO and HA had lower structural integrity, with inner tissues well colonized by microbes, and had less amount of adsorbed nanoCuO comparing to leaves exposed to nanoCuO alone. Due to their small size and high reactive surfaces, nanoparticles are prone to aggregation and sorption onto organic materials (Holsapple et al., 2005). Indeed, the surface coating of small iron oxide nanoparticles (<10 nm) by Suwannee River humic acid (SRHA) was demonstrated, and the coating thickness increased with increasing SRHA concentration (Baalousha et al., 2008). Therefore, it is conceivable that in our study more interactions between HA and smaller size CuO nanoparticles had occurred leading to a greater surface-coating by HA. The ability of humic substances (SHRA) to act as a physical barrier between metal nanoparticles and biological cells was shown by TEM (Fabrega et al., 2009), and supports the role of HA in alleviating nanoCuO toxicity. Additionally, the electrosteric hindrance due to nanoparticle surface coating by HA could also be one of the mechanisms of alleviating nanoparticle effects (Chen et al., 2011).

In our study, microbial degradation of HA in the presence of nanoCuO can not be ignored because fungal biomass, fungal sporulation and leaf decomposition were slightly higher in mixtures with HA and nanoCuO than in treatments without nanoCuO. Fungi are able to use HA as carbon source (Mishra and Srivastava, 1986; Steffen et al., 2002) through the activity of Cu^{2+} dependent extracellular oxidoreductase enzymes, such as laccases (Junghanns et al., 2005). Because Cu^{2+} can stimulate laccase activity in aquatic fungi (Junghanns et al., 2005) and Cu^{2+} can be leached from nanoCuO (Blinova et al., 2010; Pradhan et al., 2012), increased bioavailability of this ion could have contributed to microbial degradation of HA unbound to nanoparticles. Conversely, in the absence of nanoCuO, laccase activity could be compromised due to insufficient amount of copper required for the enzyme activity (Keum and Li, 2004) and HA would become more toxic to microbes. Further studies are required to better understand the mechanisms underlying the interactive effects between nanoCuO and HA on biological systems.

In our study, the exposure to nanoCuO with or without HA decreased fungal species richness and led to shifts in the community composition. Effects were more prominent with increasing nanoCuO concentration and decreasing nanoCuO size. Also, the presence of HA alleviated the stress imposed by nanoCuO. In the absence of stressors, *A. tetracladia* was the dominant species on decomposing leaves contributing with more than 80% to the total spores produced. The exposure to the highest tested concentrations of nanoCuO and/or HA increased the contribution of *H. lugdunensis* that became the co-dominant fungus. The species *A. tetracladia* and *H. lugdunensis* are reported to occur in metal-polluted streams and some strains of these species were found to be resistant to high concentrations of metals (Braha et al., 2007; Jaeckel et al., 2005; Pascoal et al., 2005b). The shift in the community structure of sporulating fungi suggests a change towards a better-adapted community to cope with the stress induced by nanoCuO and/or HA.

Overall, our study shows that nanoCuO induced toxicity to microbial decomposers of plant litter by decreasing microbial biomass, fungal reproduction and diversity with a concomitant decrease of leaf decomposition. Bacterial communities were more sensitive than fungal communities to nanoCuO exposure. Moreover, fungal reproduction was the most sensitive measure for assessing the impacts of nanoparticles. NanoCuO toxicity was dose dependent and increased with the decrease in nanoparticle size. Humic acid, an important component of natural organic matter in freshwaters, also had negative effects on microbial activity and diversity. However, HA alleviated the toxicity induced by nanoCuO of smaller size. Therefore, the impacts of nanoCuO on the functional and structural properties of microbial decomposers in streams may be attenuated by the presence of HA, but if HA decrease nanoCuO bioavailability it might contribute to increase the residence time of nanoCuO in streams with further impacts on organic matter turnover at longer times.

References

Al-Reasi HA, Wood CM, Smith DS, 2011. Physicochemical and spectroscopic properties of natural organic matter (NOM) from various sources and implications for ameliorative effects on metal toxicity to aquatic biota. Aquat Toxicol 103, 179–190.

Aruoja V, Dubourguier HC, Kasemets K, Kahru A, 2009. Toxicity of nanoparticles of CuO, ZnO and TiO_2 to microalgae *Pseudokirchneriella subcapitata*. Sci Total Environ 407, 1461–1468.

Azam A, Ahmed AS, Oves M, Khan MS, Memic A, 2012. Size-dependent antimicrobial properties of CuO nanoparticles against Gram-positive and -negative bacterial strains. Int J Nanomedicine, 7, 3527–3535.

Baalousha M, Manciulea A, Cumberland S, Kendall K, Lead JR, 2008. Aggregation and surface properties of iron oxide nanoparticles: influence of pH and natural organic matter. Environ Toxicol Chem, 27, 1875–1882

Bang SH, Le T-H, Lee SK, Kim P, Kim JS, Min J, 2011. Toxicity Assessment of Titanium (IV) Oxide Nanoparticles Using *Daphnia magna* (Water Flea). Environ Health Toxicol, 26, e2011002 (6 pp), doi: 10.5620/eht.2011.26.e2011002.

Batista D, Pascoal C, Cássio F, 2012. Impacts of warming on aquatic decomposers along a gradient of cadmium stress. Environ Pollut 169, 35–41.

Blinova I, Ivask A, Heinlaan M, Mortimer M, Kahru A, 2010. Ecotoxicity of nanoparticles of CuO and ZnO in natural water. Environ Pollut 158, 41–47.

Braha B, Tintemann H, Krauss G, Ehrman J, Bärlocher F, Krauss GJ, 2007. Stress response in two strains of the aquatic hyphomycete *Heliscus lugdunensis after* exposure to cadmium and copper ions. Biometals 20, 93–105.

Buffet PE, Tankoua OF, Pan JF, Berhanu D, Herrenknecht C, Poirier L, Amiard-Triquet C, Amiard JC, Bérard, JB, Risso C, Guibbolini M, Roméo M, Reip P, Valsami-Jones E, Mouneyrac C, 2011. Behavioural and biochemical responses of two marine invertebrates *Scrobicularia plana* and *Hediste diversicolor* to copper oxide nanoparticles. Chemosphere 84, 166–174.

Carnes LC, Klabunde KJ, 2003. The catalytic methanol synthesis over nanoparticle metal oxide catalysts. J Mol Catal A: Chem 194, 227–236.

Chen J, Xiu Z, Lowry GV, Alvarez PJJ, 2011. Effect of natural organic matter on toxicity and reactivity of nano-scale zero-valent iron. Water Res 45, 1995–2001.

De Schamphelaere KAC, Heijerick DG, Janssen CR, 2002. Refinement and field validation of a biotic ligand model predicting acute copper toxicity to *Daphnia magna*. Comp Biochem Physiol C Toxicol Pharmacol 133, 243–258.

Duarte S, Pascoal C, Cássio F, 2008. High diversity of fungi may mitigate the impact of pollution on plant litter decomposition in streams. Microb Ecol 56, 688–695.

Duarte S, Pascoal C, Cássio F, 2009. Functional stability of stream-dwelling microbial decomposers exposed to copper and zinc stress. Freshwat Biol 54, 1683–1691.

Dutta A, Das D, Grilli ML, Di Bartolomeo E, Traversa E, Chakravorty D, 2003. Preparation of sol–gel nano-composites containing copper oxide and their gas sensing properties. J Sol–Gel Sci Technol 26, 1085–1089.

Ehrman JM, Bärlocher F, Wennrich R, Krauss G-J, Krauss G, 2008. Fungi in a heavy metal precipitating stream in the Mansfeld mining district, Germany. Sci Total Environ 389, 486–496.

Erickson RJ, Benoit DA, Mattson VR, Nelson HP Jr, Leonard EN, 1996. The effects of water chemistry on the toxicity of copper to fathead minnows. Environ Toxicol Chem 15, 181–193.

Fabrega J, Fawcett SR, Renshaw JC, Lead JR, 2009. Silver nanoparticle impact upon bacterial growth: effect of pH, concentration, and organic matter. Environ Sci Technol 43, 7285–7290.

Fernandes I, Duarte S, Pascoal C, Cássio F, 2009. Mixtures of zinc and phosphate affect leaf litter decomposition by aquatic fungi in streams. Sci Total Environ 407, 4283–4288.

Gessner MO, 2005. Ergosterol as a measure of fungal biomass. In: Graça MAS, Bärlocher F, Gessner MO (Eds) Methods to study litter decomposition: a practical guide, Springer, Dordrecht, Netherlands, pp 189–196.

Gessner MO, Chauvet E, 2002. A case for using litter breakdown to assess functional stream integrity. Ecol Appl 12, 498–510.

Glover CN, Playle RC, Wood CM, 2005. Heterogeneity of natural organic matter amelioration of silver toxicity to *Daphnia magna*: effect of source and equilibration time. Environ Toxicol Chem. 24, 2934–2940.

Hartmann NB, Kammer FVD, Hofmann T, Baalousha M, Ottofuelling S, Baun A, 2010. Algal testing of titanium dioxide nanoparticles - testing considerations, inhibitory effects and modification of cadmium bioavailability. Toxicology 269, 190–197.

Heinlaan M, Ivask A, Blinova I, Dubourguier HC, Kahru A, 2008. Toxicity of nanosized and bulk ZnO, CuO and TiO_2 to bacteria *Vibrio fischeri* and crustaceans *Daphnia magna* and *Thamnocephalus platyurus*. Chemosphere 71, 1308–1316.

Holsapple MP, Farland WH, Landry TD, Monteiro-Riviere NA, Carter JM, Walker NJ, Thomas KV, 2005. Research strategies for safety evaluation of nanomaterials, part II: toxicological and safety evaluation of nanomaterials, current challenges and data needs. Toxicol Sci 88, 12–17.

Jaeckel P, Krauss GJ, Krauss G, 2005. Cadmium and zinc response of the fungi *Heliscus lugdunensis* and *Verticilliumcf.alboatrum* isolated from highly polluted water. Sci Total Environ 346, 274–279.

Junghanns C, Moeder M, Krauss G, Martin C, Schlosser D, 2005. Degradation of the xenoestrogen nonylphenol by aquatic fungi and their laccases. Microbiology 151, 45–57.

Kahru A, Dubourguier HC, Blinova I, Ivask A, Kasemets K, 2008. Biotests and biosensors for ecotoxicology of metal oxide nanoparticles: a minireview. Sensors 8, 5153–5170.

Keum, Y-S, Li QX, 2004. Copper dissociation as a mechanism of fungal laccase denaturation by humic acid. Appl Microbiol Biotechnol 64, 588–592.

Li L-Z, Zhou D-M, Peijnenburg WJGM, van Gestel CAM, Jin S-Y, Wang Y-J, Wang P, 2011. Toxicity of zinc oxide nanoparticles in the earthworm, *Eisenia fetida* and subcellular fractionation of Zn. Environ Int 37, 1098–1104.

Lorenzo JI, Nieto O, Beiras R, 2002. Effects of humic acids on speciation and toxicity of copper to *Paracentrotus lividus* larvae in seawater. Aquat Toxicol 58, 27–41.

Ma H, Allen HE, Yin Y, 2001. Characterization of isolated fractionations of dissolved organic matter from natural waters and a wastewater effluent. Water Res 35, 985–996.

Meems N, Steinberg CEW, Wiegand C, 2004. Direct and interacting toxicological effects on the waterflea (*Daphnia magna*) by natural organic matter, synthetic humic substances and cypermethrin. Sci Total Environ, 319, 123–136.

Mishra B, Srivastava LL, 1986**.** Degradation of humic acid of a forest soil by some fungal isolates. Plant Soil, 96, 413–416.

Moreirinha C, Duarte S, Pascoal C, Cássio F, 2011. Effects of cadmium and phenanthrene mixtures on aquatic fungi and microbially mediated leaf litter decomposition. Arch Environ Contam Toxicol, 61, 211–219.

Mortimer M, Kasemets K, Kahru A, 2010. Toxicity of ZnO and CuO nanoparticles to ciliated protozoa *Tetrahymena thermophila*. Toxicology 269, 182–189.

Niyogi DK, Lewis Jr WM, McKnight DM, 2002. Effects of stress from mine drainage on diversity, biomass, and function of primary producers in mountain streams. Ecosystems 5, 554–567.

Norland S, 1993. The relationship between biomass and volume of bacteria. In: Kemp PF, Sherr BF, Sherr EB, Cole JJ (Eds) Handbook of Methods in Aquatic Microbial Ecology, Lewis publishers, Boca Raton, Florida, pp 303–307.

Pascoal C, Cássio F, 2004. Contribution of fungi and bacteria to leaf litter decomposition in a polluted river. Appl Environ Microbiol 70, 5266–5273.

Pascoal C, Cássio F, Gomes P, 2001. Leaf breakdown rates: a measure of water quality? Int Rev Hydrobiol 86, 407–416.

Pascoal C, Cássio F, Marcotegui A, Sanz B, Gomes P, 2005a. Role of fungi, bacteria, and invertebrates in leaf litter breakdown in a polluted river. J N Am Benthol Soc 24, 784–797.

Pascoal C, Marvanová L, Cássio F, 2005b. Aquatic hyphomycete diversity in streams of Northwest Portugal. Fungal Divers 19, 109–128

Pflugmacher S, Tidwell LF, Steinberg CEW, 2001. Dissolved humic substances directly affect freshwater organisms. Acta hydrochim hydrobiol 29, 34–40.

Pradhan A, Seena S, Pascoal C, Cássio F, 2011. Can metal nanoparticles be a threat to microbial decomposers of plant litter in streams? Microb Ecol 62, 58–68.

Pradhan A, Seena S, Pascoal C, Cássio F, 2012. Copper oxide nanoparticles can induce toxicity to the freshwater shredder *Allogamus ligonifer*. Chemosphere 89, 1142–1150.

Ren G, Hu D, Cheng EWC, Vargas-Reus MA, Reip P, Allaker RP, 2009. Characterisation of copper oxide nanoparticles for antimicrobial applications. Int J Antimicrob Agents 33, 587–590.

Saison C, Perreault F, Daigle JC, Fortin C, Claverie J, Morin M, Popovic R, 2010. Effect of core-shell copper oxide nanoparticles on cell culture morphology and photosynthesis (photosystem II energy distribution) in the green alga, *Chlamydomonas reinhardtii*. Aquat Toxicol 96, 109–114.

Sakuma, M., 1998. Probit analysis of preference data. Appl Entomol Zool 33, 339–347.

Steffen KT, Hatakka A, Hofrichter M, 2002. Degradation of humic acids by the litter-decomposing basidiomycete *Collybia dryophila*. Appl Environ Microbiol 68, 3442–3448.

Steinberg CEW, Kamara S, Prokhotskaya VYu, Manusadžianas L, Karasyova T, Timofeyev MA, Zhang J, Paul A, Meinelt T, Farjalla VF, Matsuo AYO, Burnison BK, Menzel R, 2006. Dissolved humic substances – ecological driving forces from the individual to the ecosystem level? Freshwater Biol 51, 1189–1210.

Sun BK, Tanji Y, Unno H, 2006. Extinction of cells of cyanobacterium *Anabaena circinalis* in the presence of humic acid under illumination. Appl Microbiol Biotechnol 72, 823–828.

Timofeyev MA, Wiegand C, Burnison BK, Shatilina ZM, Pflugmacher S, Steinberg CEW, 2004. Direct impact of natural organic matter (NOM) on freshwater amphipods. Sci Total Environ 319, 115–121.

Timofeyev MA, Shatilina ZM, Kolesnichenko AV, Bedulina DS, Kolesnichenko VV, Pflugmacher S, Steinberg CEW, 2006. Natural organic matter (NOM) induces oxidative stress in freshwater amphipods *Gammarus lacustris* Sars and *Gammarus tigrinus* (Sexton). Sci Total Environ 366, 673–681.

Tsiridis V, Petala M, Samaras P, Hadjispyrou S, Sakellaropoulos G, Kungolos A, 2006. Interactive toxic effects of heavy metals and humic acids on *Vibrio fischeri.* Ecotoxicol Environ Saf 63, 158–167.

Van Hoecke K, Quik JT, Mankiewicz-Boczek J, De Schamphelaere KA, Elsaesser A, Van der Meeren P, Barnes C, McKerr G, Howard CV, Van de Meent D, Rydzyński K, Dawson KA, Salvati A, Lesniak A, Lynch I, Silversmit G, De Samber B, Vincze L, Janssen CR, 2009. Fate and effects of CeO_2 nanoparticles in aquatic ecotoxicity tests. Environ Sci Technol 43, 4537–4546.

Wall NA, Choppin GR, 2003. Humic acids coagulation: influence of divalent cations. Appl Geochem 18, 1573–1582.

Yang HL, Hseu YC, Hseu YT, Lu FJ, Lin E, Lai JS 2004. Humic acid induces apoptosis in human premyelocytic leukemia HL-60 cells. Life Sci 75, 1817–1831.

Zar JH, 2009. Biostatistical analysis, fifth ed, Prentice Hall, Upper Saddle River, New Jersey.

Zhang X, Zhang D, Ni X, Song J, Zheng H, 2008. Synthesis and electrochemical properties of different sizes of the CuO particles. J Nanopart Res 10, 839–844.

Chapter 4

Copper oxide nanoparticles can induce toxicity to the freshwater shredder Allogamus ligonifer

Published as:

Copper oxide nanoparticles can induce toxicity to the freshwater shredder *Allogamus ligonifer*.

Pradhan A, Seena S, Pascoal C, Cássio, F

***Chemosphere*, 89, 1142–1150 in 2012**

Abstract

Increased commercialisation of nanometal-based products augments the possibility of their deposition into aquatic ecosystems; this, in turn, may pose risks to aquatic biota and associated ecological functions. Freshwater invertebrate shredders mostly use microbially-colonized plant litter as food resource and play an important role in aquatic detritus food webs. We assessed lethal effects of nanoCuO on the shredder *Allogamus ligonifer* (Trichoptera, Limnephilidae) by determining the concentration that induced 50% of death (LC_{50}), and sublethal effects of nanoCuO on the feeding behaviour and growth of the shredder by exposing the animals to: i) stream water supplemented with nanoCuO and microbially-colonized leaves, and ii) stream water (without nanoCuO) and microbially-colonized leaves pre-exposed to nanoCuO. Results from acute lethal tests showed that the 96 h LC_{50} of nanoCuO was very high (569 mg L^{-1}). In the absence of nanoparticles, leaf consumption rate was 0.27 mg DM day^{-1} and the shredder growth rate was 56 µg animal DM mg^{-1} animal DM day^{-1}. A significant inhibition in leaf consumption rate (up to 47%) and invertebrate growth rate (up to 46%) was observed when shredders were exposed to the higher tested sublethal concentration of nanoCuO (75 mg L^{-1}) through either contaminated stream water or pre-contaminated food. The exposure to increased nanoCuO concentration via water or pre-contaminated food led to higher accumulation of copper in the larval body. Leached water-soluble ionic copper from the nanoCuO adsorbed or accumulated in the shredder (up to 10.2% of total Cu) seemed to influence the feeding behaviour and growth of the shredder.

Keywords: NanoCuO, freshwater shredder, lethal effect, sublethal effects, aqueous and dietary exposure, feeding behaviour

4.1. Introduction

Nanoecotoxicology research is currently in the limelight due to high propagation of nanotechnology-based industries and nanomaterial-based products (Colvin, 2003; Aitken et al., 2006; Navarro et al., 2008). The extensive use of engineered nanomaterials may increase the possibilities of their leaching and deposition into aquatic reservoirs (e.g. Kaegi et al., 2008). Therefore, it is essential to understand the risks associated with tailored nanoparticles in aquatic ecosystems (Moore, 2006; MacCormack and Goss, 2008). Metal oxide nanoparticles are among the most frequently used nanomaterials having a broad range of applications, like in sunscreens and cosmetics (Nel et al., 2006), antimicrobial paints (Hochmannova and Vytrasova, 2010), textiles (Becheri et al., 2008; Kathirvelu et al., 2009), electrospray disinfectants (Wang et al., 2010), drug delivery and gene therapy (Jin and Ye, 2007). Over the last decade, several studies have reported that metal oxide nanoparticles are potentially toxic (see Reijnders, 2006 and Gajjar et al., 2009), but few attempts have been made to assess the ecotoxicity of nanometal oxides in aquatic systems (Blaise et al., 2008; Lee et al., 2009; Miller et al., 2010; Pradhan et al., 2011). Most studies were performed with nanometal oxides enlisted in the OECD guidance manual (OECD, 2010), like nanotitanium dioxide, nanozinc oxide, nanoaluminium oxide and nanocerium dioxide (Lovern et al., 2007; Zhu et al., 2008; Van Hoecke et al., 2009). However, the OECD guidance manual stresses that the enlisted nanoparticles have to be considered as a “snapshot in time” and those not included in the list can be of importance in the future (OECD, 2010).

Although nanocopper oxide (CuO) is not in the OECD list, it is one of the commercially manufactured metal oxide nanoparticles with wide range of applications (Carnes and Klabunde, 2003; Dutta et al., 2003; Zhang et al., 2008; Ren et al., 2009) and, therefore, its potential toxicity should not be ignored (Blinova et al., 2010; Saison et al., 2010; Buffet et al., 2011). The toxicity of the nano-sized metals in aquatic systems can be questionable (Sharma, 2009) as they have different properties than their bulk or ionic forms (Christian et al., 2008). Karlsson et al. (2009) showed in human cell lines that nanoparticles of CuO could be more toxic than the bulk micrometer particles. However, the toxicity of nanoCuO and other metal oxide nanoparticles to yeasts (Kasemets et al., 2009) and other organisms that are crucial in aquatic food webs, like microalgae (Aruoja et al., 2009), protozoa

(Mortimer et al., 2010), bacteria and crustaceans (Heinlaan et al., 2008), was attributed to the leached ionic form of the metal.

In freshwaters, invertebrate shredders decompose plant litter from the riparian vegetation and play a key role in detritus food web by transferring energy from plant litter to higher trophic levels (Graça and Canhoto, 2006). They prefer to feed on litter colonized by aquatic microbes, predominantly fungi, which activity increases the food quality and palatability to shredders (Suberkropp et al., 1983). Invertebrates are important test organisms in ecotoxicological studies as they are abundant, distributed worldwide, have short life span with high reproduction rates, and are sensitive to contaminants and toxicants including ionic metals (e.g., De Schamphelaere et al., 2004; Gerhardt et al., 2004) and nanometal oxides (Cattaneo et al., 2009; Galloway et al., 2010; Buffet et al., 2011). Moreover, ecotoxicological tests using freshwater invertebrate shredders are fast, cost-effective and easy to perform as invertebrates adapt quickly to the laboratory conditions.

Most studies reporting lethal toxicity of ionic copper, nano-sized copper and its oxides on aquatic invertebrates are based on the assumption that metal toxicity to aquatic biota occurs through waterborne exposure (Griffitt et al., 2008; Heinlaan et al., 2008, 2011). Indeed, very few studies have shown that ionic copper can have sublethal toxic impacts to aquatic invertebrates through dietary exposure (Hatakeyama, 1989; De Schamphelaere et al., 2007), but according to our knowledge none of the studies reported the dietary effects of nanocopper oxide on stream invertebrates.

The aim of this study was to investigate the potential impacts of nanoCuO on *Allogamus ligonifer*, a common invertebrate shredder in Southwest European streams that prefers high quality stream water (Bonada et al., 2008). We hypothesised that nanoCuO can pose toxicity to the invertebrate shredder by exposure to contaminated stream water and/or contaminated food, and impacts would be partially attributed to the bioavailable ionic copper leached from nanoCuO. We assessed the acute lethal effect of nanoCuO through aqueous exposure by monitoring the mortality of *A. ligonifer* up to 96 h. The sublethal toxicity was examined by assessing the feeding behaviour and growth rate of the invertebrate shredder when exposure occurred via: i) pre-contaminated food, i.e. assuming an input of contaminated plant litter into streams, and ii) contaminated water which, in turn, may contaminate plant litter entering in streams. Total copper in water, water-soluble ionic copper, and adsorbed and accumulated copper in leaves, body and

case of the shredder were determined in a tentative to better understand nanocopper toxicity.

4.2. Material and Methods

4.2.1. Microbial colonization of leaves in the stream

Leaves of *Alnus glutinosa* (L.) Gaertn. (alder) were collected from a single tree in autumn and air dried at room temperature. The leaves were soaked in deionised water, cut into 12 mm-diameter disks, and placed into fine-mesh bags (15 × 15 cm, 0.5-mm mesh size to prevent invertebrate colonization). In Spring 2010, leaf bags were immersed in the Maceira Stream (N 41°45'58.79'', W 8°08'49.39'', altitude 867 m, Cávado River basin, Northwest Portugal) to allow microbial colonization. After 10 days, leaf bags were retrieved and leaf disks from each replicate bag were rinsed with deionised water and used for the feeding experiment. Further information on the Maceira Stream can be found elsewhere (Duarte et al., 2009; Pradhan et al., 2011).

4.2.2. Collection of invertebrates and acclimation to the laboratory

Early-stage larvae of the caddisfly Allogamus ligonifer (McLachlan, 1876) with similar size (14 ± 1 mm length) were collected in the upper reach of the Cávado River in Spring 2010 and transported to the laboratory in plastic containers with stream water and sand. This stream detritivore that belongs to Limnephilidae occurs in Southwest Europe (Bonada et al., 2008) and is common in low-order streams of North Portugal (Varandas and Cortes, 2010). Further information on the Cávado River can be found elsewhere (Pascoal et al., 2001). In the laboratory, animals were placed in an aquarium with filtered (MN GF-3 filter paper, Macherey-Nagel, Germany) and sterile stream water and sand (121°C, 20 min) under aeration, at 14°C with a 12 h light : 12 h dark photoperiod, and were allowed to feed on alder leaves for 2 weeks before the experiment.

4.2.3. Preparation and characterization of nanocopper oxide suspension

The stock suspension of nanocopper oxide (CuO nanopowder <50 nm, 99.5%, Sigma-Aldrich, St. Louis, MO) was prepared in sterile stream water by sonication at 42 kHz in a sonication bath (Branson 2510, Danbury, CT, USA) for 30 min in dark before use (Heinlaan et al., 2008). The stream water had silica 9.6 ± 2 mg L^{-1}, Na^{+} 4.1 ± 0.4 mg L^{-1}, Ca^{2+} 1.3 ± 0.3 mg L^{-1}, K^{+} 0.6 ± 0.1 mg L^{-1}, HCO_3^{-} 8.0 ± 0.8 mg L^{-1}, Cl^{-} 4.2 ± 0.4 mg L^{-1}, and SO_4^{-} 1.0 ± 0.2 mg L^{-1}. The pH of nanoCuO stock suspension was adjusted to stream water pH (5.8 ± 0.2). The stock suspension was examined with UV-visible spectrophotometry (UV – 1700 PharmaSpec, Shimadzu, Kyoto, Japan) followed by scanning electron microscopy (SEM, Leica Cambridge S 360, Cambridge, UK) coupled to an energy dispersive X-ray microanalysis setup (EDX, 15 KeV) as described by Pradhan et al. (2011). NanoCuO showed a plasmon peak at 359 nm, and SEM confirmed that the size of CuO nanoparticles ranged from 30 to 50 nm as shown elsewhere (Fig. 1B in Pradhan et al., 2011).

The size distribution was also monitored by dynamic light scattering (DLS) using a zetasizer (Malvern, Zetasizer Nano ZS) to check agglomeration of nanoCuO in the stock suspension. DLS data showed that the size distribution of nanoCuO ranged from 120 to 340 nm with an average size of 202 nm and poly-dispersive index (PdI) of 0.186 (Fig. 4.1). The stability was confirmed up to 3 weeks.

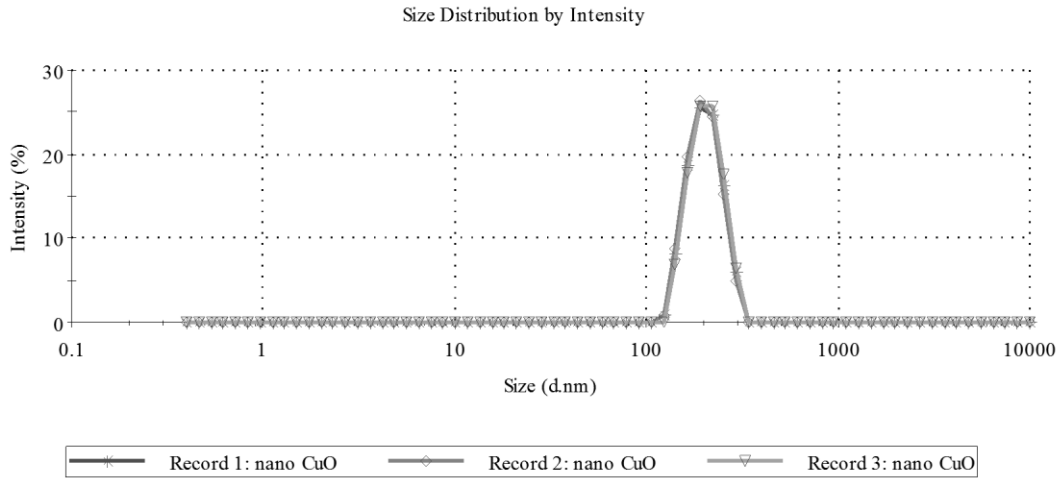

Figure 4.1 Size distribution of nanoCuO in stock suspension by dynamic light scattering.

The increased average particle size observed by DLS compared to the measured particle size by SEM indicated agglomeration of nanoCuO in the stream

water. This agrees with previous reports of CuO nanoparticles agglomeration in deionized water (Buffet et al., 2011) and in liquid culture medium (Karlsson et al., 2009). Discrepancies in nanoparticle size may also be attributed to differences in sample preparation by each technique: in SEM, nanoparticle suspension was air-dried and coated under vacuum and, so, only single particles were measured, while in DLS, the agglomerated particles could be measured with minimum perturbation of the aqueous suspension (Hassellöv et al., 2008).

4.2.4. Acute lethality tests

Acute lethality tests were performed to evaluate the sensitivity of the invertebrate to nanoCuO and to establish a range of sublethal concentrations to be used in the feeding experiments (see section 4.2.5). Invertebrate shredders were starved for 24 h and placed in 150 mL flasks containing 100 mL of nanoCuO suspensions (5 animals per flask, 3 replicates per treatment). The animals were exposed to 0, 50, 100, 250, 500 and 1000 mg L^{-1} nominal concentrations of nanoCuO prepared in sterilized stream water. The flasks were aerated with constant air flow and incubated for 96 h at 14°C, under a 12 h light : 12 h dark photoperiod. The invertebrates were not fed during the exposure period. In each 24 h, the animals that did not show any movement after mechanical stimulation were considered dead and mortality was recorded.

4.2.5. Invertebrate feeding experiments

To determine effects of nanoCuO on the feeding behaviour of the invertebrate shredder, one premeasured early-stage larvae of *A. ligonifer* was allocated to each of 150 mL flask containing 10 leaf disks and 100 mL sterile stream water. To assess the effects of nanoparticles via contaminated water, microcosms with stream water were supplemented with nanoCuO at 25 mg L^{-1} or 75 mg L^{-1} and microbially-colonized leaf disks not previously exposed to nanoCuO. To test the effects of nanoparticles via pre-contaminated food, microcosms were supplemented with stream water (without nanoCuO) and microbially-colonized leaf disks pre-exposed (5 days) to 25 mg L^{-1} or 75 mg L^{-1} of nanoCuO. Additional microcosms with sterile stream water and microbially-colonized leaf disks unexposed to nanoCuO served as control. A total of 75 flasks were used (15 replicates).

For determining the contribution of microorganisms to leaf litter decomposition, an equal number of unexposed or pre-exposed leaf disks to nanoCuO was enclosed in 0.5 mm fine mesh bag (to prevent the access of invertebrates) and placed in each replicate microcosms of the respective treatment. All flasks were aerated with constant air flow and incubated at 14°C, under a 12 h light : 12 h dark photoperiod. The experiment was continued for 10 days until >50% of leaf disks were decomposed in the control microcosms. The stream water with or without nanoCuO was renewed every 5 days to minimise the interference of released fine particles or excreted compounds with nanoparticles or invertebrates.

4.2.6. Leaf mass loss

To determine leaf mass loss, leaf disks from each replicate were freeze-dried (Christ alpha 2–4, B. Braun, Germany) and weighed to the nearest 0.001 mg, before and after microbial colonization in the stream, and before and after the feeding experiment.

4.2.7. Leaf consumption by invertebrates and microbes

Dry mass (DM, mg) of leaves consumed by the invertebrate (L_e) was determined as $(L_i – L_f) – (L_i \times (C_i – C_f)/C_i)$, where L_i and L_f are the initial and final dry mass (mg) of leaves exposed to the invertebrates, respectively, and C_i and C_f are the initial and final dry mass (mg) of control leaves (inaccessible to invertebrate), respectively. Microbial leaf decomposition rate was determined by $(C_i – C_f)/t$ where t is time (t=10 days). Leaf consumption rate by the invertebrate was calculated as $L_e/(I_f \times t)$, where If is the invertebrate dry mass (mg) at time t (day 10), and results were expressed as mg leaf DM mg^{-1} animal DM day^{-1} (Ferreira et al., 2010). Total consumption rate was determined as $((C_i – C_f) + Le)/t$ and expressed as mg leaf DM mg^{-1} $microcosm^{-1}$ day^{-1}.

4.2.8. Invertebrate growth rate

Growth rate of invertebrates (µg animal DM mg^{-1} animal DM day^{-1}) was determined as $I_e/(I_f \times t)$, where I_e is the dry mass (DM, µg) gained by the invertebrate during the elapsed time (t=10 days). The I_e was calculated by the difference between final (day 10) and initial dry mass (µg), and If is the final dry mass (mg) of

the animal at time t (Ferreira et al., 2010). For determining initial dry mass of invertebrates, the diameter of the case opening of each individual was measured under a stereoscopic microscope at 16× before the feeding experiment, and the individual dry mass was estimated according to the regression model DM = 0.0069 × CO – 0.0194 (r^2 = 0.72, *P<0.001*, n = 37), where DM is dry mass (g) and CO is case opening (mm).

4.2.9. Sample preparation and metal analysis

To determine total copper (nano and ionic forms) and ionic copper (Cu^{2+}) in water, equal volume of water samples of all replicate flasks were mixed. A fraction of 25 mL of water sample was treated with analytical grade concentrated HCl (5 mL) for quantification of total copper (Fig. 4.2). A separate fraction of 25 mL was ultra-centrifuged at 75,600 g for 60 min (Beckman Avanti J-25I, USA). The supernatant was consecutively filtered through two different size polycarbonate membranes (0.2 and 0.05 µm pore size, Millipore, Billerica, MA), and a mixed cellulose ester membrane (0.025 µm pore size, Millipore). The filtrate was employed to determine water-soluble Cu^{2+} content (Fig. 4.2).

At the end of the feeding experiment, Cu^{2+} leached from adsorbed or accumulated nanoCuO to leaves and to case and body of *A. ligonifer* was determined. For that, freeze-dried (Christ alpha 2–4, B. Braun, Germany) samples of leaves, larval case and body were revived in 25 mL ultrapure (Milli Q) water for 60 min to allow the leaching of water-soluble Cu^{2+}. Samples were ultra-centrifuged and filtered as described above before Cu^{2+} quantification (Fig. 4.2). To determine the adsorbed nanocopper, all pellets from ultra-centrifugation and residues from filtration of each sample were pooled and soaked in 25 mL of 5% HCl at 60°C; the solution was filtered through a polycarbonate membrane filter of 0.2 µm pore size and collected for analysis (Fig. 4.2). The remaining residue was mineralized in the furnace at 550°C (16 h for leaves, 20 h for larval case and 10 h for larval body) followed by digestion with HCl (1 mL) to determine the total accumulated copper. The digested solution was diluted with 5% HCl in a final volume of 25 mL, and filtered through a polycarbonate membrane (0.2 µm pore size) before quantification of accumulated copper (Fig. 4.2).

Copper concentration in all biological and water samples was determined by flame atomic absorption spectrometry (flame-AAS; Varian SpectrAA-250 Plus

apparatus) at the Scientific and Technological Research Assistance Centre (C.A.C.T.I., University of Vigo, Spain) with detection limit of 0.005 mg L^{-1}.

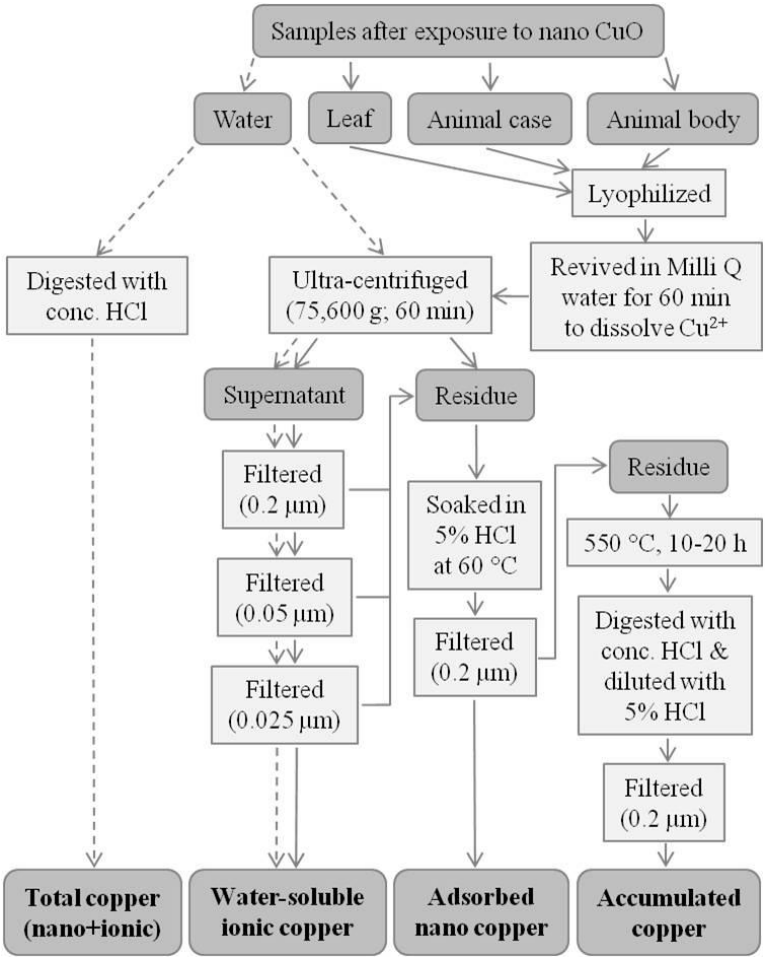

Figure 4.2 Graphical representation of sample preparation of stream water, leaves, animal case and animal body for further quantification of total copper, water-soluble ionic copper, adsorbed copper and accumulated copper by flame-AAS. Dashed lines refer to steps followed to prepare stream water samples, while straight lines refer to steps followed to prepare the remaining samples.

4.2.10. Data analyses

Mortality of shredders was recorded, and the concentration inducing 50% of death (LC_{50}) at 96 h of exposure with the respective 95% C.I. was calculated using PriProbit 1.63 (Sakuma, 1998; http://bru.gmprc.ksu.edu/proj/priprobit/download.asp). Repeated-measures analysis of variance (ANOVA) was used to test the effects of concentrations of nanoCuO on the percentage of animal survival in the acute lethality test with matched observations of exposure time (Zar, 2009). Two-way ANOVAs were used to determine the effects of sublethal concentrations of nanoCuO and the type of exposure (pre-contaminated food or contaminated water)

on leaf decomposition by microbes, leaf consumption rate by invertebrates and invertebrate growth rate (Zar, 2009). Significant differences between control and treatments were analysed by Bonferroni post-tests (Zar, 2009). To achieve normal distribution and homoscedasticity, percentage data of invertebrate survival during acute tests were arcsine square root transformed and the remaining data were ln-transformed (Zar, 2009). Multivariate correlations were used to examine the relationships between different forms of copper in leaves or stream water and different forms of copper in invertebrate body for both exposure types. Analyses were performed with Statistica 6.0 (Statsoft, Inc., Tulsa, OK, USA).

4.3. Results

4.3.1. Acute lethal effect of nanoCuO on invertebrates

The exposure of the invertebrate *Allogamus ligonifer* for 96 h to nanoCuO had a significant effect on its survival (repeated-measures ANOVA, *P<0.05*). The mortality increased with increasing concentration of nanoCuO and exposure time (Fig. 4.3). The 96 h LC_{50} (95% C.l.) of nanoCuO was 569 (328–1780) mg L^{-1} and the lowest observed effect concentration (LOEC) corresponded to 250 mg L^{-1} (Bonferroni test *P<0.05*).

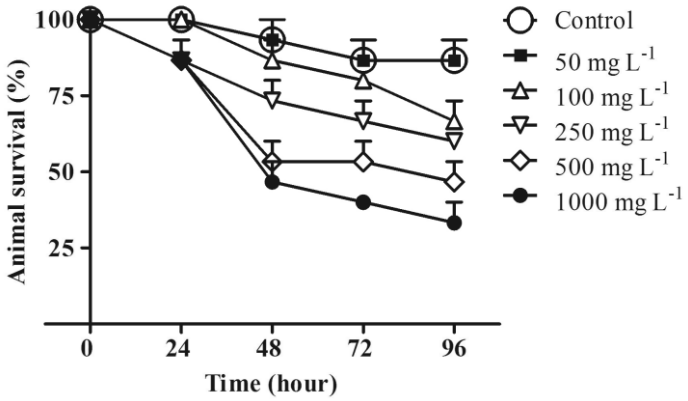

Figure 4.3 Acute lethal toxicity of nanoCuO to early-stage larvae of the invertebrate *Allogamus ligonifer* with respect to time.

4.3.2. Effects of nanoCuO on leaf consumption by invertebrates and microbes

Leaf consumption rate by *A. ligonifer* during 10 days was 0.27 mg leaf DM mg^{-1} animal DM day^{-1} in control (Fig. 4.4) and was affected by both nanoparticle concentration and type of exposure (two-way ANOVA, *P<0.05*). Higher inhibition was observed when animals were exposed to 75 mg L^{-1} nanoCuO via stream water (0.14 mg leaf DM mg^{-1} animal DM day^{-1}, Fig. 4.4A, Bonferroni *P<0.05*) followed by the treatment where the animals were fed on leaves pre-exposed to 75 mg L^{-1} nanoCuO (0.20 mg leaf DM mg^{-1} animal DM day^{-1}, Fig. 4.4B, Bonferroni *P<0.05*). Leaf consumption rate was not affected by exposure to the lower tested nanoCuO concentration (25 mg L^{-1}) via contaminated water or pre-contaminated food (Fig. 4.4A and B, Bonferroni *P>0.05*).

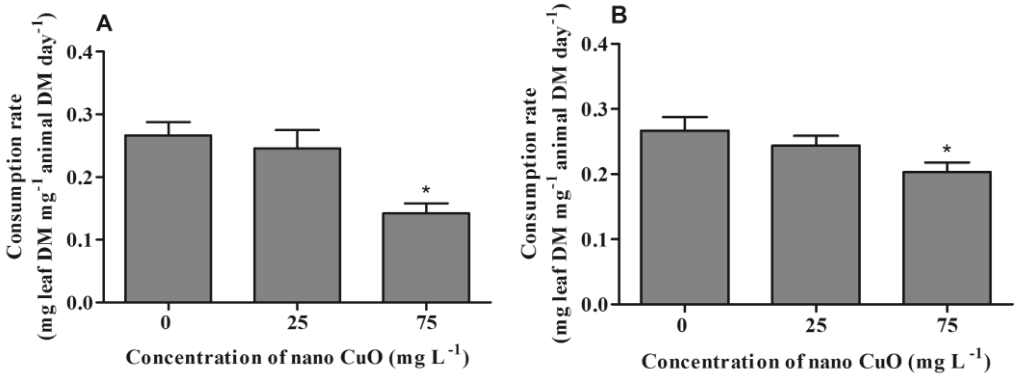

Figure 4.4 Leaf consumption rates by the early-stage larvae of *Allogamus ligonifer* for 10 days at 14ºC. The animals were exposed to nanoCuO through contaminated stream water (A), or through pre-contaminated leaves (B). Mean ± SEM, n=15. *, treatments that differ significantly from control (Bonferroni tests, *P<0.05*).

Leaf decomposition rate by microbes during 10 days was 1.3 mg leaf DM $microcosm^{-1}$ day^{-1} in control, corresponding to almost 34% of the total leaf consumption rate in the presence of the invertebrate (3.84 mg leaf DM $microcosm^{-1}$ day^{-1} in control, Fig. 4.5). Both concentration of nanoCuO and type of exposure had significant effects on microbial decomposition of leaf litter (two-way ANOVA, *P<0.05*). Microbial decomposition rate decreased significantly after exposure to 25 and 75 mg L^{-1} nanoCuO via water (Fig. 4.5A, Bonferroni *P<0.05*) and to leaves pre-exposed to 75 mg L^{-1} of nanoCuO (Fig. 4.5B, Bonferroni *P<0.05*).

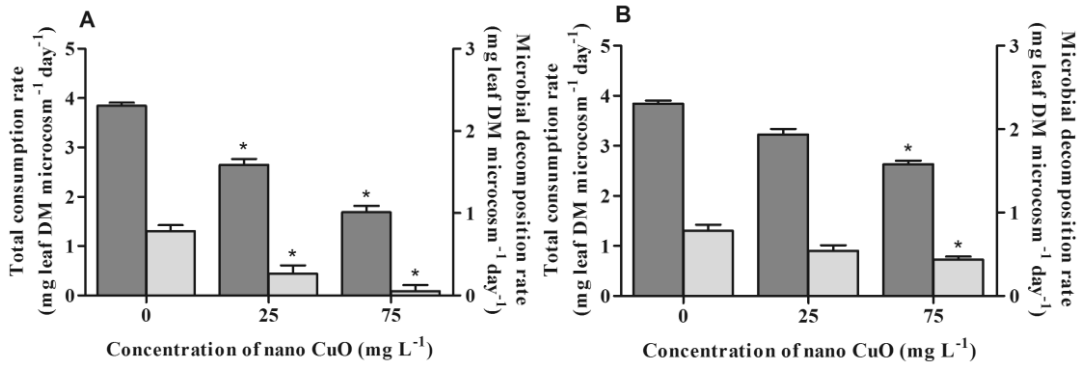

Figure 4.5 Total leaf consumption by the shredder *Allogamus ligonifer* (dark grey bars) and microbial decomposition of leaf litter (light grey bars) during 10 days in microcosms at 14ºC. The animals and microbes were exposed to nanoCuO through contaminated stream water (A), or through pre-contaminated leaves (B). Mean ± SEM, n=15. *, treatments that differ significantly from control (Bonferroni tests, *P<0.05*).

4.3.3. Effects of nanoCuO on invertebrate growth

The growth rate of the invertebrate shredder was affected by the concentration of nanoCuO, regardless the type of exposure, i.e. via water or pre-contaminated food (two-way ANOVA, *P<0.05* and *P>0.05*, respectively). In control, mean growth rate of the invertebrate was 56 µg animal DM mg^{-1} animal DM day^{-1} (Fig. 4.6). The growth rate decreased significantly in treatments where animals were exposed for 10 days to 75 mg L^{-1} nanoCuO via water (30 µg animal DM mg^{-1} animal DM day^{-1}, Fig. 4.6A, Bonferroni *P<0.05*), followed by treatments with animals that were fed on leaves pre-exposed to 75 mg L^{-1} nanoCuO (41 µg animal DM mg^{-1} animal DM day^{-1}, Fig. 4.6B, Bonferroni *P<0.05*). Similarly to that found for invertebrate feeding rates, the exposure to the lower tested concentration of nanoCuO through water or pre-exposed leaves had no effect on animal growth rates (Fig. 4.6A and B, Bonferroni *P>0.05*).

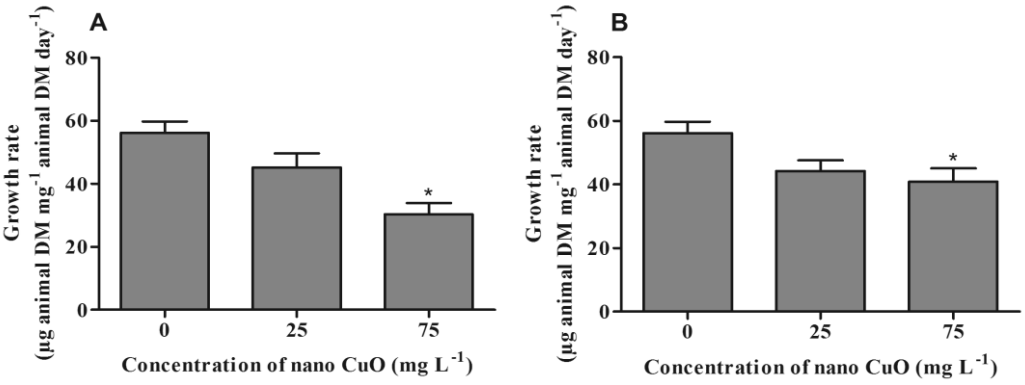

Figure 4.6 Growth rates of the early-stage larvae of *Allogamus ligonifer* feeding on microbially-colonized leaves for 10 days at 14ºC. The animals were exposed to nanoCuO through contaminated stream water (A), or through pre-contaminated leaves (B). Mean ± SEM, n=15. *, treatments that differ significantly from control (Bonferroni tests, *P<0.05*).

4.3.4. Copper in water, adsorbed and accumulated in leaves and invertebrates

In control, total copper and dissolved ionic copper (Cu^{2+}) in the stream water were below the detection limit (<0.005 mg L^{-1}) either at the initial time (t_0) or at the end of the feeding experiment (t_{10}) (Table 4.1). In the stream water supplemented with 25 mg L^{-1} nanoCuO, total Cu content varied little during the experiment (t_0, 20.98; t_{10}, 19.10 mg L^{-1}), and dissolved Cu^{2+} (t_0, <0.005 mg L^{-1}) increased till 0.6 mg L^{-1} (t_{10}). In the stream water supplemented with 75 mg L^{-1} nanoCuO, total Cu decreased 7% during the experiment (t_0, 61.167; t_{10}, 56.857 mg L^{-1}), whereas Cu^{2+} increased 12 times (t_0, 0.156; t_{10}, 1.87 mg L^{-1}). In microcosms with leaves pre-exposed to nanoCuO, the initial total Cu or Cu^{2+} content in water was below the detection limit, but at the end of the experiment total Cu increased up to 0.476 and 1.017 mg L^{-1} at 25 and 75 mg L^{-1}, respectively. Also, Cu^{2+} increased till 0.064 mg L^{-1} in treatments with water containing leaves pre-exposed to 75 mg L^{-1} nanoCuO after 10 days of exposure, but no detectable increase was observed at the lower tested concentration (25 mg L^{-1}).

After 10 days of exposure via stream water to nanoCuO, a substantial contamination of leaves occurred concomitantly with accumulation and adsorption of Cu to larval body (Table 4.1). The adsorbed Cu was higher on leaves, intermediate on the larval case and lower on the larval body (Table 4.1). However, when exposure occurred via pre-contaminated food, the adsorbed Cu was lower on the larval case than on the larval body.

The accumulated Cu was also higher in leaves, intermediate in larval body, and lower in the larval case, regardless the type of exposure (Table 4.1). In all treatments, the accumulation of Cu was lower than the adsorption. The content of Cu^{2+} and Cu adsorbed or accumulated in leaves, larval case or body increased with increasing nanoCuO concentration in both exposure types, but it was higher when exposure occurred via contaminated water (Table 4.1). However, the percentage of Cu^{2+} or Cu adsorbed or accumulated in leaves and larval body with respect to the total copper (sum of all Cu forms) obtained from all samples (water, leaves, larval body and case) were higher when exposure occurred via pre-contaminated food (Table 4.1).

Table 4.1 Total and ionic copper concentrations in water, and adsorbed and accumulated in leaves and invertebrates after 10 days (t_{10}) exposure to nanoCuO via pre-contaminated food or contaminated stream water. Exposure conditions: via contaminated water - leaves were in microcosms with stream water for 5 days and then were exposed to nanoCuO for further 10 days; via pre-contaminated food - leaves were pre-exposed for 5 days to nanoCuO and then released from nanoCuO and incubated with stream water in microcosms for further 10 days.

Sample	Concentration	Control	NanoCuO exposure			
			Via contaminated water		Via pre-contaminated food	
	Added nanoCuO (mg L^{-1})	**0**	**25**	**75**	**25**	**75**
Water	**Cu (mg L^{-1})**	**t_0 / t_{10}**	**t_0 / t_{10}**	**t_0 / t_{10}**	**t_0 / t_{10}**	**t_0 / t_{10}**
	Total Cu	nd/nd	20.982/ 19.1	61.167/ 56.857	nd/0.476	nd/1.017
	Cu^{2+}	nd/nd	nd/0.6	0.156/1.87	nd/nd	nd/0.064
	(a) % of Cu^{2+}	-	nd/3.141	0.255/3.289	-	nd/6.293
Leaves	**Cu after exposure**	**t_{10}**	**t_{10}**	**t_{10}**	**t_{10}**	**t_{10}**
	Adsorbed Cu (mg g^{-1})	0.007	11.676	15.832	2.359	3.316
	(b) % of adsorbed Cu	-	25.836	13.353	59.261	48.092
	Accumulated Cu (mg g^{-1})	0.003	4.086	12.889	0.485	1.229
	(b) % of accumulated Cu	-	7.266	10.271	11.827	17.323
	Cu^{2+} (mg g^{-1})	nd	0.076	0.113	0.011	0.013
	(b) % of Cu^{2+}	-	0.168	0.095	0.277	0.191
	(c) % of Cu^{2+}	-	0.48	0.392	0.385	0.285
Larval case	**Cu after exposure**	t_{10}	t_{10}	t_{10}	t_{10}	t_{10}
	Adsorbed Cu (mg g^{-1})	0.021	1.394	3.112	0.064	0.162
	(b) % of adsorbed Cu	-	2.929	2.061	1.823	2.139
	Accumulated Cu (mg g^{-1})	0.013	0.162	0.619	0.016	0.021
	(b) % of accumulated Cu	-	0.282	0.384	0.366	0.223
	Cu^{2+} (mg g^{-1})	0.003	0.084	0.158	0.005	0.013
	(b) % of Cu^{2+}	-	0.176	0.104	0.138	0.170
	(c) % of Cu^{2+}	8.108	5.122	4.063	5.882	6.633
Larval body	**Cu after exposure**	**t_{10}**	**t_{10}**	**t_{10}**	**t_{10}**	**t_{10}**
	Adsorbed Cu (mg g^{-1})	0.011	0.893	2.962	0.241	0.529
	(b) % of adsorbed Cu	-	0.374	0.56	1.699	1.88
	Accumulated Cu (mg g^{-1})	0.052	0.3	0.942	0.14	0.496
	(b) % of accumulated Cu	-	0.079	0.111	0.756	1.857
	Cu^{2+} (mg g^{-1})	nd	0.065	0.331	0.035	0.116
	(b) % of Cu^{2+}	-	0.027	0.063	0.249	0.411
	(c) % of Cu^{2+}	-	5.167	7.816	8.413	10.167

nd: below detection limit.
(a) With respect to total copper (nano and ionic forms).
(b) With respect to total copper (adsorbed, accumulated and ionic) obtained from all samples (water, leaves, larval case and body) of each treatment.
(c) With respect to total copper (adsorbed, accumulated and ionic) obtained in each sample.

After 10 days of exposure to nanoCuO via contaminated water, the total Cu or Cu^{2+} in water and accumulated Cu in leaves were positively correlated with adsorbed and accumulated Cu in the larval body (Table 4.2, *P<0.05*). In the exposure via pre-contaminated leaves, total Cu in water and accumulated Cu in leaves were significantly correlated with the adsorbed Cu in the larval body (Table 4.2, *P<0.05*). In the latter exposure route, Cu^{2+} in water was not correlated with adsorbed or accumulated Cu in the larval body.

Table 4.2 Multivariate correlations between copper in water or leaves and copper in the body of *Allogamus ligonifer* after 10 days exposure to nanoCuO via contaminated water or pre-contaminated leaves.

Route of nanoCuO exposure	Sample	Concentration	Copper in larval body (mg g^{-1})					
			Adsorbed Cu		Accumulated Cu		Cu^{2+}	
			r	*P*-value	*r*	*P*-value	*r*	*P*-value
Contaminated water	**Water**							
		Total Cu (mg L^{-1})	0.9992	0.026	0.9980	0.040	0.9888	0.095
		Cu^{2+} (mg L^{-1})	0.9997	0.015	0.9989	0.029	0.9911	0.085
	Leaves							
		Adsorbed Cu (mg g^{-1})	0.8796	0.316	0.8689	0.330	0.8227	0.385
		Accumulated Cu (mg g^{-1})	0.9998	0.013	0.9991	0.027	0.9917	0.082
		Cu^{2+} (mg g^{-1})	0.9111	0.270	0.9018	0.285	0.8608	0.340
Pre-contaminated leaves	**Water**							
		Total Cu (mg L^{-1})	0.9996	0.018	0.9558	0.190	0.9823	0.120
		Cu^{2+} (mg L^{-1})	0.8965	0.292	0.9823	0.120	0.9558	0.190
	Leaves							
		Adsorbed Cu (mg g^{-1})	0.9544	0.193	0.8397	0.365	0.8943	0.295
		Accumulated Cu (mg g^{-1})	0.9983	0.037	0.9775	0.135	0.9948	0.065
		Cu^{2+} (mg g^{-1})	0.9027	0.283	0.7547	0.456	0.8223	0.385

r, coefficient of correlation

4.4. Discussion

Acute lethality tests are of primary importance in ecotoxicology to assess sensitivity, viability and acute stress response of biota for predicting the impacts of toxicants or contaminants to ecosystem functioning (Valenti et al., 2005). Although very few studies on toxicity of metal oxide nanoparticles to aquatic biota are available (see Petersen and Nelson, 2010), acute toxicity of nanoCuO to freshwater crustaceans, *Daphnia magna* and *Thamnocephalus platyurus*, and to the ciliate protozoan *Tetrahymena thermophila* was shown based on mobility, mortality or growth inhibition (Blinova et al., 2010). In the current study, the 96 h acute lethality test on the shredder *Allogamus ligonifer* showed that this freshwater invertebrate was able to survive up to 100 mg L^{-1} of nanoCuO in the stream water. However, survival of this species was severely affected when exposed to higher concentrations of nanoCuO during the acute toxicity test. Although there is no estimated or predicted data for nanoCuO concentration in aquatic environments, copper concentration in the chemical mechanical planarization waste water of Taiwan often exceeds 100 ppm, 49% of which can be nanoCuO (Hsiao et al., 2001;

Huang et al., 2006). Therefore, the obtained high lethal concentrations of nanoCuO cannot be ignored.

Feeding behaviour of invertebrates is one of the most accepted and sensitive monitoring tools in ecotoxicology for assessing sublethal effects of metals (Pestana et al., 2007) and nanometals (Galloway et al., 2010; Buffet et al., 2011). In control, the feeding rate of A. ligonifer (0.27 mg leaf DM mg^{-1} animal DM day^{-1}) was within the typical range reported for stream invertebrate shredders (0.04 to 0.5 mg leaf DM mg^{-1} animal DM day^{-1}; Arsuffi and Suberkropp, 1989). After exposure of animals to contaminated stream water or pre-contaminated leaves with two sublethal concentrations of nanoCuO (25 and 75 mg L^{-1}), we found a significant reduction of leaf consumption and growth rates of the shredder by exposure to the higher concentration of nanoCuO (75 mg L^{-1}) via water or pre-contaminated food. The outcome of our study shows that the nanometal toxicity to aquatic organisms can occur via food or water, and not only via waterborne exposure as often assumed for ionic metals (see Brinkman and Johnston, 2008). Results also indicate that examining sublethal effects of nanometals can be more rational and useful to assess toxicity than merely rely on lethal effects. Maximum decrease in leaf consumption rate (47% inhibition) and growth rate (46% inhibition) was obtained when the animals were exposed to nanoCuO via contaminated water. This agrees with the recent report on decreased feeding rates of the marine invertebrate *Scrobicularia plana* exposed to nanoCuO via water (Buffet et al., 2011). In our study, the decrease in leaf consumption and invertebrate growth appeared to be lower after exposure via pre-contaminated food than via contaminated water. We should point out that in the latter case food also became contaminated by nanoCuO. Our results encourage the use of feeding behaviour of invertebrate shredders as an endpoint for assessing toxicity of metal nanoparticles in aquatic environments.

In this study, the decrease in invertebrate feeding and growth by nanoCuO exposure may be related to the food avoidance behaviour of shredders (Wilding and Maltby, 2006). Alder leaves have a high nutrient content, and leaves that are well colonized by microbes are more palatable for invertebrate shredders, including Trichoptera (Arsuffi and Suberkropp, 1989; Graça, 2001; Chung and Suberkropp, 2009). We previously reported that ionic copper (Duarte et al., 2008) and nanoCuO (Pradhan et al., 2011) have negative effects on microbes colonizing leaf litter. In our study, alder leaves were pre-colonized by microbes, so leaf quality and palatability for shredders might also be affected by the impacts of nanoCuO on microbial

communities. Indeed, we found a severe reduction in microbial decomposition during invertebrate feeding under nanoCuO exposure, particularly when exposure occurred via contaminated water. Thus, the stress induced by nanoparticles may have affected the invertebrate shredder directly or indirectly due to the effects on microbes.

Under aqueous exposure, great amounts of copper were adsorbed and accumulated in the leaves (at 75 mg L^{-1}: 15.832 and 12.889 mg g^{-1}, respectively). This was accompanied by high levels of Cu adsorption and accumulation in the larval case and body. However, the percentage of adsorbed or accumulated Cu in leaves or larval body was lower when exposure occurred via water than via pre-contaminated food. Copper adsorbed and/or accumulated in larval body were mainly correlated with Cu in the stream water or accumulated in leaves in both exposure types. The accumulation of Cu in the shredder body increased with the increase in CuO nanoparticle concentration in water or food, suggesting the intake of CuO nanoparticles. The ionic copper, leached from the CuO nanoparticles, may play an important role in enhancing the toxicity or ecotoxicity (Kahru et al., 2008; Aruoja et al., 2009; Kasemets et al., 2009). Blinova et al. (2010) using a Cu-sensor bacteria reported about 12% dissolution of Cu^{2+} from nanoCuO in freshwaters. Before our feeding experiment, Cu^{2+} in water attained 0.156 mg L^{-1} in microcosms supplemented with the higher concentration of nanoCuO (75 mg L^{-1}) via water. During the feeding experiment, the Cu^{2+} content increased, particularly when exposure occurred via contaminated water. Consistently, the highest levels of Cu^{2+} associated with the larval body were found after exposure to the higher sublethal concentration of nanoparticles via water. This may be a consequence of Cu^{2+} leached from nanoCuO, as nanoparticles were the only source of Cu^{2+}. Taking into account that toxicity of nanometals can depend on the leached ionic metal (Heinlaan et al., 2008; Mortimer et al., 2010), Cu^{2+} might have contributed to the inhibition of invertebrate feeding and growth after aqueous or dietary exposure to 75 mg L^{-1} of nanoCuO. Moreover, Cu^{2+} in stream water correlated significantly with adsorbed and accumulated Cu in larval body when exposure occurred via water, probably explaining the strongest inhibition of invertebrate growth and feeding under these conditions.

In our study, the leached ionic copper may have greatly contributed to the toxicity of nanoCuO at lethal or sublethal concentrations. This is supported by previous studies on nanoCuO toxicity to aquatic organisms including crustaceans

(Heinlaan et al., 2008; Blinova et al., 2010). But further investigation is needed pertaining to the mechanisms of toxicity and other possible factors that might be involved in toxicity. Some studies reported that leached metal ions are insufficient in explaining the toxicity of nanoparticles. Griffitt et al. (2008) showed very low dissolution of nanocopper that could account only for 10-15% of the toxicity to *Daphnia pulex* and zebrafish. Lower dissolution of nanoCuO was reported by Buffet et al. (2011). However, the toxicity can be further argued by intracellular dissolution of nanoparticles. The oral toxicity of copper nanoparticles was attributed to the high reactivity of nano Cu that could lead to metabolic alkalosis or intracellular dissolution leading to excessive accumulation of copper ions (Meng et al. 2007). Perhaps this is the explanatory bridge between the observed negative effects on larval feeding and growth and the high amounts of accumulated copper inside the larval body after exposure to the higher concentration of nanoCuO (75 mg L^{-1}) via water or pre-contaminated food. Accumulated Cu and adsorbed Cu^{2+} into leaves and larval body was higher after exposure to higher sublethal concentration of nanoCuO via contaminated stream water than via pre-contaminated food, probably contributing to the strongest inhibition of invertebrate feeding and growth in the former exposure type.

Overall, we found that copper oxide nanoparticles can have toxic effects on the invertebrate shredder *A. ligonifer*. Nanoparticle exposure led to lethal effects to this shredder only at very high concentrations. However, at sublethal levels, nanoCuO was potent to decrease the feeding and growth rates of the shredder through both aqueous and dietary exposure. Results also suggested that leached ionic copper play a role in the toxicity of nanoCuO, but further investigation is needed to comprehend the actual mode of action of nanometal oxides.

References

Aitken RJ, Chaudhry MQ, Boxall ABA, Hull M, 2006. Manufacture and use of nanomaterials: current status in the UK and global trends. Occup Med 56, 300–306.

Arsuffi TL, Suberkropp K, 1989. Selective feeding by shredders on leaf-colonizing stream fungi: comparison of macroinvertebrate taxa. Oecologia 79, 30–37.

Aruoja V, Dubourguier HC, Kasemets K, Kahru A, 2009. Toxicity of nanoparticles of CuO, ZnO and TiO_2 to microalgae *Pseudokirchneriella subcapitata*. Sci Total Environ 407, 1461–1468.

Becheri A, Dürr M, Nostro PL, Baglioni P, 2008. Synthesis and characterization of zinc oxide nanoparticles: application to textiles as UV-absorbers. J Nanopart Res 10, 679–689.

Blaise C, Gagné F, Férard J, Eullaffroy P, 2008. Ecotoxicity of selected nano-materials to aquatic organisms. Environ Toxicol 23, 591–598.

Bonada N, Zamora-Muñoz C, El Alami M, Múrria C, Prat N, 2008. New records of Trichoptera in reference Mediterranean-climate rivers of the Iberian Peninsula and North of Africa: Taxonomical, faunistical and ecological aspects. Graellsia 64, 189–208.

Blinova I, Ivask A, Heinlaan M, Mortimer M, Kahru A, 2010. Ecotoxicity of nanoparticles of CuO and ZnO in natural water. Environ Pollut 158, 41–47.

Brinkman SF, Johnston WD, 2008. Acute toxicity of aqueous copper, cadmium, and zinc to the mayfly *Rhithrogena hageni*. Arch Environ Contam Toxicol 54, 466–472.

Buffet PE, Tankoua OF, Jin-Fen Pan JF, Berhanu D, Herrenknecht C, Poirier L, Amiard-Triquet C, Amiard JC, Bérard JB, Risso C, Guibbolini M, Roméo M, Reip P, Valsami-Jones E, Mouneyrac C, 2011. Behavioural and biochemical responses of two marine invertebrates *Scrobicularia plana* and *Hediste diversicolor* to copper oxide nanoparticles. Chemosphere 84, 166–174.

Carnes LC, Klabunde KJ, 2003. The catalytic methanol synthesis over nanoparticle metal oxide catalysts. J Mol Catal A Chem 194, 227–236.

Cattaneo AG, Gornati R, Chiriva-Internati M, Bernardini G, 2009. Ecotoxicology of nanomaterials: the role of invertebrate testing. Invertebrate Surviv J 6, 78–97.

Christian P, Von der Kammer F, Baalousha M, Hofmann T, 2008. Nanoparticles: structure, properties, preparation and behaviour in environmental media. Ecotoxicology 17, 326–343.

Chung N, Suberkropp E, 2009. Effects of aquatic fungi on feeding preferences and bioenergetics of *Pycnopsyche gentilis* (Trichoptera: Limnephilidae). Hydrobiologia 630, 257–269.

Colvin VL, 2003. The potential environmental impact of engineered nanomaterials. Nat Biotechnol 21, 1166–1170.

De Schamphelaere KAC, Forrez I, Dierckens K, Sorgeloos P, Janssen CR, 2007. Chronic toxicity of dietary copper to *Daphnia magna*. Aquat Toxicol 81, 409–418.

De Schamphelaere KAC, Vasconcelos FM, Allen HE, Janssen CR, 2004. The effect of dissolved organic matter source on acute copper toxicity to *Daphnia magna*. Environ Toxicol Chem 23, 1248–1255.

Duarte S, Pascoal C, Alves A, Correia A, Cássio F, 2008. Copper and zinc mixtures induce shifts in microbial communities and reduce leaf litter decomposition in streams. Freshwat Biol 53, 91–101.

Duarte S, Pascoal C, Garabétian F, Cássio F, Charcosset JY, 2009. Microbial decomposer communities are mainly structured by trophic status in circumneutral and alkaline streams. Appl Environ Microbiol 75, 6211–6221.

Dutta A, Das D, Grilli ML, Di Bartolomeo E, Traversa E, Chakravorty D, 2003. Preparation of sol–gel nano-composites containing copper oxide and their gas sensing properties. J Sol–Gel Sci Technol 26, 1085–1089.

Ferreira V, Gonçalves AL, Godbold DL, Canhoto C, 2010. Effect of increased atmospheric CO_2 on the performance of an aquatic detritivore through changes in water temperature and litter quality. Glob Change Biol 16, 3284–3296.

Gajjar P, Pettee B, Britt DW, Huang W, Johnson WP, Anderson AJ, 2009. Antimicrobial activities of commercial nanoparticles against an environmental soil microbe, *Pseudomonas putida* KT2440. J Biol Eng 3, pp 13, doi:10.1186/1754-1611-3-9.

Galloway T, Lewis C, Dolciotti I, Johnston BD, Moger J, Regoli F, 2010. Sublethal toxicity of nano-titanium dioxide and carbon nanotubes in a sediment dwelling marine polychaete. Environ Pollut 158, 1748–1755.

Gerhardt A, de Bisthoven LJ, Soares AMVM, 2004. Macroinvertebrate response to acid mine drainage: community metrics and on-line behavioural toxicity bioassay. Environ Pollut 130, 263–274.

Graça MAS, 2001. The role of invertebrates on leaf litter decomposition in streams – A review. Internat Rev Hydrobiol 86, 383–393.

Graça MAS, Canhoto C, 2006. Leaf litter processing in low order streams. Limnetica 25, 1–10.

Griffitt RJ, Luo J, Bonzongo JC, Barber DS, 2008. Effects of particle composition and species on toxicity of metallic nanomaterials in aquatic organisms. Environ Toxicol Chem 27, 1972–1978.

Hassellöv M, Readman JW, Ranville JF, Tiede K, 2008. Nanoparticle analysis and characterization methodologies in environmental risk assessment of engineered nanoparticles. Ecotoxicology 17, 344–361.

Hatakeyama S, 1989. Effect of copper and zinc on the growth and emergence of *Epeorus latifolium* (Ephemeroptera) in an indoor model stream. Hydrobiologia 174, 17–27.

Heinlaan M, Ivask A, Blinova I, Dubourguier HC, Kahru A, 2008. Toxicity of nanosized and bulk ZnO, CuO and TiO_2 to bacteria *Vibrio fischeri* and crustaceans *Daphnia magna* and *Thamnocephalus platyurus*. Chemosphere 71, 1308–1316.

Heinlaan M, Kahru A, Kasemets K, Arbeille B, Prensier G, 2011. Changes in the *Daphnia magna* midgut upon ingestion of copper oxide nanoparticles: A transmission electron microscopy study. Water Res 45, 179–190.

Hochmannova L, Vytrasova J, 2010. Photocatalytic and antimicrobial effects of interior paints. Prog Org Coat 67, 1–5.

Hsiao MC, Wang HP, Yang YW, 2001. EXAFS and XANES studies of copper in a solidified fly ash. Environ Sci Technol 35, 2532–2535.

Huang HL, Wang HP, Wei GT, Sun IW, Huang JF, Yang YW, 2006. Extraction of nanosize copper pollutants with an ionic liquid. Environ Sci Technol 40, 4761–4764.

Jin S, Ye K, 2007. Nanoparticle-mediated drug delivery and gene therapy. Biotechnol Prog 23, 32–41.

Kaegi R, Ulrich A, Sinnet B, Vonbank R, Wichser A, Zuleeg S, Simmler H, Brunner S, Vonmont H, Burkhardt M, Boller M, 2008. Synthetic TiO_2 nanoparticle emission from exterior facades into the aquatic environment. Environ Pollut 156, 233–239.

Kahru A, Dubourguier HC, Blinova I, Ivask A, Kasemets K, 2008. biotests and biosensors for ecotoxicology of metal oxide nanoparticles: A minireview. Sensors 8, 5153–5170.

Karlsson HL, Gustafsson J, Cronholm P, Möller L, 2009. Size-dependent toxicity of metal oxide particles–A comparison between nano- and micrometer size. Toxicol Lett 188, 112–118.

Kasemets K, Ivask A, Dubourguier HC, Kahru A, 2009. Toxicity of nanoparticles of ZnO, CuO and TiO_2 to yeast *Saccharomyces cerevisiae*. Toxicol in Vitro 23, 1116–1122.

Kathirvelu S, D'Souza L, Dhurai B, 2009. UV protection finishing of textiles using ZnO nanoparticles. Indian J Fibre Text 34, 267–273.

Lee SW, Kim SM, Choi J, 2009. Genotoxicity and ecotoxicity assays using the freshwater crustacean *Daphnia magna* and the larva of the aquatic midge *Chironomus riparius* to screen the ecological risks of nanoparticle exposure. Environ Toxicol Pharmacol 28, 86–91.

Lovern SB, Strickler JR, Klaper R, 2007. Behavioral and physiological changes in *Daphnia magna* when exposed to nanoparticle suspensions (titanium dioxide, nano-C_{60}, and $C_{60}HxC_{70}Hx$). Environ Sci Technol 41, 4465–4470.

MacCormack TJ, Goss GG, 2008. Identifying and predicting biological risks associated with manufactured nanoparticles in aquatic ecosystems. J Ind Ecol 12, 286–296.

Meng H, Chen Z, Xing G, Yuan H, Chen C, Zhao F, Zhang C, Zhao Y, 2007. Ultrahigh reactivity provokes nanotoxicity: Explanation of oral toxicity of nanocopper particles. Toxicol Lett 175, 102–110.

Miller RJ, Lenihan HS, Muller EB, Tseng N, Hanna SK, Keller AA, 2010. Impacts of metal oxide nanoparticles on marine phytoplankton. Environ Sci Technol 44, 7329–7334.

Moore MN, 2006. Do nanoparticles present ecotoxicological risks for the health of the aquatic environment? Environ Int 32, 967–976.

Mortimer M, Kasemets K, Kahru A, 2010. Toxicity of ZnO and CuO nanoparticles to ciliated protozoa *Tetrahymena thermophila*. Toxicology 269, 182–189.

Navarro E, Baun A, Behra R, Hartmann NB, Filser J, Miao AJ, Quigg A, Santschi PH, Sigg L, 2008. Environmental behavior and ecotoxicity of engineered nanoparticles to algae, plants, and fungi. Ecotoxicology 17, 372–386.

Nel A, Xia T, Mädler L, Li N, 2006. Toxic potential of materials at the nanolevel. Science 311, 622–627.

OECD, 2010. Guidance Manual for the Testing of Manufactured Nanomaterials: OECD's sponsorship programme, ENV/JM/MONO(2009)20REV. OECD Environment, Health and Safety Publications, Series on the Safety of Manufactured Nanomaterials No. 25, Organisation for Economic Co-operation and Development, Paris.

Pascoal C, Cássio F, Gomes P, 2001. Leaf breakdown rates: a measure of water quality? Int Rev Hydrobiol 86, 407–416.

Pestana JLT, Ré A, Nogueira AJA, Soares AMVM, 2007. Effects of cadmium and zinc on the feeding behaviour of two freshwater crustaceans: *Atyaephyra desmarestii* (Decapoda) and *Echinogammarus meridionalis* (Amphipoda). Chemosphere 68, 1556–1562.

Petersen EJ, Nelson BC, 2010. Mechanisms and measurements of nanomaterial-induced oxidative damage to DNA. Anal Bioanal Chem 398, 613–650.

Pradhan A, Seena S, Pascoal C, Cássio F, 2011. Can metal nanoparticles be a threat to microbial decomposers of plant litter in streams? Microb Ecol 62, 58–68.

Reijnders L, 2006. Cleaner nanotechnology and hazard reduction of manufactured nanoparticles. J Clean Prod 14, 124–133.

Ren G, Hu D, Cheng EWC, Vargas-Reus MA, Reip P, Allaker RP, 2009. Characterisation of copper oxide nanoparticles for antimicrobial applications. Int J Antimicrob Agents 33, 587–590.

Saison C, Perreault F, Daigle JC, Fortin C, Claverie J, Morin M, Popovic R, 2010. Effect of core-shell copper oxide nanoparticles on cell culture morphology and photosynthesis (photosystem II energy distribution) in the green alga, *Chlamydomonas reinhardtii*. Aquat Toxicol 96, 109–114.

Sakuma M, 1998. Probit analysis of preference data. Appl. Entomol. Zool. 33, 339–347.

Sharma VK, 2009. Aggregation and toxicity of titanium dioxide nanoparticles in aquatic environment – a review. J Environ Sci Health A 44, 1485–1495.

Suberkropp K, Arsuffi TL, Anderson JP, 1983. Comparison of degradative ability, enzymatic activity, and palatability of aquatic hyphomycetes grown on leaf litter. Appl Environ Microbiol 46, 237–244.

Valenti W, Chaffin JL, Cherry DS, Schreiber ME, Valett HM, Charles M, 2005. Bioassessment of an appalachian headwater stream influenced by an abandoned arsenic mine. Arch Environ Contam Toxicol 49, 488–496.

Van Hoecke K, Quik JT, Mankiewicz-Boczek J, De Schamphelaere KA, Elsaesser A, Van der Meeren P, Barnes C, McKerr G, Howard CV, Van de Meent D, Rydzyński K, Dawson KA, Salvati A, Lesniak A, Lynch I, Silversmit G, De Samber B, Vincze L, Janssen CR, 2009. Fate and effects of CeO_2 nanoparticles in aquatic ecotoxicity tests. Environ Sci Technol 43, 4537–4546.

Varandas SG, Cortes RMV, 2010. Evaluating macroinvertebrate biological metrics for ecological assessment of streams in northern Portugal. Environ Monit Assess 166, 201–221.

Wang Z, Lee YH, Wu B, Horst A, Kang Y, Tang YJ, Chen DR, 2010. Anti-microbial activities of aerosolized transition metal oxide nanoparticles. Chemosphere 80, 525–529.

Wilding J, Maltby L, 2006. Relative toxicological importance of aqueous and dietary metal exposure to a freshwater crustacean: implication for risk assessment. Environ Toxicol Chem 25, 1795–1801.

Zar JH, 2009. Biostatistical Analysis, fifth ed, Prentice-Hall, Upper Saddle River, New Jersey.

Zhang X, Zhang D, Ni X, Song J, Zheng H, 2008. Synthesis and electrochemical properties of different sizes of the CuO particles. J Nanopart Res 10, 839–844.

Zhu X, Zhu L, Duan Z, Qi R, Li Y, Lang Y, 2008. Comparative toxicity of several metal oxide nanoparticle aqueous suspensions to Zebrafish (*Danio rerio*) early developmental stage. J Environ Sci Health A 43, 278–284.

Chapter 5

Size-dependent effects of nanoCuO on the feeding behaviour of freshwater shredders may change in the presence of natural organic matter

Abstract

Nanoparticle size and the presence of natural organic matter (NOM) may alter the toxicity of nanoCuO to aquatic biota. Invertebrate shredders play a key role in plant-litter decomposition in streams with important consequences to higher trophic levels. We investigated the feeding behaviour of the freshwater shredder *Allogamus ligonifer* in the absence or presence of two sublethal concentrations of nanoCuO (50 and 100 mg L^{-1}) with three particle sizes (12, 50 and 80 nm) in the absence or presence of humic acid (HA, 100 mg L^{-1}) as a proxy of NOM. In addition, we examined the ability of animals to recover when released from the stress induced by exposure to nanoCuO and/or HA. In the absence of nanoCuO and HA, the feeding rate of the shredder was 0.416 mg leaf DM mg^{-1} animal DM day^{-1}. The exposure to increased nanoCuO concentrations significantly inhibited the shredder-feeding rate, with smaller size nanoparticles having greater effects (up to 83.3% for 12 nm particle size). The exposure to HA alone inhibited in 52.7% the shredder-feeding rate. However, the co-exposure to nanoCuO and HA alleviated the inhibitory effects promoted by smaller size nanoCuO on the feeding rate (recovery of 29.5 and 25.9% for 12 and 50 nm, respectively). The post-exposure feeding experiment showed a slight improvement in the invertebrate feeding rate after stress removal. Shredders pre-exposed only to HA or lower concentration of 80 nm nanoCuO recovered faster.

Keywords: NanoCuO, particle size, humic acid, invertebrate shredder, feeding behaviour, stress recovery.

5.1. Introduction

Nanocopper oxide (nanoCuO) is one of the most frequently used nanometal oxide with applications in electronics, catalysis, gas sensors and antimicrobial therapy (Carnes and Klabunde, 2003; Dutta et al., 2003; Zhang et al., 2008; Ren et al., 2009). The enhanced use of this nanomaterial increases the probability of its release into the environment, ultimately reaching surface waters. There is a lack of global data on the amounts of nanoCuO in natural waters, but in industrial wastewaters copper can exceed 100 mg L^{-1} of which up to 49% consisted of nanoCuO (Huang et al., 2006). Although not yet included in the OECD list (OECD, 2010) for toxicological and risk assessment studies, nanoCuO can be toxic to aquatic organisms (bacteria and invertebrates, Heinlaan et al., 2008; ciliated protozoa, Mortimer et al., 2010; and green algae, Saison et al., 2010). However, the toxicity of metal oxide nanoparticles may depend on their physicochemical properties, which may vary with the particle size and environmental factors (Aruoja et al., 2009, Hartmann et al., 2010).

Natural organic matter (NOM) is commonly present in freshwaters up to 100 mg L^{-1} (Wall and Choppin, 2003; Steinberg et al., 2006), and is known to affect stability and bioavailability of metals and metal oxide nanoparticles with implications to their toxicity (Lowry and Wiesner, 2007; Wigginton et al., 2007; Blinova et al., 2010). About 30% of NOM in natural waters consists of humic acid (HA; Ma et al., 2001). Some authors found that HA can mitigate the toxicity of metals or metal-based nanoparticles to freshwater organisms (copper ions to crustaceans, De Schamphelaere et al., 2002; silver nanoparticles to bacteria, Fabrega et al., 2009; iron nanoparticles to bacteria, Chen et al., 2011). Conversely, HA was reported to exhibit toxicity against organisms, including freshwater invertebrates (Meems et al., 2004; Timofeyev et al., 2006).

Freshwater invertebrates are often used in ecotoxicology because they are easy to manipulate and maintain under laboratorial conditions, and they have shown high sensitivity to anthropogenic stressors, such as ionic copper (De Schamphelaere et al., 2004; Gerhardt et al., 2004) or nanoCuO (Cattaneo et al., 2009; Buffet et al., 2011; Pradhan et al 2012). However, most toxicological studies on aquatic invertebrates with ionic or nano copper have assessed lethal toxicity (Griffitt et al., 2008; Heinlaan et al., 2008, 2011), and only few assessed sublethal

toxicity by examining the feeding behaviour (Hatakeyama, 1989; De Schamphelaere et al., 2007; Pradhan et al., 2012) or burrowing activity (Buffet et al., 2011).

In low-order forested streams, invertebrate shredders play a key role in plant litter decomposition that falls from riparian vegetation (Graça and Canhoto, 2006). Freshwater shredders prefer to feed on plant-litter colonized by microbes, predominantly aquatic fungi, because their activity on leaves increases the food quality and palatability for shredders (Graça, 2001). *Allogamus ligonifer* is a common invertebrate shredder in Southwest European streams with good ecological quality (Bonada et al., 2008). In a previous study, we showed that sublethal concentrations of nanoCuO affect the feeding behaviour and growth of *A. ligonifer* (Pradhan et al., 2012). In this following up study, we investigated how effects of nanoCuO on the feeding behaviour of *A. ligonifer* depended on the particle size and the presence of humic acid, under the hypotheses that i) smaller size nanoparticles would be able to induce higher toxicity than larger size nanoparticles; ii) HA would mitigate the toxicity of nanoparticles depending on the nanoparticle size and concentration; iii) HA might have negative impacts on invertebrates; iv) invertebrate recovery from nanoCuO exposure would depend on the severity of stress. To test these hypotheses, we measured leaf consumption by the invertebrate shredder and fine particulate organic matter (FPOM) production after exposure to nanoCuO and/or HA and after releasing the animals from exposure to these chemicals. Nanoparticles in the stream water and on FPOM were analysed by SEM-EDX and DLS to examine the interactions among nanoCuO, HA and FPOM.

5.2. Material and Methods

5.2.1. Microbial colonization of leaves

Leaves of *Alnus glutinosa* (L.) Gaertn. (alder), a common riparian tree in the Iberian Peninsula, were collected from a single tree in autumn and air dried at room temperature. The leaves were soaked in deionised water, cut into 12 mm-diameter disks, and placed into fine-mesh bags (15 × 15 cm; 0.5-mm size mesh for preventing invertebrate colonization). Leaf bags were immersed in the Maceira Stream (N 41°45'58.79'', W 8°08'49.39'', altitude 867 m, Cávado River basin, Northwest Portugal) to allow microbial colonization. After 7 days of immersion, leaf bags were retrieved from the stream and leaf disks from each replicate bag were

rinsed with deionised water and used for feeding experiments. Detailed information on the Maceira Stream can be found in Pradhan et al. (2011).

5.2.2. Collection and maintenance of invertebrate shredders

Allogamus ligonifer (McLachlan, 1876) is an invertebrate shredder that belongs to the Limnephilidae family. *A. ligonifer* is reported to occur in Southwestern European streams (Bonada et al., 2008) and it is quite common in low-order streams of North Portugal (Varandas and Cortes, 2010). Early-stage larvae of the caddisfly, with similar size (14 ± 1 mm length), were collected from the upper reach of the Cávado River during autumn 2011. The animals were transported to the laboratory in plastic containers with stream water and sand. In the laboratory, the animals were placed in an aquarium with filtered (MN GF-3, Macherey-Nagel, Germany) and autoclaved (121°C, 20 min) stream water and sand, at 14°C under aeration with a 12 h light : 12 h dark photoperiod, and were allowed to feed on alder leaves for 4 weeks before the experiment. Detailed information on the Cávado River can be found in Pascoal et al. (2001).

5.2.3. Preparation and characterization of nanoCuO in the absence and presence of HA

Stock suspensions of nanocopper oxide with three different sizes, namely i) 12 nm CuO nanopowder (99.5%, Ionic Liquid Technology: IO-LI-TEC, Heilbronn, Germany), ii) 50 nm CuO nanopowder (99.5%, Sigma-Aldrich, St. Louis, MO), and iii) 80 nm (99.9%, IO-LI-TEC), were prepared in autoclaved stream water by sonication at 42 kHz (Branson 2510, Danbury, CT, USA) for 30 min in dark before use (Heinlaan et al., 2008). The pH of all nanoCuO stock suspensions was adjusted to the stream water pH (5.8 ± 0.2). Stock solution of humic acid (Sigma-Aldrich, St. Louis, MO) was freshly prepared in sterile stream water by overnight (10 h) stirring before use. The stream water contained silica 9.6 ± 2 mg L^{-1}, Na^{+} 4.1 ± 0.4 mg L^{-1}, K^{+} 0.6 ± 0.1 mg L^{-1}, Ca^{2+} 1.3 ± 0.3 mg L^{-1}, Cl^{-} 4.2 ± 0.4 mg L^{-1}, HCO_3^{-} 8.0 ± 0.8 mg L^{-1}, and SO_4^{-} 1.0 ± 0.2 mg L^{-1}.

NanoCuO suspensions with three different size nanoparticles and mixed suspensions containing nanoCuO and HA were examined before and after the feeding experiment by scanning electron microscopy (SEM, Leica Cambridge S 360, Cambridge, UK) coupled to an energy dispersive X-ray microanalysis setup (EDX,

15 KeV) as described by Pradhan et al. (2011). Size distribution of particles in the stream water was also examined by dynamic light scattering (DLS) using a zetasizer (Malvern, Zetasizer Nano ZS) for checking agglomeration (Pradhan et al. 2012).

5.2.4. Feeding experiment

For assessing the individual or combined effects of nanoCuO size and HA on the feeding behaviour of the invertebrate shredder, two premeasured larvae of *A. ligonifer* were allocated to each 150-mL flask containing 10 microbially-colonized leaf disks and 100 mL of autoclaved stream water supplemented or not with nanoCuO (50 mg L^{-1} or 100 mg L^{-1}) and/or HA (100 mg L^{-1}). Seven replicates were used per treatment. Microbially-colonized leaf disks used in the microcosms were previously exposed for 20 days to similar concentration of the respective chemical.

The contribution of microorganisms to leaf litter decomposition was determined by enclosing an equal number of leaf disks treated as above in 0.5 mm fine-mesh bags (to prevent the access of invertebrates), which were placed in each replicate microcosms of the respective treatment.

All flasks were aerated with constant air flow and incubated at 14°C, under a 12 h light : 12 h dark photoperiod. The experiment was run for 5 days.

5.2.5. Post-exposure feeding experiment

After the feeding experiments with nanoCuO and/or HA, the two invertebrates of each microcosm were placed in flasks with autoclaved stream water, and the water was renewed every 30 min until 6 h. Then, the rescued invertebrates of each treatment were placed in 150-mL flask with 100 mL of autoclaved stream water and allowed to feed on microbially-colonized leaves (10 disks) non-exposed to the chemicals. Animals were kept under the conditions of aeration and photoperiod described above, and the feeding rates were determined after 5 days. Microbial contribution to litter decomposition was determined by using 10 microbially-colonized leaf disks enclosed in fine-mesh bags as above.

5.2.6. Leaf mass loss

For determination of leaf mass loss, leaf disks from each replicate were freeze-dried (Christ alpha 2–4, B. Braun, Germany) and weighed to the nearest 0.001 mg before and after the feeding and post-exposure feeding experiments.

5.2.7. Leaf consumption by invertebrates and microbes

Leaf mass consumed by the invertebrate shredder (L_e) was determined as $(L_i - L_f) - (L_i \times (C_i - C_f)/C_i)$, where L_i and L_f are the initial and final dry mass (DM, mg) of leaves exposed to the invertebrates, respectively, and C_i and C_f are the initial and final dry mass (DM, mg) of control leaves that are inaccessible to invertebrates, respectively (Pradhan et al., 2012). Leaf decomposition rate by microbes was determined by $(C_i - C_f)/t$, where t is time (t=5 days). Leaf consumption rate by the invertebrate was calculated as $L_e/(I_f \times t)$, where I_f is the dry mass (DM, mg) of invertebrates at time t (day 5), and results were expressed as mg leaf DM mg^{-1} animal DM day^{-1} (Pradhan et al., 2012).

5.2.8. FPOM quantification and visualization under SEM

After the feeding experiments the fine particulate organic matter, i.e. invertebrate faeces and leaf detritus, was sieved (0.5 mm mesh) and collected on membranes by filtration (0.45 µm pore size, Millipore, Billerica, MA, USA). FPOM on the membranes was washed twice with ultrapure (Milli Q) water and freeze-dried (Christ alpha 2–4, B. Braun, Germany) before weighed to the nearest 0.001 mg. FPOM was, then, fixed in 2.5% (v/v) glutaraldehyde for 24 h, and dehydrated in ethanol (v/v) as follows: 20%, 8 h; 40%, 6 h; 60%, 4 h; 80%, 2 h; and 100%, 1 h. The filters containing the FPOM were glued onto 20-mm diameter metal mounts, coated with gold under vacuum and scanned by SEM-EDX as above.

5.2.9. Data analyses

Three-way ANOVAs were used to determine the effects of concentration and size of nanoCuO in the absence or presence of HA on leaf decomposition rate by microbes or leaf consumption rate by invertebrates (Zar, 2009). Significant differences between control and treatments were analysed by Bonferroni post-tests (Zar, 2009). To achieve normal distribution and homoscedasticity, the data in percentage were arcsine square root transformed (Zar, 2009). Analyses were performed with Statistica 6.0 (Statsoft, Inc., Tulsa, OK, USA).

5.3. Results

5.3.1. Characterization of CuO nanoparticles and HA in the stream water

The CuO nanoparticles in stream water were observed under SEM (Fig. 5.1) and the presence of Cu was further confirmed by EDX analysis (not shown). DLS analysis of stream water supplemented with nanoCuO showed that suspensions of nanoparticles with 12, 50 or 80 nm had average sizes of 101.8 nm (PdI 0.137), 202.4 nm (PdI 0.181) and 267.6 nm (PdI 0.296), respectively (Table 5.1). Taking into consideration the manufacturer information on the size of primary nanoparticles, the higher values found by DLS indicated agglomeration of nanoCuO in the stream water. The average size of all CuO nanoparticles increased in the presence of HA (1.2 times for 50 and 80 nm particles, and 1.5 times for 12 nm particles; Table 5.1). After the feeding experiment, the average size of nanoparticles in the stream water further increased, indicating agglomeration with time mainly for 80 nm nanoCuO (Table 5.1, Fig. 5.1). However, in the presence of HA, the size of smaller nanoparticles decreased after the feeding experiment (147.9 vs. 124.3 nm and 248.1 vs. 232.8 nm for 12 and 50 nm sizes, respectively), although sizes were still higher than those in the absence of HA (Table 5.1, Fig. 5.1). The decrease in PdI values after the feeding experiment in mixtures of smaller size nanoCuO with HA confirmed higher nanoparticle dispersion and stability (Table 5.1). In contrast, the presence of HA increased the size of 80 nm nanoparticles (330.4 nm) after the feeding experiment indicating increased aggregation/agglomeration with time as supported by the PdI (Table 5.1).

Table 5.1 Size distribution of nanoCuO in the stream water before and after the feeding experiment in the presence or absence of humic acid (HA)

Treatments	PdI	Z-average (d.nm)	Size range (d.nm)
	Before / after the feeding experiment		
NanoCuO size (nm)			
12	0.137 / 0.161	101.8 / 116.0	20–290 / 40–320
50	0.181 / 0.207	202.4 / 220.1	80–340 / 90–420
80	0.296 / 0.367	267.6 / 319.8	110–590 / 120–700
12 + HA	0.224 / 0.182	147.9 / 124.3	50–475 / 40–360
50 + HA	0.249 / 0.218	248.1 / 232.8	100–620 / 90–480
80 + HA	0.380 / 0.405	323.6 / 330.4	110–760 / 105–790

d.nm: diameter in nanometer unit. PdI: polydispersity index.

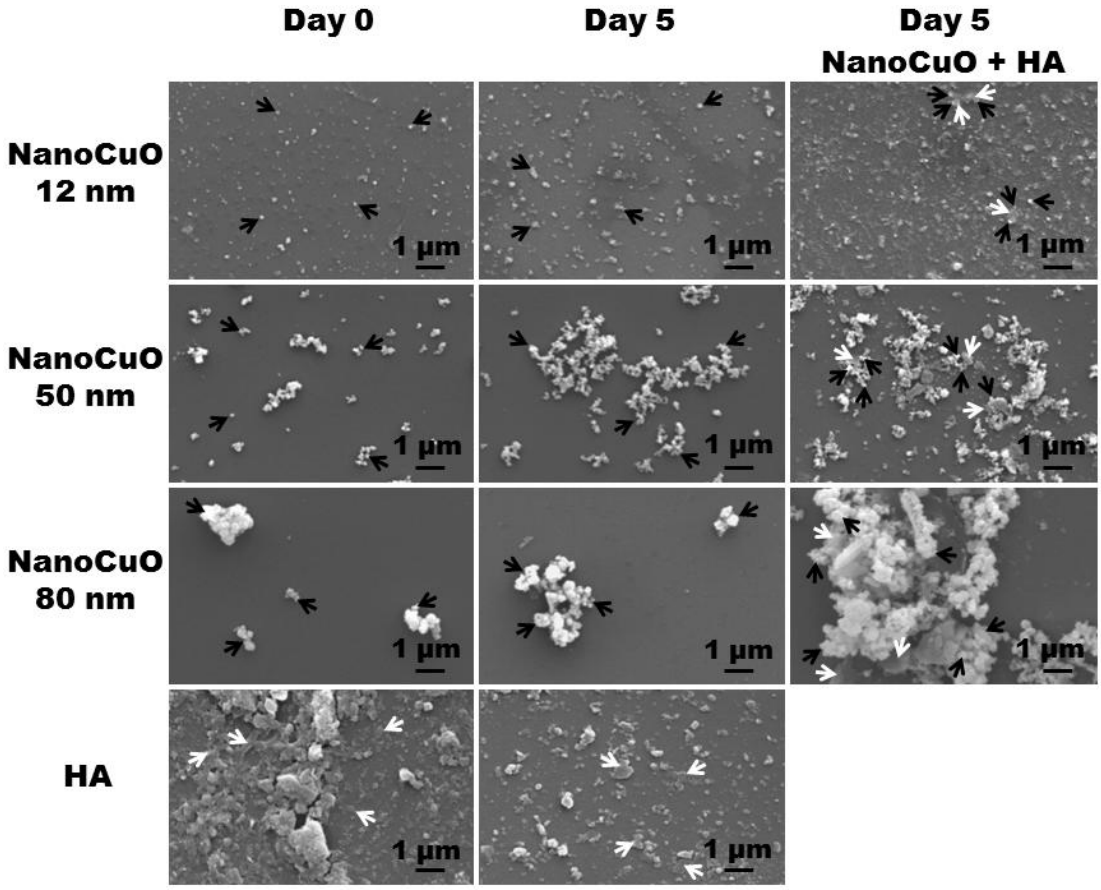

Figure 5.1 Scanning electron microscopy (SEM) of nanoCuO with 12, 50 and 80 nm size in the absence and/or presence of humic acid (HA) in the stream water before (day 0) and/or after (day 5) the invertebrate feeding experiment. Black arrows indicate nanoCuO and white arrows indicate HA.

5.3.2. Effects of nanoCuO and HA on invertebrate feeding and microbial decomposition

In the absence of nanoCuO or HA, the feeding rate of the invertebrate shredder *A. ligonifer* was 0.416 mg leaf DM mg^{-1} animal DM day^{-1}. The feeding rate of the shredder was significantly affected by the presence of HA, and by the size and concentration of nanoCuO (three-way ANOVA, $P<0.05$). The strongest inhibitions of feeding rates were 83.3, 74.0 and 53.0% after exposure to 100 mg L^{-1} of 12, 50 and 80 nm of nanoCuO, respectively ($P<0.05$; Fig. 5.2A-C). The feeding rate was not significantly reduced by exposure to the lowest concentration of 80 nm nanoCuO ($P>0.05$; Fig. 5.2C), but decreased significantly after exposure to the lowest concentration of smaller nanoparticles (69.7 and 58.2% inhibition with 12 and 50 nm, respectively) ($P<0.05$; Fig. 5.2A and B). In the absence of nanoCuO, the exposure to HA significantly inhibited the shredder feeding rate by 52.7% ($P<0.05$; Fig. 5.2A-C). However, the co-exposure to HA and to the highest concentration of

smaller size nanoparticles attenuated the negative effects of nanoCuO on the feeding rate in 29.5 and 25.9% for 12 and 50 nm, respectively (*P<0.05*; Fig. 5.2A and B), but this was not observed for the largest nanoparticles (*P>0.05*; Fig. 5.2C).

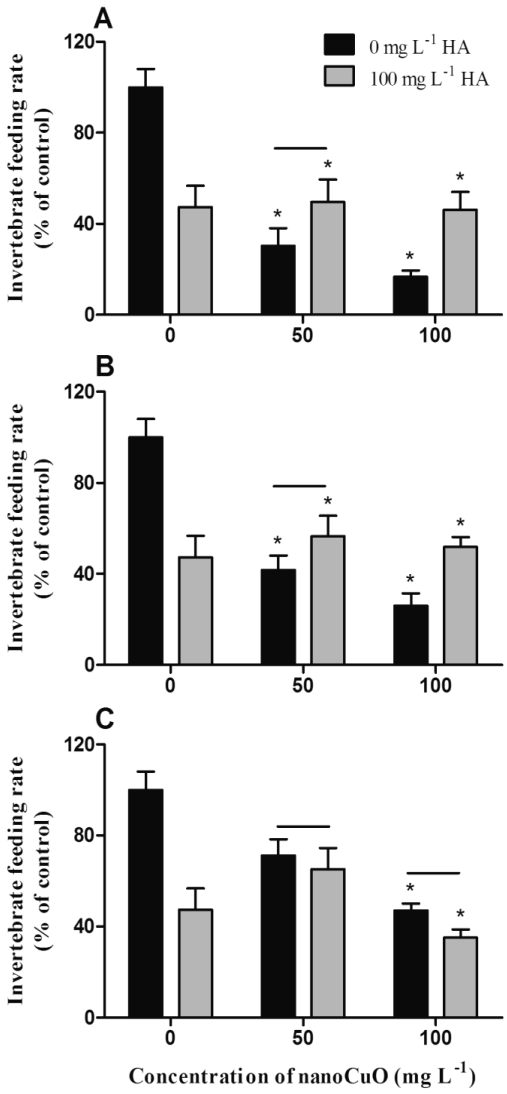

Figure 5.2 Leaf consumption rate by the invertebrate shredder *Allogamus ligonifer* exposed to increasing concentration of nanoCuO with 12 nm (A), 50 nm (B) and 80 nm (C) in the presence or absence of humic acid (HA). Mean ± SEM, n=7. *, treatments that differ significantly from control (Bonferroni tests, *P<0.05*). Horizontal lines indicate no significant differences between treatments.

In the absence of nanoCuO and HA, leaf decomposition rate by microbes was 0.616 mg leaf DM microcosm^{-1} day^{-1}, corresponding to 7.8% of the total leaf consumption rate (microbes and invertebrates). Leaf decomposition by microbes was affected by the presence of HA, the concentration and the size of nanoCuO (three-way ANOVA, *P<0.05*). The highest inhibition of microbial decomposition rates was found after exposure to the highest concentration of nanoCuO with 12 nm or 50 nm, and corresponded to a reduction of 76.8 and 67.4%, respectively (*P<0.05*; Fig.

5.3A and B). The exposure to 80 nm did not show any significant effect (*P>0.05*; Fig. 5.3C). In the absence of nanoCuO, HA decreased in 70% the microbial decomposition rate (*P<0.05*; Fig. 5.3A-C). Similarly to that found for the invertebrate, the presence of HA attenuated the negative effects of 12 and 50 nm nanoCuO on microbial decomposition rate, which recovered up to 26.2% (*P<0.05*; Fig. 5.3A and B). Moreover, the mitigation effect of HA was not observed when microbially-colonized leaves were co-exposed to nanoCuO with 80 nm (*P>0.05*; Fig. 5.3C).

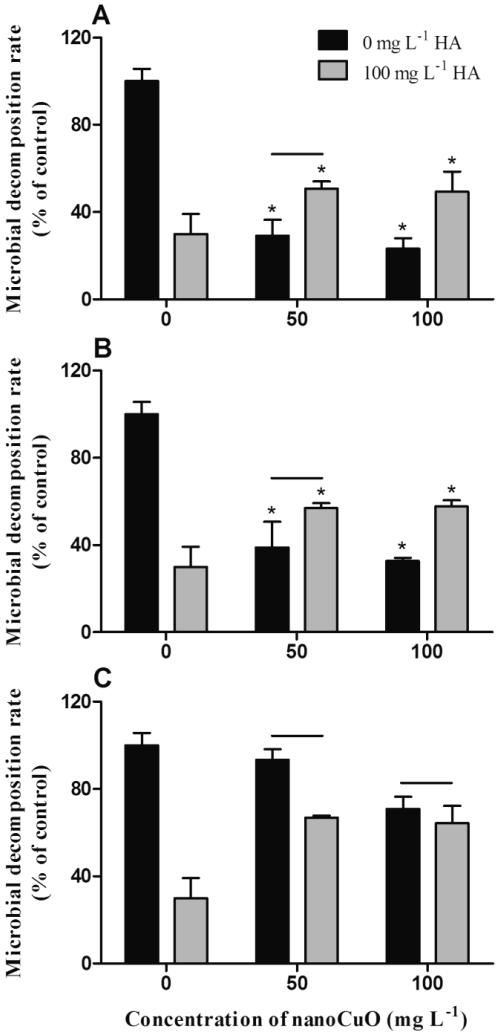

Figure 5.3 Microbial decomposition rate of leaves exposed to increasing concentration of nanoCuO with 12 nm (A), 50 nm (B) and 80 nm (C) in the presence or absence of humic acid (HA). Mean ± SEM, n=7. *, treatments that differ significantly from control (Bonferroni tests, *P<0.05*). Horizontal lines indicate no significant differences between treatments.

In the post-exposure feeding experiment, invertebrates that were not exposed to nanoCuO or HA had a feeding rate of 0.422 mg leaf DM mg^{-1} animal DM day^{-1}, similar to that found in the feeding experiment in the absence of stressors. In the post-exposure experiment, the feeding behaviour of shredders was significantly

affected by pre-exposure to HA and nanoCuO with diferent sizes and concentrations (three-way ANOVA, *P<0.05*; Fig. 5.4A-C). The feeding recovery of animals rescued from exposure to 100 mg L^{-1} of nanoCuO with 12, 50 and 80 nm in the absence of HA was very low (Fig. 5.4A-C vs. Fig. 5.2A-C), and corresponded to 3.4, 4.6 and 9.2%, respectively (Table 5.2). A slightly higher recovery in the feeding rates occurred after release from exposure to the smaller size nanoCuO and HA (*P<0.05*; Fig. 5.4A and B vs. Fig. 5.2A and B; Table 5.2).

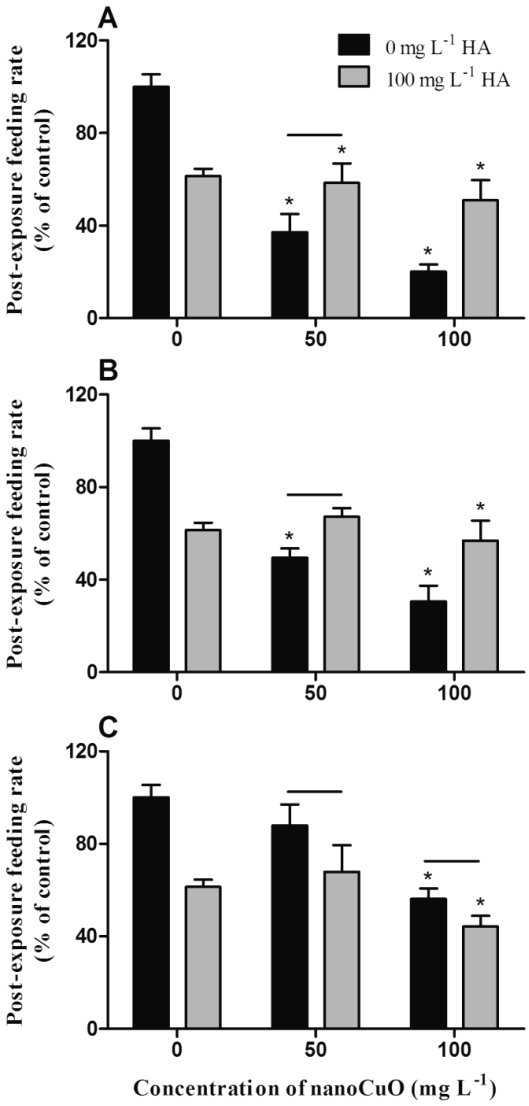

Figure 5.4 Leaf consumption rate by the invertebrate shredder *Allogamus ligonifer* in the post-exposure feeding experiment in which animals were previously exposed for 5 days to increasing concentrations of nanoCuO with 12 nm (A), 50 nm (B) and 80 nm (C) in the presence or absence of humic acid (HA) and then placed in stream water without the chemicals for further 5 days. Mean ± SEM, n=7. *, treatments that differ significantly from control (Bonferroni tests, *P<0.05*). Horizontal lines indicate no significant differences between treatments.

Animals rescued from exposure to HA without nanoCuO showed a significant decrease in the post-exposure feeding rate (*P<0.05*; Fig. 5.4A-C), which corresponded to a feeding rate recovery of 14.9% comparing to the exposure conditions (Table 5.2). Shredders rescued from exposure to the lowest concentration of the largest CuO nanoparticle in the absence of HA had the highest recovery in the feeding rates (16.7%, Table 5.2).

Table 5.2 Recovery of invertebrate feeding rates after release from exposure to different size nanoCuO and/or humic acid (HA)

Treatments	NanoCuO (mg L^{-1})	Feeding rate recovery (%)	
		Without HA	With HA
Absence of nanoCuO	0	0	14.0
12 nm nanoCuO	50	6.9	8.9
	100	3.4	4.8
50 nm nanoCuO	50	7.8	10.6
	100	4.6	5.0
80 nm nanoCuO	50	16.7	5.0
	100	9.2	9.0

5.3.3 Effects of nanoCuO and HA on FPOM production

In the absence of nanoparticles and HA, 32.6 mg of FPOM was produced per microcosm. The presence of HA reduced FPOM production to 61.7% (Table 5.3). FPOM production decreased with exposure to increasing concentrations of nanoCuO and decrease in nanoparticle size (Table 5.3). Maximum reductions in FPOM production were found in treatments with 100 mg L^{-1} of 12 and 50 nm nanoCuO leading to 21.2% and 30.4% production of the FPOM, respectively (Table 5.3). The co-exposure to 100 mg L^{-1} of both HA and nanoCuO with 12 or 50 nm increased the production to 45.1 and 56.7%, respectively; however, similar FPOM production was observed under exposure to 80 nm nanoCuO with or without HA (Table 5.3).

During the post-exposure feeding experiment, the production of FPOM in control (31.9 mg per microcosm) was similar to that found in the exposure experiment. The recovery in FPOM production was very low in microcosms with animals previously exposed to nanoCuO, mainly in treatments with 100 mg L^{-1} of 12 nm nanoCuO (recovery of 0.7%, Table 5.3). The highest recoveries in FPOM production (9.4 and 8.8%) were obtained in microcosms with invertebrates

previously exposed to 50 mg L^{-1} of the largest nanoparticles without HA, and to HA without nanoparticles (Table 5.3).

Table 5.3 Fine particulate organic matter (FPOM) produced in microcosms after exposure to increasing concentrations of 12, 50 and 80 nm size nanoCuO and/or humic acid (HA) during the exposure feeding experiment or the post-exposure feeding experiment

Treatments	NanoCuO (mg L^{-1})	FPOM production (% of control)			
		Exposure experiment		Post-exposure experiment	
		Without HA	With HA	Without HA	With HA
Absence of nanoCuO	0	100.0	61.7	100.0	70.5
12 nm nanoCuO	50	51.8	62.0	53.6	64.3
	100	21.2	45.1	21.9	48.0
50 nm nanoCuO	50	60.4	66.6	63.0	69.0
	100	30.4	56.7	32.6	59.6
80 nm nanoCuO	50	83.4	82.2	92.8	90.0
	100	70.6	69.3	74.3	72.7

SEM analysis revealed that the surface of FPOM produced in control microcosms was granular with 3-7 µm diameter average grain size (Fig. 5.5). The surface morphology of FPOM altered after exposure to nanoCuO and/or HA, even after stress release, i.e. in the post-exposure feeding experiment (Fig. 5.5). The surface of FPOM in treatments with nanoCuO without HA seemed to be less granular and covered with nanoCuO (Fig. 5.5). In treatments with smaller size nanoparticles, the size and self-aggregation of nanoparticles seemed to decrease while the number of nanoparticles seemed to increase (Fig. 5.5). The presence of Cu from nanoCuO was further confirmed by EDX (not shown). Layers of HA and alteration of the granular surface of FPOM were found in microcosm exposed to HA, this effect decreased remarkably after release from the chemicals (Fig. 5.5). FPOM from microcosms with HA and smaller nanoCuO (12 and 50 nm) had less amount of nanoparticles on the surface, which was less altered than that found in the absence of HA. However, this difference was not observed in FPOM from treatments with 80 nm nanoparticles (Fig. 5.5). NanoCuO were also observed on FPOM produced during post-exposure experiment in the microcosms containing invertebrates rescued from exposure to nanoCuO with or without HA (Fig. 5.5). However, the amount of nanoCuO on FPOM was lower and the FPOM surface was less altered after the post-exposure experiment than after the exposure experiment (Fig. 5.5).

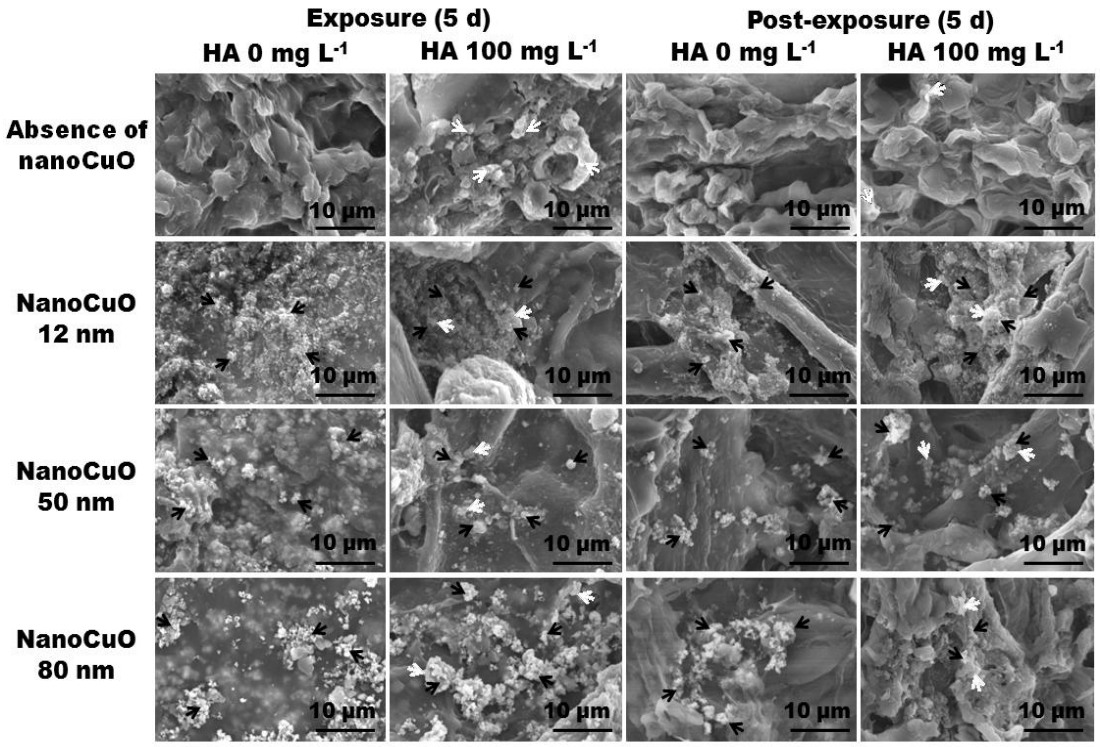

Figure 5.5 Scanning electron microscopy analysis of the FPOM produced in microcosms during the feeding experiment under exposure or not to 100 mg L^{-1} nanoCuO and/or to HA, and during the post-exposure feeding experiment after removal of the chemicals. Black arrows indicate nanoCuO and white arrows indicate HA layer.

5.4. Discussion

Most ecotoxicological studies assessing the impacts of nanometal oxides, including nanoCuO, on stream invertebrates used acute lethality tests (Heinlaan et al., 2008; Blinova et al., 2010), which may not demonstrate the actual hazard of nanoparticles because lethality can be achieved at high concentrations with low environmental realism. Indeed, studies assessing sublethal effects by examining the feeding behaviour of invertebrates pointed it as one of the most sensitive and widely accepted tools for monitoring ecotoxicity of ionic metals (Pestana et al., 2007) and nanometal oxides (Galloway et al., 2010; Buffet et al., 2011; Pradhan et al., 2012). In our study, the feeding rate of *A. ligonifer* in control microcosms (0.42 mg leaf DM mg^{-1} animal DM day^{-1}) was within the typical range for freshwater invertebrate shredders (0.04 to 0.5 mg leaf DM mg^{-1} animal DM day^{-1}; Arsuffi and Suberkropp, 1989). Exposure to nanoCuO prominently inhibited the shredder feeding rate as previously found for marine and freshwater invertebrates (Buffet et al., 2011; Pradhan et al., 2012), and toxicity was correlated with the accumulation and

adsorption of nano and/or leached ionic copper in the invertebrate body and food (Pradhan et al. 2012).

In the present study, the inhibitory effects of nanoCuO were stronger as nanoparticle size decreased and concentration increased; maximum inhibition of invertebrate feeding rate (83.3% inhibition) was found after exposure to the highest concentration (100 mg L^{-1}) of nanoCuO with the smaller size (12 nm). One should point out that the size of nanoparticles determined by DLS in our study was higher than the size of primary particles indicated by the manufacturer or by SEM-EDX analysis, probably due to nanoparticle agglomeration in aqueous environments (Buffet et al., 2011; Pradhan et al., 2012). Previous studies showed that the toxicity of nanometal oxides was higher than their bulk size particles (Aruoja et al., 2009; Karlsson et al., 2009; Kasemets et al., 2009), however, only few attempts were taken for size-based comparative toxicity assessment of nanometal oxides to aquatic organisms (Hartmann et al., 2010). Our findings on nanoCuO effects were supported by earlier observations with CeO_2 nanoparticles against freshwater invertebrates in which chronic toxicity tended to increase with the decrease in nanoparticle size (Van Hoecke et al., 2009). The size-dependent toxicity of nanoCuO to the invertebrate shredder might be related to the increased free reactive surface to volume ratio of smaller nanoparticles and lower aggregation with higher dispersion and stability in aqueous suspension, as shown by the lower polydispersity index, comparing to similar concentrations of nanoCuO with larger sizes.

In our study, the negative effects of nanoparticles to the invertebrates were accompanied by morphological alterations of the surface of FPOM, produced by the invertebrate feeding activity, and by the presence of a considerable amount of nanoparticles associated with FPOM, mainly after exposure to smaller size nanoparticles. The release from nanoparticle exposure led only to a slight recovery of invertebrate feeding rate. The feeding recovery was lower for shredders previously exposed to smaller nanoparticles than to larger nanoparticles. The presence of nanoparticles on the surface of FPOM after animals were rescued from exposure to nanoCuO suggested that the ingestion of contaminated leaves led to accumulation of nanoparticles in the gut of shredders and this might have contributed to the low feeding recovery. This agrees with our earlier observation of a positive correlation between Cu accumulation in nanoCuO-contaminated leaves and in the shredder body (Pradhan et al., 2012).

In our study, the presence of HA inhibited in 52.7% the feeding rate of *A. ligonifer*. Adverse effects of high concentrations of NOM on freshwater crustaceans (Meems et al., 2004; Timofeyev et al., 2006) and bivalve zebra mussel (Pflugmacher et al., 2001) or HA on cyanobacteria (Sun et al., 2005) were previously reported. Although the exact mode of action of NOM or HA was not revealed, the toxicity of these compounds was mainly explained by their ability to induce oxidative stress (Timofeyev et al., 2006). Interestingly, the release from HA exposure led to a 14.0% recovery of the invertebrate feeding rate, an increased production of FPOM and less alterations in the surface of FPOM. Moreover, in our study, the presence of HA reduced the negative effects of smaller size (12 or 50 nm) nanoCuO on leaf consumption by the invertebrate shredder. This agrees with other studies in which NOM or HA contributed to alleviate the toxicity induced by ionic metals or nanometals, including nanoCuO (De Schamphelaere et al., 2002; Blinova et al., 2010; Chen et al., 2011; Li et al., 2011). The mechanisms behind the mitigation effects of NOM/HA on nanoparticle-induced toxicity are unclear and effects may vary with the NOM source, concentration and exposure time (Fabrega et al., 2009; Al-Reasi et al., 2011). For instance, commercial HA (Sigma-Aldrich) was less effective than other NOM sources in alleviation of Ag^+ toxicity (48 h EC_{50}) to *Daphnia magna* (Glover et al. 2005). Nanoparticles tend to aggregate and adsorb onto organic materials due to their small size and reactive surface (Holsapple et al., 2005). Thus, it is conceivable that in the presence of HA, smaller nanoparticles have lower chance to interact with leaves and invertebrates than larger nanoparticles, contributing to explain the lower toxicity of the latter particles. Although nanoparticle adsorption to leaves or uptake by the invertebrates was not measured in this study, FPOM surface had lower amounts of smaller nanoparticles in the presence than in the absence of HA. The interaction and coating of nanoparticles with HA were also shown by TEM (Fabrega et al., 2009; Chen et al., 2011). Thus, our findings supported that HA could alleviate nanoparticle toxicity by acting as a physical barrier and masking the active nanoparticle surfaces reducing nanoparticle interactions with biota (Fabrega et al., 2009; Chen et al., 2011). Furthermore, our study highlighted that the role of HA in alleviating nanoparticle toxicity depended on nanoparticle size.

The decreased rate of invertebrate feeding by exposure to nanoCuO or HA could be also related to food avoidance behaviour (Wilding and Maltby, 2006). In our study, we examined the consumption of high quality food (alder leaves), which was previously colonized by microbes that increase leaf palatability for invertebrate

shredders (Arsuffi and Suberkropp, 1989). Thus, in the present study, the treatment of microbially-colonized leaves with nanoparticles and/or HA, prior to the feeding experiment, might have affected leaf quality and palatability for shredders. Indeed, a severe decrease in microbial decomposition was accompanied by a strong inhibition of invertebrate feeding in the presence of smaller size nanoCuO or HA. Similarly to that found for the invertebrate feeding behaviour, the inhibitory effects of smaller nanoparticles on microbial decomposition were mitigated by HA. This suggests that in addition to direct effects of nanoCuO and/or HA on invertebrates, indirect effects might also have occured through effects on microbes.

Overall, our study shows that nanoCuO induced sublethal toxicity to the invertebrate shredder *A. ligonifer* in a dose-dependent manner, and toxicity increased with the decrease in nanoparticle size. Humic acid, an important component of NOM, alleviated the toxicity of smaller nanoparticle sizes but not of larger nanoparticles. In the absence of nanoparticles, HA had negative effects on the feeding behaviour of invertebrate shredders. After release from exposure to nanoCuO and/or HA, the recovery of leaf consumption by the shredders was very low. The recovery of feeding rate was higher for invertebrates rescued from pre-exposure to HA alone or to lower concentration of nanoCuO with larger size.

References

Al-Reasi HA, Wood CM, Smith DS, 2011. Physicochemical and spectroscopic properties of natural organic matter (NOM) from various sources and implications for ameliorative effects on metal toxicity to aquatic biota. Aquat Toxicol 103, 179–190.

Arsuffi TL, Suberkropp K, 1989. Selective feeding by shredders on leaf-colonizing stream fungi: comparison of macroinvertebrate taxa. Oecologia 79, 30–37.

Aruoja V, Dubourguier HC, Kasemets K, Kahru A, 2009. Toxicity of nanoparticles of CuO, ZnO and TiO_2 to microalgae *Pseudokirchneriella subcapitata*. Sci Total Environ 407, 1461–1468.

Blinova I, Ivask A, Heinlaan M, Mortimer M, Kahru A, 2010. Ecotoxicity of nanoparticles of CuO and ZnO in natural water. Environ Pollut 158, 41–47.

Bonada N, Zamora-Muñoz C, El Alami M, Múrria C, Prat N, 2008. New records of Trichoptera in reference Mediterranean-climate rivers of the Iberian Peninsula and North of Africa: Taxonomical, faunistical and ecological aspects. Graellsia 64, 189–208.

Buffet PE, Tankoua OF, Pan JF, Berhanu D, Herrenknecht C, Poirier L, Amiard-Triquet C, Amiard JC, Bérard, JB, Risso C, Guibbolini M, Roméo M, Reip P, Valsami-Jones E, Mouneyrac C, 2011. Behavioural and biochemical responses of two marine invertebrates *Scrobicularia plana* and *Hediste diversicolor* to copper oxide nanoparticles. Chemosphere 84, 166–174.

Carnes LC, Klabunde KJ, 2003. The catalytic methanol synthesis over nanoparticle metal oxide catalysts. J Mol Catal A: Chem 194, 227–236.

Cattaneo AG, Gornati R, Chiriva-Internati M, Bernardini G, 2009. Ecotoxicology of nanomaterials: the role of invertebrate testing. Invertebrate Surviv J 6, 78–97.

Chen J, Xiu Z, Lowry GV, Alvarez PJJ, 2011. Effect of natural organic matter on toxicity and reactivity of nano-scale zero-valent iron. Water Res 45, 1995–2001.

De Schamphelaere KAC, Heijerick DG, Janssen CR, 2002. Re-finement and field validation of a biotic ligand model predicting acute copper toxicity to *Daphnia magna*. Comp Biochem Physiol C Toxicol Pharmacol 133, 243–258.

De Schamphelaere KAC, Vasconcelos FM, Allen HE, Janssen CR, 2004. The effect of dissolved organic matter source on acute copper toxicity to *Daphnia magna*. Environ Toxicol Chem 23, 1248–1255.

De Schamphelaere KAC, Forrez I, Dierckens K, Sorgeloos P, Janssen CR, 2007. Chronic toxicity of dietary copper to *Daphnia magna*. Aquat Toxicol 81, 409–418.

Dutta A, Das D, Grilli ML, Di Bartolomeo E, Traversa E, Chakravorty D, 2003. Preparation of sol–gel nano-composites containing copper oxide and their gas sensing properties. J Sol–Gel Sci Technol 26, 1085–1089.

Fabrega J, Fawcett SR, Renshaw JC, Lead JR, 2009. Silver nanoparticle impact upon bacterial growth: effect of pH, concentration, and organic matter. Environ Sci Technol 43, 7285–7290.

Galloway T, Lewis C, Dolciotti I, Johnston BD, Moger J, Regoli F, 2010. Sublethal toxicity of nano-titanium dioxide and carbon nanotubes in a sediment dwelling marine polychaete. Environ Pollut 158, 1748–1755.

Gerhardt A, de Bisthoven LJ, Soares AMVM, 2004. Macroinvertebrate response to acid mine drainage: community metrics and on-line behavioural toxicity bioassay. Environ Pollut 130, 263–274.

Glover CN, Playle RC, Wood CM, 2004. Heterogeneity of natural organic matter amelioration of silver toxicity to *Daphnia magna*: effect of source and equilibration time. Environ Toxicol Chem. 24, 2934–2940.

Graça MAS, 2001. The role of invertebrates on leaf litter decomposition in streams – a Review. Int Rev Hydrobiol 86, 383–393.

Graça MAS, Canhoto C, 2006. Leaf litter processing in low order streams. Limnetica 25, 1–10.

Griffitt RJ, Luo J, Bonzongo JC, Barber DS, 2008. Effects of particle composition and species on toxicity of metallic nanomaterials in aquatic organisms. Environ Toxicol Chem 27, 1972–1978.

Hartmann NB, Kammer FVD, Hofmann T, Baalousha M, Ottofuelling S, Baun A, 2010. Algal testing of titanium dioxide nanoparticles - testing considerations, inhibitory effects and modification of cadmium bioavailability. Toxicology 269, 190–197.

Hatakeyama S, 1989. Effect of copper and zinc on the growth and emergence of *Epeorus latifolium* (Ephemeroptera) in an indoor model stream. Hydrobiologia 174, 17–27.

Heinlaan M, Ivask A, Blinova I, Dubourguier HC, Kahru A, 2008. Toxicity of nanosized and bulk ZnO, CuO and TiO_2 to bacteria *Vibrio fischeri* and crustaceans *Daphnia magna* and *Thamnocephalus platyurus*. Chemosphere 71, 1308–1316.

Heinlaan M, Kahru A, Kasemets K, Arbeille B, Prensier G, 2011. Changes in the *Daphnia magna* midgut upon ingestion of copper oxide nanoparticles: A transmission electron microscopy study. Water Res 45, 179–190.

Holsapple MP, Farland WH, Landry TD, Monteiro-Riviere NA, Carter JM, Walker NJ, Thomas KV, 2005. Research strategies for safety evaluation of nanomaterials, part II: toxicological and safety evaluation of nanomaterials, current challenges and data needs. Toxicol Sci 88, 12–17.

Huang HL, Wang HP, Wei GT, Sun IW, Huang JF, Yang YW, 2006. Extraction of nanosize copper pollutants with an ionic liquid. Environ. Sci. Technol. 40, 4761–4764.

Karlsson HL, Gustafsson J, Cronholm P, Möller L, 2009. Size-dependent toxicity of metal oxide particles – a comparison between nano- and micrometer size. Toxicol Lett 188, 112–118.

Kasemets K, Ivask A, Dubourguier HC, Kahru A, 2009. Toxicity of nanoparticles of ZnO, CuO and TiO2 to yeast *Saccharomyces cerevisiae*. Toxicol in Vitro 23, 1116–1122.

Li L-Z, Zhou D-M, Peijnenburg WJGM, van Gestel CAM, Jin S-Y, Wang Y-J, Wang P, 2011. Toxicity of zinc oxide nanoparticles in the earthworm, *Eisenia fetida* and subcellular fractionation of Zn. Environ Int 37, 1098–1104.

Lowry GV, Wiesner MR, 2007. Environmental considerations: occurrences, fate, and characterization of nanoparticles in the environment. In Nanotoxicology: characterization, dosing and health effects (ed: Monteiro-Riviere NA, Tran CL), Informa Healthcare USA, Inc., NY, 369–389.

Ma H, Allen HE, Yin Y, 2001. Characterization of isolated fractions of dissolved organic matter from natural waters and a wastewater effluent. Water Res 35, 985–996.

Meems N, Steinberg CEW, Wiegand C, 2004. Direct and interacting toxicological effects on the waterflea (*Daphnia magna*) by natural organic matter, synthetic humic substances and cypermethrin. Sci Total Environ, 319, 123–136.

Mortimer M, Kasemets K, Kahru A, 2010. Toxicity of ZnO and CuO nanoparticles to ciliated protozoa *Tetrahymena thermophila*. Toxicology 269, 182–189.

OECD, 2010. Guidance Manual for the testing of manufactured nanomaterials: OECD's sponsorship programme, ENV/JM/MONO(2009) 20REV. OECD Environment, Health and Safety Publications, Series on the Safety of Manufactured Nanomaterials No. 25, Organisation for Economic Co-operation and Development, Paris.

Pascoal C, Cássio F, Gomes P, 2001. Leaf breakdown rates: a measure of water quality? Int Rev Hydrobiol 86, 407–416.

Pestana JLT, Ré A, Nogueira AJA, Soares AMVM, 2007. Effects of cadmium and zinc on the feeding behaviour of two freshwater crustaceans:*Atyaephyra desmarestii* (Decapoda) and *Echinogammarus meridionalis* (Amphipoda). Chemosphere 68, 1556–1562.

Pflugmacher S, Tidwell LF, Steinberg CEW, 2001. Dissolved humic substances directly affect freshwater organisms. Acta hydrochim hydrobiol 29, 34–40.

Pradhan A, Seena S, Pascoal C, Cássio F, 2011. Can metal nanoparticles be a threat to microbial decomposers of plant litter in streams? Microb Ecol 62, 58–68.

Pradhan A, Seena S, Pascoal C, Cássio F, 2012. Copper oxide nanoparticles can induce toxicity to the freshwater shredder *Allogamus ligonifer*. Chemosphere 89, 1142–1150.

Ren G, Hu D, Cheng EWC, Vargas-Reus MA, Reip P, Allaker RP, 2009. Characterisation of copper oxide nanoparticles for antimicrobial applications. Int J Antimicrob Agents 33, 587–590.

Saison C, Perreault F, Daigle JC, Fortin C, Claverie J, Morin M, Popovic R, 2010. Effect of core-shell copper oxide nanoparticles on cell culture morphology and photosynthesis (photosystem II energy distribution) in the green alga, *Chlamydomonas reinhardtii*. Aquat Toxicol 96, 109–114.

Steinberg CEW, Kamara S, Prokhotskaya VYu, Manusadžianas L, Karasyova T, Timofeyev MA, Zhang J, Paul A, Meinelt T, Farjalla VF, Matsuo AYO, Burnison BK, Menzel R, 2006. Dissolved humic substances – ecological driving forces from the individual to the ecosystem level? Freshwater Biol 51, 1189–1210.

Sun BK, Tanji Y, Unno H, 2005. Influences of iron and humic acid on the growth of the cyanobacterium *Anabaena circinalis*. Biochem Eng J 24, 195–201.

Timofeyev MA, Shatilina ZM, Kolesnichenko AV, Bedulina DS, Kolesnichenko VV, Pflugmacher S, Steinberg CEW, 2006. Natural organic matter (NOM) induces oxidative stress in freshwater amphipods *Gammarus lacustris* Sars and *Gammarus tigrinus* (Sexton). Sci Total Environ 366, 673–681.

Van Hoecke K, Quik JT, Mankiewicz-Boczek J, De Schamphelaere KA, Elsaesser A, Van der Meeren P, Barnes C, McKerr G, Howard CV, Van de Meent D, Rydzyński K, Dawson KA, Salvati A, Lesniak A, Lynch I, Silversmit G, De Samber B, Vincze L, Janssen CR, 2009. Fate and effects of CeO_2 nanoparticles in aquatic ecotoxicity tests. Environ Sci Technol 43, 4537–4546.

Varandas SG, Cortes RMV, 2010. Evaluating macroinvertebrate biological metrics for ecological assessment of streams in northern Portugal. Environ Monit Assess 166, 201–221.

Wall NA, Choppin GR, 2003. Humic acids coagulation: influence of divalent cations. Appl Geochem 18, 1573–1582.

Wigginton NS, Haus KL, Hochella MF, 2007. Aquatic environmental nanoparticles. J Environ Monit, 9, 1306–1316.

Wilding J, Maltby L, 2006. Relative toxicological importance of aqueous and dietary metal exposure to a freshwater crustacean: implication for risk assessment. Environ Toxicol Chem 25, 1795–1801.

Zar JH, 2009. Biostatistical analysis, fifth ed, Prentice Hall, Upper Saddle River, New Jersey.

Zhang X, Zhang D, Ni X, Song J, Zheng H, 2008. Synthesis and electrochemical properties of different sizes of the CuO particles. J Nanopart Res 10, 839–844.

Chapter 6

Physiological responses to nanoCuO in fungi from non-polluted and metal-polluted streams

Abstract

Nanocopper oxide (nanoCuO) is among the most commercially used metal oxide nanoparticles increasing the chance of their release in freshwaters. Aquatic fungi are the major microbial decomposers of plant litter in streams. Fungal laccases are multicopper oxidase enzymes that are involved in the degradation of lignin and various xenobiotic compounds. Therefore, it is interesting to study the effects of nanoCuO on laccase activity in fungal decomposers with different background. We investigated the effects of nanoCuO (5 levels, ≤ 200 mg L^{-1}) on four fungal isolates collected from metal-polluted and non-polluted streams. The exposure to nanoCuO decreased the biomass produced by all fungi in a concentration- and time-dependent manner. Inhibition of biomass production was stronger in fungi from non-polluted ($EC_{50(10\ days)}$ ≤ 31 mg L^{-1}) than from metal-polluted streams ($EC_{50(10\ days)}$ ≥ 65.2 mg L^{-1}). NanoCuO exposure led to cell shrinkage and mycelial degeneration, particularly in fungi collected from non-polluted streams. Adsorption of nanoCuO to fungal mycelia increased with the concentration of nanoCuO in the medium and was higher in fungi from non-polluted streams. Extracellular laccase activity was induced by nanoCuO in two fungal isolates in a concentration-dependent manner, and was highly correlated with adsorbed Cu and/or ionic Cu leached from nanoCuO. Putative laccase gene fragments were also detected in these fungi. Lack of substantial laccase activity in the other fungal isolates was corroborated by the absence of laccase-like gene fragments in these fungi.

Keywords: NanoCuO, fungal biomass, mycelial morphology, biosorption, laccases

6.1. Introduction

Nanocopper oxide (nanoCuO) is among the most commercially used metal oxide nanoparticles having a broad range of applications in electronics, medical and pharmaceutical fields and daily life products (Carnes and Klabunde, 2003; Dutta et al., 2003; Ren et al., 2009; Zhang et al., 2008). Unlike their bulk forms, metal oxide nanoparticles have special intrinsic properties, and gained recent ecotoxicological attention (Navarro et al., 2008; Rousk et al., 2012) as their increased commercialisation enhances the chance of these nanoparticles to reach the environment. Natural surface waters are likely to serve as the ultimate sink of nanomaterials, and there is some evidence on the occurrence of metal or metal oxide nanoparticles in streams (e.g. Wigginton et al., 2007; Kaegi et al., 2008).

Ionic forms of many metals are known to be toxic to aquatic biota and the processes they drive (Duarte et al., 2009). Recent studies have pointed to potential ecotoxicity of nanometal oxides to aquatic organisms (Blaise et al., 2008; Lee et al., 2009; Miller et al., 2010; Pradhan et al., 2012). Moreover, nanoparticles of CuO are likely to be more toxic than their bulk particles to a variety of aquatic organisms (Heinlaan et al., 2008; Aruoja et al., 2009; Mortimer et al., 2010).

In streams, aquatic fungi play an important role in organic matter turnover and energy transfer to higher trophic levels (Graça, 2001). Our earlier study showed that nanoCuO and Cu^{2+} strongly affected the activity and diversity of aquatic fungal communities (Pradhan et al., 2011). However, information on how fungal populations with different background respond to nanoCuO remains unexplored. Adaptive mechanisms underlying the tolerance/resistance against several metal ions, including Cu^{2+}, were shown in aquatic fungi contributing to explain their survival in metal-polluted environments (Jaeckel et al., 2005; Azevedo et al., 2007; Guimarães-Soares et al. 2007; Krauss et al., 2011).

Laccases are extracellular multicopper-containing oxidoreductase enzymes, which catalyze one-electron oxidation of aromatic amines, phenolic and nonphenolic compounds with concomitant reduction of oxygen to water through its copper reduction centre (Junghanns et al., 2005; Castilho et al., 2009). Due to their high redox potential (≈ +800 mV), fungal laccases have a wide range of applications in lignin degradation, wastewater treatment, food processing, and as biosensors (Wesenberg et al., 2003; Brondani et al., 2009; Brijwani et al., 2010). Fungal laccases are also capable to degrade humic acids (Steffen et al., 2002), which are

present in natural organic matter in soils or surface waters (Steinberg et al., 2006). Moreover, Cu^{2+} stimulates laccase activity in fungi, including those involved in plant litter decomposition in streams (Junghanns et al., 2005, 2008). Conversely, laccase activity of the terrestrial wood decomposing fungus *Trametes versicolor* decreased by short-term exposure to Cu nanoparticles, while no effects were observed in the presence of Cu^{2+} (Shah et al., 2010). This suggests that nanoCu can have a different mode of action than its ionic form, making it important to better understand the effects of nanometal oxides on laccase activity.

We investigated the effects of nanoCuO on four fungal isolates belonging to three species: two isolates were collected from non-polluted streams and the other two isolates were collected from metal-polluted streams. We hypothesized that i) nanoCuO induces toxicity to aquatic fungi by inhibiting biomass production and leading to mycelial morphological alterations, ii) fungal populations from non-polluted streams would be more affected by nanoCuO than those from metal-polluted streams, and iii) copper ions leached from nanoCuO would modulate laccase activity in fungi. For that, we examined the morphology of fungal mycelia, biomass production and extracellular laccase activity after exposure to increasing nanoCuO concentrations at two exposure times. In addition, we quantified total adsorbed copper to fungal mycelia, and leached ionic and nanoparticulate copper in the growth medium to better understand the effects of nanoCuO on aquatic fungi. Finally, because laccase activity in aquatic fungi is highly dependent on the growth conditions, the presence of laccase-like multicopper oxidase genes was checked under non-exposure conditions.

6.2. Material and Methods

6.2.1. Fungal cultures and exposure conditions

Four aquatic fungal isolates were used for the experiment, namely *Articulospora tetracladia* UMB-072.01 (At72) and *Phoma* sp. UHH 5-1-03 (P5), collected from non-polluted streams, and *A. tetracladia* UMB-061.01 (At61) and *Clavariopsis aquatica* WD(A)-00-1 (Ca1), collected from polluted streams. The isolate At72 was collected from foam in the Maceira stream at the Peneda-Gerês National Park (Portugal), while At61 was collected from decomposing leaves in a

metal-polluted site of the Este River, near the industrial park of the city of Braga (Portugal). The isolate Ca1 was collected from a stream (Waldau/Zeitz, Germany) containing high Fe and Mn in the sediment and polluted with tar oil residues leached from former lignite-processing industries, while P5 was isolated from water in the Saale River (Germany). Further information of sampling sites can be found elsewhere (Portuguese streams, Pascoal et al. 2005; German streams, Junghanns et al., 2005, 2008, Sridhar et al., 2008).

One agar plug (12-mm of diameter) of each fungal culture was homogenized (Ultraturrax, IKA, Staufen, Germany) in 1 mL of 1% (v/v) malt extract (ME) liquid medium, and 0.75 mL of the homogenate was transferred, aseptically, into 250-mL Erlenmeyer flasks containing 75 mL of 1% ME. After 48 h of fungal growth, nanoCuO was added to the cultures at the following final concentrations: 0, 5, 25, 100 and 200 mg L^{-1}. Fungal cultures were then incubated for 3 and 10 days on a shaker (140 rpm), at 14°C, in the dark. Experiments were run in triplicates.

6.2.2. Preparation and characterization of nanoCuO suspensions

The stock suspension of copper oxide nanoparticles (CuO nanopowder <50 nm, 99.5%, Sigma-Aldrich, St. Louis, MO, USA) was prepared by suspending nanoCuO powder in sterile (121°C, 20 min) Milli Q water and the suspension was sonicated in a water bath (42 kHz, 100 W; Branson 2510, Danbury, CT, USA) for 30 min in the dark before use (Pradhan et al., 2012).

NanoCuO in the stock suspension and growth medium was examined by scanning electron microscopy (SEM; Leica Cambridge S 360, Cambridge, UK) coupled to an energy dispersive X-ray (EDX) microanalysis setup (15 keV), as described in Pradhan et al. (2012). Briefly, 20 µl of nanoCuO suspension was loaded on a clean grease-free slide in the dark, air-dried and coated with gold in vacuum. Coated slides were scanned by SEM-EDX to confirm the presence of CuO nanoparticles. Size distribution of nanoCuO in stock suspension and growth medium was monitored by dynamic light scattering (DLS) (Malvern Zetasizer Nano ZS, Malvern Instruments Limited, UK) to check nanoparticle agglomeration.

6.2.3. Visualization of mycelial morphology

Fungal mycelia were harvested by filtration (5 µm pore size; Millipore, Billerica, MA, USA), washed with Milli Q water and re-suspended in 2 mL

phosphate-buffered saline (1× PBS, GIBCO, pH 7.4). Mycelia were fixed in 2.5% (v/v) glutaraldehyde for 24 h, and dehydrated in ethanol (v/v) as follows: 20%, 8 h; 40%, 6 h; 60%, 4 h; 80%, 2 h; and 100%, 1 h. Mycelial suspensions (20 µL) were loaded on slides, coated with gold in vacuum, and scanned by SEM-EDX as above.

6.2.4. Activity of extracellular laccase

The activity of laccase (EC 1.10.3.2) was quantified by using the methodology described in Junghanns et al. (2008). Briefly, the oxidation of 2,2'-azino-bis(3-ethylbenzothiazoline-6-sulfonate) (ABTS) was followed in McIlvaine buffer (pH 4.0) at 420 nm (ε_{420} = 36 mM^{-1} cm^{-1}) in 96-well flat-bottom microtiter plates (VWR, Darmstadt, Germany), using a microplate reader (SLT Spectra, Tecan, Crailsheim, Germany). Each well contained 160 µL of buffer, 20 µL of ABTS (20 mM) and 20 µL of mycelium-free medium. The measured values were corrected with a blank containing 20 µL of buffer instead of mycelium-free medium. Enzyme activity was expressed as units (U), where 1 U equals to 1 µmol product formed per minute.

6.2.5. Fungal biomass quantification

Fungal mycelia were harvested and washed, as above, dried at 80°C to constant mass (48 ± 8 h), and weighed to the nearest 0.001 g.

6.2.6. Biosorption and metal analysis

To quantify the biosorption of nanoCuO to fungal cell-walls, mycelia were harvested and washed, as above, and soaked for 12 h at 60°C in a mixture containing 4% HCl and 1% formic acid to dissolve nanoCuO to ionic Cu, and 1 mM EDTA as chelating agent. The solution was filtered through a polycarbonate membrane (0.2 µm pore size; Millipore, Billerica, MA) before copper quantification.

To quantify ionic Cu leached from nanoCuO and the nano form of copper in the culture medium, the mycelium-free medium was centrifuged at 75,600 g for 90 min (Beckman Avanti J-25I, USA). The supernatant containing the leached Cu^{2+} was filtered through a polycarbonate membrane (0.2 µm pore size). The filtered supernatant, the residue from filtration, and the pellet from centrifugation of each sample were treated, individually, with 5% HCl and 10% HNO_3 at 60°C for 8 h,

before copper quantification by inductively coupled plasma mass spectrometry (ICP-MS, X Seris 2, Thermo Scientific).

6.2.7. Screening for laccase-like multicopper oxidase genes

The genomic DNA was extracted from the four aquatic fungi grown in the absence of nanoCuO using the UltraClean Soil DNA kit (MoBio Laboratories, Solana Beach, CA, USA). Putative laccase gene fragments flanked by conserved sequences of laccase genes near the two pairs of histidines in two out of the four laccase copper binding regions of asco- and basidiomycetes (domains II and III; Lyons et al., 2003) were amplified with the degenerate primer pair Lac2for, 5' GGI ACI WII TGG TAY CAY WSI CA 3' and Lac3rev, 5' CCR TGI WKR TGI AWI GGR TGI GG 3' (Lyons et al., 2003; Castilho et al., 2009). Ambiguous bases were defined as follows: R=A/G, W=A/T, Y=C/T, S=C/G, K=T/G and I=inosine. For polymerase chain reaction (PCR), 1× Go Taq Green Master Mix (Promega corporation, Madison, WI, USA), 60 µM of each primer and 2 µL DNA (5 ng μL^{-1}) were mixed gently with nuclease-free water in a final volume of 25 µL. DNA amplification programme started with a denaturation for 3 min at 95°C, followed by 35 cycles of denaturation for 30 s at 95°C, primer annealing for 30 s at 45°C and elongation for 2 min at 70°C, followed by a final elongation for 5 min at 70°C. A PCR reaction without DNA template served as negative control. DNA amplification was performed in a Doppio thermal cycler (VWR International, Leuven, Belgium). Five µL of each amplification product was loaded on 1.3% agarose gel (BioRad, Danbury, CT, USA) and electrophoresis was carried out for 45 min at 90 V in 1 × Tris-acetate-EDTA (TAE) buffer. The GeneRuler^{TM} 50 bp DNA ladder (Thermo Scientific, Wilmington, DE, USA) was used as a marker. GelStar (Lonza Rockland, Inc., USA) was used for detecting the bands on the gel. The gel images were captured under UV light in a transiluminator Eagle eye II (Stratagene, La Jolla, CA, USA).

6.2.8. Data analyses

Two-way ANOVAs (Zar 2009) were used to assess how fungal endpoints (fungal biomass production and laccase activity) varied with the fungal isolate and nanoCuO concentration. Data were analysed for both time periods, separately. Bonferroni post-tests (Zar 2009) were used to check which treatments differed significantly from the respective control. Data in percentage were arcsine square

root transformed to achieve normal distribution and homoscedasticity (Zar 2009). The effective nanoCuO concentration inducing 50% of decrease in fungal biomass (EC_{50}) after 3 and 10 days of exposure was calculated using PriProbit 1.63 (Sakuma, 1998). Correlations were used to examine the relationships between fungal biomass or laccase activity and adsorbed copper to fungal mycelia or leached ionic copper or nanoparticulate copper in the growth medium. Analyses were done with Statistica 6.0 (Statsoft, Inc., Tulsa, OK).

6.3. Results

6.3.1. Characterization of nanoCuO by SEM and DLS

SEM analysis of nanoCuO in the aqueous stock suspension showed that the size of CuO nanoparticles ranged from 30 to 50 nm (not shown). However, DLS showed a single peak ranging between 100–340 nm with a z-average of 216 nm (Fig. 6.1) and a polydispersity index (PdI) of 0.196 in the stock suspension. In the growth medium (1% ME), the PdI increased to 0.387 and an additional peak between 75–165 nm (z-average of 114.4 nm) with 7.2% of area intensity was observed. Also, in the growth medium, the major peak shifted to 220–550 nm (z-average of 379.6 nm) corresponding to 92.8% area intensity (Fig. 6.1). This suggests that nanoparticle agglomeration increased in the growth medium compared to aqueous stock suspension probably due to interactions between components of the medium and nanoparticles and/or self-agglomeration. However, the additional smaller peak in the growth medium indicated that self-agglomeration of a little fraction of nanoparticles decreased, probably by increased affinity of O groups from nanoCuO towards H^+ due to decreased pH of the medium (pH ≤5.5) compared to that of the aqueous stock (pH 6.0).

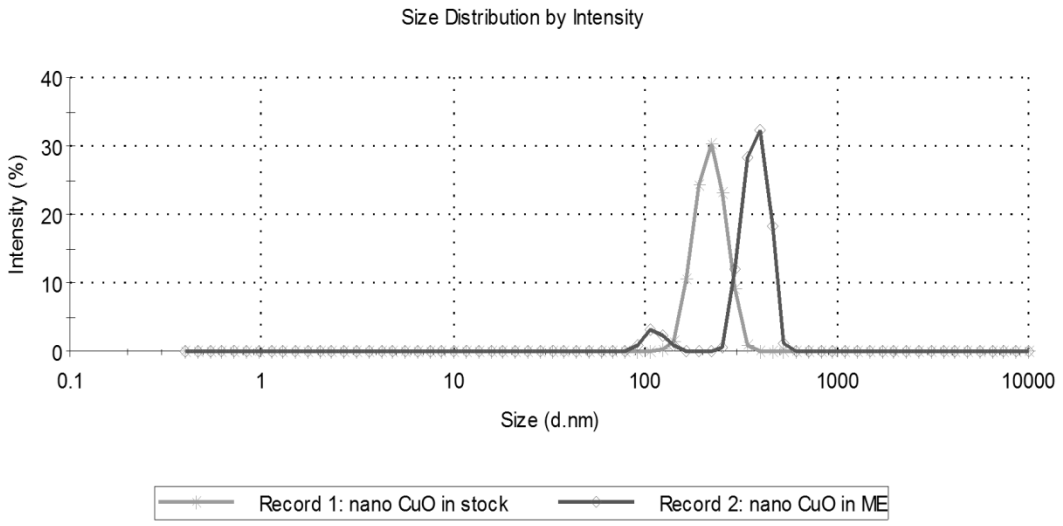

Figure 6.1 Size distribution of nanoCuO by dynamic light scattering in aqueous stock suspension and in 1% ME medium.

6.3.2. Mycelial morphology and nanoCuO adsorption

SEM analysis of fungal mycelia revealed that the exposure to nanoCuO promoted alterations in mycelial morphology, namely shrinkage and degeneration of cell-walls in all fungal isolates (Fig. 6.2). The morphological changes in fungal mycelia increased with exposure time (from 3 to 10 days) and with increasing concentrations of nanoCuO. Adsorption of nanoCuO to fungal mycelia was detected (pointed arrows; Fig. 6.2) and the presence of Cu was confirmed by EDX (Fig. 6.3). A clear difference in mycelial morphological alterations and nanoCuO adsorption was observed between fungi from non-polluted streams (At72 and P5) and metal-polluted streams (At61 and Ca1): the exposure to 200 mg L^{-1} of nanoCuO led to more severe effects on mycelia of At72 and P5 and to more nanoCuO adsorbed to mycelia (Fig. 6.2 and 6.3).

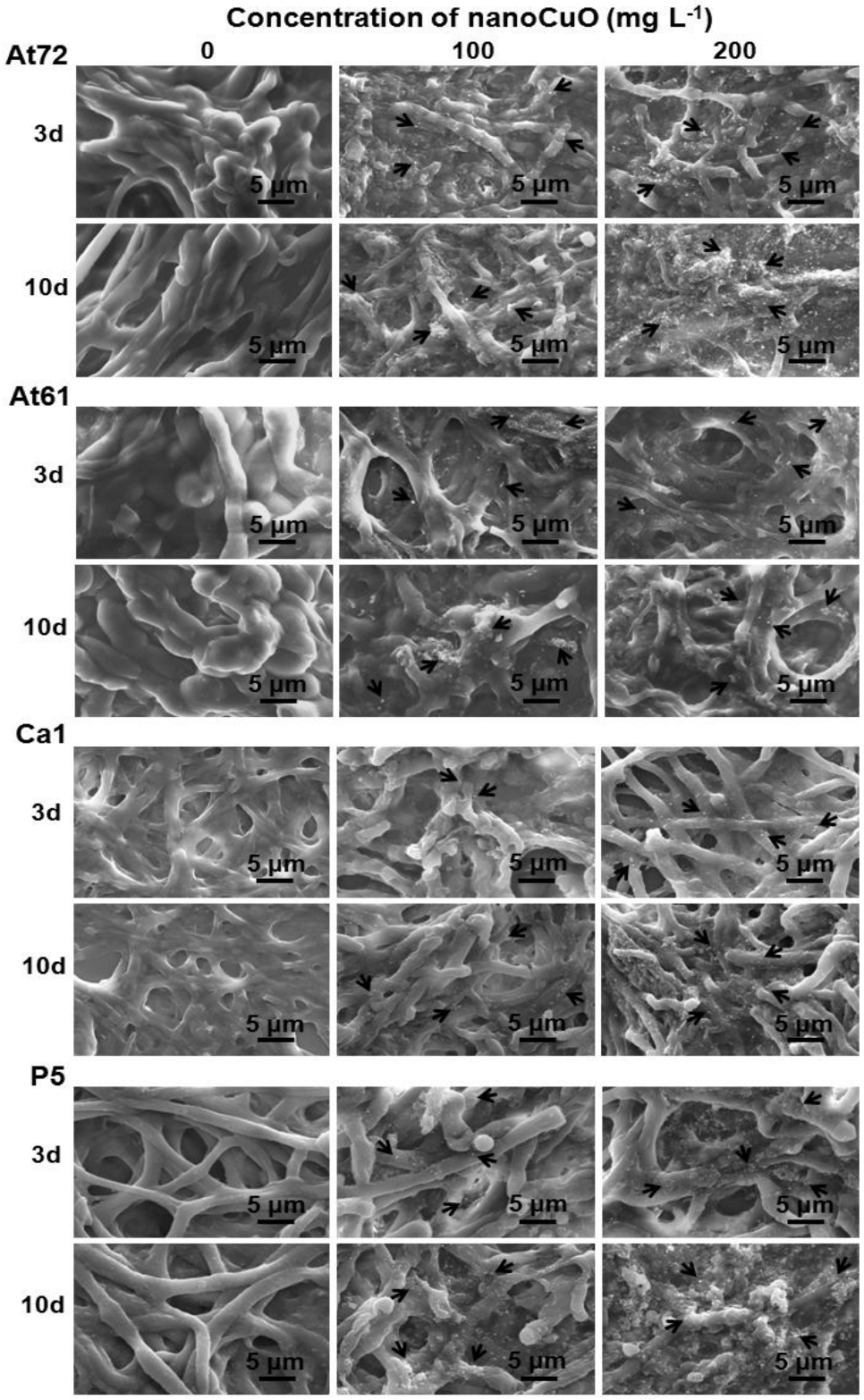

Figure 6.2 SEM visualization of mycelial morphology of aquatic fungi isolated from non-polluted streams (At72, *Articulospora tetracladia* UMB-072.01; and P5, *Phoma* sp. UHH 5-1-03) and from metal-polluted streams (At61, *A. tetracladia* UMB-061.01; and *Clavariopsis aquatica* WD(A)-00-1, Ca1) unexposed or exposed to increasing concentrations of nanoCuO (100 and 200 mg L^{-1}) for 3 days and 10 days.

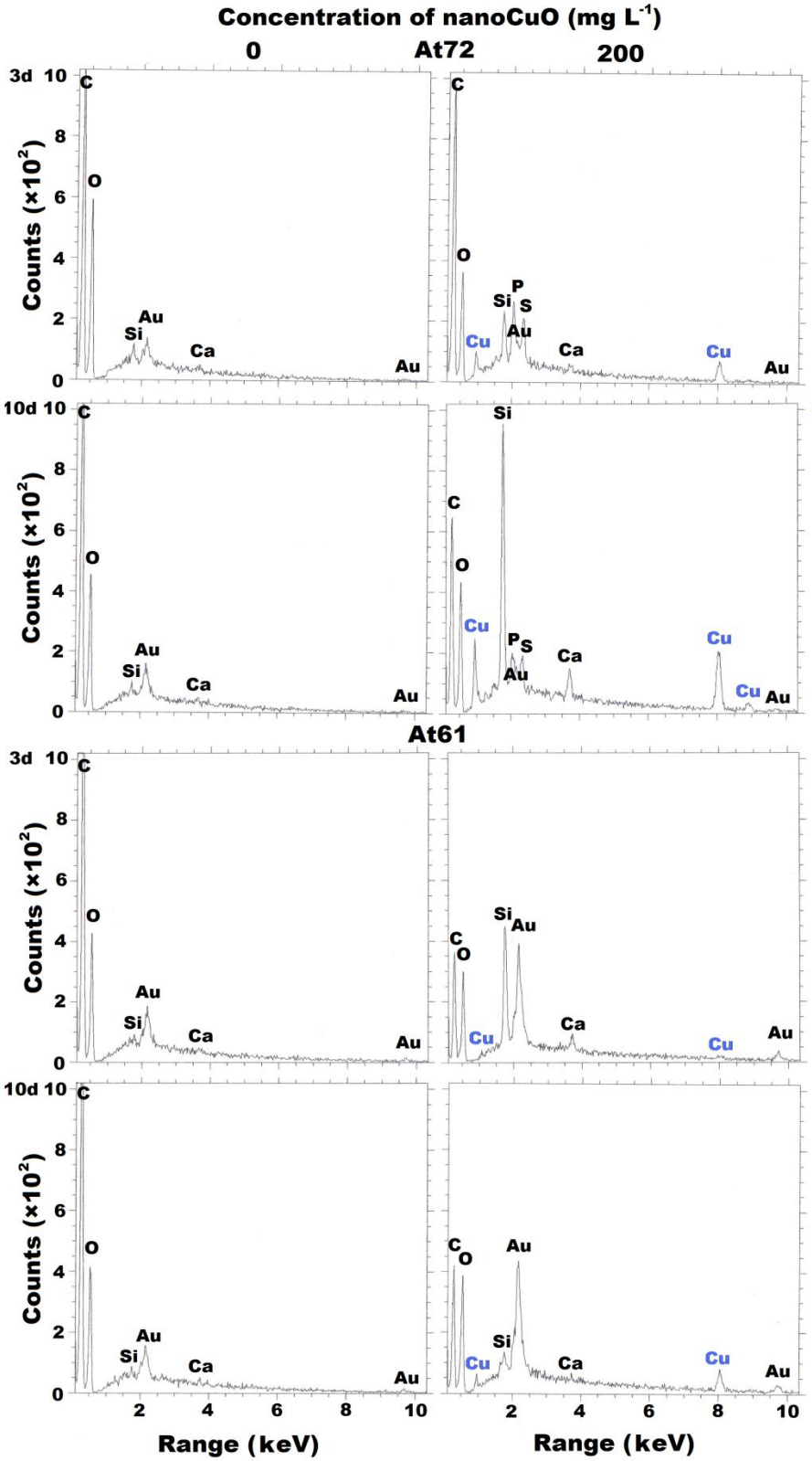
Concentration of nanoCuO (mg L-1)
0
At72
200
3d
10d
At61
Counts (×10²)
Range (keV)
C
O
Si
Au
Ca
Cu
P
S

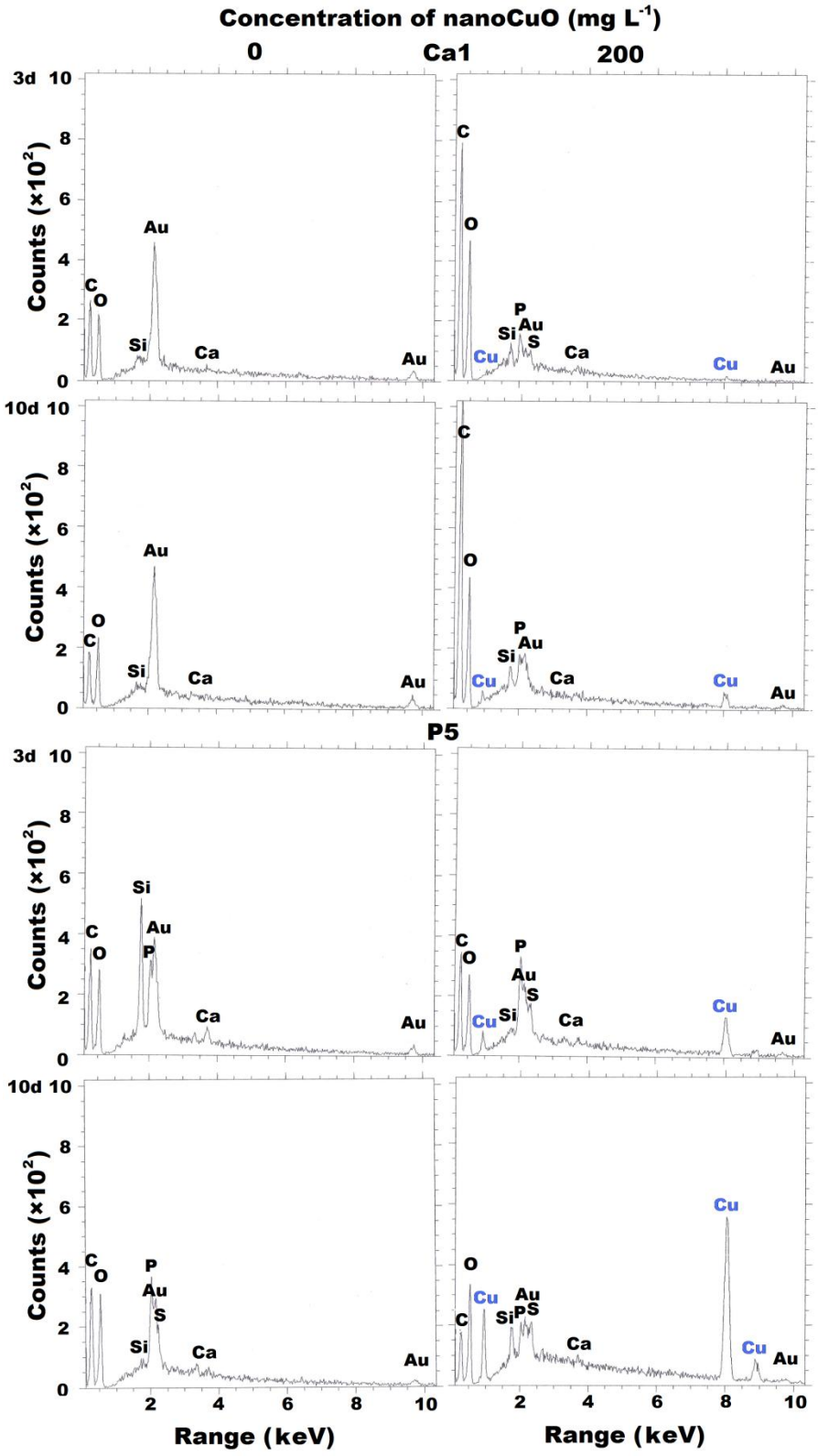

Figure 6.3 EDX profiles showing copper adsorption to mycelia of aquatic fungi isolated from non-polluted streams (At72, *Articulospora tetracladia* UMB-072.01; and P5, *Phoma* sp. UHH 5-1-03) and from metal-polluted streams (At61, *A. tetracladia* UMB-061.01; and *Clavariopsis aquatica* WD(A)-00-1, Ca1) unexposed or exposed to 200 mg L^{-1} of nanoCuO for 3 days and 10 days.

6.3.3. Copper in the growth medium and adsorbed to fungal mycelia

In the absence of nanoCuO, copper adsorption to mycelial surface was not detected in any fungal isolate (Fig. 6.4A). Under nanoCuO exposure, copper adsorbed to mycelia increased with nanoCuO concentration, and the highest copper adsorption was found after exposure to 200 mg L^{-1} of nanoCuO in mycelia of fungal isolates from non-polluted streams, namely P5 (1752.5 µg microcosm^{-1}) and At72 (978 µg microcosm^{-1}) (Fig. 6.4A). The amount of nanoparticulate copper in the growth medium increased with increasing nanoCuO concentration, and was higher in cultures of fungi from non-polluted streams (At72 and P5, 3418.9 and 1890.1 µg microcosm^{-1}, respectively) than from metal-polluted streams (Ca1 and At61, 1464.3 and 143.4 µg microcosm^{-1}, respectively) (Fig. 6.4B). Large amounts of Cu^{2+} leached from nanoCuO were found in the growth medium of all fungal isolates, and the amount increased with the increase of nanoCuO concentration in the medium (Fig. 6.4C). After exposure to the highest nanoCuO concentration, the amount of leached Cu^{2+} in the medium was highest in P5 cultures (7838.6 µg microcosm^{-1}) and lowest in At72 cultures (3528.8 µg microcosm^{-1}) (Fig. 6.4C).

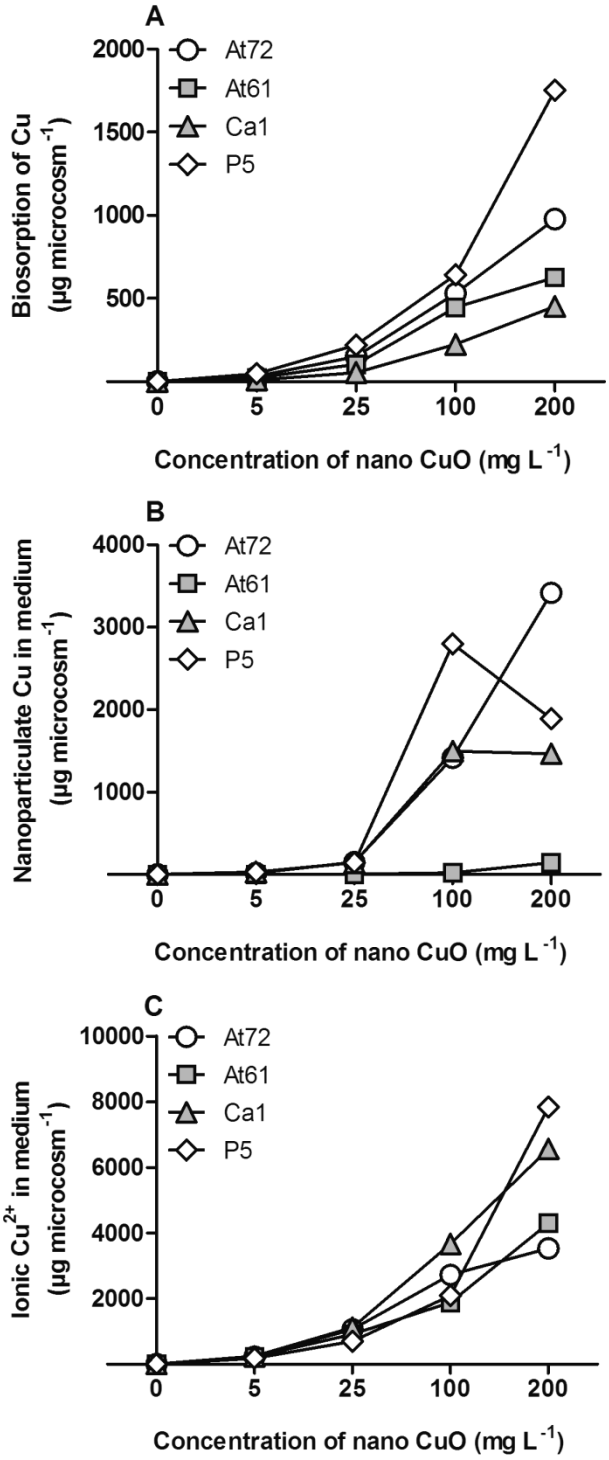

Figure 6.4 Biosorption of copper to fungal mycelia (A), nanoparticulate copper in the culture medium (B) and ionic copper in the culture medium (C). Aquatic fungi isolated from non-polluted streams (At72, *Articulospora tetracladia* UMB-072.01; and P5, *Phoma* sp. UHH 5-1-03) and from metal-polluted streams (At61, *A. tetracladia* UMB-061.01; and *Clavariopsis aquatica* WD(A)-00-1, Ca1) were unexposed or exposed to increasing concentrations of nanoCuO (5, 25, 100 and 200 mg L^{-1}) for 3 days.

6.3.4. Effects of nanoCuO on fungal biomass production

In the absence of nanoCuO, the biomass of each aquatic fungus increased with exposure time (Table 6.1). The top biomass producer was At61 (0.96 and 2.48 g L^{-1} after 3 and 10 days, respectively) while the worst biomass producer was Ca1 (0.67 and 2.1 g L^{-1} after 3 and 10 days, respectively) (Table 6.1). The exposure to nanoCuO significantly decreased biomass produced by all fungi in a concentration-dependent manner (two-way ANOVAs, *P<0.05*), and effects were more severe at the longer exposure time (Fig. 6.5A and B for 3 and 10 days, respectively). LOEC values for nanoCuO were 5 mg L^{-1} for fungal isolates collected from non-polluted streams (At72 and P5) and were 5 times higher for fungal isolates from metal-polluted streams (At61 and Ca1) (Table 6.1). Also, EC_{50} values for nanoCuO estimated after 3 days of exposure were lower for fungi collected from non-polluted streams (At72, 28.3 mg L^{-1} and P5, 41.2 mg L^{-1}) than for fungi from metal-polluted streams (At61, 80.5 mg L^{-1} and Ca1, 108.7 mg L^{-1}) (Table 6.1). Although a similar pattern was observed at the longer exposure time (10 days), EC_{50} values decreased for all fungal isolates (Table 6.1).

Table 6.1 Biomass production by aquatic fungi in the absence of nanoCuO and toxicity parameters (LOEC- lowest observed effective concentration and EC_{50}- median effective concentration) in aquatic fungi exposed for 3 and 10 days to nanoCuO. At72, *Articulospora tetracladia* UMB-072.01 and P5, *Phoma* sp. UHH 5-1-03, isolated from non-polluted streams; At61, *A. tetracladia* UMB-061.01 and Ca1, *Clavariopsis aquatica* WD(A)-00-1, isolated from metal-polluted streams.

Fungi	Fungal biomass* (g dry mass L^{-1})		LOEC (mg L^{-1})		EC_{50} (mg L^{-1})	
	3 days	10 days	3 days	10 days	3 days	10 days
At72	0.96 ± 0.05	2.48 ± 0.1	5	5	28.3 (22.2–35.5)	24.0 (19.4–29.2)
At61	1.11 ± 0.08	2.72 ± 0.17	25	25	80.5 (61.6–109)	65.2 (52.9–81)
Ca1	0.67 ± 0.07	2.1 ± 0.21	25	25	108.7 (81.3–155.3)	77.4 (55.5–115.1)
P5	0.86 ± 0.05	2.29 ± 0.12	5	5	41.2 (32.2–52)	31.0 (24.1–39.2)

*Mean ± SD, n=3.

After 3 days of exposure to nanoCuO, biomass of all fungal isolates was negatively correlated with copper adsorbed to mycelia (*P<0.05*, Table 6.2). Fungal biomass was also negatively correlated with Cu^{2+} leached from nanoCuO in the growth medium, except in the case of P5 (Table 6.2). Apart from Ca1, biomass of the other fungi was not significantly correlated with nanoparticulate copper in the medium.

Table 6.2 Correlations between fungal biomass or extracellular laccase activities and copper adsorbed to mycelia or nanoparticulate or leached ionic copper in the medium after 3 days of exposure to nanoCuO. At72, *Articulospora tetracladia* UMB-072.01 and P5, *Phoma* sp. UHH 5-1-03, isolated from non-polluted streams; At61, *A. tetracladia* UMB-061.01 and Ca1, *Clavariopsis aquatica* WD(A)-00-1, isolated from metal-polluted streams.

Parameter	Aquatic fungi	Copper (µg microcosm^{-1})					
		Adsorbed Cu to fungi		Nanoparticulate Cu in medium		Leached Cu^{2+} in medium	
		r	*P*	*r*	*P*	*r*	*P*
Fungal biomass (g L^{-1})							
	At72	-0.9322	0.021	-0.8733	0.0531	-0.9834	0.0026
	At61	-0.9852	0.0022	-0.8172	0.0912	-0.9466	0.0147
	Ca1	-0.9486	0.0139	-0.9391	0.0179	-0.9677	0.0069
	P5	-0.8958	0.0397	-0.8623	0.0601	-0.8476	0.0698
Laccase activity (U L^{-1})							
	Ca1	0.9939	0.0006	0.9116	0.0311	0.9887	0.0014
	P5	0.8899	0.0431	0.6850	0.2019	0.8579	0.0629

r, Coefficient of correlation

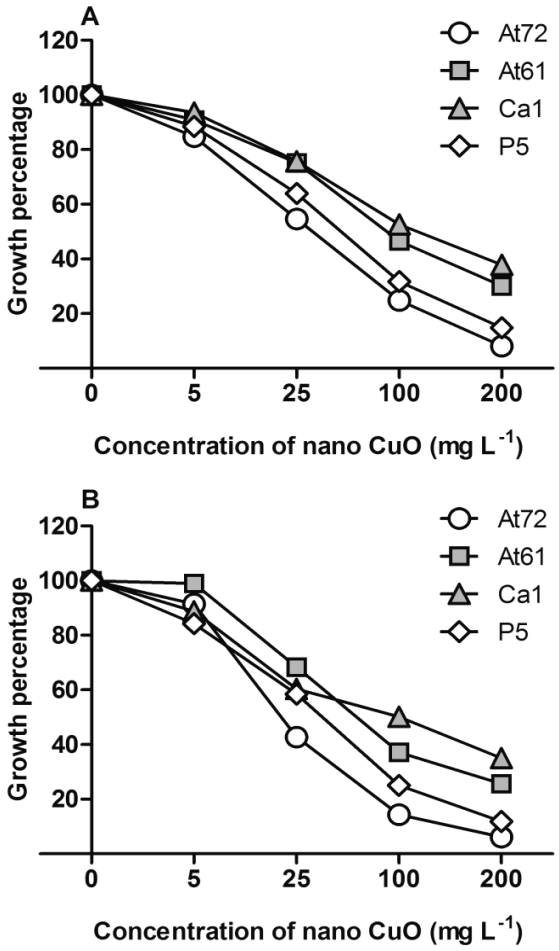

Figure 6.5 Biomass of aquatic fungi isolated from non-polluted streams (At72, *Articulospora tetracladia* UMB-072.01; and P5, *Phoma* sp. UHH 5-1-03) and from metal-polluted streams (At61, *A. tetracladia* UMB-061.01; and *Clavariopsis aquatica* WD(A)-00-1, Ca1) unexposed or exposed to increasing concentrations of nanoCuO (5, 25, 100 and 200 mg L^{-1}) for 3 days (A) and 10 days (B).

6.3.5. Activity of extracellular laccase

In the absence of nanoCuO, the activity of extracellular laccase at day 3 was only detected in P5 (3.2 U L^{-1}; Fig. 6.6A). At day 10, laccase activity increased mainly in P5 (11.6 U L^{-1}; Fig. 6.6B). The exposure to nanoCuO led to an increase in fungal laccase activity in a concentration-dependent manner (two-way ANOVAs, *P<0.05*; Fig. 6.6). The highest laccase activity was observed in P5 (15 and 546.2 U L^{-1} after 3 and 10 days, respectively), followed by Ca1 (3 and 69.3 U L^{-1} after 3 and 10 days, respectively). Only minor ABTS oxidation activity was detected in the other fungal strains (Fig. 6.6A and B).

After 3 day of exposure to nanoCuO, a significant correlation was found between laccase activity and adsorbed copper to P5 and Ca1 mycelia (*P<0.05*, Table 6.2). Additionally, extracellular laccase activity of Ca1 was also correlated with both forms (ionic and nano) of copper in the growth medium (Table 6.2).

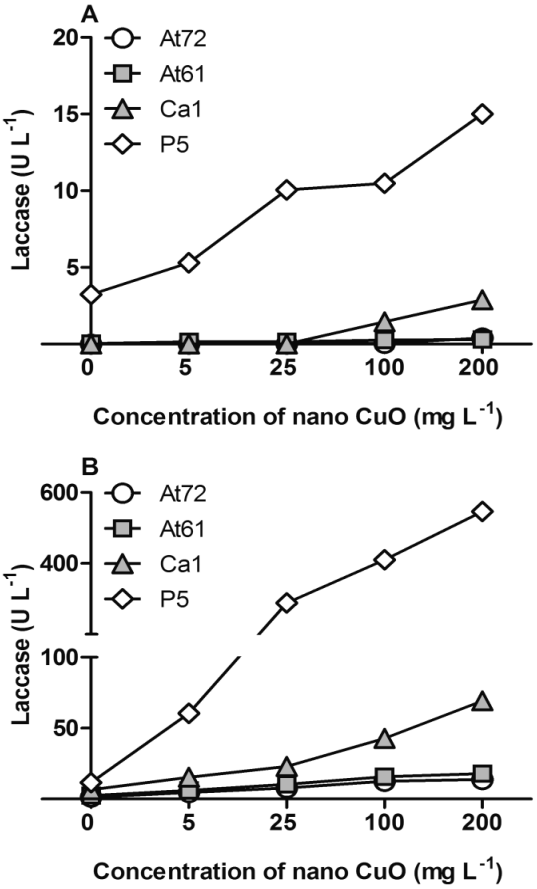

Figure 6.6 Activity of extracellular laccase in aquatic fungi isolated from non-polluted streams (At72, *Articulospora tetracladia* UMB-072.01; and P5, *Phoma* sp. UHH 5-1-03) and from metal-polluted streams (At61, *A. tetracladia* UMB-061.01; and *Clavariopsis aquatica* WD(A)-00-1, Ca1) unexposed or exposed to increasing concentrations of nanoCuO (5, 25, 100 and 200 mg L^{-1}) for 3 days (A) and 10 days (B).

6.3.6. Laccase-like multicopper oxidase genes

Gel electrophoresis revealed the presence of laccase-like multicopper oxidase gene fragments in the laccase copper binding regions II and III in the PCR amplified products of the fungal isolates Ca1 and P5, which were grown in the absence of nanoCuO (Fig. 6.7). We observed four less intense bands of about 900 bp, 750 bp, 350 bp and <200 bp and a prominent band of about 600 bp in Ca1, while only a strong single band of about 500 bp was observed in P5 (Fig. 6.7). No DNA bands were found for At72 and At61 (Fig. 6.7).

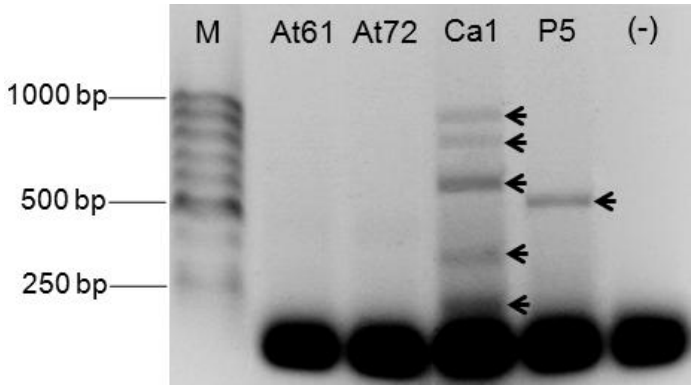

Figure 6.7 Fragments of laccase-like genes *lac2* and *lac3* (pointed with black arrow) in agarose gel obtained from aquatic fungi isolated from non-polluted streams (At72, *Articulospora tetracladia* UMB-072.01; and P5, *Phoma* sp. UHH 5-1-03) and from metal-polluted streams (At61, *A. tetracladia* UMB-061.01; and *Clavariopsis aquatica* WD(A)-00-1, Ca1). M: DNA ladder; (-) negative control.

6.4. Discussion

In this study, the exposure to nanoCuO led to a decrease in the biomass produced by all fungi in a concentration- and time-dependent manner. These results agree with our previous report in which nanoCuO inhibited biomass production by stream-dwelling fungal communities on decomposing plant litter (Pradhan et al., 2011). However, compared to fungal communities, fungal isolates in malt extract medium seemed to be more sensitive to nanoCuO. Indeed, the inhibition of biomass production by the four fungal isolates after 10 days exposure to 200 mg L^{-1} nanoCuO varied between 64.9–93.9%, whereas fungal biomass at the community level was inhibited only in 16.1 and 19.3% after 7 and 14 days of exposure to a similar nanoCuO concentration. Two main reasons might account to explain these differences: i) the high number of fungal species or strains in stream-dwelling communities increases the chance of encountering more tolerant/resistant species

and/or ii) fungal mycelia growing inside plant litter are somehow protected against direct contact with nanoCuO.

Our results clearly showed that fungal isolates collected from non-polluted streams were more sensitive to nanoCuO comparing to fungal isolates from metal-polluted streams, as shown by the lower LOEC and EC_{50} values for biomass production. Although there is a lack of information on the tolerance/resistance of aquatic fungi against nanoCuO, biomass production by fungi collected from metal-polluted streams was less affected by ionic metals than that of fungi from non-polluted streams (Jaeckel et al., 2005; Miersch et al., 2005). The exposure to Cu^{2+} led to a lower inhibition of biomass production by *Heliscus submersus* isolated from a metal-polluted stream compared to *Varicosporium elodeae* from a non-polluted stream (Azevedo et al., 2007). Also, the growth of strains of *Articulospora tetracladia* and *Tetracladium marchalianum* collected from copper-polluted streams was much less affected by Cu^{2+} than strains of the same species isolated from non-polluted streams (Miersch et al., 1997). Similarly, we found intraspecific differences in the biomass production under nanoCuO stress within isolates of *A. tetracladia* collected from metal-polluted (At61) and non-polluted streams (At72). Adaptive mechanisms of exposure to high levels of metal ions have been shown in aquatic fungi and include changes in the activity of antioxidant enzymes (Azevedo et al. 2007) and in the levels of glutathione (GSH) or other thiol-containing compounds (Guimarães-Soares et al., 2006, 2007; Braha et al., 2007).

The differential inhibition pattern of biomass production after nanoCuO exposure in fungal isolates with different background was consistent with the alterations in mycelial morphology, with evidence of more severe cell-wall shrinkage and mycelial degeneration in fungi from non-polluted streams. A similar alteration in cell-wall morphology was previously shown in aquatic fungi after exposure to Cu^{2+} (Azevedo et al., 2007). SEM-EDX analyses showed higher biosorption of nanoparticulate copper to mycelia of fungi from non-polluted streams (P5 and At72) than from metal-polluted streams (Ca1 and At61). Moreover, our results agree with those found by others showing that Cu^{2+} biosorption in aquatic fungi increase in a dose-dependent manner (Braha et al., 2007).

In this study, mean size of most nanoCuO in the growth medium was larger (379.6 nm with PdI of 0.387) than that measured in the stream water (202 nm; PdI, 0.186; Pradhan et al., 2012), but nanoCuO toxicity to fungal populations in the growth medium (this study) was higher than to fungal communities in the stream

water (Pradhan et al., 2011). The presence of nanoCuO with smaller particle size (114.4 nm) in the growth medium found in our study might also have contributed to the increased toxicity because smaller nanoparticles are generally more toxic to living organisms (Van Hoecke et al., 2009). Also, the lower pH (≤5.5) of the growth medium compared to the stream water (pH 5.8; Pradhan et al., 2012) may have played a role in nanoCuO toxicity by promoting the leaching of Cu^{2+} from nanoparticles. In our study, negative correlations between fungal biomass (except for P5) and the amount of Cu^{2+} in the medium were found. However, some studies reported that leached Cu^{2+} alone could not fully explain nanoparticle toxicity (Griffitt et al., 2008; Buffet et al., 2011). Negative correlations between adsorbed copper and fungal biomass were also found in our study in all fungi. The toxicity of nanoCuO may occur directly by adsorption of nanoparticles to cells or indirectly by the entrance of nanoCuO followed by its degradation in the lysosomes leading to an intracellular accumulation of Cu^{2+} (Petersen and Nelson, 2010).

Laccases, as multicopper oxidoreductase enzymes, are modulated by copper availability in the media (Junghanns et al., 2005; Castilho et al., 2009). Also, growth conditions such as nutrient availability and pH are recognised to affect the activity of these enzymes in aquatic fungi (Abdel-Raheem, 1997). In our study, *Phoma* sp. (P5) was the only fungus able to show laccase activity (11.6 U L^{-1}) in 1% malt extract without nanoCuO, and laccase activity in this fungus did not exceed 20.9 U L^{-1} in 2% malt extract (Junghanns et al., 2005). Earlier studies showed that Cu^{2+} stimulates laccase activity in P5 and *C. aquatica* (Ca1) (Junghanns et al., 2005, 2008), and depletion of these ions can inactivate the enzyme (Keum and Li, 2004). However, a reduction of laccase activity in the white-rot fungus *T. versicolor* was found after short-term exposure to highly aggregated nanoCu (Shah et al., 2010). In our study, the exposure to nanoCuO stimulated laccase activity in P5 and Ca1, and laccase activity in these fungi was correlated with adsorbed nanoCuO to fungal mycelia. In addition, the highest Cu^{2+} amount was measured in the growth medium of P5 followed by Ca1, suggesting that Cu^{2+} leached from nanoCuO might have contributed to the stimulated laccase activity. The clearly measurable extracellular laccase activities in P5 and Ca1 are well corroborated by the detection of one and five laccase-like gene fragments, respectively, in these fungi. Moreover, our results regarding these putative laccase gene fragments are in agreement with the presence of one single and five putative laccase genes detected upon targeting laccase copper binding regions I and III in P5 and Ca1, respectively (Junghanns et

al., 2009; Solé et al., 2012). Such differences in the laccase gene inventory might have contributed to the observed differences in laccase activities between P5 and Ca1. By contrast, even under nanoCuO exposure, only minor laccase activities (perhaps representing unspecific ABTS oxidation activities attributable to other factors than laccase) could be detected in the isolates of *A. tetracladia* (At72 and At61). These findings agree with the absence of laccase-like gene fragments in the *A. tetracladia* strains.

Overall results suggested that nanoCuO induce toxicity to aquatic fungi by inhibiting fungal biomass production and altering the mycelium morphology in a dose- and time-dependent manner. Laccase activity varied greatly among fungi and appeared to be related to the presence of laccase-like genes with a copper oxidase domain. Laccase activity and fungal biomass production were related to the amounts of nanoCuO adsorbed to mycelium and Cu^{2+} leached from nanoCuO in the growth medium. Different physiological responses to nanoCuO exposure were found in fungi collected from non-polluted and metal-polluted streams as shown by i) stronger inhibition in biomass production, ii) more pronounced alterations of mycelial morphology, and iii) higher nanoparticle biosorption in fungi from non-polluted streams. These differences were also observed at the intraspecific level (At61 and At72), further supporting higher tolerance/resistance to nanoCuO-induced stress in fungi from metal-polluted streams.

References

Abdel-Raheem AM, 1997. Laccase activity of lignicolous aquatic hyphomycetes isolated from the River Nile in Egypt. Mycopathologia, 139, 145-50.

Aruoja V, Dubourguier HC, Kasemets K, Kahru A, 2009. Toxicity of nanoparticles of CuO, ZnO and TiO_2 to microalgae *Pseudokirchneriella subcapitata*. Sci Total Environ 407, 1461–1468.

Azevedo MM, Carvalho A, Pascoal C, Rodrigues F, Cássio F, 2007. Responses of antioxidant defenses to Cu and Zn stress in two aquatic fungi. Sci Total Environ 377, 233–243.

Blaise C, Gagné F, Férard J, Eullaffroy P, 2008. Ecotoxicity of selected nano-materials to aquatic organisms. Environ Toxicol 23, 591–598.

Braha B, Tintemann H, Krauss G, Ehrman J, Bärlocher F, Krauss GJ, 2007. Stress response in two strains of the aquatic hyphomycete *Heliscus lugdunensis after* exposure to cadmium and copper ions. Biometals 20, 93–105.

Brijwani K, Rigdon A, Vadlani PV, 2010. Fungal laccases: production, function, and applications in food processing. Enzyme Res 149748 (10 pp), doi:10.4061/2010/149748.

Brondani D, Scheeren CW, Dupont J, Vieira IC, 2009. Biosensor based on platinum nanoparticles dispersed in ionic liquid and laccase for determination of adrenaline. Sens Actuators B Chem 140, 252–259.

Buffet PE, Tankoua OF, Pan JF, Berhanu D, Herrenknecht C, Poirier L, Amiard-Triquet C, Amiard JC, Bérard, JB, Risso C, Guibbolini M, Roméo M, Reip P, Valsami-Jones E, Mouneyrac C, 2011. Behavioural and biochemical responses of two marine invertebrates *Scrobicularia plana* and *Hediste diversicolor* to copper oxide nanoparticles. Chemosphere 84, 166–174.

Carnes LC, Klabunde KJ, 2003. The catalytic methanol synthesis over nanoparticle metal oxide catalysts. J Mol Catal A: Chem 194, 227–236.

Castilho FJD, Torres RA, Barbosa AM, Dekker RFH, Garcia JE, 2009. On the diversity of the laccase gene: a phylogenetic perspective from *Botryosphaeria rhodina* (ascomycota: fungi) and other related taxa. Biochem Genet 47, 80–91.

Duarte S, Pascoal C, Cássio F, 2009. Functional stability of stream-dwelling microbial decomposers exposed to copper and zinc stress. Freshwat Biol 54, 1683–1691.

Dutta A, Das D, Grilli ML, Di Bartolomeo E, Traversa E, Chakravorty D, 2003. Preparation of sol–gel nano-composites containing copper oxide and their gas sensing properties. J Sol–Gel Sci Technol 26, 1085–1089.

Graça MAS, 2001. The role of invertebrates on leaf litter decomposition in streams – a Review. Int Rev Hydrobiol, 86, 383–393.

Griffitt RJ, Luo J, Bonzongo JC, Barber DS, 2008. Effects of particle composition and species on toxicity of metallic nanomaterials in aquatic organisms. Environ Toxicol Chem 27, 1972–1978.

Guimarães-Soares L, Felícia H, Bebianno MJ, Cássio F, 2006. Metal-binding proteins and peptides in the aquatic fungi *Fontanospora fusiramosa* and *Flagellospora curta* exposed to severe metal stress. Sci Total Environ 372, 148-156.

Guimarães-Soares L, Pascoal C, Cássio F, 2007. Effects of heavy metals on the production of thiol compounds by the aquatic fungi *Fontanospora fusiramosa* and *Flagellospora curta*. Ecotoxicol Environ Saf 66, 36–43.

Heinlaan M, Ivask A, Blinova I, Dubourguier HC, Kahru A, 2008. Toxicity of nanosized and bulk ZnO, CuO and TiO_2 to bacteria *Vibrio fischeri* and crustaceans *Daphnia magna* and *Thamnocephalus platyurus*. Chemosphere 71, 1308–1316.

Jaeckel P, Krauss GJ, Krauss G, 2005. Cadmium and zinc response of the fungi *Heliscus lugdunensis* and *Verticilliumcf.alboatrum* isolated from highly polluted water.

Junghanns C, Krauss G, Schlosser D, 2008. Potential of aquatic fungi derived from diverse freshwater environments to decolourise synthetic azo and anthraquinone dyes, Bioresource Technol 99, 1225–1235.

Junghanns C, Moeder M, Krauss G, Martin C, Schlosser D, 2005. Degradation of the xenoestrogen nonylphenol by aquatic fungi and their laccases. Microbiology 151, 45–57.

Junghanns C, Pecyna MJ, Böhm D, Jehmlich N, Martin C, von Bergen M, Schauer F, Hofrichter M, Schlosser D, 2009. Biochemical and molecular genetic characterisation of a novel laccase produced by the aquatic ascomycete *Phoma* sp. UHH 5-1-03. Appl Microbiol Biotechnol 84, 1095–1105.

Kaegi R, Ulrich A, Sinnet B, Vonbank R, Wichser A, Zuleeg S, Simmler H, Brunner S, Vonmont H, Burkhardt M, Boller M, 2008. Synthetic TiO_2 nanoparticle emission from exterior facades into the aquatic environment. Environ Pollut 156, 233–239.

Keum, Y-S, Li QX, 2004. Copper dissociation as a mechanism of fungal laccase denaturation by humic acid. Appl Microbiol Biotechnol 64, 588–592.

Krauss G-J, Solé M, Krauss Gudrun, Schlosser D, Wesenberg D, Bärlocher F, 2011. Fungi in freshwaters: ecology, physiology and biochemical potential. FEMS Microbiol Rev 35, 620–651.

Lee SW, Kim SM, Choi J, 2009. Genotoxicity and ecotoxicity assays using the freshwater crustacean *Daphnia magna* and the larva of the aquatic midge *Chironomus riparius* to screen the ecological risks of nanoparticle exposure. Environ Toxicol Pharmacol 28, 86–91.

Lyons JL, Newell SY, Buchan A, Moran MA, 2003. Diversity of ascomycete laccase gene sequences in a southeastern US salt marsh. Microbial Ecol 45, 270–281.

Miersch J, Bärlocher F, Bruns I, Krauss GJ, 1997. Effects of cadmium, copper, and zinc on growth and thiol content of aquatic hyphomycetes. Hydrobiologia 346, 77–84.

Miersch J, Neumann D, Menge S, Bärlocher F, Baumbach R, Lichtenberger O, 2005. Heavy metals and thiol pool in three strains of *Tetracladium marchalianum*. Mycol Prog 4, 185–194.

Miller RJ, Lenihan HS, Muller EB, Tseng N, Hanna SK, Keller AA, 2010. Impacts of metal oxide nanoparticles on marine phytoplankton. Environ Sci Technol 44, 7329–7334.

Mortimer M, Kasemets K, Kahru A, 2010. Toxicity of ZnO and CuO nanoparticles to ciliated protozoaTetrahymena thermophila. Toxicology 269, 182–189.

Navarro E, Baun A, Behra R, Hartmann NB, Filser J, Miao AJ, Quigg A, Santschi PH, Sigg L, 2008. Environmental behavior and ecotoxicity of engineered nanoparticles to algae, plants, and fungi. Ecotoxicology 17, 372–386.

Pascoal C, Marvanová L, Cássio F, 2005. Aquatic hyphomycete diversity in streams of Northwest Portugal. Fung Divers 19, 109-128.

Petersen EJ, Nelson BC, 2010. Mechanisms and measurements of nanomaterial-induced oxidative damage to DNA. Anal Bioanal Chem 398, 613–650.

Pradhan A, Seena S, Pascoal C, Cássio F, 2011. Can metal nanoparticles be a threat to microbial decomposers of plant litter in streams? Microb Ecol 62, 58–68.

Pradhan A, Seena S, Pascoal C, Cássio F, 2012. Copper oxide nanoparticles can induce toxicity to the freshwater shredder *Allogamus ligonifer*. Chemosphere 89, 1142–1150.

Ren G, Hu D, Cheng EWC, Vargas-Reus MA, Reip P, Allaker RP, 2009. Characterisation of copper oxide nanoparticles for antimicrobial applications. Int J Antimicrob Agents 33, 587–590.

Rousk J, Ackermann K, Curling SF, Jones DL, 2012. Comparative toxicity of nanoparticulate CuO and ZnO to soil bacterial communities. PLoS One, 7(3):e34197, doi: 10.1371/journal.pone.0034197.

Sakuma, M., 1998. Probit analysis of preference data. Appl Entomol Zool 33, 339–347.

Shah V, Dobiášová P, Baldrian P, Nerud F, Kumar A, Seal S, 2010. Influence of iron and copper nanoparticle powder on the production of lignocellulose degrading enzymes in the fungus *Trametes versicolor*. J Hazard Mater 178, 1141–1145.

Solé M, Müller I, Pecyna MJ, Fetzer I, Harms H, Schlosser D, 2012. Differential regulation by organic compounds and heavy metals of multiple laccase genes in the aquatic hyphomycete *Clavariopsis aquatica*. Appl Environ Microbiol 78, 4732–4739.

Sridhar KR, Bärlocher F, Wennrich R, Krauss G-J, Krauss G, 2008. Fungal biomass and diversity in sediments and on leaf litter in heavy metal contaminated waters of Central Germany. Fundam Appl Limnol 171, 63–74.

Steffen KT, Hatakka A, Hofrichter M, 2002. Degradation of humic acids by the litter-decomposing basidiomycete *Collybia dryophila*. Appl Environ Microbiol 68, 3442–3448.

Steinberg CEW, Kamara S, Prokhotskaya VYu, Manusadžianas L, Karasyova T, Timofeyev MA, Zhang J, Paul A, Meinelt T, Farjalla VF, Matsuo AYO, Burnison BK, Menzel R, 2006. Dissolved humic substances – ecological driving forces from the individual to the ecosystem level? Freshwater Biol 51, 1189–1210.

Van Hoecke K, Quik JT, Mankiewicz-Boczek J, De Schamphelaere KA, Elsaesser A, Van der Meeren P, Barnes C, McKerr G, Howard CV, Van de Meent D, Rydzyński K, Dawson KA, Salvati A, Lesniak A, Lynch I, Silversmit G, De Samber B, Vincze L, Janssen CR, 2009. Fate and effects of CeO_2 nanoparticles in aquatic ecotoxicity tests. Environ Sci Technol 43, 4537–4546.

Wesenberg D, Kyriakides I, Agathos SN, 2003. White-rot fungi and their enzymes for the treatment of industrial dye effluents. Biotechnol Adv 22, 161–187.

Wigginton NS, Haus KL, Hochella MF, 2007. Aquatic environmental nanoparticles. J Environ Monit 9, 1306–1316.

Zar JH, 2009. Biostatistical analysis, fifth ed, Prentice Hall, Upper Saddle River, New Jersey.

Zhang X, Zhang D, Ni X, Song J, Zheng H, 2008. Synthesis and electrochemical properties of different sizes of the CuO particles. J Nanopart Res 10, 839–844.

Chapter 7

Fungi from metal-polluted streams have high ability to cope with the stress induced by nanoCuO

Abstract

Increased commercialization of products based on nanometal oxides increases the chance of their release into aquatic environments making it relevant to assess their potential impacts on aquatic biota. Aquatic fungi are worldwide distributed and play a key role in organic matter turnover in freshwater ecosystems. We investigated the biochemical and physiological responses induced by exposure to nanoCuO (5 levels, ≤ 200 mg L^{-1}) on five fungal isolates collected from metal-polluted or non-polluted streams. The exposure to nanoCuO led to lower intracellular ROS accumulation, plasma membrane disruption and DNA-strand breaks in fungi from metal-polluted streams than in those from non-polluted streams. The activities of glutathione reductase and superoxide dismutase were higher in fungi from metal-polluted than from non-polluted streams, although the opposite was found for glutathione peroxidase activity. Overall results showed that fungi from metal-polluted streams have higher capacity to deal with the oxidative stress induced by nanoCuO, probably due to their ability to maintain a high GSH:GSSG ratio.

.

Keywords: NanoCuO, ROS accumulation, DNA-strand breaks, plasma membrane disruption, antioxidant enzymes

7.1. Introduction

Copper oxide nanoparticles (nanoCuO) are among the commercially used metal nanoparticles with a wide range of applications in research and daily-life products (Dutta et al., 2003; Zhang et al., 2008; Ren et al., 2009). Because commercialization of products based on nanoCuO has been growing quickly, the chance of their release into aquatic environments increases. NanoCuO is reported to induce toxicity in biological systems (e.g., yeasts, Kasemets et al., 2009; human cell lines, Karlsson et al., 2009), but only few studies were conducted on aquatic organisms (e.g. Mortimer et al., 2010; Saison et al., 2010). Although some studies have revealed lethal and sublethal effects of nanoCuO (marine invertebrates, Buffet et al., 2011; freshwater invertebrates, Pradhan et al., 2012), the mechanisms underlying the toxicity of metal nanoparticles are not fully understood.

The toxicity of nanosized metals and metal oxides to living cells has been attributed to their ability to induce oxidative stress by producing intracellular reactive oxygen species (ROS). This generally leads to i) mitochondrial membrane depolarization, ii) DNA-strand breaks, and iii) cell membrane damage by lipid peroxidation (Lin et al., 2006; Limbach et al., 2007; Karlsson et al., 2009; Lee et al., 2009; Petersen and Nelson, 2010). For instance, TiO_2 nanoparticles induced oxidative stress in planktonic assemblages in biofilms or free-living cells in stream microcosms (Battin et al., 2009), and the exposure to nanoCuO altered the activity of several antioxidant enzymes (SOD, superoxide dismutase; CAT, catalase; and GST, glutathione-S-transferase) in marine invertebrates (Buffet et al., 2011). Most of these antioxidant enzymes are associated with the ascorbate-glutathione cycle, in which the reduced form of glutathione (GSH) is converted in its oxidized form (GSSG) via formation of a disulfide linkage under oxidative stress. The maintenance of a high GSH:GSSG ratio is crucial for regulating the cellular redox state and controlling the oxidative stress to prevent cellular damage (Penninckx, 2002; Huang et al., 2010). The two major enzymes involved in maintaining the GSH:GSSG ratio are glutathione reductase (GR) and glutathione peroxidase (GPx), which also play key roles in oxidative stress defense (Israr et al., 2006); GR mediates the conversion of GSSG to GSH with the help of NADPH, while GPx converts GR to GSSG when encountered with peroxides/hydroperoxides (Townsend et al., 2003). The antioxidant activity of SOD is associated with the conversion of $O_2^{\bullet -}$ radicals into H_2O_2, which is consumed by CAT or peroxidases (Fridovich, 1986).

Aquatic fungi are worldwide distributed and play a key role in organic matter decomposition within trophic networks in streams (Graça 2001; Pascoal et al., 2005a). Several reports document their occurrence in metal-polluted streams and have provided evidence that fungi may develop adaptive mechanisms towards tolerance/resistance against metals, helping them to survive in metal-polluted environments (Jaeckel et al., 2005; Azevedo et al. 2007; Braha et al., 2007; Guimarães-Soares et al. 2007; Miersch and Grancharov, 2008; Krauss et al., 2011). Metals, including copper, are able to induce oxidative stress in aquatic fungi leading to plasma membrane damage and DNA-strand breaks with increased accumulation of intracellular ROS (Azevedo et al., 2009). Interestingly, various antioxidant enzymes associated with the ascorbate-glutathione cycle exhibit different activities under metal exposure in fungal isolates from non-polluted and metal-polluted streams (Azevedo et al., 2007; Braha et al., 2007). This raises the question whether fungal populations with different background (i.e., adapted or not to metal stress) may show different physiological and biochemical responses under exposure to metal or metal oxide nanoparticles.

We investigated the impacts of CuO nanoparticles on cellular targets and antioxidant defenses in five aquatic fungi collected from metal-polluted or non-polluted streams, under the hypotheses that i) nanoCuO induces oxidative stress to aquatic fungi, and ii) fungal isolates from metal-polluted streams would better cope with the stress induced by nanoCuO than isolates from non-polluted streams, resulting in less cellular damages in the former fungal strains. We assessed intracellular accumulation of ROS, plasma membrane integrity, and DNA-strand breaks, as well as the activities of GR, GPx and SOD representing antioxidant enzymatic responses after exposure to increasing concentrations of nanoCuO.

7.2. Material and Methods

7.2.1. Preparation and characterization of nanoCuO stock suspension

Nanocopper oxide (nanopowder <50 nm, 99.5%; Sigma-Aldrich, St. Louis, MO) stock suspension was mixed with autoclaved Milli Q water (121°C, 20 min), and sonicated (42 kHz, 100 W; Branson 2510, Danbury, CT) for 30 min in the dark before use (Pradhan et al., 2012). The stock suspension was characterized by spectrophotometry (UV–1601, Shimadzu, Kyoto, Japan), followed by scanning

electron microscopy (SEM, Leica Cambridge S 360, Cambridge, UK) coupled to an energy dispersive X-ray (EDX) microanalysis setup (15 keV), as described in Pradhan et al. (2011). NanoCuO showed a plasmon peak at 359 nm, and SEM-EDX confirmed that the size of CuO nanoparticles ranged between 30–50 nm as shown elsewhere (Fig. 1b in Pradhan et al., 2011). Size distribution of nanoparticles was monitored by dynamic light scattering (DLS) using a zetasizer (Malvern Zetasizer Nano ZS, Malvern Instruments Limited, UK) as described by Pradhan et al. (2012). Size distribution of nanoCuO ranged between 100–340 nm with an average size of 216 nm and polydispersity index (PdI) of 0.196. The stability of the stock suspension was confirmed up to 3 weeks.

7.2.2. Fungal cultures and exposure conditions

Five fungal isolates were used: two were obtained from non-polluted streams, namely *Articulospora tetracladia* UMB-072.01 (At72) and *Phoma* sp. UHH 5-1-03 (P5), while the other three were obtained from metal-polluted streams, namely *A. tetracladia* UMB-061.01 (At61), *Heliscus lugdunensis* H-4-2-4 (H4) and *Clavariopsis aquatica* WD(A)-00-1 (Ca1). The isolate At72 was collected in the Maceira stream at the Peneda-Gerês National Park (Portugal), while At61 was isolated in the Este River at the industrial park of the city of Braga (Portugal). The isolate H4 was collected from a stream in the Mansfelder Land area (Germany), the isolate Ca1 was collected from a stream with high levels of Fe and Mn in sediments and tar oil residues leached from former lignite-processing industries (Waldau/Zeitz, Germany), and P5 was isolated in the Saale River (Germany). Further information of sampling sites can be found elsewhere (Portuguese streams, Pascoal et al. 2005b; German streams, Junghanns et al., 2005; Braha et al., 2007; Junghanns et al., 2008, Sridhar et al., 2008).

One agar plug (12 mm diameter) of 15 day-old cultures of each fungus grown on malt extract medium (ME, 1% w/v; agar, 1.5% w/v) was homogenized (Ultraturrax IKA, Staufen, Germany) in 1 mL sterile liquid medium (ME 1%), and 0.75 mL of the homogenate was inoculated in 250 mL Erlenmeyer flask containing 75 mL of ME medium. Each fungus was exposed to increasing concentrations of nanoCuO (0, 5, 25, 100 and 200 mg L^{-1}) and to 25 mg L^{-1} of Cu^{2+} ($CuCl_2.2H_2O$, >99%; Sigma-Aldrich, St. Louis, MO) in triplicates. Chemicals were added after 48 h of growth. Fungal cultures were incubated at 14°C on a shaker (140 rpm) in the dark. Fungal mycelia were collected after 3 and 10 days of exposure to the

chemicals for assessing intracellular accumulation of ROS, plasma membrane integrity, DNA-strand breaks, total protein concentration and activity of antioxidant enzymes.

7.2.3. Detection of intracellular reactive oxygen species

The accumulation of intracellular ROS was assessed with MitoTracker Red CM-H_2XRos (Molecular Probes, Eugene, OR). The dye in its reduced form does not fluoresce until it enters an actively respiring cell, where it is oxidized by intracellular ROS to form a red fluorescent compound, which is sequestered in mitochondria (Azevedo et al. 2009). A solution of the dye (1 mM) in dimethyl sulfoxide (DMSO; ≥99.9%, Sigma-Aldrich) was prepared in the dark before use. Mycelium suspensions were washed twice in phosphate-buffered saline (1× PBS, pH 7.4; GIBCO) by centrifugation (1000 rpm; 5 min), and incubated with 40 µg mL^{-1} of MitoTracker Red for 15 min at room temperature in the dark. Mycelia were scanned under an epifluorescence microscope (1000×; Leica DM5000B, Germany), and images were acquired with a digital camera (Leica DFC 350 FX R2) using the software LAS AF V1.4.1.

7.2.4. Assessment of plasma membrane integrity

The effects of nanoCuO on plasma membrane integrity were assessed by propidium iodide (PI; Molecular Probes, Eugene, OR), a membrane impermeable dye, which enters the cells and binds to nucleic acids when plasma membrane disruption occurs (Azevedo et al., 2007). Mycelium with intense red fluorescence was considered to have plasma membrane disruption. Fungal mycelia were washed as above and incubated with PI (5 µg mL^{-1}) for 15 min at room temperature in the dark. Stained mycelia were placed on a grease-free slide and covered with a cover-slip after mixing with an anti-fading and anti-photobleaching reagent (Vectashield Mounting Medium for fluorescence, H-1000; Vector Laboratories). Mycelia were scanned under an epifluorescence microscope as above.

7.2.5. TUNEL assay and DAPI staining

DNA-strand breaks in fungal mycelia were visualized by terminal deoxynucleotidyl transferase mediated dUTP nick end labelling (TUNEL) using the *In situ* Cell Death Detection Kit Fluorescein (Roche) (Azevedo et al., 2009). TUNEL

labels the free 3'-OH termini with FITC-labelled dUTP, and green fluorescence was detected by epifluorescence microscopy. Fungal mycelium was fixed with formaldehyde (4%, v/v) and cell wall was digested with zymolyase (0.5 µg μL^{-1}) in 2-mercaptoethanol (1%, v/v) during 2 h at 37°C under shaking (150 rpm). Then, mycelia were washed twice in PBS (1×, pH 7.4) by centrifugation at 1000 rpm for 5 min. Mycelia were then mounted on grease free slides and incubated with a permeabilization solution (0.1% (v/v) Triton X-100 in 0.1% sodium citrate) for 10 min at room temperature, rinsed twice in PBS (1×, pH 7.4) and incubated with the TUNEL reaction mixture. Slides were incubated in the dark under a humidified atmosphere for 1 h at 37°C. To co-localize DNA, slides were incubated for 15 min with 50 µL of 0.1 µg μL^{-1} of 4',6-diamidino-2-phenylindole (DAPI; Sigma), which forms a blue fluorescent complex with the double-stranded DNA. Then, slides were washed with PBS (1×, pH 7.4), and 10 µL of a mixture containing 100 µL of the anti-fading agent Vectashield and 2 µL of RNase (0.5 µg mL^{-1}) was added to each slide. Mycelia were observed by epifluorescence microscopy.

7.2.6. Preparation of cell-free extracts

Fungal mycelia were harvested by filtration (5 µm pore size, Millipore, Billerica, MA), washed three times with Milli Q water, and pressed between two layers of filter paper to remove the excess of water. Mycelia were mixed with sterile glass beads and ground in a liquid nitrogen in a cooled mortar. The mixture was homogenized in a buffer solution (1:5, w/v), containing 100 mM KH_2PO_4, 100 mM Tris/HCl (pH 7.8), 5 mM EDTA and 2% polyvinylpyrrolidone (PVP), and sonicated (42 kHz, 100 W, Branson 2510, Danbury, CT, USA) for 5 × 30 s at 0-4°C (cooled on ice after each sonication cycle). The cell-free extract was obtained by centrifugation (4000 g for 10 min and 13,800 g for 30 min; at 4°C) and used to measure concentration of intracellular protein and antioxidant enzymatic activities.

7.2.7. Activity of antioxidant enzymes and concentration of intracellular protein

The activity of glutathione reductase (GR) was measured according to a modified method of Esterbauer and Grill (1978). The cell-free extract (25 µL) was added to a 200 µL reaction mixture containing 100 mM potassium phosphate buffer (pH 7.8), 100 mM Tris/HCl, 30 mM EDTA, 3 mM $MgCl_2$, 0.1% BSA, 1.6 mM GSSG

and 0.25 mM NADPH. The oxidation of NADPH was followed at 340 nm (extinction coefficient: 6.2 mM^{-1} cm^{-1}). The GR activity was calculated from the slope of NADPH absorbance curve.

The activity of glutathione peroxidase **(**GPx) was measured according to a modified method of Anderson and Davis (2004). The cell-free extract (25 µL) was added to a 200 µL reaction mixture containing 100 mM potassium phosphate buffer (pH 7.8), 100 mM Tris/HCl, 1.25 mM EDTA, 1.25 mM NaN_3, 1.0 mM GSH, 0.25 mM NADPH, 0.6 U GR (from yeast) and 1.2 mM cumene hydroperoxide. GPx activity was calculated from the slope of NADPH absorbance curve as above.

The activity of superoxide dismutase (SOD) was determined according to a modified method of Beyer and Fridovich (1987) and Jevremović et al. (2010) by measuring the reduction of nitroblue tetrazolium (NBT) at 560 nm. The cell-free extract (25 µL) was added to a 200 µL reaction mixture containing 12.5 mM potassium phosphate buffer (pH 7.8), 0.1 mM EDTA, 16.5 mM L-methionine, 0.08 mM NBT and 0.04 mM riboflavin. The reaction mixture was kept under a fluorescent light for 5 min. One SOD unit was defined as the enzyme amount inhibiting by 50% the NBT reduction rate.

All enzymatic activities were measured spectrophotometrically (UV–1601, Shimadzu, Kyoto, Japan) at 25°C. Total intracellular protein concentration in cell-free extracts was determined according to Bradford (1976) using BSA as standard.

7.2.8. Data analyses

Two-way ANOVAs (Zar 2009) were used to assess how measured endpoints varied with fungal isolate and nanoCuO concentration. Data were analysed for each time, separately. Significant differences between treatments and respective controls were analysed by Bonferroni post-tests (Zar 2009). Data in percentage were arcsine square root transformed to achieve normal distribution and homoscedasticity (Zar 2009). Analyses were done with Statistica 6.0 (Statsoft, Inc., Tulsa, OK).

7.3. Results

7.3.1. Intracellular accumulation of reactive oxygen species

Intracellular accumulation of ROS did not occur in the absence of nanoCuO or Cu^{2+} as indicated by the absence of red fluorescence after MitoTracker Red CM-

H_2XRos staining of fungal mycelia (Fig. 7.1). The exposure to nanoCuO or Cu^{2+} led to intracellular accumulation of ROS as shown by red fluorescence (Fig. 7.1). Intracellular ROS accumulation promoted by nanoCuO was dose dependent. Mycelia exposed to the highest nanoCuO concentrations (100 and 200 mg L^{-1}) and to 25 mg L^{-1} of Cu^{2+} showed higher intracellular ROS accumulation after 10 than after 3 days of exposure (Fig. 7.1B versus Fig. 7.1A). The exposure to nanoCuO led to higher ROS accumulation in fungi from non-polluted streams (At72 and P5) than from metal-polluted streams (Fig. 7.1). Moreover, accumulation of ROS was higher after exposure to 25 mg L^{-1} of Cu^{2+} than to the same concentration of nanoCuO (Fig. 7.1).

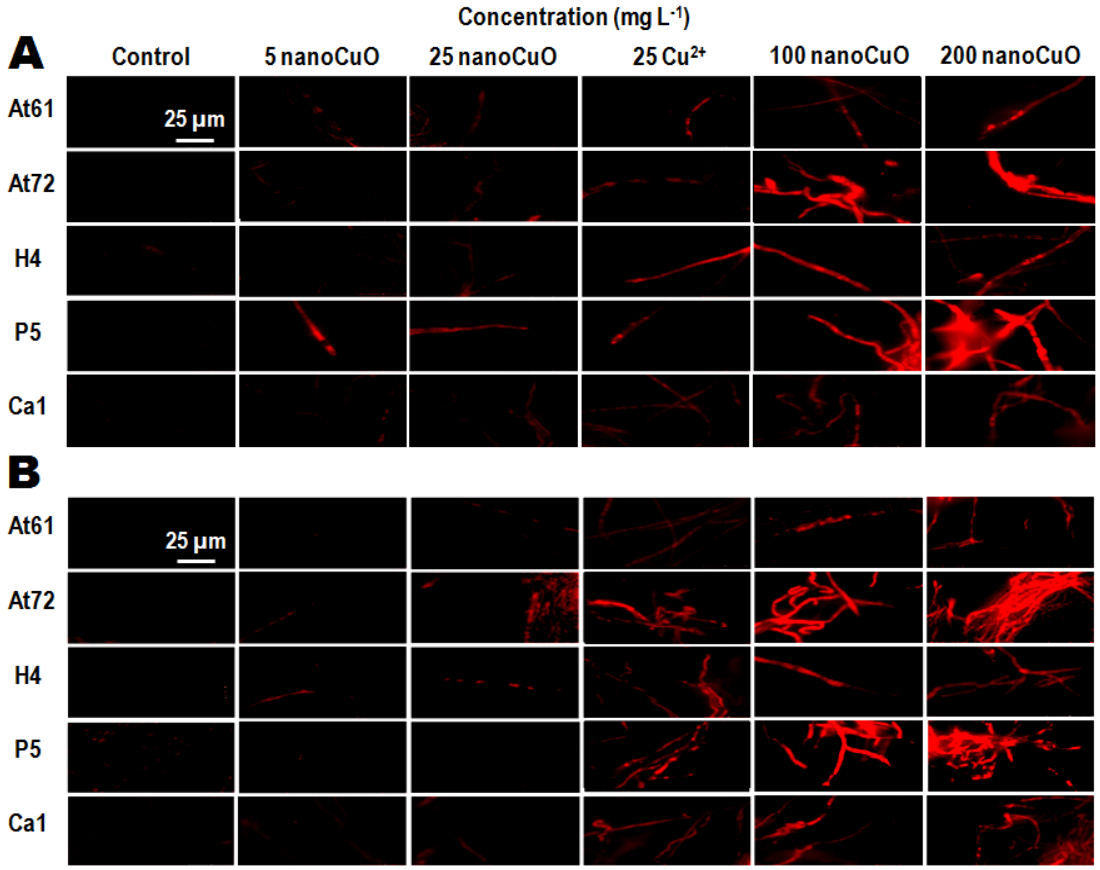

Figure 7.1 ROS accumulation, shown by red fluorescence after MitoTracker Red CM-H_2XRos staining, in mycelia of aquatic fungi isolated from non-polluted streams (At72, *Articulospora tetracladia* UMB-072.01; and P5, *Phoma* sp. UHH 5-1-03) and from metal-polluted streams (At61, *A. tetracladia* UMB-061.01; H4, *Heliscus lugdunensis* H-4-2-4; and *Clavariopsis aquatica* WD(A)-00-1, Ca1) exposed to increasing concentrations of nanoCuO (0, 5, 25, 100 and 200 mg L^{-1}) and to 25 mg L^{-1} of Cu^{2+} for 3 days (A) and 10 days (B).

7.3.2. Plasma membrane integrity

In the absence of nanoCuO or Cu^{2+}, plasma membrane disruption was not observed in fungi after 3 and 10 days of experiment, as indicated by the absence of

red fluorescence after PI staining (Fig. 7.2A and B). The exposure for 3 days to nanoCuO or Cu^{2+} led to plasma membrane disruption of fungal mycelia, and the effects increased with increasing nanoCuO concentration (Fig. 7.2A). At the longer time (10 days), the intensity of red fluorescence and the frequency of PI-positive cells further increased after exposure to higher nanoCuO concentrations or to 25 mg L^{-1} of Cu^{2+} (Fig. 7.2B). Under exposure to the highest nanoCuO concentrations (100 and 200 mg L^{-1}), plasma membrane disruption was higher in fungi isolated from non-polluted streams, namely At72 and P5, comparing to fungi from metal-polluted streams (At61, H4 and Ca1), particularly after 10 days of exposure (Fig. 7.2B). Effects of 25 mg L^{-1} of Cu^{2+} on plasma membrane disruption were more pronounced than those promoted by the same concentration of nanoCuO (Fig. 7.2).

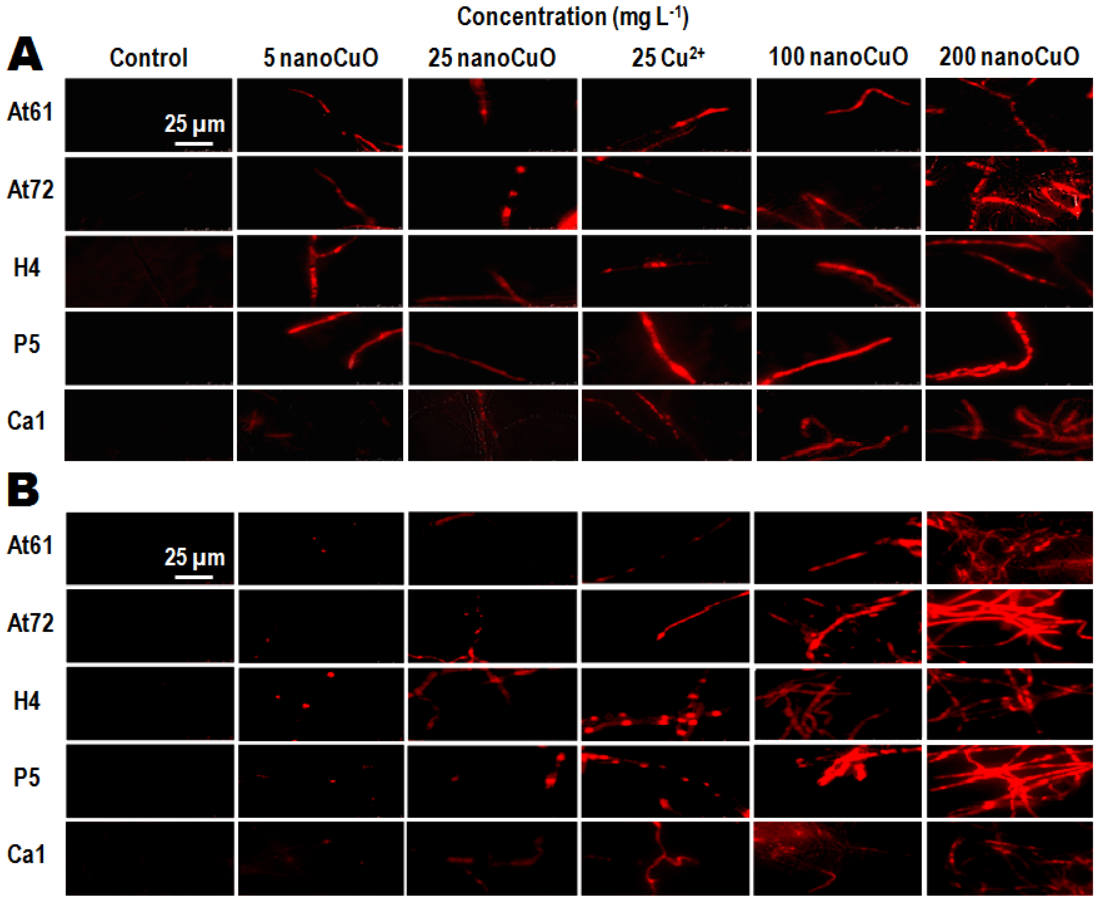

Figure 7.2 Plasma membrane damage, shown by red fluorescence after propidium iodide staining, in aquatic fungi isolated from non-polluted streams (At72, *Articulospora tetracladia* UMB-072.01; and P5, *Phoma* sp. UHH 5-1-03) and from metal-polluted streams (At61, *A. tetracladia* UMB-061.01; H4, *Heliscus lugdunensis* H-4-2-4; and *Clavariopsis aquatica* WD(A)-00-1, Ca1) exposed to increasing concentrations of nanoCuO (0, 5, 25, 100 and 200 mg L^{-1}) and to 25 mg L^{-1} of Cu^{2+} for 3 days (A) and 10 days (B).

7.3.3. DNA-strand breaks

In the absence of nanoCuO or Cu^{2+}, fungal nuclei showed blue fluorescence indicative of DAPI bound to double-stranded DNA, and no TUNEL-positive phenotype was detected (absence of green fluorescence) (Fig. 7.3). The exposure for 3 days to increasing nanoCuO concentrations resulted in a TUNEL-positive phenotype, indicative of DNA-strand breaks, as shown by an increased green fluorescence and a decreased blue fluorescence of DAPI in fungal hyphae (Fig. 7.3A).

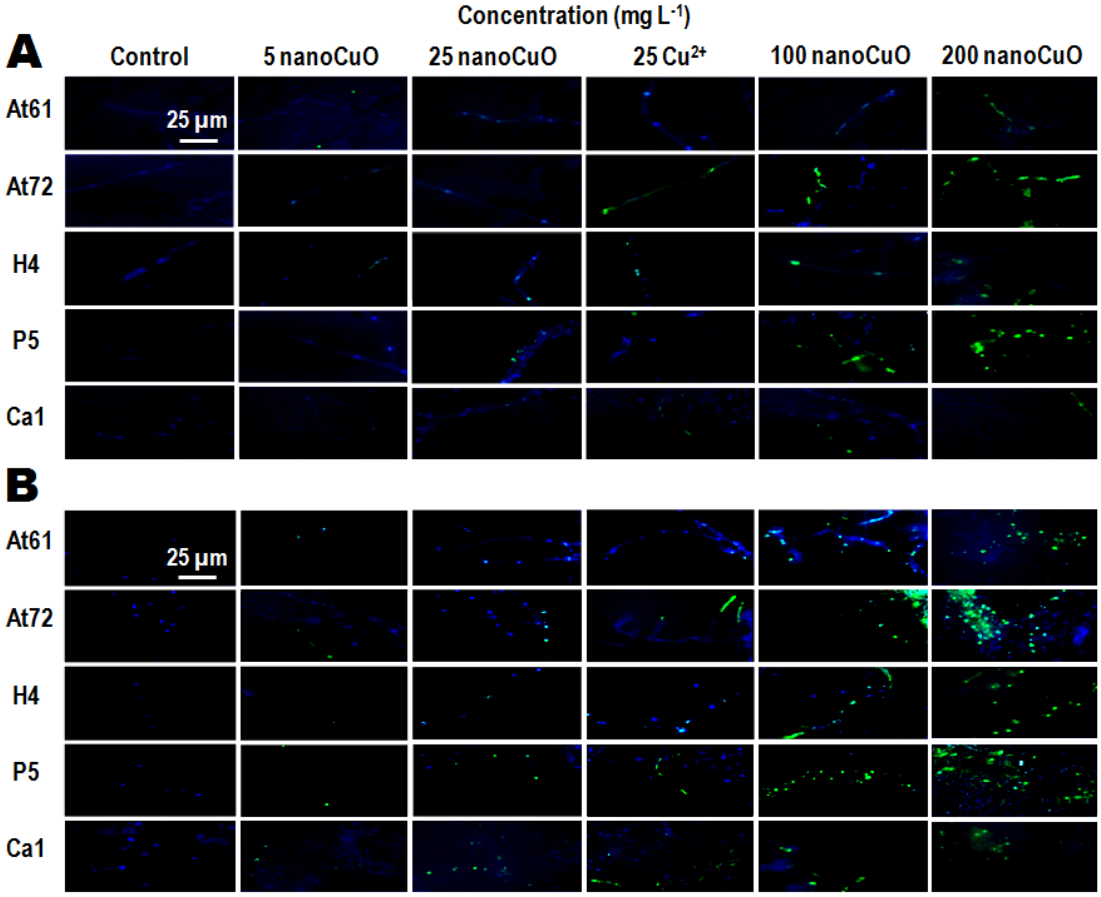

Figure 7.3 *In situ* detection of DNA-strand breaks by fluorescence staining with TUNEL (green) and DAPI (blue) isolated from non-polluted streams (At72, *Articulospora tetracladia* UMB-072.01; and P5, *Phoma* sp. UHH 5-1-03) and from metal-polluted streams (At61, *A. tetracladia* UMB-061.01; H4, *Heliscus lugdunensis* H-4-2-4; and *Clavariopsis aquatica* WD(A)-00-1, Ca1) exposed to increasing concentrations of nanoCuO (0, 5, 25, 100 and 200 mg L^{-1}) and to 25 mg L^{-1} of Cu^{2+} for 3 days (A) and 10 days (B).

The occurrence of DNA-strand breaks increased after 10 days of exposure to increasing nanoCuO concentration (Fig. 7.3B). Also, fungal isolates from non-polluted streams (At72 and P5) showed higher number of cells with TUNEL-positive

phenotype than isolates from metal-polluted streams, mainly after 10 days of exposure (Fig. 7.3B). At this exposure time, 25 mg L^{-1} of Cu^{2+} seemed to induce higher number of cells with DNA-strand breaks than the same concentration of nanoCuO in At72 and P5 (Fig. 7.3).

7.3.4. Total intracellular protein

In the absence of nanoCuO, concentration of total intracellular protein differed with the fungal isolate and the exposure time (Table 7.1). Upon exposure to nanoCuO, the intracellular protein increased in a dose- and time-dependent manner in all fungi (two-way ANOVAs, *P<0.05*, Table 7.1; Fig. 7.4A and B). Exposure to increased nanoCuO concentrations led to higher levels of intracellular protein in fungi from non-polluted streams than in those from metal-polluted streams (two-way ANOVAs, *P<0.05*, Table 7.1; Fig. 7.4A and B). Maximum increase in intracellular protein was found after 10 days of exposure to the highest nanoCuO concentration as follows: At72, 13.5×; P5, 6.8×; At61, 5.4×; H4, 2.5×; and Ca1, 2×.

Table 7.1 Total intracellular protein concentration in aquatic fungi isolated from non-polluted streams (At72, *Articulospora tetracladia* UMB-072.01; and P5, *Phoma* sp. UHH 5-1-03) and from metal-polluted streams (At61, *A. tetracladia* UMB-061.01; H4, *Heliscus lugdunensis* H-4-2-4; and *Clavariopsis aquatica* WD(A)-00-1, Ca1) exposed or not to increasing concentrations of nanoCuO for 3 days and 10 days

NanoCuO (mg L^{-1})	Total intracellular protein (mg g^{-1} fungal dry mass)									
	At72		At61		H4		P5		Ca1	
	3d	10d	3d	10d	3d	10d	3d	10d	3d	10d
0	0.010	0.010	0.010	0.011	0.051	0.038	0.024	0.025	0.028	0.029
5	0.010	0.010	0.010	0.012	0.052	0.045	0.024	0.030	0.028	0.027
25	0.016	0.021*	0.012	0.015	0.055	0.054	0.032	0.045	0.041	0.040
100	0.034*	0.044*	0.017	0.040*	0.061	0.063	0.054*	0.086*	0.042	0.052*
200	0.117*	0.135*	0.030*	0.059*	0.074	0.094*	0.125*	0.167*	0.052	0.059*

*, treatments that differ significantly from the respective control (Bonferroni tests, P<0.05).

7.3.5. Activity of oxidative stress enzymes

The activity of GR increased significantly with increasing concentration of nanoCuO in all fungi for both exposure times (two-way ANOVAs, *P<0.05*, Table 7.2; Fig. 7.4C and D). In the absence of nanoCuO, the GR activity after 3 days of experiment varied from 0.903 to 1.048 nanoKat mg^{-1} protein in H4 and Ca1, respectively (Table 7.2). At this time, the exposure to nanoCuO increased the relative GR activity more in fungi collected from metal-polluted streams (up to 185.4,

175.1 and 172.4% for At61, H4 and Ca1, respectively) than in fungi from non-polluted streams (145.9% and 157.5% for At72 and P5, respectively) (Fig. 7.4C). After longer time, GR activity increased remarkably in fungi isolated from metal-polluted streams (At61, 226.8%; H4, 205.9%; Ca1, 250.2%) compared to fungi from non-polluted streams (At72, 137.3%; P5, 169.2%) (Fig. 7.4D).

In the absence of nanoCuO, the GPx activity ranged from 0.756 to 1.653 nanoKat mg^{-1} protein in At72 and At61 after 3 days of experiment (Table 7.2). Maximum GPx activity was found in AT61 after 10 days and corresponded to 1.706 nanoKat mg^{-1} protein (Table 7.2). Exposure to increased concentrations of nanoCuO significantly increased the activity of GPx in all fungi (two-way ANOVAs, $P<0.05$, Table 7.2; Fig. 7.4E and F). After 3 and 10 days of exposure to nanoCuO, maximum increase in the activity of GPx was found in fungi collected from clean streams, namely P5 (313.3% 3 days; 330.9%, 10 days) and At72 (288.4% 3 days; 374%, 10 days), comparing to fungi from metal-polluted streams, namely At61 (163.8% 3 days; 164.3%, 10 days), H4 (269.7% 3 days; 309.1%, 10 days) and Ca1 (203.6% 3 days; 189.9%, 10 days) (Table 7.2; Fig. 7.4E and F).

In the absence of nanoCuO, the activity of SOD ranged from 0.119 to 0.566 nanoKat mg^{-1} protein in H4 and in P5, respectively. The exposure for 3 days to increased concentrations of nanoCuO significantly increased SOD activity in all fungi (two-way ANOVAs, $P<0.05$, Table 7.2; Fig 7.4G). Higher increases in SOD activity were found in fungi collected from metal-polluted streams (H4, 880.4%; Ca1, 362.9%; and At61, 237.2%) comparing with fungi from non-polluted streams (At72, 213.6%; and P5, 225.9%) (Fig. 7.4G).

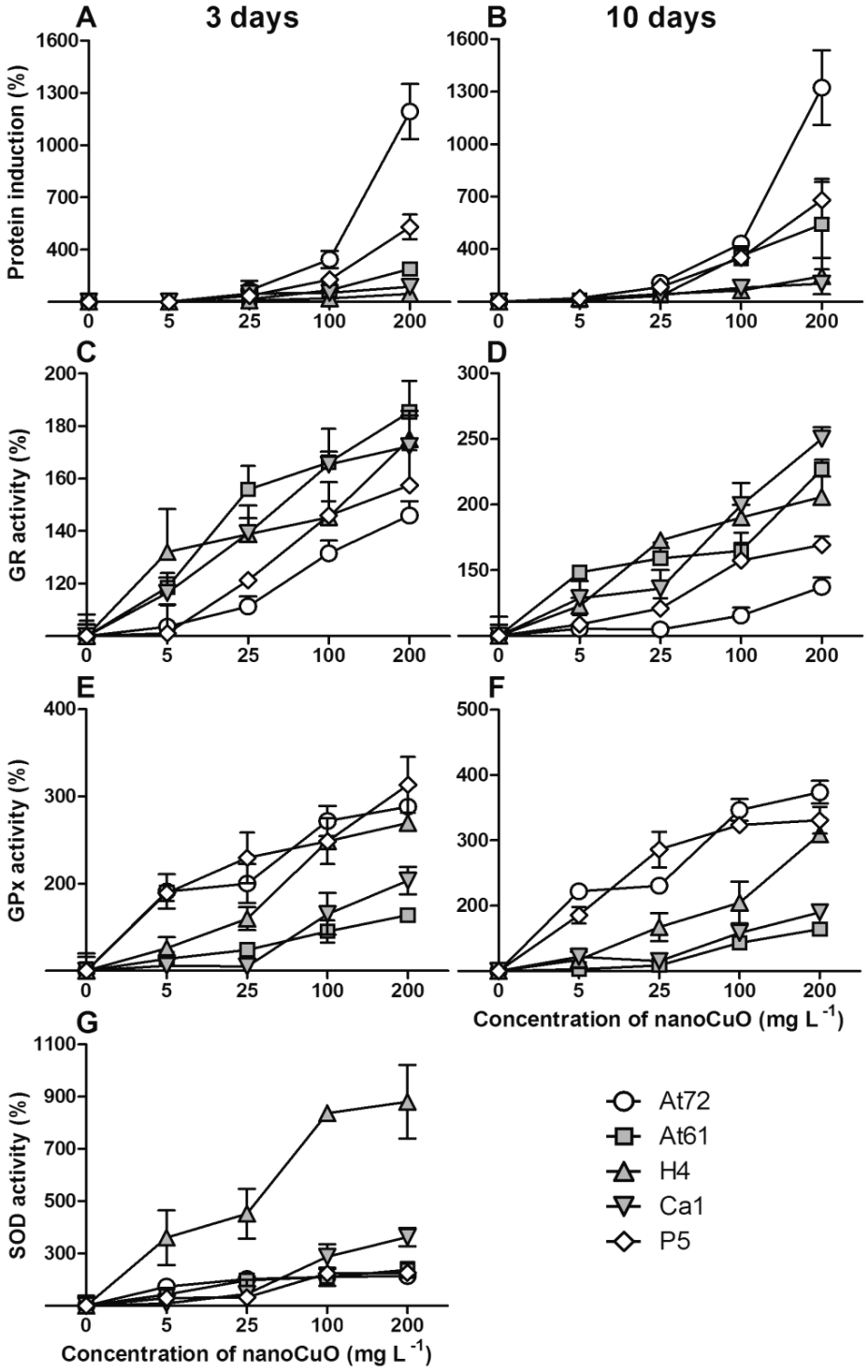

Figure 7.4 Protein increase and enzymatic activities in mycelia of aquatic fungi isolated from non-polluted streams (At72, *Articulospora tetracladia* UMB-072.01; and P5, *Phoma* sp. UHH 5-1-03) and from metal-polluted streams (At61, *A. tetracladia* UMB-061.01; H4, *Heliscus lugdunensis* H-4-2-4; and *Clavariopsis aquatica* WD(A)-00-1, Ca1) exposed to increasing concentrations of nanoCuO (0, 5, 25, 100 and 200 mg L^{-1}). Protein increase after exposure for 3 days (A) and 10 days (B); glutathione reductase (GR) activity after exposure for 3 days (C) and 10 days (D); glutathione peroxidase (GPx) activity after exposure for 3 days (E) and 10 days (F); and superoxide dismutase (SOD) activity after exposure for 3 days (G). Mean ± SEM, n=3.

Table 7.2 Activity of glutathione reductase (GR), glutathione peroxidase (GPx) and superoxide dismutase (SOD) in aquatic fungi isolated from non-polluted streams (At72, *Articulospora tetracladia* UMB-072.01; and P5, *Phoma* sp. UHH 5-1-03) and from metal-polluted streams (At61, *A. tetracladia* UMB-061.01; H4, *Heliscus lugdunensis* H-4-2-4; and *Clavariopsis aquatica* WD(A)-00-1, Ca1) exposed or not to increasing concentrations of nanoCuO for 3 days and 10 days.

Enzyme	NanoCuO (mg L^{-1})	Enzyme activity (nanoKat mg^{-1} protein)									
		At72		At61		H4		P5		Ca1	
		3d	10d	3d	10d	3d	10d	3d	10d	3d	10d
GR	0	0.973	1.109	1.008	1.027	0.903	0.973	1.029	1.041	1.048	0.921
	5	1.008	1.170	1.195	1.524*	1.192	1.196	1.040	1.132	1.221	1.185
	25	1.083	1.164	1.571*	1.635*	1.253*	1.680*	1.248	1.259	1.459*	1.254*
	100	1.28*	1.281	1.675*	1.692*	1.312*	1.851*	1.503*	1.638*	1.734*	1.84*
	200	1.42*	1.523*	1.868*	2.330*	1.581*	2.002*	1.621*	1.761*	1.807*	2.305*
GPx	0	0.756	0.823	1.653	1.706	0.792	0.770	0.804	0.868	1.095	1.230
	5	1.446*	1.829*	1.883	1.754	0.999	0.902	1.519*	1.609*	1.161	1.499
	25	1.514*	1.900*	2.054	1.857	1.267*	1.29*	1.845*	2.482*	1.152	1.419
	100	2.055*	2.853*	2.402*	2.443*	1.970*	1.576*	1.998*	2.808*	1.809*	1.948*
	200	2.182*	3.079*	2.708*	2.802*	2.137*	2.380*	2.518*	2.871*	2.229*	2.335*
SOD	0	0.513	-	0.497	-	0.119	-	0.566	-	0.246	-
	5	0.891	-	0.709	-	0.430*	-	0.735	-	0.270	-
	25	1.038*	-	0.983*	-	0.539*	-	0.746	-	0.358	-
	100	1.081*	-	1.046*	-	0.998*	-	1.268*	-	0.710*	-
	200	1.096*	-	1.479*	-	1.05*	-	1.278*	-	0.894*	-

-, not measured; *, treatments that differ significantly from the respective control (Bonferroni tests, *P<0.05*).

7.4. Discussion

Our study showed that exposure to nanoCuO induced oxidative stress in aquatic fungi by increasing accumulation of intracellular ROS, and led to plasma membrane disruption and DNA-strand breaks in a dose-dependent manner. In other biological systems like human cell lines (Karlsson et al., 2009), protozoa (Mortimer et al., 2010), human lung cells (Lin et al., 2006; Petersen and Nelson, 2010) and marine invertebrates (Buffet et al., 2011), nanoparticles of metal oxides, including nanoCuO, are reported to induce intracellular accumulation of ROS by mitochondrial membrane depolarization, plasma membrane damage by lipid peroxidation and DNA-strand breaks leading to apoptotic or necrotic death.

In our previous studies, the structure of aquatic fungal communities in stream microcosms changed after exposure to nanoCuO (Pradhan et al., 2011) or Cu^{2+} (Duarte et al., 2008, 2009) suggesting that fungi may adapt to the stress induced by nanoCuO as found for metal ions (Azevedo et al., 2007, 2009; Guimarães-Soares et al., 2007). Our study also revealed different response patterns to the stress induced by nanoCuO between fungi collected from metal-polluted streams and from non-

polluted streams. Indeed, the levels of ROS accumulation, membrane damage, and DNA-strand breaks were higher in fungi from non-polluted streams (At72 and P5) compared to fungi from metal-polluted streams (At61, H4, Ca1). Differences were more prominent after longer time (10 days) of exposure to higher nanoCuO concentrations. However, effects of exposure to the lowest nanoCuO concentration (5 mg L^{-1}) were more pronounced at short than at long time suggesting that fungi have the ability to repair membrane damages under low nanoCuO stress. This agrees with the reported recovery of plasma membrane integrity in the aquatic fungus *H. submersus* after long time of exposure to Cu^{2+} (Azevedo et al., 2007).

In our study, the activity of the enzymes GR, GPx and SOD increased after exposure to nanoCuO in a dose-dependent manner, supporting their role in coping with oxidative stress and contributing to cellular detoxification (Israr et al., 2006; Lin et al., 2006; Fahmy and Cormier, 2009; Buffet et al., 2011). In our study, the activity of SOD increased more than the activity of other antioxidant enzymes after 3 days of exposure to nanoCuO, suggesting that SOD may be involved in early defence against ROS, particularly in fungi from metal-polluted streams. The maintenance of high GSH:GSSG ratio in cells is needed to protect them against oxidative stress (Townsend et al., 2003); GR is a key enzyme to keep the pool of glutathione in its reduced form (GSH), whereas GPx interacts with free peroxides/hydroperoxides and converts GSH to GSSG (Townsend et al., 2003; Israr et al. 2006). Under metal-induced oxidative stress, the increase in glutathione pool is often observed in metal-tolerant fungi, including aquatic fungi from metal-polluted streams (Jaeckel et al., 2005; Braha et al., 2007). Although the activities of all tested enzymes had increased with nanoCuO concentration and exposure time, the response differed among fungal isolates as summarized in Fig 7.5. Fungi from non-polluted streams (At72 and P5) showed lower GR activity and higher GPx activity (Fig. 7.5A) compared to fungi from metal-polluted streams (At61, H4 and Ca1) (Fig. 7.5B), and differences became more pronounced at the longer exposure time. This suggests that GSH pool in fungi from polluted streams was higher compared to that in fungi from non-polluted streams, probably because free peroxide/hydroperoxide radicals were not so efficiently scavenged by antioxidant enzymes in the latter fungi (Fig 7.5). The high oxidative stress and cytotoxicity induced by nanoCuO to airway epithelial cells was explained by the increase in GPx activity and a decrease in the GR activity, leading to an increase in the ratio of oxidized to total glutathione (Fahmy and Cormier, 2009). Thus, the antioxidant enzymatic responses clearly provide a

key explanation to the lower level of intracellular ROS accumulation, plasma membrane damage and DNA-strand breaks in fungi from metal-polluted streams by conferring them a more effective cellular protection against nanoCuO in comparison to fungi from non-polluted streams. Moreover, fungi from non-polluted streams had higher increases in the levels of total intracellular proteins, suggesting that proteins/enzymes, other than those investigated in this study, can play a role in copping with the stress induced by nanoCuO. Under metal exposure, aquatic fungi have shown increased levels of Cu-binding small peptides, most likely glutathione and phytochelatins, and metallothionein-like proteins with a minor role in metal-binding but probably acting as ROS scavengers (Guimarães-Soares et al., 2006).

The effects of Cu^{2+} on aquatic fungi were stronger than those observed for nanoCuO either at the community level (Pradhan et al., 2011) or at the population level (this study), probably because copper bioavailability in the ionic form is higher than in the nano form. The toxicity or ecotoxicity of nanoCuO has been often attributed to the ionic form of copper leached from nanoCuO (Kahru et al., 2008; Aruoja et al., 2009; Kasemets et al., 2009). Indeed, Blinova et al. (2010) reported about 12% dissolution of Cu^{2+} from nanoCuO in freshwaters using Cu-sensor bacteria. However, when metal dissolution is very low, the contribution of metal ions leached from metal oxide nanoparticles to overall toxicity can be questioned (Griffitt et al., 2008; Buffet et al., 2011). Toxicity can also result from intracellular dissolution of nanoparticles leading to accumulation of metal ions as demonstrated for nanoCu (Meng et al., 2007). Lysosomes mediate intracellular degradation of nanoCuO into Cu^{2+}, which is subsequently released into the cytoplasm where is reduced by $O_2^{\bullet -}$ to Cu^{+} (Petersen and Nelson, 2010). Ionic metals undergoing the redox and/or ascorbate-glutathione cycle can directly or indirectly cause an increase in intracellular ROS accumulation, cell membrane disruption and DNA damage in aquatic fungi (Azevedo et al. 2007, 2009). Therefore, we cannot discard the hypothesis that Cu^{2+} might have played a role in the effects of nanoCuO on aquatic fungi.

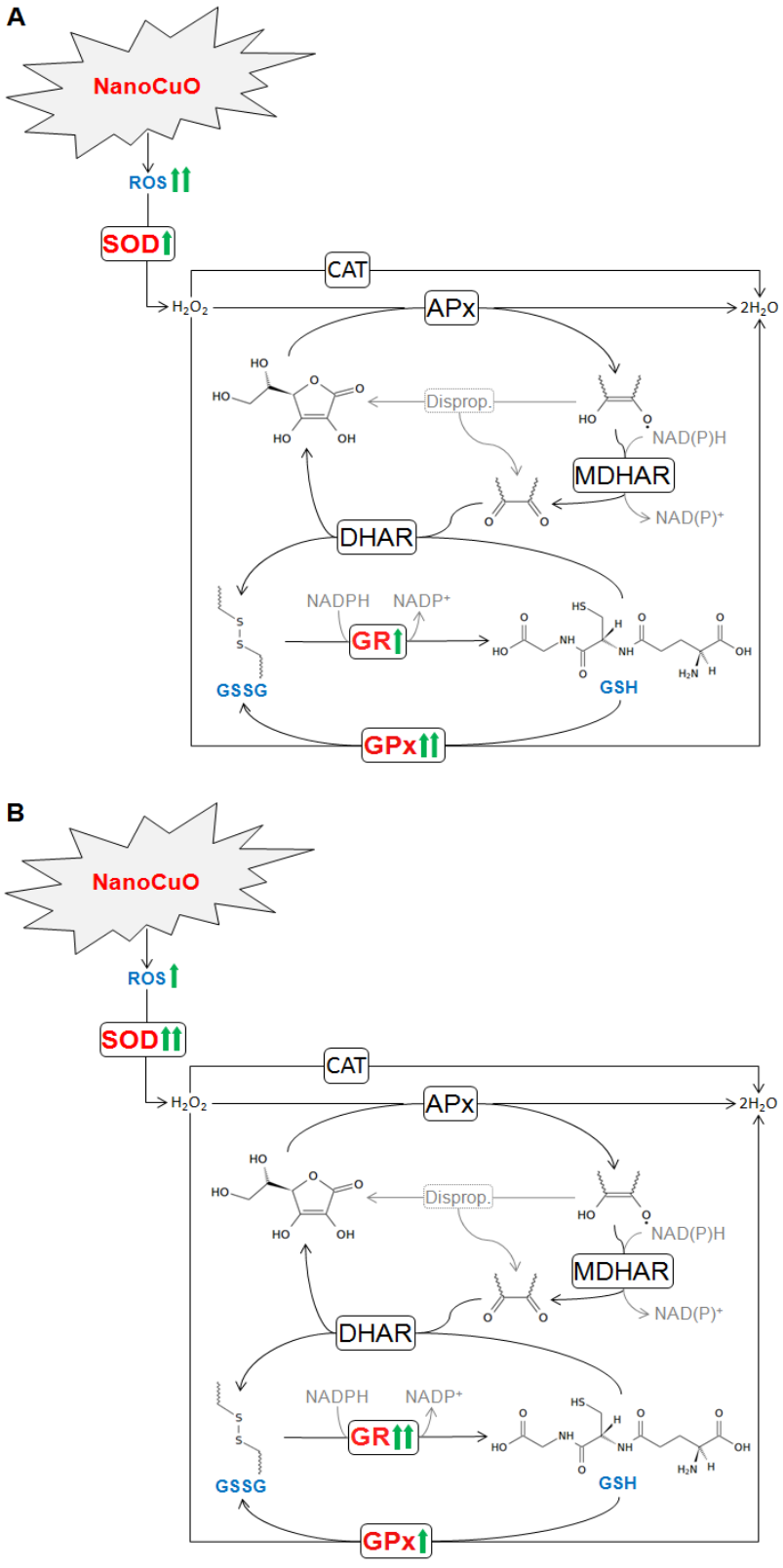

Figure 7.5 Diagrammatic representation of ascorbate-glutathione cycle highlighting the differences in the activity of glutathione reductase (GR), glutathione peroxidase (GPx), and superoxide dismutase (SOD) after nanoCuO exposure in fungi isolated from non-polluted streams (A) and metal-polluted streams (B).

Overall, our study showed that nanoCuO induced oxidative stress in aquatic fungi by intracellular ROS accumulation, and led to plasma membrane damage and DNA-strand breaks in a concentration- and time-dependent manner. Mycelia of fungi collected from metal-polluted streams showed less oxidative stress and higher responses of antioxidant enzymes related to the maintenance of glutathione (GSH) pool under nanoCuO exposure compared to fungi from non-polluted streams. The observed differences in the cellular responses to the stress induced by nanoCuO between fungi with different background were also confirmed at the intraspecific level (At61 from metal-polluted streams versus At72 from non-polluted streams). These findings suggest that fungal populations adapted to metals may develop mechanisms of tolerance/resistance to cope with the stress induce by metal nanoparticles. This means that the genetic background of populations should be taken into account in further studies when examining the toxicity of metal or metal oxide nanoparticles.

References

Anderson JV, Davis DG, 2004. Abiotic stress alters transcript profiles and activity of glutathione S-transferase, glutathione peroxidase, and glutathione reductase in *Euphorbia esula*. Physiol Plant 120, 421–433.

Aruoja V, Dubourguier HC, Kasemets K, Kahru A, 2009. Toxicity of nanoparticles of CuO, ZnO and TiO_2 to microalgae *Pseudokirchneriella subcapitata*. Sci Total Environ 407, 1461–1468.

Azevedo MM, Almeida B, Ludovico P, Cássio F, 2009. Metal stress induces programmed cell death in aquatic fungi. Aquat Toxicol 92, 264–270.

Azevedo MM, Carvalho A, Pascoal C, Rodrigues F, Cássio F, 2007. Responses of antioxidant defenses to Cu and Zn stress in two aquatic fungi. Sci Total Environ 377, 233–243.

Battin TJ, Kammer FVD, Weilhartner A, Ottofuelling S, Hofmann T, 2009. Nanostructured TiO_2: transport behavior and effects on aquatic microbial communities under environmental conditions. Environ Sci Technol 43, 8098–8104

Beyer WF, Fridovich I, 1987. Assaying for superoxide dismutase activity: some large consequences of minor changes in conditions. Anal Biochem 161, 559–566.

Blinova I, Ivask A, Heinlaan M, Mortimer M, Kahru A, 2010. Ecotoxicity of nanoparticles of CuO and ZnO in natural water. Environ Pollut 158, 41–47.

Bradford MM, 1976. A rapid and sensitive method for the quantitation of microgram quantities of protein utilizing the principle of protein-dye binding. Anal Biochem, 72, 248–254.

Braha B, Tintemann H, Krauss G, Ehrman J, Bärlocher F, Krauss GJ, 2007. Stress response in two strains of the aquatic hyphomycete *Heliscus lugdunensis after* exposure to cadmium and copper ions. Biometals 20, 93–105.

Buffet PE, Tankoua OF, Pan JF, Berhanu D, Herrenknecht C, Poirier L, Amiard-Triquet C, Amiard JC, Bérard, JB, Risso C, Guibbolini M, Roméo M, Reip P, Valsami-Jones E, Mouneyrac C, 2011. Behavioural and biochemical responses of two marine invertebrates *Scrobicularia plana* and *Hediste diversicolor* to copper oxide nanoparticles. Chemosphere 84, 166–174.

Dutta A, Das D, Grilli ML, Di Bartolomeo E, Traversa E, Chakravorty D, 2003. Preparation of sol–gel nano-composites containing copper oxide and their gas sensing properties. J Sol–Gel Sci Technol 26, 1085–1089.

Esterbauer H, Grill D, 1978. Seasonal variation of glutathione and glutathione reductase in needles of *Picea abies*. Plant Physiol 61, 119–121.

Fahmy B, Cormier SA, 2009. Copper oxide nanoparticles induce oxidative stress and cytotoxicity in airway epithelial cells. Toxicol in Vitro 23 1365–137.

Fridovich I, 1986. Biological effects of the superoxide radical. Arch Biochem Biophys 24, 1–11.

Graça MAS, 2001. The role of invertebrates on leaf litter decomposition in streams – a Review. Int Rev Hydrobiol 86, 383–393.

Griffitt RJ, Luo J, Bonzongo JC, Barber DS, 2008. Effects of particle composition and species on toxicity of metallic nanomaterials in aquatic organisms. Environ Toxicol Chem 27, 1972–1978.

Guimarães-Soares L, Felícia H, Bebianno MJ, Cássio F, 2006. Metal-binding proteins and peptides in the aquatic fungi *Fontanospora fusiramosa* and *Flagellospora curta* exposed to severe metal stress. Sci Total Environ 372, 148-156.

Guimarães-Soares L, Pascoal C, Cássio F, 2007. Effects of heavy metals on the production of thiol compounds by the aquatic fungi *Fontanospora fusiramosa* and *Flagellospora curta*. Ecotoxicol Environ Saf 66, 36-43.

Hassellöv M, Readman JW, Ranville JF, Tiede K, 2008. Nanoparticle analysis and characterization methodologies in environmental risk assessment of engineered nanoparticles. Ecotoxicology 17, 344–361.

Heinlaan M, Ivask A, Blinova I, Dubourguier HC, Kahru A, 2008. Toxicity of nanosized and bulk ZnO, CuO and TiO_2 to bacteria *Vibrio fischeri* and crustaceans *Daphnia magna* and *Thamnocephalus platyurus*. Chemosphere 71, 1308–1316.

Huang GY, Wang YS, Sun CC, Dong JD, Sun ZX, 2010. The effect of multiple heavy metals on ascorbate, glutathione and related enzymes in two mangrove plant seedlings (*Kandelia candel* and *Bruguiera gymnorrhiza*). Oceanol Hydrobiol Stud 39, 11–25.

Israr M, Sahi S, Datta R, Sarkar D, 2006. Bioaccumulation and physiological effects of mercury in *Sesbania drummondii*, Chemosphere, 65, 591–598.

Jaeckel P, Krauss GJ, Krauss G, 2005. Cadmium and zinc response of the fungi *Heliscus lugdunensis* and *Verticillium cf.alboatrum* isolated from highly polluted water. Sci Total Environ 346, 274–279.

Jevremović S, Petrić M, Živković S, Trifunović M, Subotić A, 2010. Superoxide dismutase activity and isoenzyme profiles in bulbs of snake's head fritillary in response to cold treatment. Arch Biol Sci, Belgrade 62, 553–558.

Junghanns C, Krauss G, Schlosser D, 2008. Potential of aquatic fungi derived from diverse freshwater environments to decolourise synthetic azo and anthraquinone dyes, Bioresource Technol 99, 1225–1235.

Junghanns C, Moeder M, Krauss G, Martin C, Schlosser D, 2005. Degradation of the xenoestrogen nonylphenol by aquatic fungi and their laccases. Microbiology 151, 45–57.

Kahru A, Dubourguier HC, Blinova I, Ivask A, Kasemets K, 2008. Biotests and biosensors for ecotoxicology of metal oxide nanoparticles: a minireview. Sensors 8, 5153–5170.

Karlsson HL, Gustafsson J, Cronholm P, Möller L, 2009. Size-dependent toxicity of metal oxide particles – a comparison between nano- and micrometer size. Toxicol Lett 188, 112–118.

Kasemets K, Ivask A, Dubourguier HC, Kahru A, 2009. Toxicity of nanoparticles of ZnO, CuO and TiO_2 to yeast *Saccharomyces cerevisiae*. Toxicol in Vitro 23, 1116–1122.

Krauss G-J, Sole M, Krauss Gudrun, Schlosser D, Wesenberg D, Bärlocher F, 2011. Fungi in freshwaters: ecology, physiology and biochemical potential. FEMS Microbiol Rev 35, 620-651

Lee SW, Kim SM, Choi J, 2009. Genotoxicity and ecotoxicity assays using the freshwater crustacean *Daphnia magna* and the larva of the aquatic midge *Chironomus riparius*to screen the ecological risks of nanoparticle exposure. Environ Toxicol Pharmacol 28, 86–91.

Limbach LK, Wick P, Manser P, Grass RN, Bruinink A, Stark WJ, 2007. Exposure of engineered nanoparticles to human lung epithelial cells: influence of chemical composition and catalytic activity on oxidative stress. Environ Sci Technol 41, 4158–4163.

Lin W, Huang Y, Zhou XD, Ma Y, 2006. Toxicity of cerium oxide nanoparticles in human lung cancer cells. Int J Toxicol 25, 451–457.

Meng H, Chen Z, Xing G, Yuan H, Chen C, Zhao F, Zhang C, Zhao Y, 2007. Ultrahigh reactivity provokes nanotoxicity: explanation of oral toxicity of nanocopper particles. Toxicol Lett 175, 102–110.

Miersch J, Grancharov K, 2008. Cadmium and heat response of the fungus *Heliscus lugdunensis* isolated from highly polluted and unpolluted areas. Amino Acids 34, 271–277.

Moriwaki H, Osborne MR, Phillips DH, 2008. Effects of mixing metal ions on oxidative DNA damage mediated by a Fenton-type reduction. Toxicol in Vitro 22, 36–44.

Mortimer M, Kasemets K, Kahru A, 2010. Toxicity of ZnO and CuO nanoparticles to ciliated protozoa *Tetrahymena thermophila*. Toxicology 269, 182–189

Pascoal C, Cássio F, Marcotegui A, Sanz B, Gomes P, 2005a. Role of fungi, bacteria, and invertebrates in leaf litter breakdown in a polluted river. J N Am Benthol Soc 24, 784–797.

Pascoal C, Marvanová L, Cássio F, 2005b. Aquatic hyphomycete diversity in streams of Northwest Portugal. Fung Divers 19, 109-128.

Penninckx MJ, 2002. An overview on glutathione in *Saccharomyces* versus non-conventional yeasts. FEMS Yeast Res 2, 295–305.

Petersen EJ, Nelson BC, 2010. Mechanisms and measurements of nanomaterial-induced oxidative damage to DNA. Anal Bioanal Chem 398, 613–650.

Pradhan A, Seena S, Pascoal C, Cássio F, 2011. Can metal nanoparticles be a threat to microbial decomposers of plant litter in streams? Microb Ecol 62, 58–68.

Pradhan A, Seena S, Pascoal C, Cássio F, 2012. Copper oxide nanoparticles can induce toxicity to the freshwater shredder *Allogamus ligonifer*. Chemosphere 89, 1142–1150.

Ren G, Hu D, Cheng EWC, Vargas-Reus MA, Reip P, Allaker RP, 2009. Characterisation of copper oxide nanoparticles for antimicrobial applications. Int J Antimicrob Agents 33, 587–590.

Saison C, Perreault F, Daigle JC, Fortin C, Claverie J, Morin M, Popovic R, 2010. Effect of core-shell copper oxide nanoparticles on cell culture morphology and photosynthesis (photosystem II energy distribution) in the green alga, *Chlamydomonas reinhardtii*. Aquat Toxicol 96, 109–114.

Sridhar KR, Bärlocher F, Wennrich R, Krauss G-J, Krauss G, 2008. Fungal biomass and diversity in sediments and on leaf litter in heavy metal contaminated waters of Central Germany. Fundam Appl Limnol 171, 63–74.

Stohs SJ, Bagchi D, 1995. Oxidative mechanisms in the toxicity of metal ions. Free Radic Biol Med 18, 321–336.

Townsend DM, Tew KD, Tapiero H, 2003. The importance of glutathione in human disease. Biomed Pharmacother 57, 145–155.

Zar JH, 2009. Biostatistical analysis, fifth ed, Prentice Hall, Upper Saddle River, New Jersey.

Zhang X, Zhang D, Ni X, Song J, Zheng H, 2008. Synthesis and electrochemical properties of different sizes of the CuO particles. J Nanopart Res 10, 839–844.

Chapter 8

Polyhydroxy fullerene can stimulate yeast growth and mitigate oxidative stress induced by cadmium

Abstract

The water-soluble polyhydroxy fullerene (PHF) is a functionalized carbon nanomaterial with several industrial and commercial applications. There have been controversial reports on the potential toxicity and/or antioxidative activity of fullerenes and their derivatives. Conversely, metals have been recognized as toxic mainly due to their ability to induce oxidative stress in living organisms. We investigated the interactive effects of PHF nanoparticles and Cd ions on the model yeast *Saccharomyces cerevisiae* by exposing cells to Cd (≤5 mg L^{-1}) in the absence or presence of PHF (≤500 mg L^{-1}) at different pH (5.8-6.8) for 14h and 26h. In the absence of Cd, PHF stimulated yeast growth up to 10.3%. Cadmium inhibited growth up to 79.7% in a dose-, time- and pH-dependent manner. Cadmium also induced intracellular accumulation of reactive oxygen species (ROS) and plasma membrane disruption. The negative effects of Cd on yeast growth were attenuated by the presence of PHF, and maximum growth recovery (53.8%) was obtained at the highest PHF concentration, at pH 6.8, after 26 h. The co-exposure to Cd and PHF decreased ROS accumulation up to 36.7% and membrane disruption up to 30.7% in a dose-, time- and pH-dependent manner. Results suggested that PHF stimulates yeast growth and mitigates the oxidative stress induced by Cd.

Keywords: Polyhydroxy fullerene, cadmium, yeasts, antioxidant agent, ROS accumulation.

8.1. Introduction

Fullerene and functionalised fullerenes are carbon-based nanoparticles with enormous developments in nanotechnology due to their applications in several fields, such as biomedical diagnostics and therapeutics (Da Ros et al., 2001; Bosi et al., 2003; Partha and Conyers, 2009) and remediation in wastewater treatment plants (Anderson and Barron, 2005). However, some studies have reported potential toxicity and ecotoxicity of fullerene (Sayes et al., 2004; Oberdörster et al., 2006) and, consequently, fullerene was placed on the top of OECD list (OECD, 2010) seeking toxicity tests and risk assessment. On the other hand, polyhydroxy fullerene (PHF), a functionalised derivative of fullerene, is in the lime light of current research due to its reported non-toxic nature and reactive oxygen species (ROS) quenching properties (Lai et al., 2000; Injac et al., 2008b; Vávrová et al., 2012). PHF has an edge over fullerene in commercial or research applications because it is stable and soluble in aqueous solution due to the presence of hydroxyl groups. As an antioxidant agent and free radical scavenger, PHF has been reported to decrease excitotoxic and apoptotic death of neurons (Dugan et al., 1996), protect against ischemia-reperfused lungs (Chen et al., 2004), protect rat brain from alcoholic injury (Tykhomyrov et al., 2008), prevent hepatotoxicity in rats and human cell lines (Injac et al., 2008a), and decrease tumour size in rats (Krishna et al., 2010). In contrast, cytotoxicity of PHF has also been observed (Sayes et al., 2004; Xu et al., 2009; Johnson-Lyles et al., 2010; Wielgus et al., 2010). Under photoexcitation, PHF can generate free radical species (Pickering and Wiesner, 2005) and induce early apoptosis and lipid peroxidation (Wielgus et al., 2010). These discrepant findings make it relevant to further assess the effects of PHF on biological systems.

Cadmium (Cd), a nonessential element for living organisms, has been used in various industrial and regular-life products, such as batteries, pigments and paints, alloys, welding and electroplating, leading to its increased release in the environment (Ayres, 1992). For instance, a quantitative estimation of Cd for Chinese rivers pointed to 4.45 t of Cd deposited per year along the Anhui section of the Yangtze River, and to a high Cd content in the suspended matter in the Shun'an River (104.8 μg g^{-1}) (Zhao et al., 2008). As a non-biodegradable element, Cd has a very long biological half-life (Sugita and Tsuchiya, 1995) and it has been reported to be toxic to macro and microorganisms, including yeasts (Chen et al., 1995; Choi, 2009; Nweke, 2010; Vestena et al., 2011). Cadmium toxicity has been shown to be

caused by oxidative stress (Brennan and Schiestl, 1996; Valko et al., 2006); Cd can indirectly generate free radicals by replacing iron or copper ions in cytoplasmic and membrane proteins leading to an increase of free or chelated metals (Valko et al., 2006), which in turn can lead to oxidative stress via Fenton reactions (Price and Joshi, 1983; Casalino et al., 1997). ROS production was involved in Cd-induced cell death in rainbow trout (Risso-de Faverney et al., 2004), murine splenocytes (Pathak and Khandelwal, 2006) and human hepatoma cells (Oh and Lim, 2006). ROS triggered by Cd can react with several biomolecules within cells and may lead to DNA mutation, alteration in protein structure and function, lipid peroxidation, variation in gene expression, and apoptosis (Valko et al., 2006; Wang et al., 2011).

We investigated the potential role of PHF in alleviating Cd toxicity in yeasts under the hypothesis that oxidative stress induced by Cd may be mitigated by PHF due to its antioxidant and free-radical scavenging properties. We selected the yeast *Saccharomyces cerevisiae* because i) it has been used as a eukaryotic model system to study oxidative stress responses (Priault et al., 2003; Landolfo et al., 2008; Chevtzoff et al., 2010; Mendes-Ferreira et al., 2010; Allen et al., 2011), and ii) mounting evidence suggests that Cd can induce oxidative stress by accumulating ROS or free radicals (Lee and Ueom, 2001; Liu et al., 2005; Muthukumar and Nachiappan, 2010). Because the uptake and toxicity of Cd to yeasts can change with pH (Mapolelo and Torto, 2004), exposure time (Blackwell and Tobin, 1999; Oliveira et al., 2012) and growth phase (Adamis et al., 2003; Anagnostopoulos et al., 2010), we assessed the effects of Cd and PHF alone or in mixture on yeast growth, intracellular ROS accumulation and plasma membrane integrity at different exposure conditions. Moreover, we used scanning electron microscopy coupled to an energy dispersive X-ray analyser (SEM-EDX) to examine putative physicochemical interactions between PHF nanoparticles and Cd ions in an attempt to better understand the mode of action of these nanoparticles.

8.2. Material and Methods

8.2.1. Yeast growth and exposure conditions

The yeast *Saccharomyces cerevisiae* PYCC 4072 was obtained from the Portuguese Yeast Culture Collection (Faculty of Sciences and Technology, New University of Lisbon, Portugal). The yeast was maintained on YPD solid medium

with the following composition: dextrose (2%, w/v), peptone (1%, w/v), yeast extract (0.5%, w/v) and agar (2%, w/v). For the assays, cells grown on YPD agar (48 h at 26°C) were inoculated in YPD liquid medium.

Erlenmeyer flasks (100-mL) with 20 ml of YPD medium were supplemented with Cd (0, 1.5 or 5 mg L^{-1}; chloride salt, 98%, Sigma) and/or PHF (0, 50, 250 or 500 mg L^{-1}; $C_{60}(OH)_{18-22}$; BuckyUSA, Houston, TX), and pH of the medium was adjusted to 5.8, 6.3 and 6.8. Exponentially growing yeast cells (5×10^5 cfu mL^{-1}) in YPD were inoculated in each replicate flask, and incubated under shaking (150 rpm) for 14 h and 26 h at 26ºC (12 chemical treatments × 3 pH × 2 exposure times × 3 replicates, in a total of 216 flasks). The yeast growth was monitored by optical density (OD; λ=600 nm) using UV-visible spectrophotometer (UV–1700 PharmaSpec, Shimadzu, Kyoto, Japan).

8.2.2. Preparation of Cd and PHF stocks

The stock solution of Cd was prepared in ultrapure (Milli Q) water and filtered through 0.2 µm pore size membrane (GTTP, Millipore, Billerica, MA) and stored at 4°C in dark. The stock of PHF was prepared by suspending the powder in sterile (121°C, 20 min) ultrapure (Milli Q) water and suspension was sonicated (42 kHz, 100 W, Branson 2510, Danbury, CT) for 10 min in the dark. A uniform aqueous suspension of PHF was obtained with no detectable precipitation after three weeks of storage at 4°C in the dark.

8.2.3. Characterization of Cd, PHF alone and in mixtures

Stock aqueous suspension with PHF nanoparticles and YPD medium containing Cd and/or PHF were examined by scanning electron microscopy (SEM, Leica Cambridge S 360, Cambridge, UK) coupled to an energy dispersive X-ray (EDX) microanalysis setup (15 keV), as described in Pradhan et al. (2011). Briefly, 20 µl of each solution/suspension was loaded on a clean grease-free slide in dark, air-dried and coated with gold in vacuum. Slides were scanned by SEM-EDX to confirm the presence of Cd or C from PHF nanoparticles.

Size distribution of PHF nanoparticles was monitored by dynamic light scattering (DLS) using a zetasizer (Malvern Zetasizer Nano ZS, Malvern Instruments Limited, UK) to check agglomeration of PHF in the stock suspension and in the YPD medium at three different pH. Unlike SEM, agglomerated particles in

the aqueous environment could be measured by DLS with minimum perturbation (Hassellöv et al., 2008).

8.2.4. Visualization of cell morphology

Yeast cells grown in YPD medium in the absence or presence of Cd and/or PHF were harvested by centrifugation (8,000 rpm, 10 min; Sigma 113 Centrifuge; Germany), washed twice and re-suspended in 2 mL phosphate-buffered saline (1× PBS, GIBCO, pH 7.4). Cells were fixed in 2.5% (v/v) glutaraldehyde for 24 h, and dehydrated in ethanol (v/v) as follows: 20%, 8 h; 40%, 6 h; 60%, 4 h; 80%, 2 h; and 100%, 1 h. Cell suspensions (20 µl) were, then, loaded on slides, coated and scanned by SEM-EDX as in section 8.2.3.

8.2.5. Flow cytometry and epifluorescence microscopy for assessing plasma membrane integrity and intracellular ROS accumulation

Plasma membrane integrity was assessed by a membrane impermeable dye, propidium iodide (PI; Molecular Probes, Eugene, OR), which enters the cells and binds to nucleic acids when plasma membrane disruption occurs. Cells with intense red fluorescence were considered as having plasma membrane disruption. Yeast cells, unexposed or exposed to Cd and/or PHF at different pH, were harvested and washed as in section 8.2.4, and re-suspended in 2 ml PBS containing 20 µg ml^{-1} of PI and 0.1 mg ml^{-1} of 4',6-diamidino-2-phenylindole (DAPI, Sigma). The mixture was incubated for 15 min at 26 °C in the dark. DAPI is known to localize nuclei by blue fluorescence.

The accumulation of intracellular ROS was assessed with MitoTracker Red CM-H_2XRos (Molecular Probes, Eugene, OR). This dye does not fluoresce in the reduced form, but entering an actively respiring cell it is oxidized by ROS in the mitochondria to form a red-fluorescent compound. Yeast cells, obtained as above, were re-suspended in 2 ml PBS containing 40 µg ml^{-1} of the dye prepared in dimethyl sulfoxide (≥99.9%, Sigma), and incubated for 15 min at 26°C in the dark.

For visualization of intracellular ROS accumulation and plasma membrane disruption, samples of yeast cells, stained as above, were placed on a grease-free slide and mixed with an equal volume of an anti-fading and anti-photobleaching reagent (Vectashield Mounting Medium; Vector Laboratories, CA). Slides were scanned under an epifluorescence microscope (1000×, Leica DM5000B, Germany)

and images were acquired with a digital camera (Leica DFC 350 FX R2) using the software LAS AF V1.4.1.

Quantitative fluorescence of yeast cells was measured using a flow cytometer (EPICS® XL-MCL™, Beckman Coulter, Germany) equipped with an argon-ion laser emitting a 488 nm beam at 15 mW. The red fluorescence of PI or MitoTracker Red was detected on FL3 log filter through a 590 nm long-pass, a 620 nm band-pass and another 670 nm long-pass. An acquisition protocol was defined to measure forward scatter (FS log), side scatter (SS log) and red fluorescence (FL3 log) on a four-decade logarithmic scale. Twenty five thousand cells per sample were scanned and data were analyzed with the software WinMDI 2.8.

8.2.6. Data analyses

Two-way ANOVAs (Zar, 2009) were used to assess i) effects of PHF and pH on yeast endpoints in the absence or presence of each Cd concentration and ii) effects of Cd and pH on yeasts at each PHF concentration. Data were analysed for 14 h and 26 h, separately. Significant differences between treatments and respective controls or between pH levels were analysed by Bonferroni post-tests (Zar, 2009). To achieve normal distribution and homoscedasticity, data in percentage were arcsine square root transformed (Zar, 2009). Analyses were done with Statistica 6.0 (Statsoft, Inc., Tulsa, OK).

8.3. Results

8.3.1. Characterization of PHF by SEM and DLS

Scanning electronic microscopy (SEM) analysis of PHF in the aqueous stock suspension showed two nanoparticle size ranges: larger particles varied between 100 and 250 nm, and smaller particles varied between 30 and 60 nm (not shown). These results were confirmed by DLS: two peaks with PHF mean sizes of 185.4 nm and 38.4 nm corresponded to 93.1% and 6.9% of area intensity, respectively (Table 8.1). In YPD medium, an additional peak ranging from 1.6 nm to 2.9 nm was found (peak 3; Table 8.1). This was probably due to nanocrystal composites of the YPD medium, because a peak with particles of similar size was observed in the absence of PHF (not shown). In YPD medium, the mean size of PHF and polydispersity index

(PdI) increased with the decrease of pH (peak 1: 198.3 vs 210.5 nm, peak 2: 43.6 vs 51.5 nm, PdI: 0.495 vs 0.597, at pH 6.8 and 5.8, respectively; Table 8.1). Also, the relative abundance of smaller size PHF nanoparticles was reduced by the decrease in pH of YPD medium (2.2% and 0.1% at pH 6.8 and pH 5.8, respectively; Table 8.1). This suggests that nanoparticle agglomeration increased with decreasing pH probably due to interactions between components of the medium and nanoparticles and/or self-agglomeration.

Table 8.1 Characterization of PHF nanoparticles in stock suspension and culture media by dynamic light scattering (size distribution by intensity)

Sample	pH	PdI	Peak 1		Peak 2		Peak 3	
			Mean size (d.nm)	Area intensity (%)	Mean size (d.nm)	Area intensity (%)	Mean size (d.nm)	Area intensity (%)
PHF in YPD	5.8	0.597	210.5	92.5	51.5	0.1	2.9	7.4
PHF in YPD	6.3	0.562	202.0	92.8	48.1	1	1.6	6.2
PHF in YPD	6.8	0.495	198.3	93.1	43.6	2.2	1.6	4.7

d.nm: diameter in nanometer unit. PdI: polydispersity index. YPD: yeast peptone dextrose liquid medium.

8.3.2. Interactions between Cd and PHF nanoparticles in YPD medium

The presence of PHF nanoparticles and Cd ions in YPD medium was confirmed by SEM-EDX (Fig. 8.1A-C). A peak of C and an increased peak of O, compared to YPD medium without PHF, confirmed the presence of PHF nanoparticles in the medium (Fig. 8.1A and Fig. 8.1C vs Fig. 8.1B). Analysis of the YPD medium supplemented with $CdCl_2$ showed peaks of Cd and Cl (Fig. 8.1B). When the YPD medium was supplemented with Cd and PHF, peaks of C, O, Cd and Cl were detected (Fig. 8.1C). Under these conditions, instead of self-agglomeration, nanoparticles of PHF interacted with Cd and Cl by keeping these elements arrested and surrounded by PHF nanoparticles, which formed crossed-links with other Cd or Cl crystals (Fig. 8.1C). Additional elements were detected by EDX in all samples (Fig. 8.1), and they were probably originated from the glass slides and culture medium (Na, Mg, Si, Ca, O) or coating (Au) during sample preparation because these elements were also found in the absence of PHF or Cd (not shown).

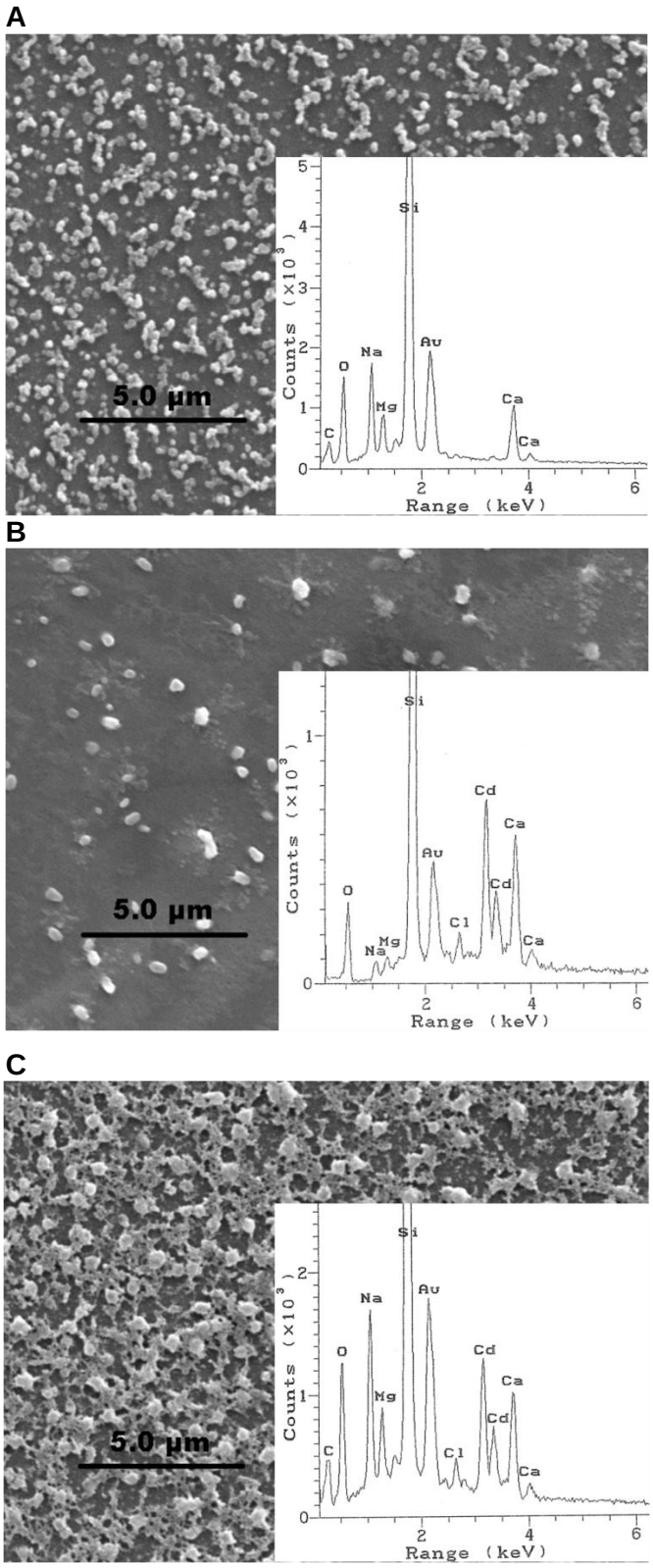

Figure 8.1 SEM and EDX microanalysis (insight) of YPD medium (pH 6.3) containing 500 mg L^{-1} of PHF (A), 5 mg L^{-1} of Cd (B) or mixture of 5 mg L^{-1} of Cd and 500 mg L^{-1} of PHF (C) after 26 h of incubation, at 26 ºC, under shaking in the absence of yeast cells.

8.3.3. Effects of PHF and Cd on yeast growth

In the absence of Cd and PHF, yeast growth was not affected by pH between 5.8 and 6.8 for 14 h (*P>0.05*, Fig. 8.2A) and 26 h (*P>0.05*, Fig. 8.2B). In the absence of Cd, PHF had a stimulatory effect on the yeast growth (two-way ANOVAs, *P<0.05*; Fig. 8.2A and B). The exposure to the highest PHF concentration (500 mg L^{-1}) for 14 h stimulated yeast growth by 6.1% and 7.0% at pH 6.3 and 6.8, respectively (*P<0.05*, Fig. 8.2A). After 26 h, growth was stimulated (6.9-10.3%) by exposure to 250 mg L^{-1} of PHF at higher pH and to the highest PHF concentration at all pH values (*P<0.05*, Fig. 8.2B).

The exposure to Cd alone inhibited the yeast growth, and the effects were stronger at higher pH and Cd concentration (two-way ANOVAs, *P<0.05*). At pH 5.8 and shorter exposure time, 1.5 mg L^{-1} of Cd reduced growth to 76.0% (Fig. 8.2C) while 5 mg L^{-1} of Cd restricted growth to 34.2% (Fig. 8.2E). Stronger inhibition of yeast growth was found at pH 6.8 after 26 h, where growth was reduced to 64.5% at lower Cd concentration (Fig. 8.2D) and to 20.3% at higher Cd concentration (Fig. 8.2F).

The presence of PHF attenuated Cd inhibitory effects on yeast growth: Cd effects were less pronounced at higher PHF concentrations and pH (two-way ANOVAs, *P<0.05*; Fig. 8.2C-F). Growth recovery from exposure to the lower Cd concentration and 500 mg L^{-1} of PHF was 28.4% after 26 h at pH 6.8 (Fig. 8.2D). At this PHF concentration and pH, growth recovery from exposure to 5 mg L^{-1} of Cd was 49.8% and 53.8% after 14 h (Fig. 8.2E) and 26 h (Fig. 8.2F), respectively.

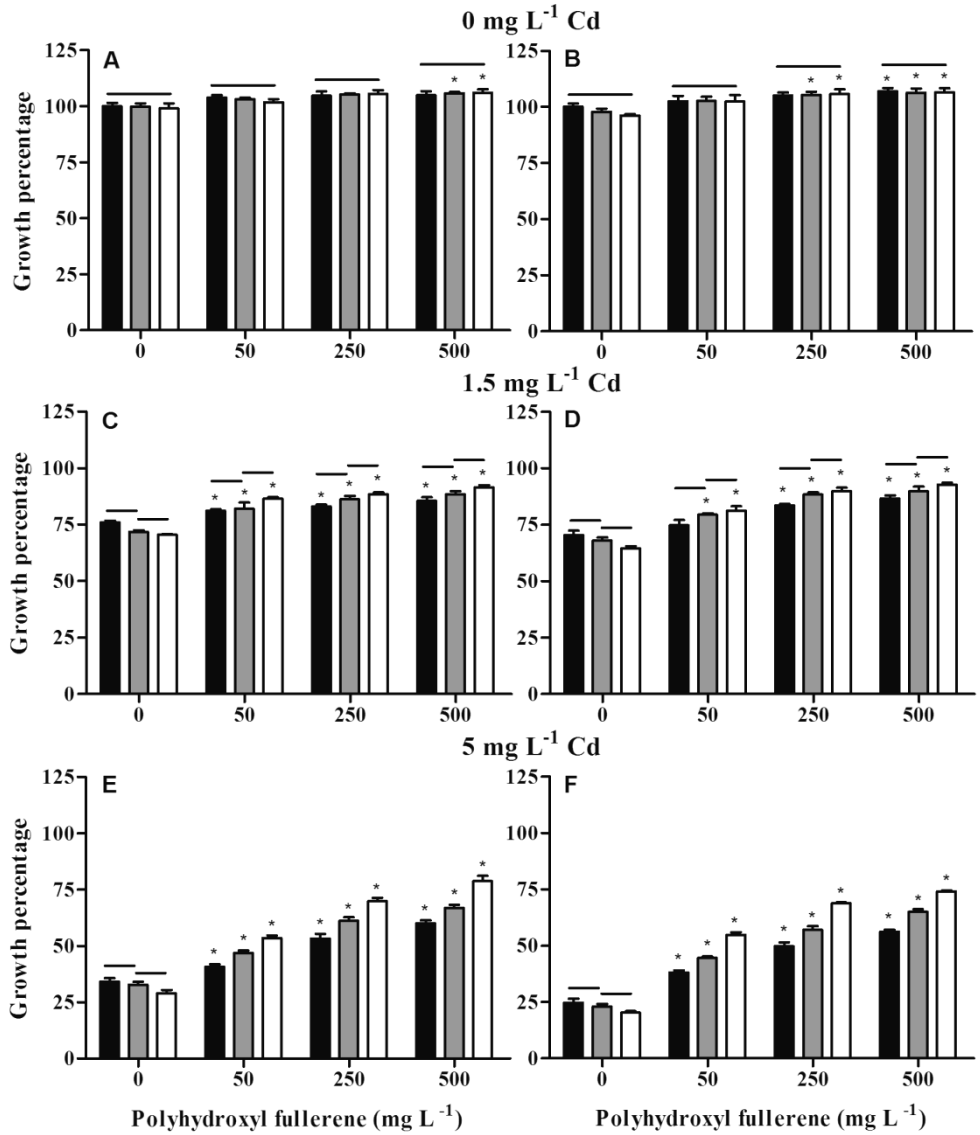

Figure 8.2 Effects of increasing concentrations of PHF on the growth of *S. cerevisiae* PYCC 4072 in the absence (A, B) and presence of 1.5 mg L^{-1} of Cd (C, D) or 5 mg L^{-1} of Cd (E, F) after 14 h (A, C, E) and 26 h (B, D, F) at pH 5.8 (black bar), pH 6.3 (grey bar) and pH 6.8 (white bar). Data are expressed are percentage of growth in the absence of PHF and Cd. Mean ± SEM, n=3. *, treatments that differ significantly from the respective control (Bonferroni tests, *P<0.05*). Horizontal line indicates no significant differences between pH treatments.

8.3.4. Effects of PHF and Cd on cell morphology

Comparing to the control, the exposure of yeasts to PHF did not lead to any morphological alteration of cells as shown by SEM (Fig. 8.3A vs Fig. 8.3B). By contrast, the exposure to Cd induced remarkable cell morphological alterations, such as cell shrinkage and degeneration (Fig. 8.3C). The co-exposure to Cd and

PHF led to minor morphological alterations in just a few number of yeast cells (Fig. 8.3D).

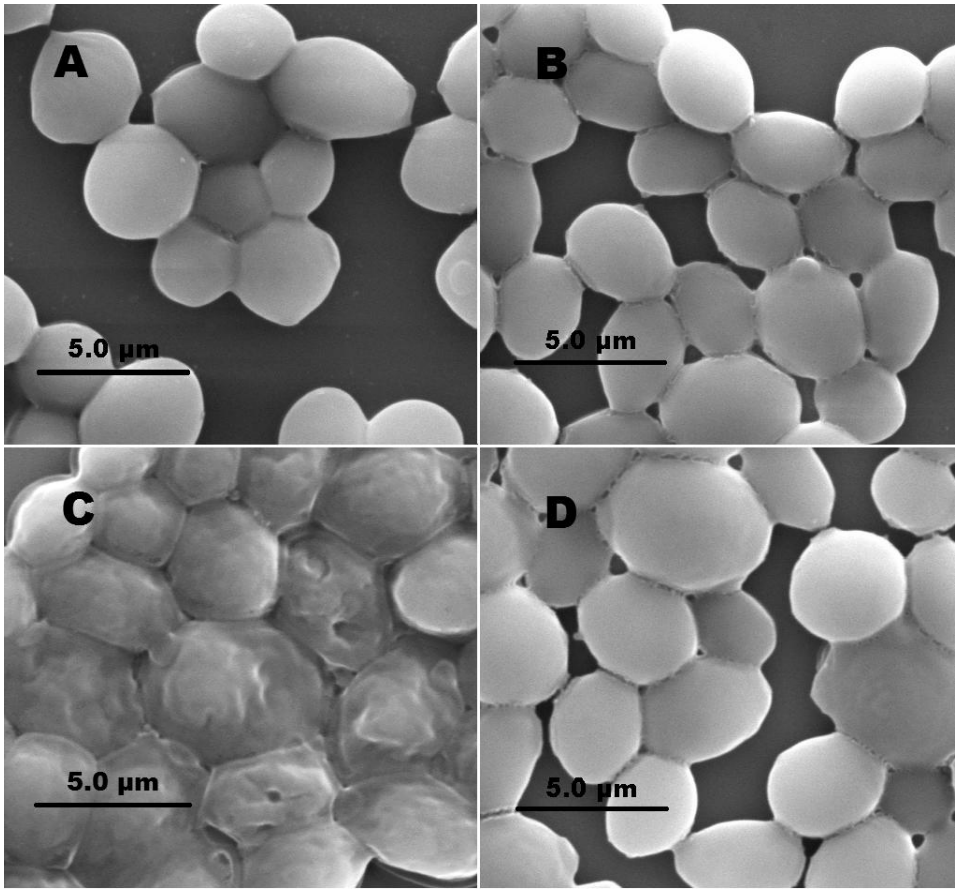

Figure 8.3 SEM visualization of cells of *S. cerevisiae* PYCC 4072 grown for 26 h in YPD medium at pH 6.3 in the absence of PHF and Cd (A), in the presence of 500 mg L^{-1} of PHF (B), in the presence of 5 mg L^{-1} of Cd (C) or in presence of both PHF and Cd (D).

8.3.5. Effects of PHF and Cd on plasma membrane integrity

In the absence of PHF and Cd, yeast cells did not show plasma membrane disruption as indicated by the absence of red fluorescence after PI staining under epifluorescence microscopy (Fig. 8.4A and B panel I); under these conditions, cell nuclei were localized by the blue fluorescence after DAPI staining. Results from flow cytometry showed that maximum number of yeast cells with plasma membrane disruption was low (≤ 1.4%) after 14 h and 26 h, at all tested pH (Fig. 8.5A and B). The number of PI-positive cells decreased with increasing PHF concentration (two-way ANOVAs, $P<0.05$; Fig. 8.5A and B).

Cadmium led to plasma membrane disruption as revealed by the presence of red fluorescence in cells (Fig. 8.4A and B panels II and III), and the effects increased with increasing Cd concentrations and pH (two-way ANOVAs, *P<0.05*; Fig. 8.5C-F). At pH 5.8, the exposure to 1.5 mg L^{-1} of Cd led to 8.5% and 11.6% of PI positive cells after 14 h and 26 h, respectively (Fig. 8.5C and D). At pH 6.8, the exposure to the lower Cd concentration led to 10.9% (14 h) and 13.8% (26 h) of PI positive cells, while exposure to the higher concentration of Cd increased the percentage of PI positive cells to 24.9% and 38.1%, after 14 h and 26 h, respectively.

Plasma membrane disruption induced by Cd was reduced when yeast cells were co-exposed to PHF as shown by a decrease in cell red fluorescence (Fig. 8.4A and B panels V and VI). The level of plasma membrane disruption induced by Cd depended on PHF concentration and pH (two-way ANOVAs, *P<0.05*; Fig. 8.5C-F). The maximum reduction in the number of PI-positive cells was found after co-exposure for 26 h to the highest concentrations of PHF and Cd, at the highest pH, and corresponded to a decrease of 30.7% in PI-positive cells compared to cells exposed only to Cd (Fig. 8.5F, *P<0.05*).

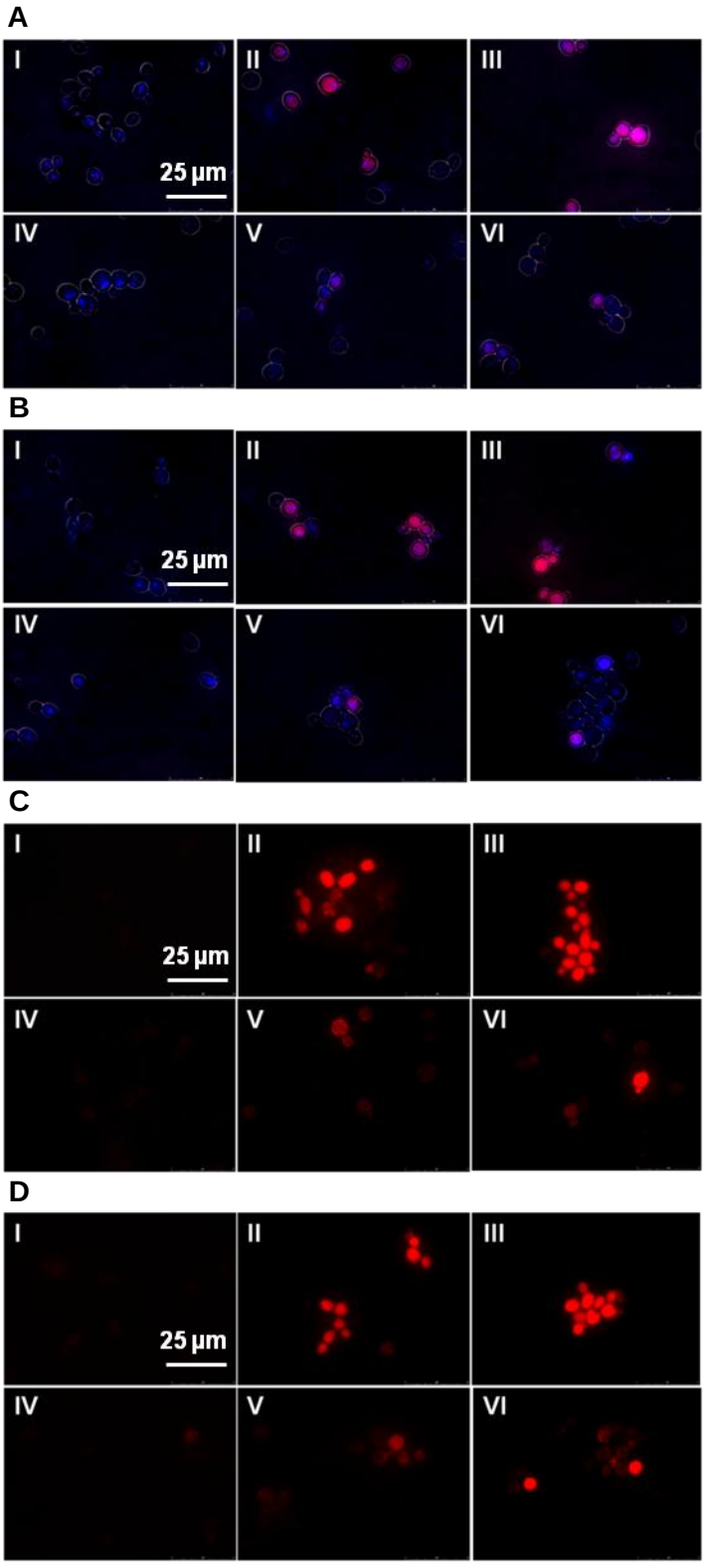

Figure 8.4 Epifluorescence microscopic visualization of plasma membrane integrity after PI and DAPI staining (A, B) and ROS accumulation after Mito-Tracker Red CM-H_2XRos staining (C, D) in cells of *S. cerevisiae* PYCC 4072 exposed for 14 h (A, C) and 26 h (B, D) to Cd at 0 (I), 1.5 (II) and 5 (III) mg L^{-1} in the absence of PHF, or to Cd at 0 (IV), 1.5 (V) and 5 (VI) mg L^{-1} in the presence of 500 mg L^{-1} PHF at pH 5.8.

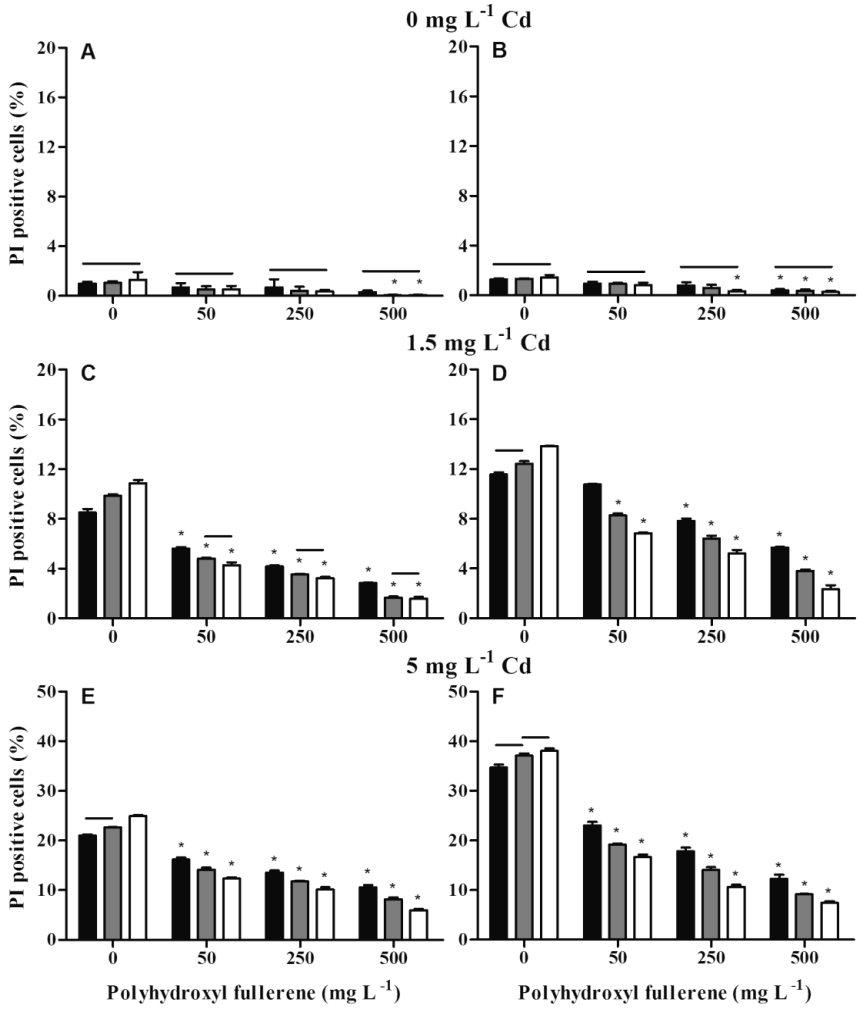

Figure 8.5 Effects of PHF on plasma membrane disruption of cells of *S. cerevisiae* PYCC 4072 assessed by PI staining in the absence (A, B) and presence of 1.5 mg L^{-1} of Cd (C, D) or 5 mg L^{-1} of Cd (E, F) after 14 h (A, C, E) and 26 h (B, D, F) at pH 5.8 (black bars), pH 6.3 (grey bars) and pH 6.8 (white bars). Mean ± SEM, n=3. *, treatments that differ significantly from control (Bonferroni tests, *P<0.05*). Horizontal line indicates no significant differences between pH treatments.

8.3.6. Effects of PHF and Cd on ROS accumulation

Epifluorescence microscopic analysis of yeast cells did not show ROS accumulation in the absence of Cd as indicated by the absence of red fluorescence after MitoTracker Red CM-H_2XRos staining (pH 5.8; Fig. 8.4C and D panel I). Consistently, results from flow cytometry showed that less than 2.9% of yeast cells unexposed to Cd had intracellular ROS accumulation at pH ranging from 5.8 to 6.8 (Fig 8.6A and B). In addition, the exposure to increasing PHF concentrations reduced ROS accumulation (two-way ANOVAs, *P<0.05*).

The exposure to Cd increased ROS accumulation in yeast cells (Fig. 8.4C and D panels II and III) in a dose- and pH-dependent manner (two-way ANOVAs, *P<0.05*; Fig. 8.6C-F). The highest number of cells showing ROS accumulation (44.1%) was detected after 26 h of exposure to 5 mg L^{-1} of Cd at pH 6.8 (Fig. 8.6F). The presence of PHF diminished the intracellular accumulation of ROS induced by Cd (Fig. 8.4C and D panels V and VI) and this mitigating effect increased with increasing PHF concentration and pH (two-way ANOVAs, *P<0.05*; Fig. 8.6C-F). The co-exposure to the highest concentrations of PHF and Cd, at pH 6.8, led to 6.3% and 7.4% of ROS-positive cells after 14 h and 26 h, respectively (Fig. 8.6E and F). This indicates that the presence of PHF decreased up to 36.7% the number of cells with ROS accumulation induced by Cd exposure.

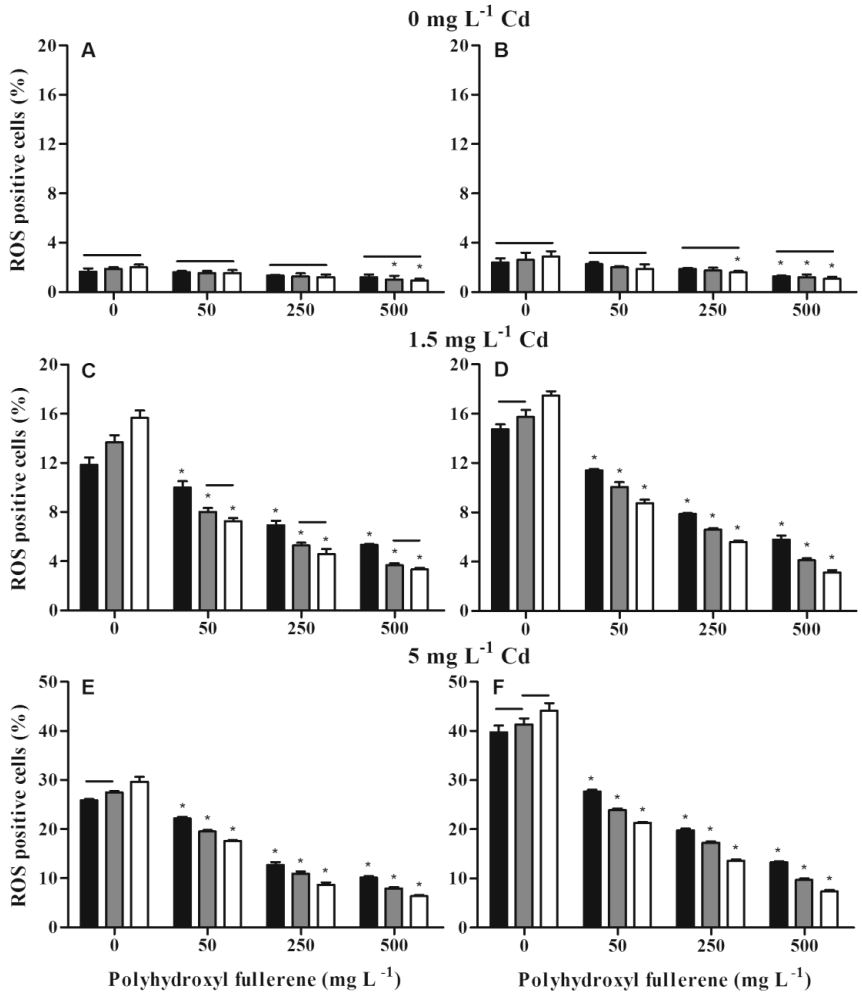

Figure 8.6 Effects of PHF on reactive oxygen species accumulation in cells of *S. cerevisiae* PYCC 4072 detected by MitoTracker Red CM-H_2XRos staining in the absence (A, B) and presence of 1.5 mg L^{-1} of Cd (C, D) or 5 mg L^{-1} of Cd (E, F) after 14 h (A, C, E) and 26 h (B, D, F) at pH 5.8 (black bars), pH 6.3 (grey bars) and pH 6.8 (white bars). Mean ± SEM, n=3. *, treatments that differ significantly from control (Bonferroni tests, *P<0.05*). Horizontal line indicates no significant differences between pH treatments.

8.4. Discussion

Although cytotoxicity of the functionalized carbon nanomaterial PHF has been reported (Xu et al., 2009; Johnson-Lyles et al., 2010; Wielgus et al., 2010), several studies have highlighted its non-toxic nature and ROS quenching properties in biological systems (Lai et al., 2000; Injac et al., 2008b; Vávrová et al., 2012). Here, we used the yeast *S. cerevisiae* as an eukaryotic model system to confirm that Cd induce oxidative stress, as shown by others (Brennan and Schiestl, 1996; Valko et al., 2006), and to provide the first evidence that PHF is able to mitigate the stress induced by metals. Similarly to that shown by other authors (Pasternakiewicz, 2006; Oliveira et al., 2012), we found that Cd inhibited the growth of *S. cerevisiae* in a dose-dependent manner. Cd effects on yeast growth became stronger at the longer exposure time (26 h), probably due to an increase in Cd uptake (Blackwell and Tobin, 1999). In our study, the negative effects of Cd on yeast growth also increased with pH from 5.8 to 6.8. In the absence of other interfering factors, the uptake of Cd by this yeast is reported to be ca. 2 times higher at pH 6.0 than at pH 5.0, probably because at lower pH the affinity of protons for binding sites on the yeast is much higher than that of metal ions (Mapolelo and Torto, 2004). Therefore, the increase in Cd toxicity with pH in our study may be related to pH dependent Cd uptake by the yeast.

Cadmium leads to oxidative injury in cells of living organisms due to intracellular accumulation of ROS (microbes: Chen et al., 1995; Choi, 2009, plants: Vestena et al., 2011, animals: Brennan and Schiestl, 1996; Valko et al., 2006, and humans: Oh and Lim, 2006). Consistently, we found that Cd induced ROS accumulation and plasma membrane disruption in cells of *S. cerevisiae* in a dose- and time-dependent manner. The more pronounced effects of Cd on plasma membrane integrity and ROS accumulation at higher pH may be related to the effects of pH on the magnitude of metal uptake by the yeast cells (see above). Moreover, results suggested that not all cells with ROS accumulation had lost their membrane integrity because the number of cells with plasma membrane disrupted (PI-positive cells) was slightly lower than that of ROS-positive cells, with differences up to 6.1% (26 h) at pH 6.8.

The exact mechanism of Cd toxicity is not fully understood yet, but most probably Cd cytotoxicity is the combination of i) apoptotic death by increased ROS accumulation saturating the antioxidant systems with mitochondrial membrane

dysfunction, and ii) membrane lipid peroxidation promoted by ROS accumulation that leads to plasma membrane permeabilization and necrotic death (Howlett and Avery, 1997; Sokolova et al., 2004; López et al., 2006; Kroemer et al., 2007). Our findings support that Cd toxicity to the yeast *S. cerevisiae* was related to oxidative stress via intracellular ROS accumulation and/or via plasma membrane disruption, which might be due to lipid peroxidation. In addition, SEM analysis showed that Cd induced alterations of cell morphology with evidence of cell shrinkage and degeneration. Thus, overall Cd-mediated toxicity might have involved apoptotic and/or necrotic cell death of *S. cerevisiae*. However, further studies are still needed to clarify this aspect.

In the absence of Cd, PHF had a stimulatory effect on the growth of *S. cerevisiae*; this agrees with studies reporting that these nanoparticles can be beneficial for the growth of many organisms including fungi (Gao et al., 2011). White rot fungi are capable of mineralising PHF and to incorporate minor amounts of carbon from PHF into biomass (Schreiner et al., 2009). We also found that PHF nanoparticles can be used as sole carbon source by the *S. cerevisiae*; however, yeast growth in mineral medium with vitamins and oligoelements supplemented with PHF (200 mg L^{-1}) was almost 7-fold lower than in YPD (20 mg L^{-1} of dextrose) (unpublished data). These findings contrast to the reported harmful impacts of other nanoparticles, including fullerene, to biota (Sayes et al., 2004; Handy et al., 2008; Pradhan et al., 2011; Pradhan et al., 2012). Comparing to the pristine fullerene (C_{60}), the functionalized surface of PHF leads to a lower ability to penetrate lipid bilayers of cell membranes, probably explaining the non-toxic nature of PHF (Qiao et al., 2007).

In our study, the co-exposure of *S. cerevisiae* to PHF nanoparticles and Cd decreased the number of cells with i) intracellular ROS accumulation, ii) plasma membrane disruption and iii) altered morphology, comparing to cells exposed to Cd alone. Moreover, the ability of PHF to mitigate Cd toxicity increased with nanoparticle concentration. These effects were consistent with the attenuated negative effects of Cd on yeast growth in the presence of PHF and indicate that PHF can protect yeast cells against metal-induced oxidative stress. PHF by reducing the levels of intracellular ROS may stabilize mitochondrial membrane potential and prevent mitochondrial dysfunction (Cai et al., 2008; Partha and Conyers, 2009), a common manifestation of Cd-induced oxidative stress that leads to apoptosis. Also, PHF can prevent oxidation of polyunsaturated fatty acid in

liposomes and lipid peroxidation (Mirkov et al., 2004). However, the mechanisms underlying the antioxidative properties of PHF nanoparticles are still unclear. Đorđević and Bogdanović (2008) explained the PHF antioxidant properties by two possible mechanisms i) an addition reaction of hydroxyl radicals (·OH, 2n) to the olefinic double bonds of PHF core and/or ii) a removal of a hydrogen from PHF by hydroxyl radical. In our study, complementarily to the antioxidative function of PHF, extracellular physicochemical interactions between PHF nanoparticles and Cd might have reduced the bioavailability of Cd to yeast cells. Indeed, SEM-EDX analysis showed that, in the extracellular medium, Cd ions were surrounded by PHF nanoparticles. This suggests that PHF nanoparticles, via interactions with their surface functionalized hydroxyl groups, could trap Cd while still having an opening face for interacting with yeast cells. In addition, the more pronounced decrease in Cd toxicity promoted by PHF at higher pH was probably due to greater availability of unbound and/or non-aggregated PHF nanoparticles with unmasked hydroxyl groups to encounter with Cd ions, as disclosed by the shift in nanoparticle size distribution towards lower size-range and PdI at higher pH (Table 8.1). Thus, pH can be a crucial factor for the stability and availability of PHF nanoparticles to the yeast cells.

Overall, this study provided the first evidence that PHF nanoparticles can play a role against metal toxicity in biological systems. Results show that PHF nanoparticles mitigated Cd effects by protecting cells against oxidative stress, as revealed by a decrease in intracellular ROS accumulation and in the number of cells with altered morphology and plasma membrane disruption (Fig. 8.7). The protective role of PHF against Cd-induced oxidative stress was pH-, dose- and time-dependent: effects were more pronounced at elevated pH and longest exposure time. In the absence of Cd, the stimulatory effect of PHF on yeast growth supported that PHF nanoparticles can be use as carbon and/or energy source. Results also suggest that extracellular physicochemical interactions between PHF nanoparticles and Cd might have occurred reducing Cd bioavailability to yeast cells. The ability of PHF nanoparticles to interact with metals opens new perspectives for the development of remediation strategies.

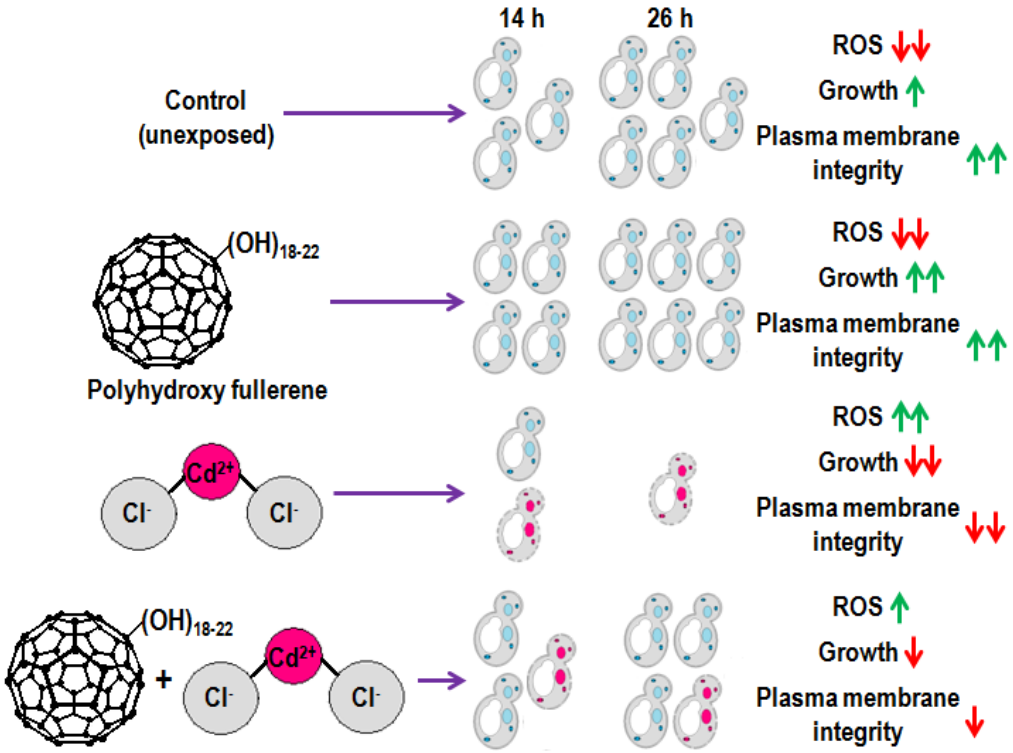

Figure 8.7 Diagrammatic representations of the overall major impacts of PHF nanoparticles on *S. cerevisiae.*

References

Adamis PDB, Panek AD, Leite SGF, Eleutherio ECA, 2003. Factors involved with cadmium absorption by wild-type strain of *Saccharomyces cerevisiae*. Braz J Microbiol 34, 55–60.

Allen SA, Clark W, McCaffery JM, Cai Z, Lanctot A, Slininger PJ, Liu ZL, Gorsich SW, 2011. Furfural induces reactive oxygen species accumulation and cellular damage in *Saccharomyces cerevisiae*. Biotechnol Biofuels 3:2, pp 10; DOI 10.1186/1754-6834-3-2.

Anagnostopoulos VA, Symeopoulos BD, Soupioni MJ, 2010. Effect of growth conditions on biosorption of cadmium and copper by yeast cells. Global NEST J 12, 288–295.

Anderson R, Barron AR, 2005. Reaction of hydroxyfullerene with metal salts: A route to remediation and immobilization. J Am Chem Soc 127, 10458–10459.

Ayres RU, 1992. Toxic heavy metals: Materials cycle optimization. Proc Natl Acad Sci 89, 815–820.

Blackwell KJ, Tobin JM, 1999. Cadmium accumulation and its effects on intracellular ion pools in a brewing strain of *Saccharomyces cerevisiae*. J Ind Microbiol Biotechnol 23, 204–208.

Bosi S, Da Ros T, Spalluto G, Prato M, 2003. Fullerene derivatives: an attractive tool for biological applications. Eur J Med Chem 38, 913–923.

Brennan RJ, Schiestl RH, 1996. Cadmium is an inducer of oxidative stress in yeast. Mutat Res 356, 171–178.

Cai X, Jia H, Liu Z, Hou B, Luo C, Feng Z, Li W, Liu J, 2008. Polyhydroxylated fullerene derivative $C_{60}(OH)_{24}$ prevents mitochondrial dysfunction and oxidative damage in an MPP^+-induced cellular model of Parkinson's disease. J Neurosci Res 86, 3622–3634.

Casalino E, Sblano C, Landriscina C, 1997. Enzyme activity alteration by cadmium administration to rats: the possibility of iron involvement in lipid peroxidation. Arch Biochem Biophys 346, 171–179.

Chen T, Li W, Schulz PJ, Furst A, Chien PK, 1995. Induction of peroxisome proliferation and increase of catalase activity in yeast, *Candida albicans*, by cadmium. Biol Trace Elem Res 50, 125–133.

Chen YW, Hwang KC, Yen CC, Lai YL, 2004. Fullerene derivatives protect against oxidative stress in RAW 264.7 cells and ischemia-reperfused lungs. Am J Physiol Regul Integr Comp Physiol 287, R21–R26.

Chevtzoff C, Yoboue ED, Galinier A, Casteilla L, Daignan-Fornier B, Rigoulet M, Devin A, 2010. Reactive oxygen species-mediated regulation of mitochondrial biogenesis in the yeast *Saccharomyces cerevisiae*. J Biol Chem 285, 1733–1742.

Choi J, 2009. Adsorption, bioavailability, and toxicity of cadmium to soil microorganisms. Geomicrobiol J 26, 248–255.

Da Ros T, Spalluto G, Prato M, 2001. Biological applications of fullerene derivatives: a brief overview. Croat Chem Acta (CCACAA) 74, 743–755.

Đorđević A, Bogdanović, G, 2008. Fullerenol - a new nanopharmaceutic? Arch Oncol 16, 42–45.

Dugan LL, Gabrielsen JK, Yu SP, Lin TS, Choi DW, 1996. Buckminsterfullerenol free radical scavengers reduce excitotoxic and apoptotic death of cultured cortical neurons. Neurobiol Dis 3, 129–135.

Gao J, Wang Y, Folta KM, Krishna V, Bai W, Indeglia P, Georgieva A, Nakamura H, Koopman B, Moudgil B, 2011. Polyhydroxy fullerenes (fullerols or fullerenols): beneficial effects on growth and lifespan in diverse biological models. PLoS One 6, e19976, pp 8.

Handy RD, Owen R, Valsami-Jones E, 2008. The ecotoxicology of nanoparticles and nanomaterials: current status, knowledge gaps, challenges, and future needs. Ecotoxicology 17, 315–325.

Hassellöv M, Readman JW, Ranville JF, Tiede K, 2008. Nanoparticle analysis and characterization methodologies in environmental risk assessment of engineered nanoparticles. Ecotoxicology 17, 344–361.

Howlett NG, Avery SV, 1997. Relationship between cadmium sensitivity and degree of plasma membrane fatty acid unsaturation in *Saccharomyces cerevisiae*. Appl Microbiol Biotechnol 48, 539–545.

Injac R, Perse M, Obermajer N, Djordjevic-Milic V, Prijatelj M, Djordjevic A, Cerar A, Strukelj B, 2008a. Potential hepatoprotective effects of fullerenol $C_{60}(OH)_{24}$ in doxorubicin-induced hepatotoxicity in rats with mammary carcinomas. Biomaterials 29, 3451–3460.

Injac R, Radic N, Govedarica B, Djordjevic A, Strukelj B, 2008b. Bioapplication and activity of fullerenol $C_{60}(OH)_{24}$. Afr J Biotechnol 7, 4940–4050.

Johnson-Lyles DN, Peifley K, Lockett S, Neun BW, Hansen M, Clogston J, Stern ST, McNeil SE, 2010. Fullerenol cytotoxicity in kidney cells is associated with cytoskeleton disruption, autophagic vacuole accumulation, and mitochondrial dysfunction. Toxicol Appl Pharmacol 248, 249–258.

Krishna V, Singh A, Sharma P, Iwakuma N, Wang Q, Zhang Q, Knapik J, Jiang H, Grobmyer SR, Koopman B, Moudgil B, 2010. Polyhydroxy fullerenes for non-invasive cancer imaging and therapy. Small 6, 2236–2241.

Kroemer G, Galluzzi L, Brenner C, 2007. Mitochondrial membrane permeabilization in cell death. Physiol Rev 87, 99–163.

Lai HS, Chen WJ, Chiang LY, 2000. Free radical scavenging activity of fullerenol on the ischemia-reperfusion intestine in dogs. World J Surg 24, 450–454.

Landolfo S, Politi H, Angelozzi D, Mannazzu I, 2008. ROS accumulation and oxidative damage to cell structures in *Saccharomyces cerevisiae* wine strains during fermentation of high-sugar-containing medium. Biochim Biophys Acta 1780, 892–898.

Lee K, Ueom J, 2001. Protection of metal stress in *Saccharomyces cerevisiae*: cadmium tolerance requires the presence of two ATP-binding domains of Hsp104 protein. Bull Korean Chem Soc 22, 514–518.

Liu J, Zhang Y, Huang D, Song G, 2005. Cadmium induced MTs synthesis via oxidative stress in yeast *Saccharomyces cerevisiae*. Mol Cell Biochem 280, 139–145.

López E, Arce C, Oset-Gasque MJ, Cañadas S, González MP, 2006. Cadmium induces reactive oxygen species generation and lipid peroxidation in cortical neurons in culture. Free Radic Biol Med 40, 940–951.

Mapolelo M, Torto N, 2004. Trace enrichment of metal ions in aquatic environments by *Saccharomyces cerevisiae*. Talanta 64, 39–47.

Mendes-Ferreira A, Sampaio-Marques B, Barbosa C, Rodrigues F, Costa V, Mendes-Faia A, Ludovico P, Leão C, 2010. Accumulation of non-superoxide anion reactive oxygen species mediates nitrogen-limited alcoholic fermentation by *Saccharomyces cerevisiae*. Appl Environ Microbiol 76, 7918–7924.

Mirkov SM, Djordjevic AN, Andric NL, Andric SA, Kostic TS, Bogdanovic GM, Vojinovic-Miloradov MB, Kovacevic RZ, 2004. Nitric oxide-scavenging activity of polyhydroxylated fullerenol, $C_{60}(OH)_{24}$. Nitric Oxide 11, 201–207.

Muthukumar K, Nachiappan V, 2010. Cadmium-induced oxidative stress in *Saccharomyces cerevisiae*. Indian J Biochem Biophys 47, 383–387.

Nweke CO, 2010. Effects of metals on dehydrogenase activity and glucose utilization by *Saccharomyces cerevisiae*. Nig J Biochem Mol Biol 25, 28–35.

Oberdörster E, Zhu S, Blickley TM, McClellan-Green P, Haasch ML, 2006. Ecotoxicology of carbon-based engineered nanoparticles: effects of fullerene (C_{60}) on aquatic organisms. Carbon 44, 1112–1120.

OECD, 2010. Guidance manual for the testing of manufactured nanomaterials: OECD's sponsorship programme, ENV/JM/MONO(2009)20REV; OECD environment, health and safety publications, series on the safety of manufactured nanomaterials No. 25; Organisation for economic co-operation and development: Paris.

Oh SH, Lim SC, 2006. A rapid and transient ROS generation by cadmium triggers apoptosis via caspase-dependent pathway in HepG2 cells and this is inhibited through N-acetylcysteine-mediated catalase upregulation. Toxicol Appl Pharmacol 212, 212–223.

Oliveira RP, Basso LC, Junior AP, Penna TC, Del Borghi M, Converti A, 2012. Response of *Saccharomyces cerevisiae* to cadmium and nickel stress: the use of the sugar cane vinasse as a potential mitigator. Biol Trace Elem Res 145, 71–80.

Partha R, Conyers JL, 2009. Biomedical applications of functionalized fullerene-based nanomaterials. Int J Nanomedicine 4, 261–275.

Pasternakiewicz A, 2006. The growth of *Saccharomyces cerevisiae* yeast in cadmium enriched media. Acta Sci Pol Technol Aliment 5, 39–46.

Pathak N, Khandelwal S, 2006. Oxidative stress and apoptotic changes in murine splenocytes exposed to cadmium. Toxicology 220, 26–36.

Pickering KD, Wiesner MR, 2005. Fulelrenol-sensitized production of reactive oxygen species in aqueous solution. Environ Sci Technol 39, 1359–1365.

Pradhan A, Seena S, Pascoal C, Cássio F, 2011. Can metal nanoparticles be a threat to microbial decomposers of plant litter in streams? Microb Ecol 62, 58–68.

Pradhan A, Seena S, Pascoal C, Cássio F, 2012. Copper oxide nanoparticles can induce toxicity to the freshwater shredder *Allogamus ligonifer*. Chemosphere 89, 1142–1150.

Priault M, Camougrand N, Kinnally KW, Vallette FM, Manon S, 2003. Yeast as a tool to study Bax/mitochondrial interactions in cell death. FEMS Yeast Res 4, 15–27.

Price DJ, Joshi JG, 1983. Ferritin. Binding of beryllium and other divalent metal ions. J Biol Chem 258, 10873–10880.

Qiao R, Roberts AP, Mount AS, Klaine SJ, Ke PC, 2007. Translocation of C_{60} and its derivatives across a lipid bilayer. Nano Lett 7, 614–619.

Risso-de Faverney C, Orsini N, de Sousa G, Rahmani R, 2004. Cadmium-induced apoptosis through the mitochondrial pathway in rainbow trout hepatocytes: involvement of oxidative stress. Aquat Toxicol 69, 247–258.

Sayes CM, Fortner JD, Guo W, Lyon D, Boyd AM, Ausman KD, Tao YJ, Sitharaman B, Wilson LJ, Hughes JB, West JL, Colvin VL, 2004. The differential cytotoxicity of water-soluble fullerenes. Nano Lett 4, 1881–1887.

Schreiner KM, Filley TR, Blanchette RA, Bowen BB, Bolskar RD, Hockaday WC, Masiello CA, Raebiger JW, 2009. White-rot basidiomycete-mediated decomposition of C_{60} fullerol. Environ Sci Technol 43, 3162–3168.

Sokolova MI, Evans S, Hughes FM, 2004. Cadmium-induced apoptosis in oyster hemocytes involves disturbance of cellular energy balance but no mitochondrial permeability transition. J Exp Biol 207, 3369–3380.

Sugita M, Tsuchiya K, 1995. Estimation of variation among individuals of biological half-time of cadmium calculated from accumulation data. Environ Res 68, 31–37.

Tykhomyrov AA, Nedzvetsky VS, Klochkov VK, Andrievsky GV, 2008. Nanostructures of hydrated C_{60} fullerene (C_{60}HyFn) protect rat brain against alcohol impact and attenuate behavioral impairments of alcoholized animals. Toxicology 246, 158–165.

Valko M, Rhodes CJ, Moncol J, Izakovic M, Mazur M, 2006. Free radicals, metals and antioxidants in oxidative stress-induced cancer. Chem Biol Interact 160, 1–40.

Vávrová J, Řezáčová M, Pejchal J, 2012. Fullerene nanoparticles and their anti-oxidative effects: a comparison to other radioprotective agents. J Appl Biomed 10, 1–8.

Vestena S, Cambraia J, Ribeiro C, Oliveira JA, Oliva MA, 2011. Cadmium-induced oxidative stress and antioxidative enzyme response in water hyacinth and salvinia. Braz J Plant Physiol 23, 131–139.

Wang L, Xu T, Lei WW, Liu DM, Li YJ, Xuan RJ, Ma JJ, 2011. Cadmium-induced oxidative stress and apoptotic changes in the testis of freshwater crab, *Sinopotamon henanense*. PLoS One 6, e27853.

Wielgus AR, Zhao B, Chignell CF, Hu DN, Roberts JE, 2010. Phototoxicity and cytotoxicity of fullerol in human retinal pigment epithelial cells. Toxicol App Pharmacol 242, 79–90.

Xu JY, Han K, Li SX, Cheng JS, Xu GT, Li WX, Li QN, 2009. Pulmonary responses to polyhydroxylated fullerenols, $C_{60}(OH)_x$. J Appl Toxicol 29, 578–584.

Zar JH, 2009. Biostatistical analysis, 5th ed.; Prentice Hall: Upper Saddle River, New Jersey.

Zhao CD, Chen FR, Chen XR, Zhao HC, Xia WL, Nie HF, Kong M, Liu F, Yang K, 2008. Methodology of tracking source of cadmium anomalies and their quantitative estimation in the Yangtze River basin. Earth Sci Front 15, 179–194.

Chapter 9

General discussion and future perspectives

General discussion and future perspectives

Since the term “nanotechnology” has been coined (Taniguchi, 1974) and brought into the public domain (Drexler, 1986), an enormous nanomaterial-based research has been carried out with incredible advancements and huge commercial success (Salata 2004; Aitken et al., 2006). This brought the “nanoworld” to our daily life. The enhanced commercialization and usage of nanomaterial-based products (Perugini et al., 2002; Nel et al., 2006; Jin and Ye, 2007; Becheri et al., 2008; Luechinger et al., 2008; Kathirvelu et al., 2009) branched off to “nanotoxicology” due to the adverse toxic impacts of nanomaterials to a wide range of living organisms including humans (Buzea et al., 2007; Petica et al., 2008; Heinlaan et al., 2008). Due to extensive applications, nanomaterials are likely to be released into the environment, particularly in aquatic ecosystems, as they are the largest terminal repositories. Researchers are currently concerned about the fate and potential impacts of nanomaterials in the environment as these materials are known to cause adverse effects to living organisms due to their unusual physicochemical properties (Schrand et al., 2010). Thus, potential ecotoxicity of engineered nanomaterials is under the limelight of current research.

Some studies have reported the release of engineered nanoparticles into streams (e.g. Wigginton et al., 2007; Kaegi et al., 2008; Kim et al., 2010; Rezić, 2011) and this raised the question about the potential risk of nanoparticles against aquatic biota and the processes they drive (Moore, 2006; Christian et al., 2008; MacCormack and Goss, 2008; Sharma, 2009). A number of studies showed the adverse effects of nanoparticles, mostly metal-based nanoparticles, against living organisms (Reijnders, 2006; Gajjar et al., 2009), but there are only few studies assessing the impacts of these nanoparticles on aquatic biota (Blaise et al., 2008; Lee et al., 2009; Miller et al., 2010). Most studies on aquatic systems were performed with nanometals/nanometal oxides enlisted in the OECD (OECD, 2010) guideline manual representing the commercial engineered nanoparticles that currently require risk assessment and toxicity studies (Lovern et al., 2007; Van Hoecke et al., 2009; Zhu et al., 2008). However, most of the existing results are mainly individual-based responses of biota that are insufficient to predict the impacts on aquatic communities and the associated ecosystem processes.

In low order forested streams, where insufficient sunlight can penetrate the water, plant-litter decomposition is a key ecosystem process linking riparian

vegetation with the activities of aquatic microbial decomposers and invertebrate detritivores (Pascoal et al., 2003, 2005a). Aquatic fungi are the dominant microbial decomposers that play a major role in organic matter turnover and constitute a significant link in detritus food webs between plant-litter and stream invertebrates (Graça, 2001; Pascoal et al., 2003, 2005a), which in turn supply the basic diet to higher trophic levels (Suberkropp et al., 1983; Graça and Canhoto, 2006) such as fishes. Aquatic bacterial communities play an important role in the process after partial breakdown of plant-litter (Graça, 2001; Pascoal and Cássio, 2004). The process of litter decomposition is sensitive to water quality, and this integrative process was proposed as a functional measure for determining the health of freshwater ecosystems (Pascoal et al., 2001; Gessner and Chauvet, 2002; Pascoal et al., 2005a).

We investigated the effects of copper oxide (<50 nm) and silver (<100 nm) nanoparticles, two commercially used metal-based nanoparticles (Nair and Laurencin, 2007; Ren et al., 2009; Zhang et al., 2009), and their ionic precursors (Ag^{+} and Cu^{2+}) on leaf-litter decomposition by freshwater microbial communities (Chapter 2). The nano and ionic metals decreased leaf decomposition rate significantly and inhibited fungal biomass (up to 82.9% of control) and bacterial biomass (up to 96.5% of control) in a concentration- and time-dependent manner. We found that bacteria were more sensitive to nano metals than fungi as noted in earlier studies for metal ions (Duarte et al., 2008, 2009; Niyogi et al., 2002). Fungal sporulation rates seemed to be the most sensitive indicator of the stress induced by nanoparticles showing inhibitions from 91.0 to 99.4%. The adverse effects of the chemicals were also shown by a reduction in microbial diversity, and shifts in the structure of fungal and bacterial communities based on DNA fingerprints and fungal spore morphology. *Articulospora tetracladia* was the dominant species in control and under nano or ionic metal-exposure, while the co-dominant species in control, *Flagellospora* sp., was replaced by *Heliscus lugdunensis* under exposure conditions. In earlier studies, *A. tetracladia* and *H. lugdunensis* were reported to be present in metal-polluted streams and some strains were found to be resistant to high concentrations of metals (Braha et al., 2007; Jaeckel et al., 2005; Pascoal et al., 2005b). The shifts in the structure of microbial communities suggest a change towards a better-adapted community to maintain ecological functions under nano or ionic metal-induced stress. In addition, the impacts of metal nanoparticles on leaf decomposition by aquatic microbes were less pronounced when compared to their

ionic forms, although the applied concentrations of metal ions were about one order of magnitude lower than those of nanometals. This corroborates that ionic metals can be more toxic to aquatic organisms than nanometal counterparts (Heinlaan et al., 2008; Aruoja et al., 2009; Blinova et al., 2010).

The toxicity of nanometals in detritus freshwater ecosystems may depend on the intrinsic physicochemical properties of nanoparticles and on factors that alter those properties in aqueous environment. A key intrinsic property is the nanoparticle size whereas natural organic matter (NOM) is one of those key driving factors in the environment. NOM is present in freshwaters up to concentration of 100 mg L^{-1} (Wall and Choppin, 2003; Paul et al., 2006; Steinberg et al., 2006). Our follow up study was carried out to assess the individual or combined effects of size of copper oxide nanoparticles (12, 50 and 80 nm) and humic acid on microbial decomposers of plant-litter (Chapter 3). We used humic acid (HA) as a model of NOM due to its significant contribution to the constitution of NOM in freshwaters (Ma et al., 2001). The inhibitory effects of nanoCuO on leaf decomposition, bacterial and fungal biomass and fungal reproduction rate increased with the decrease in nanoparticle size and increase in nanoparticle concentration. This was supported by EC_{50} and LOEC values. Results also confirmed that bacterial communities were more sensitive to nanoCuO than fungal communities. Our findings were similar to those showing an increase in toxicity with a decrease in nanoparticle size (Van Hoecke et al., 2009; Hartmann et al., 2010). Indeed, SEM and DLS analyses revealed increased self-aggregation with ascending nanoparticle size confirming that differences in toxicity could be due to differences in nanoparticle surface areas. Some studies reported that NOM or HA can hinder the toxicity of ionic metals and nanometals/nanometal oxides in living cells and organisms (Erickson et al., 1996; De Schamphelaere et al., 2002; Fabrega et al., 2009; Chen et al., 2011; Li et al., 2011). A similar trend was observed in our study for lower size nanoparticles because HA alleviated the toxicity of nanoCuO with 12 and 50 nm, but not of larger nanoparticles. This suggests that the effect of NOM on nanoparticle toxicity depends on the reactive surface area of nanoparticles. We proposed that the role of HA in alleviating the toxicity of lower size nanoCuO was probably the consequence of a decrease in reactive surfaces by greater surface-masking of less self-aggregated and highly dispersed smaller nanoparticles in the presence of HA. Thus, HA formed a physical barrier between nanoparticle surface and biological tissues. In contrast, HA might not interact with larger size nanoCuO due to lesser dispersion and higher

self-aggregation of nanoparticles. Moreover, the possibility of a copper-dependent fungal extracellular enzyme-mediated degradation of unbound HA cannot be ignored. Conversely, HA has been reported to exhibit toxicity against many organisms including freshwater invertebrates (Hseu et al., 2002; Meems et al., 2004; Yang et al., 2004; Timofeyev et al., 2006) as also observed in our study in the absence of nanoCuO. The community shift under nanoCuO and/or HA stress showed the same trend observed in our previous experiment: the co-dominance of *A. tetracladia* and *H. lugdunensis* under stress, indicating the resistance/tolerance of these species towards nanoCuO and/or HA-induced stress.

To better understand the impacts of nanoparticles in detritus foodwebs, we selected invertebrate shredders as representative of the next trophic level. Shredders prefer to feed on plant-litter colonized by aquatic microbes, predominantly fungi, whose activity increases the food quality and palatability (Suberkropp et al., 1983). Shredders play an important role in detritus foodwebs in streams by further transferring the carbon and energy from decomposed plant-litter to higher trophic levels (Graça and Canhoto, 2006). Also, the invertebrates are important in ecotoxicological studies as they are abundant, globally distributed, have short life span with high reproduction rates, and are sensitive to contaminants and toxicants including heavy metals (e.g., De Schamphelaere et al., 2004; Gerhardt et al., 2004). Here we investigated the potential lethal and sublethal effects of nanoCuO (50 nm) on *Allogamus ligonifer* (Chapter 4), a common invertebrate shredder in Southwest European streams that prefers high quality water (Bonada et al., 2008). The acute lethal tests showed that the 96 h LC_{50} of nanoCuO was very high (569 mg L^{-1}), whereas the sublethal concentrations inhibited leaf consumption up to 47% and the invertebrate growth up to 46% after 10 days of exposure. In addition, the exposure to increased sublethal concentration of nanoCuO via water or pre-contaminated food led to higher accumulation of copper in the larval body. Leached water-soluble ionic copper from nano CuO adsorbed or accumulated in the shredder (up to 10.2% of total Cu) indicated its influence in the shredder feeding behaviour and growth. This agrees to some extent with previous studies suggesting the role of leached ions in the toxicity of nanometal oxides (Heinlaan et al., 2008; Aruoja et al., 2009; Kasemets et al., 2009; Mortimer et al., 2010).

In a follow up study, we assessed the sublethal impacts of nanoparticle size (12, 50 and 80 nm nanoCuO) and/or humic acid on the shredder *A. ligonifer* (Chapter 5). An increased reduction of invertebrate feeding behaviour was observed

after 5 days exposure to increasing concentrations of nanoCuO with decreasing size; leaf consumption rates were inhibited up to 83.4% under exposure to smaller size nanoparticles. HA alone inhibited the feeding rate up to 52.6%. Similar to the trend observed previously with microbial communities (Chapter 3), HA mitigated the inhibitory effects of lower size nanoCuO by recovering the feeding rate up to 29.6%, but HA did not attenuate the toxicity promoted by larger nanoparticles. This was probably a consequence of HA adsorption to the reactive surfaces of highly dispersed small nanoparticles, while the highly self-aggregated larger particles had comparatively less opening faces for HA adsorption. Thus, it is conceivable that in the presence of HA, the smaller size nanoparticles have lower chance to interact with leaves and invertebrates than larger nanoparticles. The post-exposure feeding experiment, where the animals were rescued from the stressors and further exposed to uncontaminated stream water and food, pointed to a very low recovery of invertebrate feeding rates. The post-exposure experiment tried to mimic accidental flash-exposure to nanoparticles in streams and was an important tool to assess the potential ability of shredders to recover from the stress. Shredders exposed previously to only HA or lower concentration of 80 nm nanoCuO recovered faster indicating conditions of lower stress. The effects were also supported by alterations in the amount and morphology of fine particulate organic matter (FPOM) produced. The presence of nanoCuO and/or HA were observed by SEM in the surface of FPOM even after the post-exposure experiment. Overall, nanoparticle size and HA could influence the sublethal toxicity of nanoCuO to freshwater invertebrate shredders as observed earlier for microbial decomposer communities.

Based on the differential responses to nanoCuO of aquatic fungal species within communities, we investigated the physiological response to nanoCuO-induced stress in four fungal populations collected from metal-polluted or non-polluted streams (Chapter 6). We found a stronger inhibition of fungal biomass (lower EC_{50} values), a clearer evidence of increased mycelium morphological alterations (e.g. shrinkage and degradation), and an increased adsorption of CuO nanoparticles in populations from non-polluted streams than in those from metal-polluted streams. The increased resistance of aquatic fungi from metal-polluted streams than fungi from non-polluted streams had also been reported for metal ions (Cu^{2+}, Azevedo et al., 2007; Cd, Miersch and Grancharov, 2008). In our study, the differences were more prominent after longer exposure time. The significant correlations between the inhibition of fungal biomass production and nanoparticulate

copper adsorbed to fungi or leached Cu^{2+} in the culture media suggested that both forms of copper contributed to the observed physiological effects.

Additionally, we assessed the activity of laccase, which is an extracellular multicopper-containing oxidoreductase enzyme that is involved in the degradation of lignin and various xenobiotic compounds (Durán et al., 2002; Brondani et al., 2009). This enzyme is produced by fungi, including those involved in litter decomposition in terrestrial (Steffen et al., 2002) and aquatic environments, and requires copper for their activity (Junghann et al., 2005, 2008). Interestingly, in our study, an increase in the laccase activity with increased nanoCuO concentration was observed in two out of the four tested fungi (*Phoma* sp. UHH 5-1-03 and *Clavariopsis aquatica* WD(A)-00-1). These fungi were previously reported to exhibit laccase activity under Cu^{2+} exposure (Junghann et al., 2005, 2008). The low activity of laccase in the other two fungal strains could be attributed to the absence of laccase-like gene fragments in the copper binding domain indicating low capability of integrating copper as cofactor for their activity.

For further understanding the resistance/tolerance of aquatic fungi to nanoCuO-induced stress, we investigated the ability of nanoCuO to promote oxidative stress, cellular damages, and changes in the antioxidant enzymatic responses in five aquatic fungi collected from metal-polluted or non-polluted streams (Chapter 7). We observed clear differences among fungi in the response to nanoCuO exposure. The exposure to nanoCuO led to higher intracellular reactive oxygen species (ROS) accumulation, plasma membrane disruption and DNA-strand breaks in fungi from non-polluted streams than in those from metal-polluted streams. Superoxide dismutase (SOD) is an antioxidant enzyme involved in early defence against ROS. The maintenance of high GSH (reduced glutathione) to GSSG (oxidised glutathione) ratio in cells is required to protect them against oxidative stress (Townsend et al., 2003); glutathione reductase (GR) is the key enzyme in ascorbate-glutathione cycle to keep the pool of glutathione in its reduced form (GSH), whereas glutathione peroxidise (GPx) interacts with free peroxides/hydroperoxides and converts GSH to GSSG (Townsend et al., 2003; Israr et al. 2006). Under metal-induced oxidative stress, the increase in glutathione pool is often observed in metal-tolerant fungi, including aquatic fungi from metal-polluted streams (Jaeckel et al., 2005; Braha et al., 2007). In our study, the activities of GR and SOD were higher in fungi from polluted streams than from non-polluted streams, although the opposite was found for GPx activity. Results suggested that

fungal populations from metal-polluted streams could have higher capacity to deal with the oxidative indicating higher tolerance/resistance to nanoCuO than those from non-polluted streams.

The increased nanoCuO-induced toxicity can result directly from nanoparticles or indirectly from intracellular dissolution of nanoparticles leading to accumulation of metal ions as demonstrated for nanoCu (Meng et al., 2007). Lysosomes mediate intracellular degradation of nanoCuO into Cu^{2+}, which is subsequently released into the cytoplasm where is reduced by $O_2^{\bullet -}$ to Cu^{+} (Petersen and Nelson, 2010). Ionic metals undergoing the redox and/or ascorbate-glutathione cycle can directly or indirectly cause an increase in intracellular ROS accumulation, cell membrane disruption and DNA damage in aquatic fungi (Azevedo et al., 2007, 2009). Therefore, in our study, the involvement of Cu^{2+} in the effects of nanoCuO on aquatic fungi cannot be discarded.

Similarly to metal-based nanoparticles, carbon-based nanoparticles, such as fullerene and functionalised fullerenes, also have applications in several fields in nanotechnology such as biomedical diagnostics and therapeutics (Da Ros et al., 2001; Bosi et al., 2003; Partha and Conyers, 2009). In contrast to the adverse effects of metal/metal oxide nanoparticles, the polyhydroxy fullerene (PHF), a functionalised derivative of fullerene, has been attracting much interest due to its reported non-toxic nature and ROS-quenching properties (Lai et al., 2000; Injac et al., 2008; Vávrová et al., 2012). PHF has an edge over fullerene in commercial or research applications because of its higher stability and solubility in aqueous solution due to the presence of hydroxyl groups. We investigated the interactive effects of PHF and cadmium (Cd) on the model yeast *Saccharomyces cerevisiae* at different pH (5.8-6.8) for 14h and 26h (Chapter 8). Yeasts are unicellular fungi found in several environments including streams, and *S. cerevisiae* is a well-known eukaryotic model system to study oxidative stress responses (Priault et al., 2003; Landolfo et al., 2008; Mendes-Ferreira et al., 2010). In the absence of Cd, PHF stimulated yeast growth up to 10.3% which agreed with previous reports showing that PHF can be beneficial for the growth of many organisms, including white rot fungi which are capable of incorporating minor amounts of C from PHF into biomass (Schreiner et al., 2009; Gao et al., 2011). Cadmium inhibited growth in a concentration-, time- and pH-dependent manner. However, the negative effects of Cd on the growth were attenuated by the presence of PHF with a maximum growth recovery (53.8%) at the highest PHF concentration, at pH 6.8, after 26 h. Cadmium

induced intracellular accumulation of ROS and plasma membrane disruption, but these effects were alleviated by the presence of PHF. Results indicated that PHF could stimulate the yeast growth and mitigate the oxidative stress induced by Cd.

The overall mechanisms of the impacts of nanoparticles (metal/metal oxides and carbon-based PHF) to fungal cells based on our studies and earlier reports are schematically represented in Fig. 9.1.

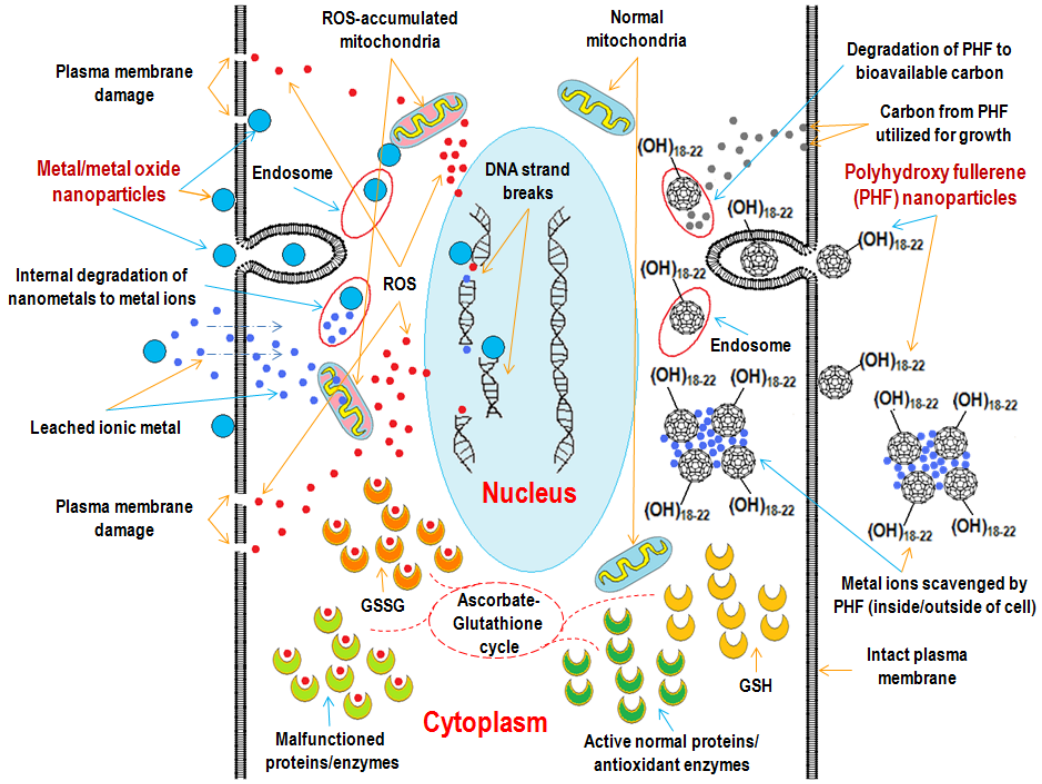

Figure 9.1 Schematic diagram of the impacts of metal-based nanoparticles and polyhydroxy fullerene on fungal cells based on observations from our study (orange arrow) and previous studies (blue arrow).

Overall, our study suggested that metal and metal oxide nanoparticles (Ag/CuO) could induce toxicity to freshwater microbial decomposers in a concentration- and time-dependent manner. Moreover, the toxicity of nanoCuO increased with the decrease in nanoparticle size. NOM, namely HA, also had negative effects in the absence of nanoparticles, but it could alleviate the toxicity of lower size nanoparticles to freshwater microbial decomposers and shredders. Bacterial communities were more sensitive than fungal communities against nanoCuO-induced stress. Also, the shifts in the community structure under nanoparticle exposure suggested that certain species are more tolerant/resistant than others to the stress induced by nanoparticles. The physiological and biochemical responses of fungal populations to nanoCuO showed that fungi isolated

from metal-polluted streams had a better ability to cope with the stress induced by nanoparticles compared to populations from non-polluted streams. Acute lethal effects of nanoCuO to freshwater invertebrate shredders may be achieved at very high and environmentally non-realistic concentrations; however, sublethal concentrations had pronounced effects on the feeding behaviour of shredders. Also, the toxicity CuO nanoparticles to invertebrate shredders was modulated by the size of particles and by the presence of HA as observed for microbial communities. In contrast to the adverse effects of nanoAg or nanoCuO on aquatic fungi and invertebrates, the polyhydroxy fullerene had a stimulatory effect on yeast growth and acted as an antioxidant agent by alleviating cadmium toxicity in yeasts. This may open new perspectives for the development of remediation strategies, which would allow the application of a clean nanotechnology. In the future, it would be interesting to examine if the negative impacts of metal-based nanoparticles can be alleviated by PHF.

Our study showed that nanometals and nanometal oxides had negative effects on plant litter decomposition and associated microbes and invertebrates in stream microcosms. This outcome suggests that plant litter decomposition might be a useful tool to assess ecotoxicity of metal nanoparticles in freshwaters. Considerring the increasing commercial applications and usage of nanoparticles and based on our results that pointed to potential toxicity of these nanomaterials to biota and the processes they drive, our work emphasizes the importance of risk assessment studies. In the near future, studies are also needed to provide the mechanistic explanations of nanometal-induced toxicity to aquatic organisms and to better discriminate the role of leached ionic and the particulate form of nanometals under realistic environmental conditions. Strategies should be further developed focusing on the risk assessment and taking precautionary steps to avoid the devastating effects like those caused by DDT or PCBs or to minimize the impacts of accidental or flash exposures such as the oil spillage in the Gulf of Mexico (2010). More regulatory frameworks are required for nanomaterials envisaging the control of exposure levels, taking into account bioactivity and biocompatiblility, and the development of alternative environmental friendly nanoparticles. To provide a safer and cleaner nanotechnology-based world, more responsibilities, awareness and precautionary care are required.

References

Aitken RJ, Chaudhry MQ, Boxall ABA, Hull M, 2006. Manufacture and use of nanomaterials: current status in the UK and global trends. Occup Med 56, 300–306.

Aruoja V, Dubourguier HC, Kasemets K, Kahru A , 2009. Toxicity of nanoparticles of CuO, ZnO and TiO2 to microalgae *Pseudokirchneriella subcapitata*. Sci Total Environ 407, 1461–1468.

Azevedo MM, Almeida B, Ludovico P, Cássio F, 2009. Metal stress induces programmed cell death in aquatic fungi. Aquat Toxicol 92, 264–270.

Azevedo MM, Carvalho A, Pascoal C, Rodrigues F, Cássio F, 2007. Responses of antioxidant defenses to Cu and Zn stress in two aquatic fungi. Sci Total Environ 377, 233–243.

Becheri A, Dürr M, Nostro PL, Baglioni P, 2008. Synthesis and characterization of zinc oxide nanoparticles: application to textiles as UV-absorbers. J Nanopart Res 10, 679–689.

Blaise C, Gagné F, Férard J, Eullaffroy P, 2008. Ecotoxicity of selected nano-materials to aquatic organisms. Environ Toxicol 23, 591–598.

Blinova I, Ivask A, Heinlaan M, Mortimer M, Kahru A, 2010. Ecotoxicity of nanoparticles of CuO and ZnO in natural water. Environ Pollut 158, 41–47.

Bonada N, Zamora-Muñoz C, El Alami M, Múrria C, Prat N, 2008. New records of Trichoptera in reference Mediterranean-climate rivers of the Iberian Peninsula and North of Africa: Taxonomical, faunistical and ecological aspects. Graellsia 64, 189–208.

Bosi S, Da Ros T, Spalluto G, Prato M, 2003. Fullerene derivatives: an attractive tool for biological applications. Eur J Med Chem 38, 913–923.

Braha B, Tintemann H, Krauss G, Ehrman J, Bärlocher F, Krauss GJ , 2007. Stress response in two strains of the aquatic hyphomycete *Heliscus lugdunensis* after exposure to cadmium and copper ions. BioMetals 20, 93–105.

Brondani D, Scheeren CW, Dupont J, Vieira IC, 2009. Biosensor based on platinum nanoparticles dispersed in ionic liquid and laccase for determination of adrenaline. Sens Actuators B Chem 140, 252–259.

Buzea C, Blandino IIP, Robbie K, 2007. Nanomaterials and nanoparticles: sources and toxicity. Biointerphases 2, MR17–MR172.

Chen J, Xiu Z, Lowry GV, Alvarez PJJ, 2011. Effect of natural organic matter on toxicity and reactivity of nano-scale zero-valent iron. Water Res 45, 1995–2001.

Christian P, Von der Kammer F, Baalousha M, Hofmann T, 2008. Nanoparticles: structure, properties, preparation and behaviour in environmental media. Ecotoxicology 17, 326–343.

Da Ros T, Spalluto G, Prato M, 2001. Biological applications of fullerene derivatives: a brief overview. Croat Chem Acta (CCACAA) 74, 743–755.

De Schamphelaere KAC, Heijerick DG, Janssen CR, 2002. Refinement and field validation of a biotic ligand model predicting acute copper toxicity to *Daphnia magna*. Comp Biochem Physiol C Toxicol Pharmacol 133, 243–258.

De Schamphelaere KAC, Vasconcelos FM, Allen HE, Janssen CR, 2004. The effect of dissolved organic matter source on acute copper toxicity to *Daphnia magna*. Environ Toxicol Chem 23, 1248–1255.

Drexler KE (foreword by Minsky M), 1986. Engines of creation: the coming era of nanotechnology. http://www.physics.utu.fi/projects/kurssit/UFYS3084/Engines%20of%20Creation.pdf

Duarte S, Pascoal C, Alves A, Correia A, Cássio F, 2008. Copper and zinc mixtures induce shifts in microbial communities and reduce leaf litter decomposition in streams. Freshwat Biol 53, 91–101.

Duarte S, Pascoal C, Cássio F, 2009. Functional stability of stream-dwelling microbial decomposers exposed to copper and zinc stress. Freshwat Biol 54, 1683–1691.

Durán N, Rosa MA, D'Annibale A, Gianfreda L., 2002. Applications of laccases and tyrosinases (phenoloxidases) immobilized on different supports: a review. Enzyme Microb Technol 31, 907–931.

Erickson RJ, Benoit DA, Mattson VR, Nelson HP Jr, Leonard EN, 1996. The effects of water chemistry on the toxicity of copper to fathead minnows. Environ Toxicol Chem 15, 181–193.

Fabrega J, Fawcett SR, Renshaw JC, Lead JR, 2009. Silver nanoparticle impact upon bacterial growth: effect of pH, concentration, and organic matter. Environ Sci Technol 43, 7285–7290.

Gajjar P, Pettee B, Britt DW, Huang W, Johnson WP, Anderson AJ, 2009. Antimicrobial activities of commercial nanoparticles against an environmental soil microbe, *Pseudomonas putida* KT2440. J Biol Eng 3, pp 13, doi:10.1186/1754-1611-3-9.

Gao J, Wang Y, Folta KM, Krishna V, Bai W, Indeglia P, Georgieva A, Nakamura H, Koopman B, Moudgil B, 2011. Polyhydroxy fullerenes (fullerols or fullerenols): beneficial effects on growth and lifespan in diverse biological models. PLoS One 6, e19976, pp 8.

Gerhardt A, de Bisthoven LJ, Soares AMVM, 2004. Macroinvertebrate response to acid mine drainage: community metrics and on-line behavioural toxicity bioassay. Environ Pollut 130, 263–274.

Gessner MO, Chauvet E, 2002. A case for using litter breakdown to assess functional stream integrity. Ecol Appl 12, 498–510.

Graça MAS, 2001. The role of invertebrates on leaf litter decomposition in streams – a Review. Int Rev Hydrobiol 86, 383–393.

Graça MAS, Canhoto C, 2006. Leaf litter processing in low order streams. Limnetica 25, 1–10.

Hartmann NB, Kammer FVD, Hofmann T, Baalousha M, Ottofuelling S, Baun A, 2010. Algal testing of titanium dioxide nanoparticles - testing considerations, inhibitory effects and modification of cadmium bioavailability. Toxicology 269, 190–197.

Heinlaan M, Ivask A, Blinova I, Dubourguier HC, Kahru A, 2008. Toxicity of nanosized and bulk ZnO, CuO and TiO_2 to bacteria *Vibrio fischeri* and crustaceans *Daphnia magna* and *Thamnocephalus platyurus*. Chemosphere 71, 1308–1316.

Hseu YC, Huang HW, Wang SY, Chen HY, Lu FJ, Gau RJ, Yang HL, 2002. Humic acid induces apoptosis in human endothelial cells. Toxicol Appl Pharmacol 182, 34–43.

Injac R, Radic N, Govedarica B, Djordjevic A, Strukelj B, 2008a. Bioapplication and activity of fullerenol $C_{60}(OH)_{24}$. Afr J Biotechnol 7, 4940–4050.

Israr M, Sahi S, Datta R, Sarkar D, 2006. Bioaccumulation and physiological effects of mercury in *Sesbania drummondii*, Chemosphere, 65, 591–598.

Jaeckel P, Krauss GJ, Krauss G, 2005. Cadmium and zinc response of the fungi *Heliscus lugdunensis* and *Verticillium* cf. *alboatrum* isolated from highly polluted water. Sci Total Environ 346, 274–279.

Jin S, Ye K, 2007. Nanoparticle-mediated drug delivery and gene therapy. Biotechnol Prog 23, 32–41.

Junghanns C, Krauss G, Schlosser D, 2008. Potential of aquatic fungi derived from diverse freshwater environments to decolourise synthetic azo and anthraquinone dyes, Bioresource Technol 99, 1225–1235.

Junghanns C, Moeder M, Krauss G, Martin C, Schlosser D, 2005. Degradation of the xenoestrogen nonylphenol by aquatic fungi and their laccases. Microbiology 151, 45–57.

Kaegi R, Ulrich A, Sinnet B, Vonbank R, Wichser A, Zuleeg S, Simmler H, Brunner S, Vonmont H, Burkhardt M, Boller M, 2008. Synthetic TiO_2 nanoparticle emission from exterior facades into the aquatic environment. Environ Pollut 156, 233–239.

Kasemets K, Ivask A, Dubourguier HC, Kahru A, 2009. Toxicity of nanoparticles of ZnO, CuO and TiO_2 to yeast *Saccharomyces cerevisiae*. Toxicol in Vitro 23, 1116–1122.

Kathirvelu S, D'Souza L, Dhurai B, 2009. UV protection finishing of textiles using ZnO nanoparticles. Indian J Fibre Text 34, 267–273.

Kim B, Park CS, Murayama M, Hochella MF, 2010. Discovery and characterization of silver sulfide nanoparticles in final sewage sludge products. Environ Sci Technol 44, 7509–7514.

Lai HS, Chen WJ, Chiang LY, 2000. Free radical scavenging activity of fullerenol on the ischemia-reperfusion intestine in dogs. World J Surg 24, 450–454.

Landolfo S, Politi H, Angelozzi D, Mannazzu I, 2008. ROS accumulation and oxidative damage to cell structures in *Saccharomyces cerevisiae* wine strains during fermentation of high-sugar-containing medium. Biochim Biophys Acta 1780, 892–898.

Lee SW, Kim SM, Choi J, 2009. Genotoxicity and ecotoxicity assays using the freshwater crustacean *Daphnia magna* and the larva of the aquatic midge *Chironomus riparius* to screen the ecological risks of nanoparticle exposure. Environ Toxicol Pharmacol 28, 86–91.

Li L-Z, Zhou D-M, Peijnenburg WJGM, van Gestel CAM, Jin S-Y, Wang Y-J, Wang P, 2011. Toxicity of zinc oxide nanoparticles in the earthworm, *Eisenia fetida* and subcellular fractionation of Zn. Environ Int 37, 1098–1104.

Lovern SB, Strickler JR, Klaper R, 2007. Behavioral and physiological changes in *Daphnia magna* when exposed to nanoparticle suspensions (titanium dioxide, nano-C_{60}, and $C_{60}HxC_{70}Hx$). Environ Sci Technol 41, 4465–4470.

Luechinger NA, Athanassiou EK, Stark WJ, 2008. Graphene-stabilized copper nanoparticles as an air-stable substitute for silver and gold in low-cost ink-jet printable electronics. Nanotechnology 19, 445201 (6 pp).

Ma H, Allen HE, Yin Y, 2001. Characterization of isolated fractionations of dissolved organic matter from natural waters and a wastewater effluent. Water Res 35, 985–996.

MacCormack TJ, Goss GG, 2008. Identifying and predicting biological risks associated with manufactured nanoparticles in aquatic ecosystems. J Ind Ecol 12, 286–296.

Meems N, Steinberg CEW, Wiegand C, 2004. Direct and interacting toxicological effects on the waterflea (*Daphnia magna*) by natural organic matter, synthetic humic substances and cypermethrin. Sci Total Environ, 319, 123–136.

Mendes-Ferreira A, Sampaio-Marques B, Barbosa C, Rodrigues F, Costa V, Mendes-Faia A, Ludovico P, Leão C, 2010. Accumulation of non-superoxide anion reactive oxygen species mediates nitrogen-limited alcoholic fermentation by *Saccharomyces cerevisiae*. Appl Environ Microbiol 76, 7918–7924.

Meng H, Chen Z, Xing G, Yuan H, Chen C, Zhao F, Zhang C, Zhao Y, 2007. Ultrahigh reactivity provokes nanotoxicity: explanation of oral toxicity of nanocopper particles. Toxicol Lett 175, 102–110.

Miersch J, Grancharov K, 2008. Cadmium and heat response of the fungus *Heliscus lugdunensis* isolated from highly polluted and unpolluted areas. Amino Acids 34, 271–277.

Miller RJ, Lenihan HS, Muller EB, Tseng N, Hanna SK, Keller AA, 2010. Impacts of metal oxide nanoparticles on marine phytoplankton. Environ Sci Technol 44, 7329–7334.

Moore MN, 2006. Do nanoparticles present ecotoxicological risks for the health of the aquatic environment? Environ Int 32, 967–976.

Mortimer M, Kasemets K, Kahru A, 2010. Toxicity of ZnO and CuO nanoparticles to ciliated protozoa *Tetrahymena thermophila*. Toxicology 269, 182–189.

Nair LS, Laurencin CT, 2007. Silver nanoparticles: synthesis and therapeutic applications. J Biomed Nanotech 3, 301–316.

Nel A, Xia T, Mädler L, Li N, 2006. Toxic potential of materials at the nanolevel. Science 311, 622–627.

Niyogi DK, Lewis Jr WM, McKnight DM, 2002. Effects of stress from mine drainage on diversity, biomass, and function of primary producers in mountain streams. Ecosystems 5, 554–567.

OECD, 2010. Guidance Manual for the Testing of Manufactured Nanomaterials: OECD's sponsorship programme, ENV/JM/MONO(2009)20REV. OECD Environment, Health and Safety Publications, Series on the Safety of Manufactured Nanomaterials No. 25, Organisation for Economic Co-operation and Development, Paris.

Partha R, Conyers JL, 2009. Biomedical applications of functionalized fullerene-based nanomaterials. Int J Nanomedicine 4, 261–275.

Pascoal C, Cássio F, 2004. Contribution of fungi and bacteria to leaf litter decomposition in a polluted river. Appl Environ Microbiol 70, 5266–5273.

Pascoal C, Cássio F, Gomes P, 2001. Leaf breakdown rates: a measure of water quality? Int Rev Hydrobiol 86, 407–416.

Pascoal C, Cássio F, Marcotegui A, Sanz B, Gomes P, 2005a. Role of fungi, bacteria, and invertebrates in leaf litter breakdown in a polluted river. J N Am Benthol Soc 24, 784–797.

Pascoal C, Marvanová L, Cássio F, 2005b. Aquatic hyphomycete diversity in streams of Northwest Portugal. Fungal Divers 19, 109–128.

Pascoal C, Pinho M, Cássio F, Gomes P, 2003. Assessing structural and functional ecosystem condition using leaf breakdown: studies on a polluted river. Freshwat Biol 48, 2033–2044.

Paul A, Stösser Zehl A, Zwirnmann E, Vogt RD, Steinberg CEW, 2006. Nature and abundance of organic radicals in natural organic matter: effect of pH and irradiation. Environ Sci Technol 40, 5897–5903.

Perugini P, Simeoni S, Scalia S, Genta I, Modena T, Conti B, Pavanetto F, 2002. Effect of nanoparticle encapsulation on the photostability of the sunscreen agent, 2-ethylhexyl-p-methoxycinnamate. Int J Pharm 246, 37–45.

Petersen EJ, Nelson BC, 2010. Mechanisms and measurements of nanomaterial-induced oxidative damage to DNA. Anal Bioanal Chem 398, 613–650.

Petica A, Gavriliu S, Lungu M, Buruntea N, & Panzaru C, 2008. Colloidal silver solutions with antimicrobial properties. Mater Sci Eng B 152, 22–27.

Priault M, Camougrand N, Kinnally KW, Vallette FM, Manon S, 2003. Yeast as a tool to study Bax/mitochondrial interactions in cell death. FEMS Yeast Res 4, 15–27.

Reijnders L, 2006. Cleaner nanotechnology and hazard reduction of manufactured nanoparticles. J Clean Prod 14, 124–133.

Ren G, Hu D, Cheng EWC, Vargas-Reus MA, Reip P, Allaker RP, 2009. Characterisation of copper oxide nanoparticles for antimicrobial applications. Int J Antimicrob Agents 33, 587–590.

Rezić I, 2011. Determination of engineered nanoparticles on textiles and in textile wastewaters. Trends Analyt Chem 30, 1159–1167.

Salata OV, 2004. Applications of nanoparticles in biology and medicine. J Nanobiotechnol 2 (6 pp).

Schrand AM, Rahman MF, Hussain SM, Schlager JJ, Smith DA, Syed AF, 2010. Metal-based nanoparticles and their toxicity assessment. Wiley Interdiscip Rev Nanomed Nanobiotechnol 2, 544–68.

Schreiner KM, Filley TR, Blanchette RA, Bowen BB, Bolskar RD, Hockaday WC, Masiello CA, Raebiger JW, 2009. White-rot basidiomycete-mediated decomposition of C_{60} fullerol. Environ Sci Technol 43, 3162–3168.

Sharma VK, 2009. Aggregation and toxicity of titanium dioxide nanoparticles in aquatic environment – a review. J Environ Sci Health A 44, 1485–1495.

Steffen KT, Hatakka A, Hofrichter M, 2002. Degradation of humic acids by the litter-decomposing basidiomycete *Collybia dryophila*. Appl Environ Microbiol 68, 3442–3448.

Steinberg CEW, Kamara S, Prokhotskaya VYu, Manusadžianas L, Karasyova T, Timofeyev MA, Zhang J, Paul A, Meinelt T, Farjalla VF, Matsuo AYO, Burnison BK, Menzel R, 2006. Dissolved humic substances – ecological driving forces from the individual to the ecosystem level? Freshwater Biol 51, 1189–1210.

Suberkropp K, Arsuffi TL, Anderson JP, 1983. Comparison of degradative ability, enzymatic activity, and palatability of aquatic hyphomycetes grown on leaf litter. Appl Environ Microbiol 46, 237–244.

Taniguchi N, 1974. Proc Intl Conf Prod Eng Tokyo, Part II, Japan Society of Precision Engineering.

Timofeyev MA, Shatilina ZM, Kolesnichenko AV, Bedulina DS, Kolesnichenko VV, Pflugmacher S, Steinberg CEW, 2006. Natural organic matter (NOM) induces oxidative stress in freshwater amphipods *Gammarus lacustris* Sars and *Gammarus tigrinus* (Sexton). Sci Total Environ 366, 673–681.

Townsend DM, Tew KD, Tapiero H, 2003. The importance of glutathione in human disease. Biomed Pharmacother 57, 145–155.

Van Hoecke K, Quik JT, Mankiewicz-Boczek J, De Schamphelaere KA, Elsaesser A, Van der Meeren P, Barnes C, McKerr G, Howard CV, Van de Meent D, Rydzyński K, Dawson KA, Salvati A, Lesniak A, Lynch I, Silversmit G, De Samber B, Vincze L, Janssen CR, 2009. Fate and effects of CeO_2 nanoparticles in aquatic ecotoxicity tests. Environ Sci Technol 43, 4537–4546.

Vávrová J, Řezáčová M, Pejchal J, 2012. Fullerene nanoparticles and their anti-oxidative effects: a comparison to other radioprotective agents. J Appl Biomed 10, 1–8.

Wall NA, Choppin GR, 2003. Humic acids coagulation: influence of divalent cations. Appl Geochem 18, 1573–1582.

Wigginton NS, Haus KL, Hochella MF, 2007. Aquatic environmental nanoparticles. J Environ Monit, 9, 1306–1316.

Yang HL, Hseu YC, Hseu YT, Lu FJ, Lin E, Lai JS 2004. Humic acid induces apoptosis in human premyelocytic leukemia HL-60 cells. Life Sci 75, 1817–1831.

Zhang F, Wu X, Chen Y, Lin H, 2009. Application of silver nanoparticles to cotton fabric as an antibacterial textile finish. Fibers Polym 10, 496–501.

Zhu X, Zhu L, Duan Z, Qi R, Li Y, Lang Y, 2008. Comparative toxicity of several metal oxide nanoparticle aqueous suspensions to Zebrafish (*Danio rerio*) early developmental stage. J Environ Sci Health A 43, 278–284.